Integrability in AdS/CFT correspondence: quasi-classical analysis

2009 J. Phys. A: Math. Theor. 42 254004

(http://iopscience.iop.org/1751-8121/42/25/254004)

IOP PUBLISHING JOURNAL OF PHYSICS A: MATHEMATICAL AND THEORETICAL

J. Phys. A: Math. Theor. **42** (2009) 254004 (106pp) doi:10.1088/1751-8113/42/25/254004

Integrability in AdS/CFT correspondence: quasi-classical analysis

Nikolay Gromov[1,2,3]

[1] Service de Physique Théorique, CNRS-URA 2306 C.E.A.-Saclay, F-91191 Gif-sur-Yvette, France
[2] LPT de l'Ecole Normale Supérieure et l'Université Paris-VI, Paris 75231, France
[3] St Petersburg INP, Gatchina, 188 300 St Petersburg, Russia

E-mail: nikgromov@gmail.com

Received 31 December 2008, in final form 24 March 2009
Published 9 June 2009
Online at stacks.iop.org/JPhysA/42/254004

Abstract

In this review, we consider a quasi-classical method applicable to integrable field theories which is based on a classical integrable structure—the algebraic curve. We apply it to the Green–Schwarz superstring on the $AdS_5 \times S^5$ space. We show that the proposed method reproduces perfectly the earlier results obtained by expanding the string action for some simple classical solutions. The construction is explicitly covariant and is not based on a particular parameterization of the fields and as a result is free from ambiguities. On the other hand, the finite size corrections in some particularly important scaling limit are studied in this paper for a system of Bethe equations. For the general superalgebra $\mathfrak{su}(N|K)$, the result for the $1/L$ corrections is obtained. We find an integral equation which describes these corrections in a closed form. As an application, we consider the conjectured Beisert–Staudacher (BS) equations with the Hernandez–Lopez dressing factor where the finite size corrections should reproduce quasi-classical results around a general classical solution. Indeed, we show that our integral equation can be interpreted as a sum of all physical fluctuations and thus prove the complete one-loop consistency of the BS equations. We demonstrate that any local conserved charge (including the AdS energy) computed from the BS equations is indeed given at one loop by the sum of the charges of fluctuations with an exponential precision for large S^5 angular momentum of the string. As an independent result, the BS equations in an $\mathfrak{su}(2)$ sub-sector were derived from Zamolodchikovs's S-matrix. The paper is based on the author's PhD thesis.

PACS numbers: 11.25.Tq, 02.30.Ik

(Some figures in this article are in colour only in the electronic version)

Contents

1. Introduction

The history of the quantum mechanics starts from Louis de Broglie, who suggested that the free particles could be described in terms of waves, like photons. This suggestion was brilliantly

confirmed by the observed interference effects in the scattering of electrons from crystals. The next step was to describe the particles in external potential. This problem was solved by Schrödinger, who discovered the non-relativistic wave equation. However, its relativistic generalization had a puzzling property of negative densities and the description of systems of interacting relativistic particles turned out to be inconsistent.

After discovering the field theory, a number of old problems were resolved or at least clarified but new difficulties of divergences in perturbative theory appeared. However, to describe all physical phenomena, which can be observed on earth, these difficulties can be overcome. The complete description of the existing experimental data so far is given by the standard model. The only ingredient of the standard model, which still lacks experimental support, is the Higgs boson particle. One can, therefore, conclude that at this moment there is no direct experimental need to go beyond the standard model.

On the other hand, there are a number of theoretical reasons to go beyond the standard model. The standard model is a relativistic quantum field theory, which describes three fundamental interactions existing in nature. The consistent quantum theory, which describes all the four known interactions at the same time, does not exist today. One of the main problems of today's physics is the integration of quantum mechanics and general relativity which leads to unification of the gravitational interaction with the others. Until now, the most reasonable and the only existing candidate has been string theory. In this theory, several problems of the quantum gravity seem to be resolved. In particular, the divergences are regularized on the Planck scale in some natural way. Unfortunately, string theory can be formulated consistently only in ten-dimensional spacetime and it seems that there are too many ways to compactify it to the four dimensions of the real world.

Besides the problem of finding the 'theory of everything', there are many open questions inside the standard model. In particular, the standard model describes the strong interaction, which is indeed the strongest force of nature. It is responsible for the major part of baryon mass and thus for the major part of all masses on the earth. Strong interactions bind nucleons in nuclei which, being dressed with electrons and bound into molecules by the much weaker electro-magnetic force, give rise to a variety of chemical properties. The part of the standard model, describing the strong interaction, quantum chromodynamics (QCD), has quarks and gluons as fundamental degrees of freedom. However, understanding the physical world also implies understanding how these fundamental constituents interact and bring into existence the entire variety of physical objects composing the universe. One of the most important features of the strong interactions—quark confinement—is still a mystery for the theorists.

String theory from its very origin is closely related to the theory of the strong interactions. It was first formulated as a theory of hadrons. However, after invention of QCD, the string research was shifted to the Planck scale. String theory in the theory of the strong interactions converted into a phenomenological tool. Nevertheless, the hope that the gauge theories with the $SU(N)$ gauge group can be described by strings came from the large N 't Hooft limit. In this limit, the Feynman graph with non-planar topology is suppressed by the powers of N. Each graph carries a topological factor N^χ, where χ is the Euler characteristic of the graph. This strongly reminds some string theory with $1/N$ coupling. Based on this, it was conjectured that in this limit QCD is described by some string theory. This idea is also supported by the experimental fact that hadrons approximately lie on linear Regge trajectories.

Then it was understood that the string theory dual to a particular four-dimensional gauge theory lives on a curved, higher dimensional manifold [1]. The formulation of this duality could be made precise in the case of $\mathcal{N} = 4$ super-Yang–Mills (SYM). Maldacena conjectured that it is dual to the type IIB string theory on $\mathrm{AdS}_5 \times S^5$ [2–4]. A great technical advantage of

the string side of duality is that string theory in the tree approximation is a two-dimensional σ-model and the string interactions are not relevant in the planar 't Hooft limit. On the other hand, there are numerous examples of the exactly solvable two-dimensional σ-models possessing an integrability. This gives us some hope that the $\mathcal{N} = 4$ super Yang–Mills theory is the first interacting four-dimensional gauge theory which could be solved at least in the planar 't Hooft limit.

In support of this hope, the one-loop integrability was discovered in $\mathcal{N} = 4$ SYM in [5] for the bosonic sector[1] where the dilatation operator was identified with the Hamiltonian of an integrable one-dimensional spin chain. Soon after, the classical integrability of the full superstring σ-model on $AdS_5 \times S^5$ was demonstrated in [8]. We will focus on this construction of major importance in the following section.

In this work, we will shortly review the main ingredients of applications of integrability to the AdS/CFT correspondence. We will then restrict ourselves to the problems related to finite size effects in integrable spin chains and quantum effects from the string side of the duality. We develop quasi-classical methods for the computation of one-loop corrections to the classical spectrum of free strings in a curved integrable background making use of the underlying integrable structures such as algebraic curves (section 3). From the spin-chain side, we describe a method of finding generic finite size corrections to the scaling limit described in section 2. We then show that the string and spin chain calculations match generically once the dressing phase chosen correctly (section 4).

In section 5, we also examine the possibility of obtaining the spectrum of AdS/CFT from some completely relativistic model by restricting ourselves to a particular subspace of the spectrum and integrating out extra degrees of freedom. This is done on the example of the $S^3 \times R$ sub-sector of the full $AdS_5 \times S^5$ string. This approach has an advantage that the spectrum is given by a simple set of Bethe equations and the complicated dressing phase in the effective Bethe equations simply stems from the existence of the extra hidden degrees of freedom. We conclude in section 6.

1.1. Integrability

The Green–Schwarz (GS) superstring on $AdS_5 \times S^5$ can be represented as a coset model with the target super-space [9]

$$\frac{PSU(2,2|4)}{SP(2,2) \times SP(4)}$$

whose bosonic part is $\frac{SU(2,2)}{SP(2,2)} \times \frac{SU(4)}{SP(4)}$, which is precisely $AdS_5 \times S^5$.

The matrix superalgebra $\mathfrak{su}(2,2|4)$ is spanned by the 8×8 supertraceless supermatrices

$$M = \left(\begin{array}{c|c} A & B \\ \hline C & D \end{array}\right),$$

where A and D belong to $\mathfrak{u}(2,2)$ and $\mathfrak{u}(4)$ respectively while the fermionic components are related by

$$C = B^\dagger \begin{pmatrix} \mathbb{I}_{2\times 2} & 0 \\ 0 & -\mathbb{I}_{2\times 2} \end{pmatrix}.$$

[1] Integrable spin chains have been discovered in (non-supersymmetric) gauge theories earlier [6, 7].

The $\mathfrak{psu}(2,2|4)$ superalgebra is the quotient of this algebra by the matrices proportional to the identity. Then we note that the $\mathfrak{psu}(2,2|4)$ algebra enjoys the automorphism

$$\Omega \circ M = \begin{pmatrix} EA^TE & -EC^TE \\ EB^TE & ED^TE \end{pmatrix}, \qquad E = \begin{pmatrix} 0 & -1 & 0 & 0 \\ 1 & 0 & 0 & 0 \\ 0 & 0 & 0 & -1 \\ 0 & 0 & 1 & 0 \end{pmatrix},$$

such that $\Omega^4 = 1$. This automatically implies that the algebra is endowed with a $\mathbb{Z}_4$ grading. This means that any algebra element can be decomposed into $\sum_{i=0}^{3} M^{(i)}$, where $\Omega \circ M^{(n)} = i^n M^{(n)}$. More explicitly,

$$\begin{aligned} M^{(0,2)} &= \tfrac{1}{2}\begin{pmatrix} A \pm EA^TE & 0 \\ 0 & D \pm ED^TE \end{pmatrix} \\ M^{(1,3)} &= \tfrac{1}{2}\begin{pmatrix} 0 & B \pm \mathrm{i}EC^TE \\ C \mp \mathrm{i}EB^TE & 0 \end{pmatrix} \end{aligned}. \tag{1}$$

We see that the $M^{(0)}$ elements belong, by definition, to the denominator algebra $\mathfrak{sp}(2,2) \times \mathfrak{sp}(4)$ of the coset. Then, the remaining bosonic elements, $M^{(2)}$, orthogonal to the former, generate the (orthogonal) complement of $\mathfrak{sp}(2,2) \times \mathfrak{sp}(4)$ in $\mathfrak{su}(2,2) \times \mathfrak{su}(4)$.

The Metsaev–Tseytlin action for the GS superstring in $\mathrm{AdS}_5 \times S^5$ is then given in terms of the algebra current

$$J = -g^{-1}\,\mathrm{d}g, \tag{2}$$

where $g(\sigma, \tau)$ is a group element of $PSU(2,2|4)$, by [10]

$$S = \frac{\sqrt{\lambda}}{4\pi} \int \mathrm{str}(J^{(2)} \wedge *J^{(2)} - J^{(1)} \wedge J^{(3)}), \tag{3}$$

Besides the obvious global $PSU(2,2|4)$ left multiplication symmetry the action (3) possesses a local gauge symmetry, $g \to gH$ with $H \in SP(2,2) \times SP(4)$, under which

$$J^{(i)} \to H^{-1} J^{(i)} H, \qquad i = 1, 2, 3,$$

while $J^{(0)}$ transforms as a connection. The equations of motion following from (3) are equivalent to the conservation of the Noether current associated with the global left multiplication symmetry

$$d * k = 0, \tag{4}$$

where $k = gKg^{-1}$ and $K = J^{(2)} + \frac{1}{2} * J^{(1)} - \frac{1}{2} * J^{(3)}$.

For a purely bosonic representative g, we can write

$$g = \left(\begin{array}{c|c} \mathcal{Q} & 0 \\ \hline 0 & \mathcal{R} \end{array}\right),$$

where $\mathcal{R} \in SU(4)$ and $\mathcal{Q} \in SU(2,2)$. Then we see that $U \equiv \mathcal{R}E\mathcal{R}^T$ is invariant under the gauge transformation $U \to \mathcal{R}HEH^T\mathcal{R}^T = U$ for $H \in SP(4)$ and thus is a good parameterization of

$$SU(4)/SP(4) \sim S^5.$$

In the same way, $V \equiv \mathcal{Q}E\mathcal{Q}^T$ describes the AdS_5 space. It is instructive to define the embedding coordinates u and v by the simple relations

$$u^j \Sigma_j^S = U, \qquad v^j \Sigma_j^A = V, \tag{5}$$

where Σ^S and Σ^A are the gamma matrices of $SO(6)$ and $SO(4,2)$ respectively. By construction, these coordinates will automatically satisfy

$$1 = u_6^2 + u_5^2 + u_4^2 + u_3^2 + u_2^2 + u_1^2, \qquad 1 = v_6^2 + v_5^2 - v_4^2 - v_3^2 - v_2^2 - v_1^2. \tag{6}$$

Then the bosonic part of the action can be expressed in the usual nonlinear σ model form:

$$S_b = \frac{\sqrt{\lambda}}{4\pi}\int_0^{2\pi} \mathrm{d}\sigma \int \mathrm{d}\tau \sqrt{h} h^{\mu\nu}(\partial_\mu u \cdot \partial_\nu u - \partial_\mu v \cdot \partial_\nu v).$$

One can also expand the action in powers of fermions. It is convenient to use the following parameterization of the $PSU(2,2|4)$ group element [11]:

$$g = \exp\begin{pmatrix} 0 & \theta \\ \bar{\theta} & 0 \end{pmatrix} \times \begin{pmatrix} \mathcal{Q} & 0 \\ 0 & \mathcal{R} \end{pmatrix}. \tag{7}$$

In this parameterization, the fermionic part of the action reads as

$$\begin{aligned} \mathcal{S}_f = \frac{\sqrt{\lambda}}{8\pi}\int \mathrm{d}^2\sigma \sqrt{h} h^{\mu\nu}\,\mathrm{tr}_4[V\partial_\mu \bar{V}(\theta\partial_\nu\bar{\theta} - \partial_\nu\theta\bar{\theta}) + U\partial_\mu\bar{U}(\partial_\nu\bar{\theta}\theta - \bar{\theta}\partial_\nu\theta)] \\ \pm \mathrm{i}\frac{\sqrt{\lambda}}{8\pi}\int \mathrm{d}^2\sigma\, \epsilon^{\mu\nu}\mathrm{tr}_4[V\partial_\mu\bar{\theta}^t\bar{U}\partial_\nu\bar{\theta} + \partial_\mu\theta U\partial_\nu\theta^t\bar{V}] + \mathcal{O}(\theta^4). \end{aligned} \tag{8}$$

1.1.1. Integrability and algebraic curve. As follows from the equations of motion and the flatness condition

$$\mathrm{d}J - J\wedge J = 0,$$

the connection

$$A(x) = J^{(0)} + \frac{x^2+1}{x^2-1}J^{(2)} - \frac{2x}{x^2-1}(*J^{(2)} - \Lambda) + \sqrt{\frac{x+1}{x-1}}J^{(1)} + \sqrt{\frac{x-1}{x+1}}J^{(3)} \tag{9}$$

is flat for any complex number x [8]. This is the crucial observation which indicates the model to be (at least classically) integrable. Indeed, we can define the monodromy matrix

$$\Omega(x) = \mathrm{Pexp}\oint_\gamma A(x), \tag{10}$$

where γ is any path starting and ending at some point (σ,τ) and wrapping the worldsheet cylinder once. Since the flatness of the connection ensures path independence, we can choose γ to be the constant τ path. Moreover, placing this loop at some other value of τ just amounts to a similarity transformation of the monodromy matrix. Thus, we conclude that the eigenvalues of $\Omega(x)$ are time independent. Since they depend on a generic complex number x, we have obtained in this way an infinite number of conserved charges thus hinting integrability. Usually, one also needs to prove that the conserved charges are local and that they are in convolution with each other to insure integrability below classical theory (for more details, see [12, 13]).

Let us construct the algebraic curve of Beisert *et al* [14], which gives the classification of the classical motions of the superstring on $\mathrm{AdS}_5 \times S^5$. We will argue below that the action variables are represented in a transparent way in terms of the algebraic curve and thus give a good starting point for the quasi-classical quantization of the superstring action.

To proceed, we note that under periodic $SP(2,2)\times SP(4)$ gauge transformations the monodromy matrix transforms by a simple similarity transformation so that the eigenvalues are also gauge invariant. We denote them as follows:

$$\{\mathrm{e}^{\mathrm{i}\hat{p}_1}, \mathrm{e}^{\mathrm{i}\hat{p}_2}, \mathrm{e}^{\mathrm{i}\hat{p}_3}, \mathrm{e}^{\mathrm{i}\hat{p}_4} \mid \mathrm{e}^{\mathrm{i}\tilde{p}_1}, \mathrm{e}^{\mathrm{i}\tilde{p}_2}, \mathrm{e}^{\mathrm{i}\tilde{p}_3}, \mathrm{e}^{\mathrm{i}\tilde{p}_4}\}.$$

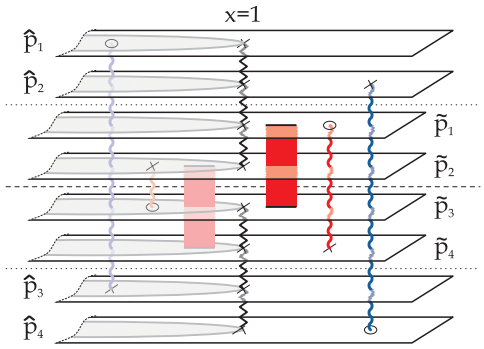

Figure 1. The eight sheets of the Riemann surface of the 'finite gap' method. The sheets could be connected by the cuts or have synchronized poles. The surface is also restricted by the $x \to 1/x$ symmetry. The singularities outside the unit circle are also reflected inside the unit circle.

In the rest of this section, we shall review the results of [14] and analyze the analytical properties of the quasi-momenta $\hat{p}$ and $\tilde{p}$. The eigenvalues are the roots of the characteristic polynomial equation and thus they define an eight-sheet Riemann surface. These sheets are connected by several cuts—see figure 1—whose branch points are the loci where the eigenvalues of the monodromy matrix become equal. The quasi-momenta can jump by a multiple of 2π at points connected by a cut[2]. For example, for a cut going from the first to the second sheet, we will have

$$\hat{p}_1^+ - \hat{p}_2^- = 2\pi n, \qquad x \in \mathcal{C}_n^{\hat{1}\hat{2}},$$

where $\tilde{p}^\pm$ stands for the value of the quasi-momenta immediately above/below the cut. This integer n, together with the filling fraction we shall introduce in following section, labels each of the cuts. Generically, we can summarize all equations as

$$p_i^+ - p_j^- = 2\pi n_{ij}, \qquad x \in \mathcal{C}_n^{ij}, \tag{11}$$

where the indices i and j take values

$$i = \tilde{1}, \tilde{2}, \hat{1}, \hat{2}, \qquad j = \tilde{3}, \tilde{4}, \hat{3}, \hat{4}, \tag{12}$$

and we denote

$$p_{\tilde{1},\tilde{2},\tilde{3},\tilde{4}} \equiv \tilde{p}_{1,2,3,4}, \qquad p_{\hat{1},\hat{2},\hat{3},\hat{4}} \equiv \hat{p}_{1,2,3,4}. \tag{13}$$

For each cut, we also associate the filling fraction

$$S_{ij} = \pm\frac{\sqrt{\lambda}}{8\pi^2 \mathrm{i}} \oint_{\mathcal{C}_{ij}} \left(1 - \frac{1}{x^2}\right) p_i(x)\,\mathrm{d}x \tag{14}$$

obtained by integrating the quasi-momenta around the square root cut. As before, the indices run over (12) and we should chose the plus sign for $i = \hat{1}, \hat{2}$ and the minus sign for the remaining excitations with $i = \tilde{1}, \tilde{2}$. Let us explain why we chose to integrate the quasi-momenta $p(x)$ around the cut with the seemingly mysterious $1 - 1/x^2$ weight. It was pointed out in [14, 15] and shown in [16] that these filling fractions are the action variables of the theory. From the AdS/CFT correspondence, these filling fractions are also expected to be integers since they correspond to an integer number of Bethe roots [18, 19]. Indeed, the likely existence of the Bethe ansatz description [20, 21] of the $\mathrm{AdS}_5 \times S^5$ superstring also

[2] Note that the derivative of the quasi-momenta is a single-valued function on the Riemann surface while $p(x)$ is not.

implies this pole structure of the exact quasi-momentum in a semi-classical limit. Moreover, in section 5 where the S^5 sub-sector is studied from the 'bootstrap' point of view we will clearly see that the quasi-momenta $p(z)$ coming from the quantum Bethe ansatz equations (BAEs) appears in the usual form $\oint p(z)\,\mathrm{d}z$, for the Zhukovsky variable $z = x + 1/x$. Thus, (14) is the good starting point for the string quasi-classical quantization.

From (1) and (9), it follows that

$$C^{-1}\Omega(x)C = \Omega^{-ST}(1/x), \qquad C = \left(\begin{array}{c|c} E & 0 \\ \hline 0 & -E \end{array}\right),$$

which translates into the inversion symmetry

$$\begin{aligned} \tilde{p}_{1,2}(x) &= -2\pi m - \tilde{p}_{2,1}(1/x) \\ \tilde{p}_{3,4}(x) &= +2\pi m - \tilde{p}_{4,3}(1/x) \\ \hat{p}_{1,2,3,4}(x) &= -\hat{p}_{2,1,4,3}(1/x) \end{aligned} \tag{15}$$

for the quasi-momenta[3].

The singularities of the connection at $x = \pm 1$ result in simple poles for the quasi-momenta. These singularities come from the current $J^{(2)}$ in (9). This current is supertraceless because it belongs to $\mathfrak{psu}(2,2|4)$ and so is its square due to the Virasoro constraints following from the variation of the action with respect to the worldsheet metric. Together with the inversion symmetry, this forces the various residues to organize as follows:

$$\{\hat{p}_1, \hat{p}_2, \hat{p}_3, \hat{p}_4 \mid \tilde{p}_1, \tilde{p}_2, \tilde{p}_3, \tilde{p}_4\} \simeq \frac{\{\alpha_\pm, \alpha_\pm, \beta_\pm, \beta_\pm | \alpha_\pm, \alpha_\pm, \beta_\pm, \beta_\pm\}}{x \pm 1}, \tag{16}$$

i.e. the residues at these points are synchronized and must be the same for the S^5 and the AdS_5 quasi-momenta $\hat{p}_i$ and $\tilde{p}_i$ respectively. This is the crucial role of the Virasoro constraints which will be of utmost importance in the remaining of this section.

Finally, for large x, one has

$$A_\sigma \simeq -g^{-1}\left(\partial_\sigma + \frac{2}{x}k_\tau\right)g,$$

where k, defined below (4), is the Noether current associated with the left global symmetry. Thus, from the behavior at infinity we can read the conserved global charges[4] [14, 25]

$$\left(\begin{array}{c} \hat{p}_1 \\ \hat{p}_2 \\ \hat{p}_3 \\ \hat{p}_4 \\ \hline \tilde{p}_1 \\ \tilde{p}_2 \\ \tilde{p}_3 \\ \tilde{p}_4 \end{array}\right) \simeq \frac{2\pi}{x\sqrt{\lambda}} \left(\begin{array}{c} +E - S_1 + S_2 \\ +E + S_1 - S_2 \\ -E - S_1 - S_2 \\ -E + S_1 + S_2 \\ \hline +J_1 + J_2 - J_3 \\ +J_1 - J_2 + J_3 \\ -J_1 + J_2 + J_3 \\ -J_1 - J_2 - J_3 \end{array}\right). \tag{17}$$

The finite gap method allow us to build, at least implicitly, classical solutions of the nonlinear equations of motion from the analytical properties of the quasi-momenta[5].

[3] Note that for $\hat{p}$, there is no $2\pi m$ imposed by requiring absence of time windings [14, 24].

[4] These are the bosonic charges, the ones which are present for a classical solution. Later we shall consider all kind of fluctuations, including the fermionic ones. Then we shall slightly generalize this expression to (182).

[5] For the inverse problem of recovering the solutions from the algebraic curve, see the monographs [26, 27] for the general formalism and [16] where this is carried over in the context of string theory for the classical bosonic string in $R \times S^3 \subset \mathrm{AdS}_5 \times S^5$ described by the KMMZ algebraic curve [18].

As we shall see in section 3, the algebraic curve can also be turned into a powerful tool to study the quantum spectrum, i.e. the energy level spacing, for energies close to that of a given classical string solution.

Integrability from the string side appears in the classical theory and its essence is contained in the algebraical curve. From the gauge side of the duality, the integrability shows up in the study of the anomalous dimensions of the long operators, where the mixing matrix acts on the single trace operators as a spin-chain Hamiltonian. An important tool in studying the integrable spin chains is the Bethe ansatz reviewed in the following sections.

1.2. Bethe ansatz equation

In 1931 Hans Bethe presented a method for obtaining the exact eigenvalues and eigenvectors of the one-dimensional spin-1/2 Heisenberg model, a linear array of electrons with uniform interaction between nearest neighbors. Bethe's parameterization of the eigenvectors, the Bethe ansatz, has become influential to an extent not imagined at the time. Today, many other systems are known to be solvable by some variant of the Bethe ansatz, and the method has been generalized and expanded far beyond the calculational tool it was originally. In particular, it seems to be a key ingredient in the AdS/CFT duality [2–4] between $\mathcal{N} = 4$ SYM and type IIB superstring theory on $AdS_5 \times S^5$.

It is very instructive to follow Bethe's original work to understand the physics beyond the algebraical constructions. The spin-1/2 Heisenberg spin chain is described in terms of the spin operators $\hat{\sigma}_n$ by the Hamiltonian

$$H = -2\sum_{n=1}^{L}\left(\hat{\sigma}_n \cdot \hat{\sigma}_{n+1} - \frac{1}{4}\right) \tag{18}$$

with periodic boundary conditions $\hat{\sigma}_{L+1} = \hat{\sigma}_1$. H acts on a Hilbert space of dimension 2^L spanned by the orthogonal basis vectors $|\sigma_1 \dots \sigma_L\rangle$, where each σ_n is $\uparrow$ or $\downarrow$.

The ferromagnetic state $|F\rangle = |\uparrow \cdots \uparrow\rangle$ is obviously an eigenstate with zero energy. To diagonalize the sector with one spin flipped, we can use the translational symmetry, which implies the plane wave form of the eigenstates

$$|p\rangle = \sum_{n=1}^{L} \mathrm{e}^{\mathrm{i}pn}|n\rangle, \tag{19}$$

where $|n\rangle$ is the ferromagnetic state with the nth spin flipped. We can also express it as $|n\rangle = \hat{\sigma}_n^-|F\rangle$. Since the states $|p\rangle$ with $Lp = 2\pi m, m = 0, \dots, L-1$, constitute the basis in the sector with one flipped spin they are automatically eigenstates of the Hamiltonian with eigenvalues

$$E = 2(1 - \cos p); \tag{20}$$

one can also use the parameterization $u = \frac{1}{2}\cot\frac{p}{2}$ of the momentum of the excitation. We will call this new quantity u—the Bethe root. In the new parameterization, one has

$$E = \frac{1}{u^2 + 1/4}. \tag{21}$$

Let us consider two excitations (or magnons). When the two flipped spins are far from each other, the Hamiltonian acts on them independently and so it is natural to assume the plane wave behavior of the wavefunction

$$|\psi\rangle = \sum_{1\leqslant n_1<n_2\leqslant L} \mathrm{e}^{\mathrm{i}(p_1n_1+p_2n_2)}\hat{\sigma}_{n_1}^-\hat{\sigma}_{n_2}^-|F\rangle + A\sum_{1\leqslant n_2<n_1\leqslant L} \mathrm{e}^{\mathrm{i}(p_1n_1+p_2n_2)}\hat{\sigma}_{n_1}^-\hat{\sigma}_{n_2}^-|F\rangle, \tag{22}$$

where the second term represents the result of the scattering of one excitation on another. Acting on this state by the Hamiltonian, one finds

$$A = -\frac{e^{i(p_1+p_2)} + 1 - 2e^{ip_2}}{e^{i(p_1+p_2)} + 1 - 2e^{ip_1}} = \frac{u_1 - u_2 - i}{u_1 - u_2 + i}; \tag{23}$$

we see that the scattering phase take a nice form in terms of u's. The periodicity of the wavefunction implies

$$A\, e^{ip_1 L} = 1, \qquad e^{ip_2 L} = A \tag{24}$$

or

$$\left(\frac{u_i + i/2}{u_i - i/2}\right)^L = \prod_{j\neq i}^{K} \frac{u_i - u_j + i}{u_i - u_j - i}, \qquad i = 1, \ldots, K, \tag{25}$$

with $K = 2$. Increasing further the number of excitations will simply lead to the same equation with K equal to the number of the magnons. This set of the equations is called the Bethe ansatz equations. The energy of the state is given by

$$E = \sum_i \frac{1}{u_i^2 + 1/4}. \tag{26}$$

This seemingly surprising fact that the multi-magnon scattering is described by the product of the two magnon phases is due to the existence of the large number of conserved charges. They commute with the Hamiltonian and thus can be diagonalized in the same basis. Their eigenvalues are given by

$$\mathcal{Q}_r = \sum_{j=1}^{K} \frac{i}{r-1}\left(\frac{1}{(u_j + i/2)^{r-1}} - \frac{1}{(u_j - i/2)^{r-1}}\right). \tag{27}$$

1.2.1. Bethe ansatz in the AdS/CFT correspondence. The $\mathcal{N} = 4$ SYM dilatation operator in the planar limit can be perturbatively computed in powers of the 't Hooft coupling λ. In the seminal work of Minahan and Zarembo [5], it was shown that the one-loop dilatation operator acts on the six real scalars of the theory exactly like an integrable $SO(6)$ nearest neighbor spin chain Hamiltonian. Restricting ourselves to two complex scalars, we obtain the same Hamiltonian considered above. The full $\mathcal{N} = 4$ one-loop dilatation operator [28] is also governed by an integrable Hamiltonian whose spectrum is given by a system of seven Bethe equations [29], corresponding to the seven nodes of the $\mathfrak{psu}(2, 2|4)$ Dynkin diagram. In [30], the all-loop generalization of the Bethe equation for the $SU(2)$ sector (25) was conjectured for the first time[6] to be

$$\left(\frac{y_j^+}{y_j^-}\right)^L = \prod_{j\neq i}^{K} \frac{u_i - u_j + i}{u_i - u_j - i}, \tag{28}$$

where $y_j(u_j)$ and $y_j^{\pm}(u_j)$ are given by

$$y + \frac{1}{y} = \frac{4\pi}{\sqrt{\lambda}} u, \qquad y^{\pm} + \frac{1}{y^{\pm}} = \frac{4\pi}{\sqrt{\lambda}}\left(u \pm \frac{i}{2}\right).$$

On the other hand, for the same sector but from the string sigma model side of the correspondence, a map between classical string solutions and Riemann surfaces was proposed [18] and then generalized to the full superstring coset [14], as we reviewed above.

[6] Consequently, it was found accurate up to three loops only at weak coupling.

The resemblance between the cuts connecting the different sheets of these Riemann surfaces and the distribution of roots of the Bethe equations in some limit seemed to indicate that the former could be the continuous limit of some quantum string Bethe ansatz. We will give more details about this so-called scaling limit in the following sections. In [20], Arutyunov, Frolov and Staudacher (AFS) proposed the following equations:

$$\left(\frac{y_j^+}{y_j^-}\right)^L = \prod_{j\neq i}^{K} \frac{u_i - u_j + \mathrm{i}}{u_i - u_j - \mathrm{i}} \sigma_{\mathrm{AFS}}^2(u_i, u_j), \tag{29}$$

where

$$\sigma_{\mathrm{AFS}}(u_i, u_j) = \frac{1 - 1/(y_j^+ y_i^-)}{1 - 1/(y_j^- y_i^+)} \left(\frac{y_j^- y_i^- - 1}{y_j^- y_i^+ - 1} \frac{y_j^+ y_i^+ - 1}{y_j^+ y_i^- - 1}\right)^{i(u_j - u_i)}. \tag{30}$$

In section 5, we will show how to derive (29) from the bootstrap approach. The striking similarity between (28) and (29) naturally leads to the proposal that both sides of the correspondence would be described by the same equation with a scalar factor σ^2 interpolating from σ_{AFS}^2 for the large 't Hooft coupling to 1 for small λ.

In [21, 31], Beisert and Staudacher (BS) conjectured the all-loop Bethe equations for the full $PSU(2,2|4)$ group to be

$$\begin{aligned}
\mathrm{e}^{\mathrm{i}\eta\phi_1 - \mathrm{i}\eta\phi_2} &= \prod_{j=1}^{K_2} \frac{u_{1,k} - u_{2,j} + \frac{\mathrm{i}}{2}}{u_{1,k} - u_{2,j} - \frac{\mathrm{i}}{2}} \prod_{j=1}^{K_4} \frac{1 - 1/x_{1,k} x_{4,j}^+}{1 - 1/x_{1,k} x_{4,j}^-},\\
\mathrm{e}^{\mathrm{i}\eta\phi_2 - \mathrm{i}\eta\phi_3} &= \prod_{j\neq k}^{K_2} \frac{u_{2,k} - u_{2,j} - \mathrm{i}}{u_{2,k} - u_{2,j} + \mathrm{i}} \prod_{j=1}^{K_3} \frac{u_{2,k} - u_{3,j} + \frac{\mathrm{i}}{2}}{u_{2,k} - u_{3,j} - \frac{\mathrm{i}}{2}} \prod_{j=1}^{K_1} \frac{u_{2,k} - u_{1,j} + \frac{\mathrm{i}}{2}}{u_{2,k} - u_{1,j} - \frac{\mathrm{i}}{2}},\\
\mathrm{e}^{\mathrm{i}\eta\phi_3 - \mathrm{i}\eta\phi_4} &= \prod_{j=1}^{K_2} \frac{u_{3,k} - u_{2,j} + \frac{\mathrm{i}}{2}}{u_{3,k} - u_{2,j} - \frac{\mathrm{i}}{2}} \prod_{j=1}^{K_4} \frac{x_{3,k} - x_{4,j}^+}{x_{3,k} - x_{4,j}^-},\\
\mathrm{e}^{\mathrm{i}\eta\phi_4 - \mathrm{i}\eta\phi_5} &= \left(\frac{x_{4,k}^-}{x_{4,k}^+}\right)^{\eta L} \prod_{j\neq k}^{K_4} \frac{u_{4,k} - u_{4,j} + \mathrm{i}}{u_{4,k} - u_{4,j} - \mathrm{i}} \prod_{j}^{K_4} \left(\frac{1 - 1/x_{4,k}^+ x_{4,j}^-}{1 - 1/x_{4,k}^- x_{4,j}^+}\right)^{\eta - 1} \sigma_{\mathrm{AFS}}^{2\eta}(x_{4,k}, x_{4,j})\, \mathrm{e}^{-\mathrm{i}\eta\mathcal{V}(u_{4,k}, u_{4,j})}\\
&\quad \times \prod_{j=1}^{K_1} \frac{1 - 1/x_{4,k}^- x_{1,j}}{1 - 1/x_{4,k}^+ x_{1,j}} \prod_{j=1}^{K_3} \frac{x_{4,k}^- - x_{3,j}}{x_{4,k}^+ - x_{3,j}} \prod_{j=1}^{K_5} \frac{x_{4,k}^- - x_{5,j}}{x_{4,k}^+ - x_{5,j}} \prod_{j=1}^{K_7} \frac{1 - 1/x_{4,k}^- x_{7,j}}{1 - 1/x_{4,k}^+ x_{7,j}},\\
\mathrm{e}^{\mathrm{i}\eta\phi_5 - \mathrm{i}\eta\phi_6} &= \prod_{j=1}^{K_6} \frac{u_{5,k} - u_{6,j} + \frac{\mathrm{i}}{2}}{u_{5,k} - u_{6,j} - \frac{\mathrm{i}}{2}} \prod_{j=1}^{K_4} \frac{x_{5,k} - x_{4,j}^+}{x_{5,k} - x_{4,j}^-},\\
\mathrm{e}^{\mathrm{i}\eta\phi_6 - \mathrm{i}\eta\phi_7} &= \prod_{j\neq k}^{K_6} \frac{u_{6,k} - u_{6,j} - \mathrm{i}}{u_{6,k} - u_{6,j} + \mathrm{i}} \prod_{j=1}^{K_5} \frac{u_{6,k} - u_{5,j} + \frac{\mathrm{i}}{2}}{u_{6,k} - u_{5,j} - \frac{\mathrm{i}}{2}} \prod_{j=1}^{K_7} \frac{u_{6,k} - u_{7,j} + \frac{\mathrm{i}}{2}}{u_{6,k} - u_{7,j} - \frac{\mathrm{i}}{2}},\\
\mathrm{e}^{\mathrm{i}\eta\phi_7 - \mathrm{i}\eta\phi_8} &= \prod_{j=1}^{K_6} \frac{u_{7,k} - u_{6,j} + \frac{\mathrm{i}}{2}}{u_{7,k} - u_{6,j} - \frac{\mathrm{i}}{2}} \prod_{j=1}^{K_4} \frac{1 - 1/x_{7,k} x_{4,j}^+}{1 - 1/x_{7,k} x_{4,j}^-}.
\end{aligned} \tag{31}$$

where $\eta = \pm 1$. Sets of equations with different η are related between each other by duality transformation, which we will discuss below. We inserted some additional parameters ϕ_i, called twists. Strictly speaking, they all should be zero. However, as we will see the situation

when all the twists vanish is a very degenerate one. We will also assume that the twists are restricted by

$$\phi_1 - \phi_2 - \phi_3 + \phi_4 = \phi_7 - \phi_8 - \phi_5 + \phi_6 = 2\pi m - \eta \sum_{j=1}^{K_4} \frac{1}{\mathrm{i}} \log \frac{x_4^+}{x_4^-}. \tag{32}$$

The phase $\mathcal{V}(y_{4,j})$ should be responsible for the interpolation between the YM and the string equations for small and large 't Hooft coupling λ.

When some configuration of the Bethe roots $u_{a,j}$ is found, the energy of the state (or anomalous dimension of the SYM operators) is given by

$$\Delta = \frac{\sqrt{\lambda}}{2\pi} \sum_{i=1}^{K_4} \left(\frac{\mathrm{i}}{y_{4,j}^+} - \frac{\mathrm{i}}{y_{4,j}^-} \right), \tag{33}$$

and the generalized expression for the local conserved changes is

$$\mathcal{Q}_r = \frac{1}{r-1} \sum_{j=1}^{K_4} \left(\frac{\mathrm{i}}{\left(y_{4,j}^+\right)^{r-1}} - \frac{\mathrm{i}}{\left(y_{4,j}^-\right)^{r-1}} \right). \tag{34}$$

In terms of them, one can rewrite the AFS phase (30) as

$$\sigma_{\mathrm{AFS}}^2(u_j, u_k) = \exp\left(2\mathrm{i}g \sum_{r=2}^{\infty} (\mathcal{Q}_r(u_k)\mathcal{Q}_{r+1}(u_j) - \mathcal{Q}_{r+1}(u_k)\mathcal{Q}_r(u_j)) \right). \tag{35}$$

In [32], based on a hypothesis for a natural extension for the quantum symmetry of the theory, Beisert found (up to a scalar factor) an S-matrix from which the BS equations would be derived. The scalar factor $\mathcal{V}$ was then conjectured in [33, 34] from the string side—using Janik's crossing relation [35]—and Beisert, Eden and Staudacher (BES) in [36, 37] from the gauge theory point of view—based on several heuristic considerations [38]. Similar to (35), one can write

$$\mathcal{V}(u_k, u_j) = \sum_{r=2} \sum_{s=r+1} c_{r,s}(g)(\mathcal{Q}_r(u_k)\mathcal{Q}_s(u_j) - \mathcal{Q}_s(u_k)\mathcal{Q}_r(u_j)) \tag{36}$$

with

$$\begin{aligned} c_{r,s}(g) &= \sum_{n=1}^{\infty} g^{1-n} \frac{((-1)^{r+s} - 1)\zeta(n)}{(-2\pi)^n \Gamma(n-1)} (r-1)(s-1) \frac{\Gamma\frac{s+r+n-3}{2} \Gamma\frac{s-r+n-1}{2}}{\Gamma\frac{s+r-n+1}{2} \Gamma\frac{s-r-n+3}{2}} \\ &\simeq ((-1)^{r+s} - 1) \left(\frac{2(r-1)(s-1)}{\pi(r-s)(r+s-2)} + \frac{1}{12g}(r-1)(s-1) + \cdots \right). \end{aligned} \tag{37}$$

The leading coefficient for $g \to \infty$ was first obtained by Hernandez and Lopez [39].

From the gauge theory side, these equations were tested quite recently up to four loops [40–42]. From the string theory point of view, the scalar factor recently passed several nontrivial checks [43–46] where several loops were probed at strong coupling. Also at strong coupling, the full structure of the BS equations was derived up to two loops in [47, 48] in a particular limit [49] where the sigma model is drastically simplified.

Another efficient way of testing the predictions of the Bethe ansatz equations is via anomalous dimensions of the twist-two operators (i.e. local operators with two scalars and S derivatives, traceless and symmetric in Lorenz indices). In the regime of a large number of derivatives, their anomalous dimensions scale logarithmical $\Delta - S = f(g) \log S$. $f(g)$ is a universal scaling function, computed up to four loops in YM [40, 50, 51]. It can also be computed up to two loops from the string side [52–54]. The methods reviewed in this work could be applied to compute two-loops prediction from the Bethe ansatz [123]. For the strong

coupling expansion, our method seems to be the most efficient by far since only some limiting cases of the results of [123] are reproduced from different methods [66, 67].

It is therefore fair to say that the advance in the last four years was spectacular. On the other hand it is also true that there is a great deal of conjectures involved one should both check and, hopefully, prove (or disprove).

In this work, we will check that the BS equations reproduce the one-loop shift around *any* classical string soliton solution with exponential precision in the large angular momentum of the string state $\mathcal{J} \equiv L/\sqrt{\lambda}$.

1.2.2. Thermodynamical limit. In this section we will review a special limit of the Bethe ansatz equations [22, 23], following closely [18, 24]. It is the so-called thermodynamical or scaling limit. It corresponds to the ferromagnetic regime of low energies $E \sim 1/L$ [7] Consider for example an $\mathfrak{sl}(2)$ Heisenberg spin-chain Bethe ansatz, which will be studied in details in the following section

$$-\left(\frac{u_j - \mathrm{i}/2}{u_j + \mathrm{i}/2}\right)^L = \prod_{k=1}^{K} \frac{u_j - u_k + \mathrm{i}}{u_j - u_k - \mathrm{i}}, \qquad j = 1, \ldots, K. \tag{38}$$

Note that under the formal replacement $L \to -L$, it becomes the above-described $\mathfrak{su}(2)$ spin chain. An important property which simplifies the analysis is that the solutions of this set of the equations are always real, which is not the case for the $\mathfrak{su}(2)$ spin chain.

Taking log of both parts of (49), we have[8]

$$2\pi \mathrm{i} n_j + L \log \frac{u_j - \mathrm{i}/2}{u_j + \mathrm{i}/2} = \sum_{k=1}^{K} \log \frac{u_j - u_k + \mathrm{i}}{u_j - u_k - \mathrm{i}}. \tag{39}$$

As we shall see in a moment in the limit $L \to \infty$, $K \sim L$ and with $n_j \sim 1$, the Bethe roots scales like L. It means that the chain is very long and the spins very smoothly change along it. The typical length of spin waves (magnons) is of the order of length L. It is instructive to introduce $x_j = u_j/L$. We can then write (39) in the form

$$2\pi n_j - \frac{1}{x_j} = \frac{2}{L} \sum_{k=1}^{K} \frac{1}{x_j - x_k}, \tag{40}$$

where we expanded (39) for large L. There is a potential danger arising from the right-hand side, since $u_j - u_k$ could be of order of 1. As we will see in section 2, these terms with $u_j - u_k \sim 1$ are responsible for the $1/L$ correction and are not important at the leading order.

Now let us consider the situation with a finite number of different mode numbers n_j and assume that the number of Bethe roots with the same mode number is of order L. If we take the ratio K/L to be small, we can neglect the right-hand side of (40) to get $x_j = 1/(2\pi n_j)$. We see that the points x_j with the same mode number are very close to each other and separated from the other roots by ~ 1. For $K/L \sim 1$, the picture is similar. The points x_j with the same mode number constitute some continuous distributions. The supports of these distributions corresponding to the different mode numbers are separated by a finite distance ~ 1. Hence, roots with the same mode number form a continuous cut in the complex plane x. One can characterize the distributions by the density

$$\rho(x) \equiv \frac{1}{L} \sum_j \delta(x - x_j) \tag{41}$$

[7] It is different from a more traditional regime $E \sim L$ widely studied since many years, especially in the condensed matter literature.

[8] Note that $\frac{\mathrm{i}}{2} \log \frac{x+\mathrm{i}}{x-\mathrm{i}} = \arctan(x) - \frac{\pi}{2}\,\mathrm{sign}(x)$ for the standard definition of log.

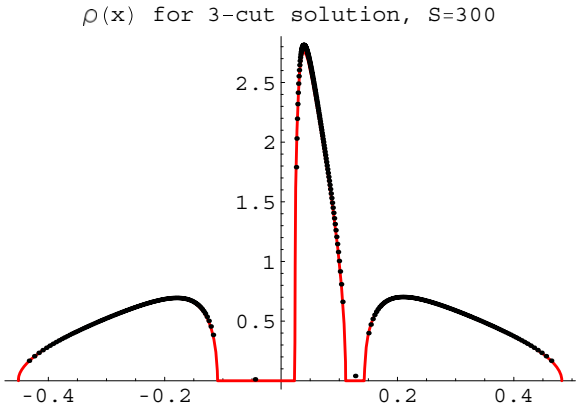

Figure 2. Density of roots. The dots correspond to numerical 3-cut solution with total number of Bethe roots $K = 300$ and equal fractions $\alpha_i = 1/6$, and $n_i = \{-1, 3, 1\}$. They are fixed from the numerical values of the roots by the (60). Solid line is the density at $L = \infty$ computed analytically from the corresponding hyper-elliptic curve. x coordinates of the dots are $\frac{u_j+u_{j+1}}{2L}$ so that the solitary points in the middle of empty cuts are artifacts of this definition.

or by the resolvent

$$G(x) \equiv \frac{1}{L}\sum_{j=1}^{K}\frac{1}{x-x_j} \simeq \int_{\mathcal{C}}\frac{\rho(y)\,\mathrm{d}y}{x-y}. \tag{42}$$

The density is non-zero on a set of cuts in the complex plane which in general consists of several non-overlapping cuts, $\mathcal{C} = \bigcup_i \mathcal{C}_i$, where the ith cut $\mathcal{C}_i$ represents roots with mode number n_i. In the case of the $\mathfrak{sl}(2)$ spin chain considered, the roots are always real and the cuts belong to the real axis.

The scaling limit of the Bethe equations can be rewritten as an integral equation for the density

$$2\not{G} = 2\fint_{\mathcal{C}}\frac{\rho(y)\,\mathrm{d}y}{x-y} = 2\pi n_i - \frac{1}{x}, \qquad x \in \mathcal{C}_i, \tag{43}$$

where $2\not{G}(x) \equiv G(x+\mathrm{i}0) + G(x-\mathrm{i}0)$. One can solve this integral equation numerically and compare with the actual density of the Bethe roots, also found numerically. For the three-cut configuration, this comparison is given in figure 2 revealing the perfect consistency of the above analysis.

Let us introduce

$$p(x) = \frac{1}{2x} + G(x), \tag{44}$$

which we shall call the quasi-momentum for reasons which will be clear soon. In terms of the analytic function $p(x)$, the above equation becomes

$$\not{p}(x) = \pi n_i, \qquad x \in \mathcal{C}_i; \tag{45}$$

in other words, it implies that $\mathrm{e}^{\mathrm{i}p}$ and $\mathrm{e}^{-\mathrm{i}p}$ are two sheets of the same two-sheet Riemann surface. This reminds the eigenvalues of the monodromy matrix in the classical finite gap analysis of section 1.1.1. However we see that our $p(x)$ has a simple pole in the origin, whereas the quasi-momenta of the $\mathrm{AdS}_5 \times S^5$ string had two poles at ± 1. But the BS equations (31)

are designed in such a way that the analogous quasi-momenta arising in the thermodynamical limit have exactly the same analytical properties as those of the classical 'finite-gap' analysis.

Indeed, for $\mathcal{J} = L/\sqrt{\lambda}$ fixed and $L \sim K_a \gg 1$ the BS equations can be summarized by $\not{p}_i - \not{p}_j = 2\pi n_{ij}$ for

$$\begin{array}{c}
p_1 = +\dfrac{2\pi\mathcal{J}x - \delta_{\eta,+1}\mathcal{Q}_1 + \delta_{\eta,-1}\mathcal{Q}_2 x}{x^2-1} + \eta(-H_1 - \bar{H}_3 + \bar{H}_4) + \phi_1 \\
\hline
p_2 = +\dfrac{2\pi\mathcal{J}x - \delta_{\eta,-1}\mathcal{Q}_1 + \delta_{\eta,+1}\mathcal{Q}_2 x}{x^2-1} + \eta(-H_1 + H_2 + \bar{H}_2 - \bar{H}_3) + \phi_2 \\
p_3 = +\dfrac{2\pi\mathcal{J}x - \delta_{\eta,-1}\mathcal{Q}_1 + \delta_{\eta,+1}\mathcal{Q}_2 x}{x^2-1} + \eta(-H_2 + H_3 + \bar{H}_1 - \bar{H}_2) + \phi_3 \\
\hline
p_4 = +\dfrac{2\pi\mathcal{J}x - \delta_{\eta,+1}\mathcal{Q}_1 + \delta_{\eta,-1}\mathcal{Q}_2 x}{x^2-1} + \eta(+H_3 - H_4 + \bar{H}_1) + \phi_4 \\
p_5 = -\dfrac{2\pi\mathcal{J}x - \delta_{\eta,+1}\mathcal{Q}_1 + \delta_{\eta,-1}\mathcal{Q}_2 x}{x^2-1} + \eta(-H_5 + H_4 - \bar{H}_7) + \phi_5 \\
\hline
p_6 = -\dfrac{2\pi\mathcal{J}x - \delta_{\eta,-1}\mathcal{Q}_1 + \delta_{\eta,+1}\mathcal{Q}_2 x}{x^2-1} + \eta(-H_5 + H_6 + \bar{H}_6 - \bar{H}_7) + \phi_6 \\
p_7 = -\dfrac{2\pi\mathcal{J}x - \delta_{\eta,-1}\mathcal{Q}_1 + \delta_{\eta,+1}\mathcal{Q}_2 x}{x^2-1} + \eta(-H_6 + H_7 + \bar{H}_5 - \bar{H}_6) + \phi_7 \\
\hline
p_8 = -\dfrac{2\pi\mathcal{J}x - \delta_{\eta,+1}\mathcal{Q}_1 + \delta_{\eta,-1}\mathcal{Q}_2 x}{x^2-1} + \eta(+H_7 + \bar{H}_5 - \bar{H}_4) + \phi_8
\end{array}, \tag{46}$$

where we introduced

$$G_a(x) = \sum_{j=1}^{K_a} \frac{\alpha(y_{a,j})}{x - y_{a,j}}, \qquad H_a(x) = \sum_{j=1}^{K_a} \frac{\alpha(x)}{x - y_{a,j}}, \qquad \alpha(x) = \frac{4\pi}{\sqrt{\lambda}} \frac{x^2}{x^2-1}.$$

For $\eta = 1$, we will also use the following notations:

$$\begin{array}{llll}
\tilde{p}_1 = p_1, & \tilde{p}_2 = p_4, & \tilde{p}_3 = p_5, & \tilde{p}_4 = p_8, \\
\hat{p}_1 = p_2, & \hat{p}_2 = p_3, & \hat{p}_3 = p_6, & \hat{p}_4 = p_7.
\end{array} \tag{47}$$

The local conserved charges are encoded into the 'middle-node' resolvent $G_4(x) \equiv -\sum_{n=0}^{\infty} \mathcal{Q}_{n+1} x^n$. To leading order, these quasi-momenta define an eight-sheet Riemann surface with exactly the same properties as in the classical analysis of the first section.

2. Finite size corrections in the Heisenberg spin chain

This part is devoted to the study of the $1/L$ finite size corrections in Bethe ansatz equations. From the string side of the duality, the finite size corrections correspond to the worldsheet loop expansion. Thus, the careful analysis of the finite size corrections can bring a new insight and can serve as a very nontrivial test of the different conjectures involved in the AdS/CFT correspondence. The main result of this section will be the integral equation, describing in a closed form the finite size corrections to the classical limit in the BS equations.

The similarity, and even the coincidence in a certain regime of the finite size corrections from the Bethe ansatz side and one-loop corrections to the classical limit from the string side was already observed earlier on particular string and chain solutions, having only one support for the Bethe roots distribution [55–62]. $1/L$ corrections were first studied for BMN states in [5], where the integrable spin chain for $\mathcal{N} = 4$ SYM was first proposed, and then in [20]. The Airy edge behavior, we will find in this section, also seems to be an important feature, because it provides some information about the system at all orders in $1/L$.

2.1. *Finite size corrections in the* $\mathfrak{sl}(2)$ *Heisenberg spin chain*

In this section, we study the integrable periodic Heisenberg XXX_s chain of non-compact quantum spins transforming under the representation $s = -1/2$ of $\mathfrak{sl}(2)$, in the thermodynamical limit reviewed in section 1. We will develop some general methods of the systematic $1/L$ expansion. In the following section we will generalize it to the so-called nested Bethe ansatz, which arises for the spin chains with a higher rank symmetry group.

The $\mathfrak{sl}(2)$ spin chain is known to be solvable by the Bethe ansatz (see, for example, [63]) and the energy of a state of K magnons in dimensionless units is given by a simple formula

$$E = \sum_{k=1}^{K} \frac{1}{u_k^2 + 1/4}, \tag{48}$$

where the Bethe roots u_j, $j = 1, 2, \ldots, K$, parameterizing the momenta of magnons, are solutions of a system of polynomial BAEs

$$-\left(\frac{u_j - \mathrm{i}/2}{u_j + \mathrm{i}/2}\right)^L = \prod_{k=1}^{K} \frac{u_j - u_k + \mathrm{i}}{u_j - u_k - \mathrm{i}}, \qquad j = 1, \ldots, K. \tag{49}$$

It can be proven that for this model, the roots are always real.

Our goal is to study the limiting $L \to \infty$ distributions of Bethe roots and the finite volume $1/L$ corrections to these distributions, to the energy and higher conserved charges. As we mentioned in section 1 in the main order this thermodynamical limit for the compact Heisenberg $XXX_{1/2}$ chain of $\mathfrak{su}(2)$ spins was already considered in [22], and later in [23] in relation to the integrable dilatation Hamiltonian in planar perturbative superconformal $\mathcal{N} = 4$ SYM theory. Its description and the general solution in terms of algebraic curves were proposed in [18] for the $\mathfrak{su}(2)$ case[9] and in [24, 65] for the $\mathfrak{sl}(2)$ chain.

The study of $1/L$ corrections in these systems was started recently in the papers [55, 56] for the simplest single support or one-cut distribution.

In this section, we will get the following results.

(1) The explicit formulae for the $1/L$ and $1/L^2$ corrections to the general multi-cut distribution of Bethe roots and to the corresponding energy of a Bethe state in terms of the underlying algebraic curve.
(2) The universal description of the distribution of Bethe roots in the vicinity of an edge of a support in terms of the zeros of the Airy function, similar to the double scaling limit in the matrix models.
(3) Asymptotics of conserved local charges $\mathcal{Q}_n(K, L)$ in the large n limit.

Unlike the papers [55, 56] using the method of a singular integral equation corrected by the so-called anomaly term[10], we will use here the exact Baxter equation written directly for the analytical function—the resolvent of the root distribution (a similar approach was used in [65]). This approach is more general and can be generalized to the higher orders in $1/L$. As an example, we apply the method to the simplest one-cut configuration.

In the following sections, we will generalize the method developed here for the more general systems of the equations and finally apply it in section 4 to the conjectured string BS equations. Then in the following section, we will show how the finite size corrections of the BS equations match with the one-loop corrections to the classical energy levels in the general classical background.

[9] Following a similar approach of [64] to a somewhat different limit of large spin.

[10] In the literature, some local term in the expansion of Bethe equations which was overlooked in early papers is called anomaly. This phenomenon of anomaly or the contribution of close roots in the thermodynamical limit of the BAE was first observed in [19].

2.1.1. Hamiltonian, transfer matrix and higher charges of the $\mathfrak{sl}(2)$ *chain.* The Hamiltonian of interaction of the neighboring spins s_l, s_{l+1} can be written in an explicit way [68]

$$H_{-1/2} = \sum_{l=1}^{L} \hat{H}^{l,l+1}_{-1/2} \tag{50}$$

with the Hamiltonian density

$$\hat{H}^{l,l+1}_{-1/2}|k, m-k\rangle = \sum_{k'=0}^{m} \left(\delta_{k=k'} \left(h(k) + h(m-k)\right) - \frac{\delta_{k\neq k'}}{|k-k'|} \right) |k', m-k'\rangle, \tag{51}$$

where $|k_1, \ldots, k_l, k_{l+1}, \ldots, k_L\rangle$ is a state vector labeled by L integers k_j ($s = -1/2$ spin components) and $h(k) = \sum_{j=1}^{k} \frac{1}{j}$ are harmonic numbers (see [63]).

The total momentum $P(u)$

$$\mathrm{e}^{\mathrm{i}P(u_j)} = \frac{u_j - \mathrm{i}/2}{u_j + \mathrm{i}/2} \tag{52}$$

satisfies the (quasi-)periodicity condition following directly from (49):

$$P_{\text{tot}} = \sum_{j=1}^{K} P(u_j) = 2\pi k/L, \qquad k \in \mathbf{Z}. \tag{53}$$

In application to the anomalous dimensions of operators[11] in $\mathcal{N} = 4$ SYM theory, one selects only cyclic Bethe states (with the trivial Bloch phase)

$$P_{\text{tot}} = 2\pi m, \qquad m \in \mathbf{Z}. \tag{54}$$

We can also study other physically interesting quantities of this model, such as the local conserved charges $\hat{\mathcal{Q}}_r$. They are defined as follows:

$$\hat{T}(v) = \exp\left(\mathrm{i} \sum_{r=1}^{\infty} \hat{\mathcal{Q}}_r v^{r-1} \right), \tag{55}$$

where the quantum transfer matrix $\hat{T}(v) \equiv \hat{T}(v; 0, 0, \ldots, 0)$ is a particular case of the inhomogeneous transfer matrix

$$\hat{T}(v; v_1, \ldots, v_L) = \mathrm{Tr}_0[\hat{R}_{0,1}(v - v_1) \cdots \hat{R}_{0,L}(v - v_L)], \tag{56}$$

and $\hat{R}_{0,j}$ is the universal $\mathfrak{sl}(2)$ R-matrix defined as [69]

$$\hat{R}_{0,1}(v) = \sum_{j=0}^{\infty} R_j(v) \mathcal{P}^{(j)}_{0,1}, \qquad R_j(v) = \prod_{k=1}^{j} \frac{v - \mathrm{i}k}{v + \mathrm{i}k} \tag{57}$$

with $\mathcal{P}^{(j)}_{01}$ being the operator projecting the direct product of two neighboring spins $s_0 = s_1 = -1/2$ to the representation j. Recall that

$$[\hat{T}(v; v_1, \ldots, v_L), \hat{T}(v'; v_1, \ldots, v_L)] = 0 \tag{58}$$

for any pair v, v', due to Yang–Baxter equations on the $\hat{R}$-matrix.

The direct calculation shows that $\hat{P}_{\text{tot}} = -\hat{\mathcal{Q}}_1$ is the operator of the momentum, $\hat{H}_{-1/2} = \hat{\mathcal{Q}}_2$ is the Hamiltonian (50), etc. These charges are local, in the sense that the charge density of $\mathcal{Q}_k$ contains $\leqslant k$ consecutive spins.

[11] The operators of type $\mathrm{Tr}(\nabla^{k_1} Z \cdots \nabla^{k_L} Z)$ in SYM, where $\nabla = \partial + A$ is a covariant derivative in a null direction and Z is a complex scalar, represent the state vectors $|k_1, \ldots, k_l, k_{l+1}, \ldots, k_L\rangle$ and the dilatation Hamiltonian is given at one loop by the $XXX_{-1/2}$ Hamiltonian.

Due to the integrability manifestly expressed by (58), all these charges commute and their eigenvalues on a Bethe state characterized by a set of Bethe roots satisfying (49) (enforcing the periodicity of the chain or the quasi-periodicity of the Bethe state) are given by [7]

$$\mathcal{Q}_r = \sum_{j=1}^{K} \frac{\mathrm{i}}{r-1}\left(\frac{1}{(u_j+\mathrm{i}/2)^{r-1}} - \frac{1}{(u_j-\mathrm{i}/2)^{r-1}}\right). \tag{59}$$

We will later estimate the behavior of $\mathcal{Q}_r$ at $r \to \infty$ and high orders of $1/L$ expansion.

2.1.2. $1/L$ expansion of the BAE. Let us start from reviewing one of the methods of solving (49) in the thermodynamical limit $L \to \infty, u_k \sim L \sim K$, before sticking with the most efficient one using the Baxter equation.

As we mentioned (49) has only real solutions, i.e. all the roots lie on the real axis. We label the roots so that $u_{j+1} > u_j$. Suppose that there exists a smooth function $X(x)$ parameterizing the Bethe roots

$$u_k = LX(k/L), \qquad \varrho(X(x)) \equiv \frac{1}{X'(x)} \simeq \frac{1}{u_{k+1}-u_k}. \tag{60}$$

For large K, the function $\varrho(x)$ has a meaning of density of Bethe roots. As follows from definition (60), its normalization is

$$\int \mathrm{d}x\, \varrho(x) = \alpha \tag{61}$$

with $\alpha = K/L$. In the thermodynamical limit, we can rewrite (39) assuming k to be far from the edges, as follows:

$$\begin{aligned}\sum_j{}' \mathrm{i}\log\left(\frac{u_j-u_k+\mathrm{i}}{u_j-u_k-\mathrm{i}}\right) &= -2\sum_j{}' \frac{1}{u_j-u_k} + \frac{2}{3}\sum_j{}' \frac{1}{(u_j-u_k)^3} - \frac{2}{5}\sum_j{}' \frac{1}{(u_j-u_k)^5} \\ &+ \frac{2}{7}\sum_j{}' \frac{1}{(u_j-u_k)^7} + \frac{\pi\varrho'[\coth(\pi\varrho)]_6}{L} - \frac{1}{12L^3}\left((\pi\varrho')^3\left[\frac{\coth(\pi\varrho)}{\sinh^2(\pi\varrho)}\right]_2\right. \\ &\left. - 2\pi^2\varrho'\varrho''\left[\frac{1}{\sinh(\pi\varrho)}\right]_3 + \pi\varrho^{(3)}[\coth(\pi\varrho)]_4\right) + \mathcal{O}\left(\frac{1}{L^5}\right),\end{aligned} \tag{62}$$

where we introduce the notation defined by $[f(\varrho)]_n \equiv f(\varrho) - \sum_{i=0}^{n-1} f^{(i)}(0)\frac{\varrho^i}{i!}$ for the functions regular at zero. For singular functions, the Taylor series should be substituted by the Laurent series so that $[f(\varrho)]_n$ is zero for $\varrho = 0$ and has first $n-1$ zero derivatives at this point. The terms in the first line represent the naive expansion of the lhs in $1/(u_j - u_k)$. It works well for the terms in the sum with $u_j \gg u_k$. The terms in the second line describe the anomalous contribution at $u_j \sim u_k$, for close roots with $i \sim j$. In this case, we can expand

$$u_j - u_k = \frac{j-k}{\varrho(u_j/L)} + \mathcal{O}(1/L) \tag{63}$$

and calculate the corresponding converging sum giving the terms in the second line. This anomaly was noted in the Bethe ansatz context in [19] although this phenomenon was known since long in the large N matrix integrals or similar character expansions [70, 71].

In our case when $L \to \infty$, it is obvious from (62), (39) that the anomaly does not contribute to the main order and the Bethe ansatz equation becomes a singular integral equation (see section 1.2.2):

$$2\pi n_k - \frac{1}{x} = 2\int_{\mathcal{C}_{\mathrm{tot}}} \frac{\mathrm{d}y\, \varrho_0(y)}{x-y}, \qquad x \in \mathcal{C}_k, \quad k = 1, \ldots, K. \tag{64}$$

2.1.3. Large L limit and $1/L$ corrections from the Baxter equation. Equation (49) can be also obtained as the condition that the transfer matrix eigenvalue $T(u)$ is a polynomial of degree L (see, for example, [72]):

$$T(u) = W(u+\mathrm{i}/2)\frac{Q(u+\mathrm{i})}{Q(u)} + W(u-\mathrm{i}/2)\frac{Q(u-\mathrm{i})}{Q(u)}, \tag{65}$$

where $Q(u) = \prod_{k=1}^{K}(u-u_k)$ and $W(u) = u^L$. This is clear from the very construction of a Bethe state in the algebraic Bethe ansatz approach [63]. The Bethe equations (49) are simply a condition that $T(u)$ has no poles.

Introducing notations: $x = u/L$, $\Phi(x) = \frac{1}{L}\sum_{k=1}^{K}\log(x-x_k)$, $V(x) = \log x$, $2t(x) = T(Lx)/(Lx)^L$, we rewrite (65) as

$$2t(x) = \exp L\left[\Phi\left(x+\frac{\mathrm{i}}{L}\right) - \Phi(x) + V\left(x+\frac{\mathrm{i}}{2L}\right) - V(x)\right] + \text{c.c.} \tag{66}$$

In these notations, the quasi-momentum (44) takes the form (exactly in $1/L$)

$$p(x) \equiv \Phi' + V'/2, \tag{67}$$

and expanding the Baxter equation in $1/L$ we get

$$t(x) = \cos p(x)\left[1 - \frac{1}{L}\left(\frac{p'(x)}{2} - \frac{V''(x)}{8}\right) + \frac{1}{2L^2}\left(\frac{p'(x)}{2} - \frac{V''(x)}{8}\right)^2\right] + \frac{1}{L^2}\sin p(x)\left(\frac{p''(x)}{6} - \frac{V^{(3)}(x)}{16}\right) + O\left(\frac{1}{L^3}\right). \tag{68}$$

According to our definition, $p(x)$ is a function of L. We will expand $p(x) = p_0(x) + \frac{1}{L}p_1(x) + \frac{1}{L^2}p_2(x) + \mathcal{O}(1/L^3)$ and $t(x) = t_0(x) + \frac{1}{L}t_1(x) + \frac{1}{L^2}t_2(x) + \mathcal{O}(1/L^3)$ and plug it into the last equation. Since $t(x)$ has no singularities, except $x = 0$, it is natural to assume that the coefficients of expansion $t_0(x), t_1(x), t_2(x), \ldots$ are the entire functions on the plane x with no cuts, having only a singularity at $x = 0$.

The quasi-periodicity property of the total momentum (53) reads up to three first orders as follows:

$$P_{\text{tot}} = -\sum_j \frac{1}{u_j} + \sum_j \frac{1}{12u_j^3} + \mathcal{O}\left(\frac{1}{L^4}\right) = 2\pi k/L \tag{69}$$

and for the cyclic states we select only $k = mL$, with integer m.

Algebraical curve from the Baxter equation. Let us restore from the Baxter equation the zero-order result of the previous section. In the zero-order approximation, we get from (68)

$$\cos p_0(x) = t_0(x) \tag{70}$$

or

$$p_0'(x) = \frac{2t_0'(x)}{\sqrt{1-t_0^2}}. \tag{71}$$

Since $t_0(x)$ is an entire function all the branch cuts of p_0 come from the square root in the denominator, after the Bethe roots condense to a set $\mathcal{C}_1, \ldots, \mathcal{C}_K$ of dense supports in the $L \to \infty$ limit. In this way, we reproduced the thermodynamical limit.

$1/L$ *correction from the Baxter equation.* To find the $1/L$ correction to the leading approximation to the density of roots, we deduce from (68)

$$p_1 = (-p_0'/2 + V''/8)\cot p_0 - \frac{t_1}{\sin p_0}. \tag{72}$$

From (71) and (45), we know about $p_0(x)$ that

$$p_0^+ = \pi n_j - \pi \mathrm{i}\rho_0, \qquad p_0^- = \pi n_j + \pi \mathrm{i}\rho_0 \tag{73}$$

so that

$$\sin p_0^+ = -\sin p_0^-, \tag{74}$$

and thus we have for the real and imaginary parts of $p_0(x)$ on the cuts

$$\pi \mathrm{i}\rho_1 = \left(\frac{V''}{8}t_0 - t_1\right)\frac{1}{\sin p_0^-}, \tag{75}$$

$$p_1' = -p_0' \cot p_0/2. \tag{76}$$

We will solve these equations below and restore the explicit form p_1.

Moreover, we see from (69) that

$$p_1(0) = 0 \tag{77}$$

and $p_1(x)$ should decreases as $\mathcal{O}(1/x^2)$ for large x.

We can build a general solution of the Riemann–Hilbert problem (76):

$$p_1(x) = \frac{x}{4\pi \mathrm{i} f(x)} \oint_{\mathcal{C}} \frac{f(y)p_0'(y)\cot p_0(y)}{y(y-x)}\,\mathrm{d}y + \sum_{j=1}^{K-2} \frac{a_j x^j}{f(x)}, \tag{78}$$

where $f^2(x) = \prod_{j=1}^{2K}(x - x_j)$ and the contour encircles all cuts $\mathcal{C}_k$ (but no other singularities). The first term on the rhs represents the Cauchy integral restoring the function from its real part on the cuts and having a zero at the origin (the value of the quasi-momentum $p(x)$ at $x = 0, \infty$ was already fixed for p_0) whereas the second one is purely imaginary on the cuts, with the polynomial in the numerator chosen in such a way that it does not spoil the behavior of $p(x)$ at $x = 0, \infty$.[12]

Thus for $K < 3$, the solution is unique. In particular, for $K = 1$ we restore from here the one-cut solution of [55]. For $K \geqslant 3$, we have to fix $K - 2$ parameters a_j. To do this, we have to use K additional conditions ensuring the right fractions α_j of the roots already chosen for p_0:

$$\oint_{\mathcal{C}_l} p_1(x)\,\mathrm{d}x = 0, \qquad l = 1, \ldots, K; \tag{79}$$

in fact, only $K - 2$ of them are linear independent (since we have already fixed the total filling fraction by the asymptotic properties of (78) at $x = \infty$: $p_1(x) = \mathcal{O}(1/x^2)$; equation (77) also restricts some linear combination of conditions (79). Hence, we completely fixed all parameters of our K-cut solution for the $1/L$ correction p_1 knowing the zero-order solution (algebraic curve) for p_0.

[12] We could also add terms $\frac{1}{f^3}, \frac{1}{f^5}, \ldots$ but they are too singular at the branch points as we shall see in the following section.

$1/L^2$ corrections from the Baxter relation. Expanding (68) up to $1/L^2$, we obtain

$$p_2 = -\frac{1}{2}\partial_x[\cot(p_0)I] - \frac{1}{8x^3} - \frac{\tilde{t}_2}{2\sin(p_0)}, \tag{80}$$

where

$$I = -\frac{\tilde{t}_1}{\sin(p_0)} = p_1 + \frac{p_0'}{2}\cot p_0. \tag{81}$$

We introduced here the notations

$$\begin{aligned}\tilde{t}_1 &= t_1 + \frac{\cos p_0}{8x^2},\\ \tilde{t}_2 &= t_2 - \frac{\cos p_0}{128x^4} + \frac{\tilde{t}_1}{8x^2} - \frac{\cos(2p_0)+5}{24\sin p_0}p_0'' + \frac{\cos p_0}{8\sin^2 p_0}\left(3(p_0')^2 + 4\tilde{t}_1^2\right)\end{aligned} \tag{82}$$

so that $\tilde{t}_1$ and $\tilde{t}_2$ are single-valued functions on the complex plane.

Note that above the cut $I^+ = \pi \mathrm{i}\rho_1$. We will find the explicit solution of these equations later, but we will need for that some results of the following section where we study the behavior of $p(x)$ near the branch points.

2.1.4. Double scaling solution near the branch point. As we stated above, the branch point singularities come only from the square roots of the denominator of (71). We define an exact branch point as a point x_*, where $t(x_*) = \pm 1$. If we approach one of the branch points $x \to x_*$, we can expand

$$t(x) \simeq \pm[1 - a(x - x_*)/2 - b(x - x_*)^2/2]. \tag{83}$$

Note that x_*, a, b themselves depend on L. We assume that they have a regular expansion in $1/L$ and define $x_* = x_0 + x_1/L + \cdots$. We call x_0 a classical branch point and x_1/L a branch point displacement.

Denoting $v = (x - x_*)L^{2/3}$ which will be our double scaling variable $v \sim 1$, we get from (65) up to $1/L^2$ terms

$$\pm 2\left(1 - \frac{av}{2L^{2/3}} - \frac{bv^2}{2L^{4/3}}\right)Q(u) = Q(u+\mathrm{i})\frac{W(u+\mathrm{i}/2)}{W(u)} + Q(u-\mathrm{i})\frac{W(u-\mathrm{i}/2)}{W(u)}. \tag{84}$$

In terms of a new function

$$q(v) = \mathrm{e}^{-n\pi v L^{1/3}}\,\mathrm{e}^{\frac{vL^{1/3}}{2x_*}}\,Q(x_*L + vL^{1/3}), \tag{85}$$

where n is such that $t(x^*) = \mathrm{e}^{\mathrm{i}\pi n}$, and after expansion in $1/L$ the last equation takes the form

$$q'' - avq = \frac{1}{L^{1/3}}\frac{4vq' + q}{4x_*^2} + \frac{1}{L^{2/3}}\left[\frac{1}{12}q^{(4)}(v) - \frac{v^2 q(v)}{4}\left(\frac{1}{x_*^4} - 4b\right)\right] + \mathcal{O}\left(\frac{1}{L}\right). \tag{86}$$

In fact, this equation can be easily solved in terms of q_0:

$$q \propto \left[1 + \frac{v^2}{4x_*^2 L^{1/3}} + \frac{1}{L^{2/3}}\left(\frac{v^4}{32x_*^4} - \frac{3b - a^2}{15a}v\right)\right]q_0\left(v - \frac{1}{4ax_*^2L^{1/3}} + \frac{a^2 + 12b}{60aL^{2/3}}v^2\right), \tag{87}$$

where $q_0(v) = \mathrm{Ai}(a^{1/3}v)$ (the Airy function). The second solution of (86), $\mathrm{Bi}(a^{1/3}v)$, has a wrong asymptotic as we will see. The sign $\propto$ means that the solution is defined up to a constant multiplier but this unknown multiplier does not affect the quasi-momentum. Now we can express the quasi-momentum only through our scaling function $q(v)$:

$$p\left(x_* + \frac{v}{L^{2/3}}\right) = \frac{\partial_v q(v, L)}{q(v, L)L^{1/3}} + \pi n + \frac{1}{2x_*}\left(\frac{1}{1 + \frac{v}{x_*L^{2/3}}} - 1\right). \tag{88}$$

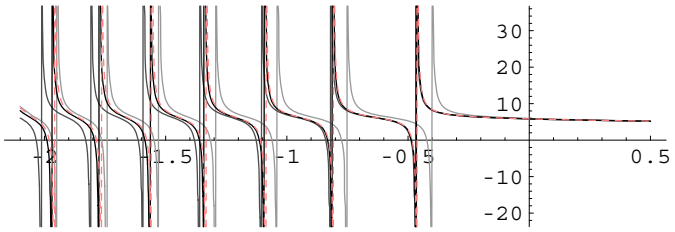

Figure 3. Quasi-momentum near the branch point as a function of the scaling variable v for $K = 200$. The poles correspond to the positions of Bethe roots u_i. Red dashed line—'exact' numerical value, light gray—zero-order approximation given by the Airy function $\mathrm{Ai}(a^{1/3}x)$, gray—first order and black—second-order approximation.

The first two terms on the rhs, if we substitute $q(v) \to q_0(v)$, represent the principal contribution to the double scaling limit near the edge, valid up to the corrections of the order $1/L^{2/3}$. We see from definition (85) that the zeros of $q(v)$ are nothing but the positions u_i of Bethe roots. Thus, we know these positions with a precision $1/L^{2/3}$ (see figure 3).

The large v asymptotic will be very helpful in fixing some unknown constant in the $1/L^2$ corrections given in the following section:

$$p(x_* + vL^{-2/3}) = \pi n + \frac{1}{L^{1/3}}\left(\underbrace{-\sqrt{av}}_{1} \underbrace{-\frac{1}{4v}}_{1/L} + \underbrace{\frac{5}{32v^2\sqrt{av}}}_{1/L^2} + \cdots\right) + \frac{1}{L^{2/3}}\left(\underbrace{\frac{1}{8x_*^2\sqrt{av}}}_{1/L} \underbrace{-\frac{1}{16ax_*^2v^2}}_{1/L^2} + \cdots\right) + \cdots, \tag{89}$$

where the cut corresponds to negative v for $a > 0$. Introducing the notation $y = vL^{-2/3}$ and rearranging the terms by the powers $1/L$, we have

$$\begin{aligned} p(x_* + y) = \pi n &+ \left[-\sqrt{ay} - \frac{(a^2 + 12b)y^{3/2}}{24\sqrt{a}} + \cdots\right] \\ &+ \frac{1}{L}\left[-\frac{1}{4y} + \frac{1}{8x_*^2\sqrt{ay}} + \frac{a^2 - 4b}{16a} + \cdots\right] \\ &+ \frac{1}{L^2}\left[\frac{5}{32y^2\sqrt{ay}} - \frac{1}{16ay^2x_*^2} + \frac{6 - x_*^4(a^2 + 12b)}{768x_*^4(ay)^{3/2}} + \cdots\right] + \cdots. \end{aligned} \tag{90}$$

Doing this re-expansion we assume that $L^{-1} \ll y \ll 1$, trying to sew together the double scaling region with the $1/L$ corrections to the thermodynamical limit. This procedure is similar to that used in higher orders of the WKB approximation in the usual one-dimensional quantum mechanics (see, for example, [73]).

To compare with p_0, p_1 and p_2, we have to re-expand around x_0:

$$p(x_0 + y) = p(x_* + y) + \frac{x_1}{L}\frac{\sqrt{a}}{2\sqrt{y}} + \frac{1}{L^2}\left[-\frac{x_1}{4y^2} + \frac{x_1}{16x_0^2y\sqrt{ay}} + \frac{\sqrt{a}x_1^2}{8y\sqrt{y}}\right], \tag{91}$$

or introducing notation

$$x_1 = \frac{2A}{\sqrt{a}} - \frac{1}{4x_0^2 a} \tag{92}$$

we get

$$\begin{aligned} p(x_0+y) = \pi n &+ \left[-\sqrt{ay} - \frac{(a^2+12b)y^2}{24\sqrt{ay}} + \cdots\right] \\ &+ \frac{1}{L}\left[-\frac{1}{4y} + \frac{A}{\sqrt{y}} + \frac{a^2-4b}{16a} + \cdots\right] + \frac{1}{L^2}\left[\frac{5}{32y^2\sqrt{ay}}\right. \\ &\left. - \frac{A}{2\sqrt{a}y^2} + \left(\frac{A^2}{2y\sqrt{ay}} - \frac{b}{64(ay)^{3/2}} - \frac{\sqrt{ay}}{768y^2}\right) + \cdots\right] + \cdots. \end{aligned} \tag{93}$$

Near the left branch point (i.e for $a < 0$ and $y < 0$), we have

$$\begin{aligned} p(x_0+y) = \pi n &+ \left[\sqrt{ay} + \frac{(a^2+12b)y^2}{24\sqrt{ay}} + \cdots\right] \\ &+ \frac{1}{L}\left[-\frac{1}{4y} - \frac{A}{\sqrt{-y}} + \frac{a^2-4b}{16a} + \cdots\right] + \frac{1}{L^2}\left[-\frac{5}{32y^2\sqrt{ay}}\right. \\ &\left. + \frac{A}{2\sqrt{-a}y^2} + \left(\frac{A^2}{2y\sqrt{ay}} + \frac{b}{64(ay)^{3/2}} + \frac{\sqrt{ay}}{768y^2}\right) + \cdots\right] + \cdots. \end{aligned} \tag{94}$$

Now we can compare it with our results of the previous sections and fix a, b and x_1.

Let us note that similar Airy-type oscillations were observed in the papers on random matrices where this behavior occurs near an endpoint of a distribution of eigenvalues [74].

Comparison with the $1/L$ *expansion.* It is instructive to establish the relations between a, b, A and the parameters of the algebraic curve.

For that, we use expansion (83) defining a, b and find from (70) for $y > 0$

$$p_0(x_0+y) = \pi n + \arccos t_0 \simeq \pi n - \sqrt{ay} - \frac{a^2+12b}{24\sqrt{a}} y^{3/2} + \mathcal{O}(y^{5/2}), \tag{95}$$

in agreement with (93), (94). We can fix a and b up to $\mathcal{O}(1/L)$ corrections from here through the parameters of the solution for p_0.

To calculate a and b up to $\mathcal{O}(1/L)$ and to fix A, we use expansion (83) with (72). Note that we have the minus sign in front of $\sqrt{ay}$, which ensures the positivity of the density on the cut (i.e. for $y < 0$ and $a > 0$) $\rho(y) \simeq \sqrt{a(-y)}/\pi$. If we had Bi instead of Ai, the sign would be plus and the density would be negative.

Now we compare this near-cut behavior to p_1. First, consider the regular part

$$p\!\!\!/_1 = -\frac{1}{2} p_0' \cot p_0 \simeq -\frac{1}{4y} + \frac{a^2-4b}{16a} + \mathcal{O}(y), \tag{96}$$

which agrees with (90). From (78), we see that

$$p_1(x_0+y) - p\!\!\!/_1(x_0+y) \simeq \frac{A}{\sqrt{y}} + \mathcal{O}\left(\frac{1}{y^{3/2}}\right), \tag{97}$$

where A can be written explicitly, again using p_0.

For the example of a one-cut solution, see (120).

2.1.5. General solution for p_2 and E_2. Now we have enough information to construct p_2 in the most general situation of an arbitrary number of cuts.

We start from a formula which immediately follows from (80):

$$\not{p}_2 = -\frac{1}{2}\partial_x\left[\cot(p_0)\left(p_1 + \frac{p_0'}{2}\cot p_0\right)\right] - \frac{1}{8x^3}, \tag{98}$$

where p_1 is given by (78). The behavior near zero and at infinity is as follows. Since from (53) and (69) it follows that $G(0) - \frac{1}{24L^2}G''(0) = 2\pi k/L + \mathcal{O}\left(\frac{1}{L^4}\right)$, we can conclude that

$$p_2(0) = \tfrac{1}{24}G_0''(0). \tag{99}$$

For large x, we again have

$$p_2(x) = O\left(1/x^2\right). \tag{100}$$

Repeating the arguments of the previous subsection, we have

$$p_2(x) = \frac{x}{4\pi \mathrm{i} f(x)}\oint_{\mathcal{C}}\frac{f(y)}{y(y-x)}\left(\frac{1}{4y^3} + \partial_y\left[\cot(p_0)p_1\right]\right) + \sum_{j=0}^{5K-1}\frac{c_j x^j}{f^5(x)}, \tag{101}$$

where path $\mathcal{C}$ is defined as in (78). Again, the first term guarantees that p_2 satisfies (98). We drop out $p_0'\coth p_0$ for simplicity. We can do this since together with $f(y)$, it forms a single-valued function without cuts and the integral is given by the poles inside of the path of integration. In fact, there are only poles at each branch point so that the result can be absorbed into the second term in (101).

So far, the second term in (101) was restricted only by conditions (99) and (100). Of course, this does not explain why we should restrict ourselves by the fifth power of $f(x)$ in the denominator. A natural explanation comes from the known behavior near the branch points (93), (94) from where we can see that

$$p_2\left(x_0^i + y\right) = \begin{cases} \frac{5}{32y^2\sqrt{a_i y}} - \frac{A_i}{2\sqrt{a_i}y^2} + \left(\frac{A_i^2}{2y\sqrt{a_i y}} - \frac{b_i}{64(a_i y)^{3/2}} - \frac{\sqrt{a_i y}}{768y^2}\right) + \mathcal{O}\left(\frac{1}{y}\right), & a_i, y > 0 \\ -\frac{5}{32y^2\sqrt{a_i y}} + \frac{A_i}{2\sqrt{-a_i}y^2} + \left(\frac{A_i^2}{2y\sqrt{a_i y}} + \frac{b_i}{64(a_i y)^{3/2}} + \frac{\sqrt{a_i y}}{768y^2}\right) + \mathcal{O}\left(\frac{1}{y}\right), & a_i, y < 0, \end{cases} \tag{102}$$

where all $6K$ constants a_i, b_i, A_i for $i = 1, \ldots, 2K$ are known since they can be determined from the near branch point behavior of p_0 and p_1 (93), (94). a_i and b_i follow from p_0:

$$p_0\left(x_0^i + y\right) = \begin{cases} -\sqrt{a_i y} - \frac{(a_i^2 + 12b_i)y^2}{24\sqrt{a_i y}} + \mathcal{O}(y^{5/2}), & a_i > 0, y > 0 \\ \sqrt{a_i y} + \frac{(a_i^2 + 12b_i)y^2}{24\sqrt{a_i y}} + \mathcal{O}(y^{5/2}), & a_i < 0, y < 0 \end{cases} \tag{103}$$

and A_i comes from p_1:

$$p_1\left(x_0^i + y\right) = \begin{cases} -\frac{1}{4y} + \frac{A_i}{\sqrt{y}} + \mathcal{O}(y^0), & a_i > 0, y > 0 \\ -\frac{1}{4y} - \frac{A_i}{\sqrt{-y}} + \mathcal{O}(y^0), & a_i < 0, y < 0. \end{cases} \tag{104}$$

In fact, (102) gives only two nontrivial conditions for each branch point which are the coefficient before the half-integer power of y so that we have $4K$ conditions. The extra K conditions come from zero A-period constraints signifying the absence of corrections to the filling fractions α_i:

$$\oint_{\mathcal{C}_l} p_2(x)\,\mathrm{d}x = 0, \qquad l = 1, \ldots, K. \tag{105}$$

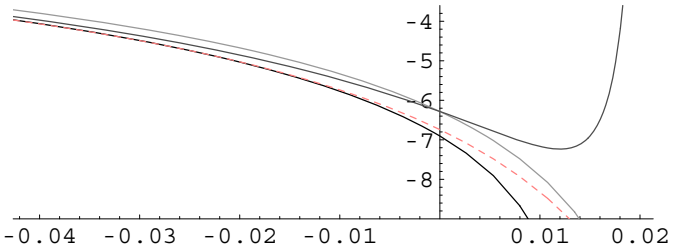

Figure 4. Resolvent far from the branch point as a function of x. Red dashed line—'exact' numerical value for one-cut solution with $K = 10, n = 2, m = 1$, light gray—zero-order approximation, gray—first order given by (78) and black—second-order approximation given by (108). Note that near the branch point ($x_0 = 0.02$), the approximation explodes and instead of it we should use the Airy function of (88), like in the usual WKB near a turning point.

To reduce the number of unknown constants, consider a branch point x_0. We can see that for small $y = x - x_0$ (we assume that the cut is on the left, i.e. $a_i > 0$),

$$I_1 \equiv \frac{x}{4\pi \mathrm{i} f(x)} \oint_{\mathcal{C}} \frac{f(z)}{z(z-x)} \left(\frac{1}{4z^3} + \partial_z (p_1 \cot p_0) \right)$$
$$= \frac{3}{16y^2\sqrt{ay}} - \frac{A}{2\sqrt{a}y^2} + \frac{1}{y^{3/2}} \left(\frac{b}{32a^{3/2}} - \frac{5\sqrt{a}}{128} \right) + \mathcal{O}\left(\frac{1}{y}\right). \tag{106}$$

Introducing the following integral

$$I_2 \equiv \frac{x}{4\pi \mathrm{i} f(x)} \oint_{\mathcal{C}} \frac{f(z)}{z(z-x)} \left((p_1 + p_0' \cot p_0) p_1 \cot p_0 - \frac{p_0''}{12} \right)$$
$$= -\frac{1}{32y^2\sqrt{ay}} + \frac{1}{y^{3/2}} \left(\frac{A^2}{2\sqrt{a}} - \frac{3b}{64a^{3/2}} + \frac{29\sqrt{a}}{768} \right) + \mathcal{O}\left(\frac{1}{y}\right), \tag{107}$$

we see that $I_1 + I_2$ reproduces the right series expansion near the branch points given by (102). Moreover, on the cuts $I_2(x + \mathrm{i}0) + I_2(x - \mathrm{i}0) = 0$ since the function under the integral is single valued. We can simply take

$$p_2(x) = I_1(x) + I_2(x) + \sum_{j=0}^{K-1} \frac{\tilde{c}_j x^j}{f(x)}, \tag{108}$$

where the remaining K constants are fixed from (105). Using that $p_2(0) = G''(0)/24$, we can fix one constant $\tilde{c}_0 = \frac{G''(0) f(0)}{24}$ before imposing condition (105).

This is our final result for the second quantum correction to the quasi-momentum. In section 2.1.7, we will specify this result for the example of the one-cut solution where it can be made much more explicit.

2.1.6. Energy. To find $1/L$ corrections to the energy, we represent the exact formula (48) as follows:

$$E = -\frac{1}{L} G'(0) + \frac{1}{24L^3} G^{(3)}(0) + \mathcal{O}\left(\frac{1}{L^5}\right), \tag{109}$$

We still have to expand $G(x) = -\frac{1}{2x} + p_0(x) + \frac{1}{L} p_1(x) + \frac{1}{L^2} p_2(x) + \mathcal{O}(1/L^3)$.

Finally, we obtain for the energy:

$$E = \frac{1}{L} E_0(x) + \frac{1}{L^2} E_1 + \frac{1}{L^3} E_2 + \mathcal{O}\left(\frac{1}{L^4}\right), \tag{110}$$

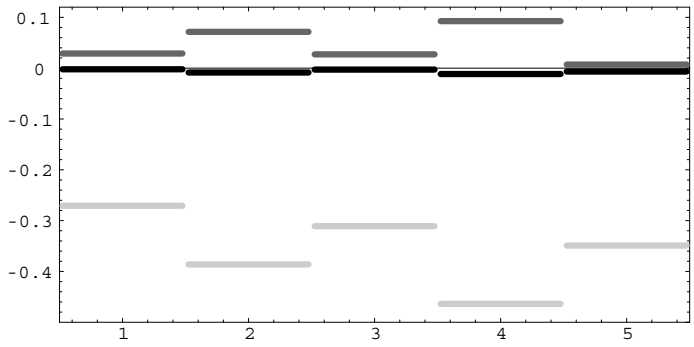

Figure 5. Relative deviation $\delta E(K)/E(K)$ of analytical computations of the energy $E(K)$ from its 'exact' value $E_{\text{exact}}(K)$ for the one-cut distribution found numerically by Mathematica (solid line corresponds to $\delta E(K) = 0$), for a finite number of roots K and a finite length L for zero-order (light gray), first-order (gray) and second-order (black) approximations. Details are summarized in the table

#	1	2	3	4	5
m, n	1, 2	2, 1	1, 3	2, 2	1, 5
E_0	$12\pi^2$	$24\pi^2$	$16\pi^2$	$32\pi^2$	$24\pi^2$
E_1	−558.4	−1563	−855.3	−2401	−1563
E_2	1160.0	5464.0	1592.0	8982.0	1504.0
K	10	40	7	20	5
L	20	20	21	20	25
$E_{\text{numerical}}$	4.66004	8.54515	5.7359	10.7876	7.0232
$E_0 + \frac{E_1}{L} + \frac{E_2}{L^2}$	4.670	8.619	5.752	10.912	7.070

where

$$E_0 = -G_0'(0), \tag{111}$$

$$E_1 = -p_1'(0) = -\frac{Q'(0)}{4\pi \mathrm{i} f(0)} \oint_{\mathcal{C}} \frac{f(y)p'(y)\cot p(y)}{Q(y)y}\,\mathrm{d}y, \tag{112}$$

and $Q(x) = \sum_{k=1}^{K-2} b_k x^k$ is related to the last term in (78). For E_2, we have from (108) the following representation:

$$E_2 = \frac{G_0^{(3)}(0)}{24} - p_2'(0) = -\frac{c_1}{f(0)} + \frac{G_0''(0)f'(0)}{24f(0)} + \frac{G_0^{(3)}(0)}{24}$$
$$- \frac{1}{4\pi \mathrm{i} f(0)} \oint \frac{f(y)}{y^2}\left(\frac{1}{4z^3} + \partial_z(p_1\cot p_0) - \frac{p_0''}{12} + (p_1 + p_0'\cot p_0)p_1\cot p_0\right). \tag{113}$$

Note that for one-cut, we should take $c_1 = 0$. We can compare our results with numerical calculations, as is done for a few one-cut solutions in figure 5.

2.1.7. One-cut case. In this section, we express corrections to the energy in terms of infinite sums for the simplest case of a one-cut solution. For this solution, the hyperelliptic curve is a

sphere. It is two complex planes connected by a single cut. The density of the Bethe roots is given by a simple formula [24]

$$\rho(x) = \frac{\sqrt{8\pi m x - (2\pi n x - 1)^2}}{2\pi x}. \tag{114}$$

We can easily find explicit expressions for a_i and b_i of (102). With the notation $M = \sqrt{m(m+n)}$, a_i and b_i become

$$\begin{aligned} a_1 &= -\frac{8Mn^4\pi^3}{(\sqrt{4M^2+n^2}-2M)^2}, \\ b_1 &= \frac{4\pi^4 n^6}{3(\sqrt{4M^2+n^2}-2M)^4}\left(12M\sqrt{4M^2+n^2}+3n^2-4n^2\pi^2M^2-24M^2\right) \end{aligned} \tag{115}$$

and

$$\begin{aligned} a_2 &= \frac{8Mn^4\pi^3}{(\sqrt{4M^2+n^2}+2M)^2}, \\ b_2 &= -\frac{4\pi^4 n^6}{3(\sqrt{4M^2+n^2}+2M)^4}\left(12M\sqrt{4M^2+n^2}-3n^2+4n^2\pi^2M^2+24M^2\right). \end{aligned} \tag{116}$$

It may be more convenient for comparison with string theory results [53] to express A defined by (93) as an infinite sum. We have to evaluate the integral in (78) and find A from the behavior near a branch point. We compute the integral by poles. To that end, we use that the solutions to the equation $\sin\left(p_0\left(x_l^{\pm}\right)\right) = 0$ are

$$x_l^{\pm} = \frac{1}{2\pi}\frac{1}{\sqrt{4M^2+n^2}\mp\sqrt{4M^2+l^2}}, \qquad l \geqslant 0. \tag{117}$$

The points $x_{l=0}^{\pm}$ are the branch points. They are inside the contour of integration and thus do not contribute.

Using that $f\left(x_l^{\pm}\right)/x_l^{\pm} = \pm\frac{l}{n}$,

$$\begin{aligned} \frac{1}{x_l^+ - x_{0,1}} - \frac{1}{x_l^- - x_{0,1}} &= -\frac{\sqrt{l^2+4M^2}}{l^2}\frac{1}{\pi x_{0,1}^2} \\ \frac{1}{x_l^+ - x_{0,2}} - \frac{1}{x_l^- - x_{0,2}} &= -\frac{\sqrt{l^2+4M^2}}{l^2}\frac{1}{\pi x_{0,2}^2}. \end{aligned} \tag{118}$$

We can evaluate the integral (78) for $x \to x_0$ (we also take x inside the contour to drop an irrelevant symmetric part of p_1):

$$\frac{1}{2\pi \mathrm{i}}\oint_C \frac{f(y)p'(y)\cot p(y)}{y(y-x)}\,\mathrm{d}y \to -\frac{1}{\mathrm{i}\pi n x_0^2}\left[\sum_{l=1}^{\infty}\left(\frac{\sqrt{l^2+4M^2}}{l}-1\right)-\frac{1}{2}\right]. \tag{119}$$

We can conclude that

$$\begin{aligned} A_2 &= -\frac{1}{2x_2^2\sqrt{a_2}}\left[\sum_{l=1}^{\infty}\left(\frac{\sqrt{l^2+4M^2}}{l}-1\right)-\frac{1}{2}\right] \\ A_1 &= -\frac{1}{2x_1^2\sqrt{-a_1}}\left[\sum_{l=1}^{\infty}\left(\frac{\sqrt{l^2+4M^2}}{l}-1\right)-\frac{1}{2}\right]. \end{aligned} \tag{120}$$

We reproduce the result of [55] for E_1 in terms of a sum from (112):

$$E_1 = -p_1'(0) = 4\pi^2 \sum_{l=1}^{\infty} l\sqrt{l^2+4M^2} \tag{121}$$

with the ζ-function regularization assumed.

We can also express our result for the next correction to energy E_2 given by (113) as a double sum. We will need the following quantity:

$$p_1\big(x_k^{\pm}\big) = \frac{\pm 1}{2\pi\big(x_k^{\pm}\big)^2 k}\left[\sum_{l=1}^{\infty}\left(\frac{l\sqrt{l^2+4M^2}-k\sqrt{k^2+4M^2}}{l^2-k^2}-1\right)+\frac{\sqrt{k^2+4M^2}}{2k}-\frac{1}{2}\right]. \tag{122}$$

Evaluating the integrals in (113), we express E_2 as a double sum:

$$E_2 = -(\mathcal{I}_1+\mathcal{I}_2+\mathcal{I}_3+\mathcal{I}_4), \tag{123}$$

where

$$\begin{aligned}
\mathcal{I}_1 &\equiv \frac{1}{4\pi \mathrm{i} f(0)}\oint \frac{f(z)}{z^2}\partial_z(p_1\cot p_0) = -2p_1'(0)\\
&\quad +\sum_{k=1}^{\infty}\left[2\pi\sum_{\pm}\left(\sqrt{4M^2+n^2}\pm 2\frac{k^2+2M^2}{\sqrt{k^2+4M^2}}\right)p_1\big(x_k^{\pm}\big)-4p_1'(0)\right]\\
\mathcal{I}_2 &\equiv \frac{1}{4\pi \mathrm{i} f(0)}\oint \frac{f(z)}{4z^5} = 4\pi^4 M^2(n^2+5M^2)\\
\mathcal{I}_3 &\equiv I_2'(0) = \frac{1}{16}\left(\frac{1}{x_{0,1}^2}+\frac{1}{x_{0,2}^2}\right)+\frac{1}{x_{0,1}}\left(\frac{7a_1}{96}-\frac{b_1}{8a_1}-A_1^2\right)+\frac{1}{x_{0,2}}\left(\frac{7a_2}{96}-\frac{b_2}{8a_2}+A_2^2\right)\\
\mathcal{I}_4 &\equiv -\frac{G_0''(0)f'(0)}{24f(0)}-\frac{G_0^{(3)}(0)}{24} = \frac{4}{3}M^2(2n^2+11M^2)\pi^4.
\end{aligned} \tag{124}$$

Note that in our new notations, $1/x_{0,i} = 4\pi M \pm 2\pi\sqrt{4M^2+n^2}$. Expressions for a_i, b_i and A_i are given in (115), (116) and (120), respectively.

2.1.8. Local charges. In this, we will calculate local charges $\mathcal{Q}_r$ in *all* powers of $1/L$ but for the *large* r from the behavior near the relevant branch point. The idea of this calculation is taken from the double scaling approach in matrix models. Namely, one can compare it to the calculation of the resolvent of eigenvalues in a Gaussian unitary matrix ensemble:

$$H_N(x) = \int \frac{\mathrm{d}^{N^2}M}{(2\pi)^{N^2}}\exp\left(-\frac{N}{2}\operatorname{Tr}M^2\right)\operatorname{Tr}(x-M)^{-1} = \sum_{g=1}^{\infty}N^{2-2g}\sum_{n=0}^{\infty}x^{-2n-1}H_{(g,n)}, \tag{125}$$

where M is the Hermitian matrix of a large size N. The coefficients $H_{(g,n)}$ actually give the number of specific planar graphs: it is given by the number of surfaces of genus g which can be done from a polygon with $2n$ edges, by the pairwise gluing of these edges. To extract the large n asymptotics of $H_{(g,n)}$ for any g, one can use that in the large N limit the density (which is the imaginary part of the resolvent on the support of eigenvalues) is given by Wigner's semi-circle law and the near-edge behavior is described by the Airy functional asymptotics [74, 75] showing the traces of individual eigenvalues in the continuous semi-circle distribution. We will try to extract similar asymptotics for the distribution of Bethe roots. The role of the $1/N$ expansion will be played by the $1/L$ expansion whereas the order of the $1/x$ expansion in the matrix model will now be played by the label r of the charge.

We start from expanding (59)

$$\mathcal{Q}_r = \sum_{m=0}^{\infty} \frac{1}{L^{r+2m-1}} \frac{(-1)^{m+1} G^{(r+2m-1)}(0)}{(2m+1)!(r-1)!2^{2m}}. \tag{126}$$

As we shall see, for large r only the $m = 0$ term contributes. We express the derivative as a contour integral around cuts

$$G^{(n)}(0) = -\frac{n!}{2\pi \mathrm{i}} \oint_{\mathcal{C}} \frac{G(x)}{x^{n+1}} \, \mathrm{d}x. \tag{127}$$

For large n, only a small neighborhood of the closest to zero branch point x_0 contributes due to the exponential suppression by the $1/x^{n+1}$ factor. Near the branch point x_0, we have from (93) (see also (94), (88)

$$G_k(x) = \delta_{k0}\left(\pi n_i - \frac{1}{2x_0}\right) + \begin{cases} c_k (x - x_0)^{\frac{1}{2}-\frac{3k}{2}} |a|^{\frac{1}{2}-\frac{k}{2}} + \mathcal{O}\big((x-x_0)^{1-\frac{3k}{2}}\big), \\ \quad a > 0, x_0 < 0 \\ (-1)^{k+1} c_k (x_0 - x)^{\frac{1}{2}-\frac{3k}{2}} |a|^{\frac{1}{2}-\frac{k}{2}} + \mathcal{O}\big((x_0-x)^{1-\frac{3k}{2}}\big), \\ \quad a < 0, x_0 > 0 \end{cases} \tag{128}$$

where the universal constants c_k can be computed from the known asymptotic of the Airy function

$$\mathrm{Ai}(z) = \frac{\mathrm{e}^{-\frac{2z^{3/2}}{3}}}{2\sqrt{\pi} z^{1/4}} \left[\sum_{k=0}^{n} \frac{\left(\frac{1}{6}\right)_k \left(\frac{5}{6}\right)_k}{k!} \left(-\frac{3}{4z^{3/2}}\right)^k + \mathcal{O}\left(\frac{1}{z^{3(n+1)/2}}\right) \right] \tag{129}$$

so that

$$c_k = \left. \frac{\mathrm{Ai}'(z)}{\mathrm{Ai}(z)} \right|_{z^{-\frac{3k-1}{2}}}, \tag{130}$$

in particular, $c_0 = -1$, $c_1 = -\frac{1}{4}$, $c_2 = \frac{5}{32}$, $c_3 = -\frac{15}{64}$, $c_4 = \frac{1105}{2048}$, $c_5 = -\frac{1695}{1024}$, $c_6 = \frac{414\,125}{65\,536}$, $c_7 = -\frac{59\,025}{2048}$.

These coefficients behave asymptotically as $c_k \sim (-1)^k k!$ at $k \to \infty$.

We assume that $k \ll n, r$ and expand (for $x_0 < 0$)

$$\begin{aligned} \oint_{-y_0}^{0} (y + x_0)^{-n} y^{\beta} \, \mathrm{d}y &= |x_0|^{\beta+1-n} (-1)^n \oint_{-y_0}^{0} y^{\beta} \, \mathrm{e}^{-n \log(1-y)} \, \mathrm{d}y \\ &\simeq |x_0|^{\beta+1-n} (-1)^n \oint_{-\infty}^{0} y^{\beta} \, \mathrm{e}^{ny} \, \mathrm{d}y. \end{aligned} \tag{131}$$

For the last integral the path of integration starts at $-\infty - \mathrm{i}0$, encircles the origin in the counterclockwise direction and returns to the point $-\infty + \mathrm{i}0$. For the first integral, the path is finite: it starts at some point $-y_0 - \mathrm{i}0$ where $0 < y_0 < |x_0|$ and ends at $-y_0 + \mathrm{i}0$. The dependence on y_0 is exponentially suppressed. The last integral is nothing but Hankel's contour integral:

$$\oint_{-y_0}^{0} (y + x_0)^{-n} y^{\beta} \, \mathrm{d}y = (-1)^n |x_0|^{\beta+1-n} n^{-\beta-1} \frac{2\pi \mathrm{i}}{\Gamma(-\beta)} \left(1 + \mathcal{O}\left(\frac{1}{n}\right)\right), \tag{132}$$

similarly,

$$\oint_{0}^{y_0} (y + x_0)^{-n} (-y)^{\beta} \, \mathrm{d}y = -|x_0|^{\beta+1-n} n^{-\beta-1} \frac{2\pi \mathrm{i}}{\Gamma(-\beta)} \left(1 + \mathcal{O}\left(\frac{1}{n}\right)\right) \tag{133}$$

so that

$$\frac{G_k^{(n)}(0)}{n!} = \begin{cases} (-1)^n \frac{c_k |a|^{\frac{1}{2}-\frac{k}{2}} n^{\frac{3k}{2}-\frac{3}{2}} |x_0|^{\frac{1}{2}-\frac{3k}{2}-n}}{\Gamma\left(\frac{3k}{2}-\frac{1}{2}\right)} \left(1+\mathcal{O}\left(\frac{1}{n}\right)\right), & a>0, x_0<0 \\ (-1)^{k+1} \frac{c_k |a|^{\frac{1}{2}-\frac{k}{2}} n^{\frac{3k}{2}-\frac{3}{2}} |x_0|^{\frac{1}{2}-\frac{3k}{2}-n}}{\Gamma\left(\frac{3k}{2}-\frac{1}{2}\right)} \left(1+\mathcal{O}\left(\frac{1}{n}\right)\right), & a<0, x_0>0. \end{cases} \tag{134}$$

As we can see from here, only the term with $m = 0$ in (126) contributes at large n. The others are suppressed as $1/n$ and the final result is

$$\mathcal{Q}_{k,r} = \begin{cases} (-1)^r \frac{c_k |a|^{\frac{1}{2}-\frac{k}{2}} r^{\frac{3k}{2}-\frac{3}{2}} |x_0|^{\frac{3}{2}-\frac{3k}{2}-r}}{\Gamma\left(\frac{3k}{2}-\frac{1}{2}\right)} (1+\mathcal{O}(r^{-1/2})), & a>0, x_0<0 \\ (-1)^k \frac{c_k |a|^{\frac{1}{2}-\frac{k}{2}} r^{\frac{3k}{2}-\frac{3}{2}} |x_0|^{\frac{3}{2}-\frac{3k}{2}-r}}{\Gamma\left(\frac{3k}{2}-\frac{1}{2}\right)} (1+\mathcal{O}(r^{-1/2})), & a<0, x_0>0, \end{cases} \tag{135}$$

where we introduced the notation

$$\mathcal{Q}_r = \frac{1}{L^{r-1}} \sum_{k=0}^{\infty} \mathcal{Q}_{k,r} \frac{1}{L^k}. \tag{136}$$

Note that $\mathcal{Q}_{k,r}$ is similar to $H_{g,n}$ of the matrix model.

2.1.9. Summary. We showed in this section on the example of $\mathfrak{sl}(2)$ Heisenberg spin chain how to find finite size corrections in the thermodynamical limit. We also propose a double scaling analysis of the near-edge distribution of Bethe roots, which gives some interesting results for the asymptotics of high conserved charges for the finite size corrections of any order.

The methods presented here can be easily carried over to the $\mathfrak{su}(2)$ quantum chain as well, though some peculiarities of this model, such as complex distributions of roots and the presence of 'string' condensates with equally distributed roots [23], should be taken into account. Only slight modifications of our results will allow one to find the $1/L$ corrections in the long-range integrable deformations of the $\mathfrak{su}(2)$ spin chain described in [76, 77]. As for more complicated models solved by the nested Bethe ansatz, $1/L$ will be discussed in the following section.

2.2. Finite size corrections in the $\mathfrak{su}(1,2)$ Heisenberg spin chain

In this section, we mainly stick to the simple example of the $\mathfrak{su}(1, 2)$ spin chain. This simple toy model has already contained all the nontrivial new features appearing due to the nested nature of the Bethe ansatz. The generalization to other (super)groups is straightforward and in particular, we shall focus on the Bethe ansatz describing the superstring in $AdS_5 \times S^5$ in section 4.

The scattering of excitations in this model is governed not by a simple phase factor as was in the $\mathfrak{su}(2)$ case considered in section 1 but rather by the S-matrix. To derive the Bethe ansatz restricting the momenta of the excitations due to the periodical boundaries, we have to solve a diagonalization problem

$$e^{-ip_k L}|\psi\rangle = \prod_{j\neq k}^{K} S(p_k, p_j)|\psi\rangle, \tag{137}$$

where $S(p_k, p_j)$ is a matrix and $|\psi\rangle$ is the multi-particle wavefunction. One can consider the matrix on the rhs as a spin-chain Hamiltonian, depending on the momenta of the initial excitations p_i as on parameters. One can show that this Hamiltonian is also integrable. The scattering of the excitations with some momenta $\tilde{p}_i$ in this auxiliary spin chain is governed by

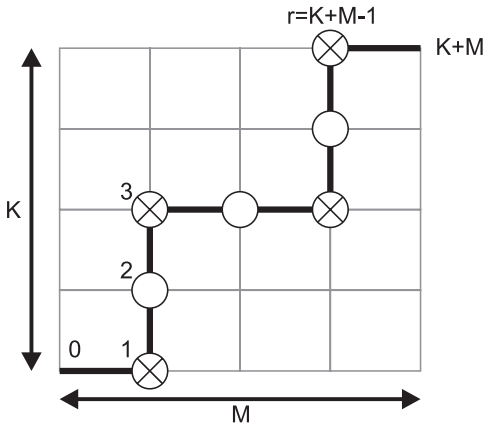

Figure 6. For $\mathfrak{su}(K|M)$ superalgebras, the Dynkin diagram is not unique. The several possible choices can be represented as paths going from the up right corner (M, K) to the origin always approaching this point with each step. The turns are the fermionic nodes whereas the straight lines correspond to the usual bosonic nodes. Different paths will correspond to different sets of Bethe equations which are related by fermionic dualities which flip a *left–down* fermionic turn into a *down–left* turn or vice versa [78].

a smaller size S-matrix. Continuing in this way, we will finally get a scalar S-matrix for which (137) is trivial. Thus for integrable rank r spin chains, each quantum state is parameterized by a set $\{u_{a,j}\}$ of Bethe roots where $a = 1, \ldots, r$ and $j = 1, \ldots, K_a$, where K_a is the excitation number of *magnons* of type a. The nested Bethe ansatz (NBA) equation from which we find these roots is given by

$$e^{i\tau_a}\left(\frac{u_{a,j}+\frac{i}{2}V_a}{u_{a,j}-\frac{i}{2}V_a}\right)^L = -\prod_{b=1}^{r}\frac{Q_b\left(u_{a,j}+\frac{i}{2}M_{ab}\right)}{Q_b\left(u_{a,j}-\frac{i}{2}M_{ab}\right)}, \tag{138}$$

where

$$Q_a(u) = \prod_{j=1}^{K_a}(u-u_{a,j})$$

are the Baxter polynomials, V_a are the Dynkin labels of the representation considered and M_{ab} is the Cartan matrix. In fact, in contrast to what happens for the usual Lie algebras, for superalgebras the Dynkin diagram (and thus the Cartan matrix) is not unique. Take for example the $\mathfrak{su}(K|M)$ superalgebra. The different possible Dynkin diagrams can be identified [78] as different paths starting from (M, K) and finishing at $(0, 0)$ (always approaching this point with each step) in a rectangular lattice of size $M \times K$ as in figure 6. The turns in this path represent the fermionic nodes whereas the bosonic nodes are those which are crossed by a straight line—see figure 6 (the index a goes along the path as indicated). The Cartan matrix M_{ab} is then given by

$$M_{ab} = (p_a + p_{a+1})\,\delta_{ab} - p_{a+1}\delta_{a+1,b} - p_a\delta_{a,b+1},$$

where p_a is associated with the link between nodes a and $a+1$ and is equal to $+1$ (-1) if this link is vertical (horizontal).

Here, we consider twisted (quasi-periodic) boundary conditions, i.e. we restrict to the states which are periodical up to the multiplication by

$$g = \mathrm{diag}(e^{i\phi_1}, \ldots, e^{i\phi_K}, e^{i\varphi_1}, \ldots, e^{i\varphi_M}) \in SU(K|M), \tag{139}$$

and the twists τ_a, appearing in (138) and associated with a Dynkin node located at (m, k) in the $M \times K$ network depicted in figure 6, are then given by [79]

$\tau_a = \phi_k - \phi_{k+1}$ for a bosonic along a vertical segment of the path

$\tau_a = \varphi_{m+1} - \varphi_m$ for a bosonic along a horizontal segment of the path

$\tau_a = \varphi_{m+1} - \phi_k + \pi$ for a fermionic node in a Γ-like turn that is with $p_{a-1} = -p_a = 1$

$\tau_a = \phi_{k+1} - \varphi_m + \pi$ for a fermionic node with $p_{a-1} = -p_a = -1$.

Note that since $g \in SU(K|M)$, we have $\sum_k \phi_k - \sum_m \varphi_m = 0 \bmod 2\pi$. We shall study these Bethe equations with generic twists and we will see that the usual case ($\tau_a = 0$) is in fact quite degenerate.

As mentioned above, we already found all the ingredients we will need for the study of the BS equations in the simple example of a $\mathfrak{su}(1, 2)$ spin chain in the fundamental representation described by the following system of NBA equations[13]:

$$e^{i\phi_1 - i\phi_2} = -\frac{Q_1(u_{1,j} + i)}{Q_1(u_{1,j} - i)} \frac{Q_2(u_{1,j} - i/2)}{Q_2(u_{1,j} + i/2)}, \qquad j = 1, \dots, K_1, \tag{140}$$

$$e^{i\phi_2 - i\phi_3} \left(\frac{u_{2,j} - \frac{i}{2}}{u_{2,j} + \frac{i}{2}} \right)^L = -\frac{Q_2(u_{2,j} + i)}{Q_2(u_{2,j} - i)} \frac{Q_1(u_{2,j} - i/2)}{Q_1(u_{2,j} + i/2)}, \qquad j = 1, \dots, K_2. \tag{141}$$

The eigenvalues of the local conserved charges are functions of roots $u_{2,j}$ only and are given by

$$\mathcal{Q}_r = \sum_{j=1}^{K_2} \frac{i}{r-1} \left(\frac{1}{(u_{2,j} + i/2)^{r-1}} - \frac{1}{(u_{2,j} - i/2)^{r-1}} \right). \tag{142}$$

We will often call these momentum-carrying roots carrying charges *middle node* roots[14].

First, consider only middle node excitations; $K_1 = 0 \neq K_2$ in the equations reduces to the $\mathfrak{sl}(2)$ case considered above

$$2\pi n^A + \phi_2 - \phi_3 = \frac{1}{x} + 2\not{G}_2(x), \qquad x \in \mathcal{C}^A, \tag{143}$$

where we introduce the resolvents

$$G_a(x) = \int \frac{\rho_a(y)}{x - y}, \qquad \rho_a(y) = \frac{1}{L} \sum_{j=1}^{K_a} \delta(x - x_{a,j}). \tag{144}$$

Let us also introduce some notation useful for what will follow. Defining the quasi-momenta as

$$\begin{aligned} p_1 &= -\frac{1}{2x} + G_1 - \phi_1, \\ p_2 &= -\frac{1}{2x} - G_1 + G_2 - \phi_2, \\ p_3 &= -\frac{3}{2x} - G_2 - \phi_3, \end{aligned} \tag{145}$$

[13] These equations are exactly the same as for the $\mathfrak{su}(3)$ spin chain except for the sign of the Dynkin labels which makes the system simpler because the Bethe roots are in general real.

[14] This name is not very proper in this situation. For the BS equations, the momentum-carrying roots are indeed in the middle of the Dynkin diagram.

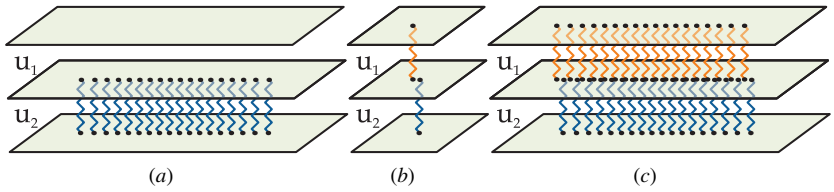

Figure 7. The *middle node* Bethe roots u_2 can condense into a line as depicted in figure 7(*a*). (The spins in this spin chain transform in a non-compact representation and thus the cuts are typically real. For the $\mathfrak{su}(2)$ Heisenberg magnet, the solutions are distributed in the complex plane as some *umbrella*-shaped curves [23].). Roots of different types can form bound states, called stacks [19], as shown in figure 7(*b*). The stacks behave as fundamental excitations and can also form cuts of stacks as represented in figure 7(*c*).

we can add indices 23 to the mode number n^A and to the cut $\mathcal{C}^A$ in (143) and recast this equation as

$$2\pi n^A_{23} = \not{p}_2 - \not{p}_3, \qquad x \in \mathcal{C}^A_{23}. \tag{146}$$

Next let us consider a state with only two roots $u_{2,1} \equiv u$ and $u_{1,1} \equiv v$ with different flavors, that is, $K_1 = K_2 = 1$. Bethe equations then yield

$$u = \frac{1}{2}\cot\frac{\phi_1 - \phi_3 + 2\pi n}{2L}, \qquad v = u + \frac{1}{2}\cot\frac{\phi_1 - \phi_2}{2}, \tag{147}$$

which tells us that if $n \sim 1$ we are in the scaling limit where $v \sim u \sim L$ and $v = u + \mathcal{O}(1)$—the two Bethe roots form a bound state, called stack [19], and can be thought of as a fundamental excitation (see figure 7(*b*)). On the other hand we note that, strictly speaking, for the usual untwisted Bethe ansatz with $\phi_a = 0$ the stack no longer exists.

Since the stack in figure 7(*b*) seems to behave as a fundamental excitation, one might wonder whether there exists a cut with $K_1 = K_2$ roots of types u_1 and u_2, like in figure 7(*c*), *dual* to the configuration plotted in figure 7(*a*). To answer affirmatively to this question, let us introduce a novel kind of duality in the Bethe ansatz which we shall call *bosonic duality*.

Indeed, as we will explain in detail in section 2.2.4, given a configuration of K_1 roots of type u_1 and K_2 roots of type u_2, we can write

$$2\mathrm{i}\sin(\tau/2)\, Q_2(u) = \mathrm{e}^{\mathrm{i}\tau/2} Q_1(u - \mathrm{i}/2)\tilde{Q}_1(u + \mathrm{i}/2) - \mathrm{e}^{-\tau/2} Q_1(u + \mathrm{i}/2)\tilde{Q}_1(u - \mathrm{i}/2), \tag{148}$$

where

$$\tilde{Q}_1(u) = \prod_{j=1}^{\tilde{K}_1}(u - \tilde{u}_{1,j}), \qquad \tilde{K}_1 = K_2 - K_1,$$

and $\tau = \phi_1 - \phi_2$. Moreover, this decomposition is unique and thus defines unambiguously the position of the new set of roots $\tilde{u}_1$. Then, as we will explain in section 2.2.4, the new set of roots $\{\tilde{u}_1, u_2\}$ is a solution of the same set of Bethe equations (138) with

$$\phi_1 \leftrightarrow \phi_2.$$

Let us then apply this duality to a configuration like that in figure 7(*a*) where the roots $u_2 \sim L$ are in the scaling limit and where there are no roots of type u_1, $K_1 = 0$. To the leading order, we see that $\tilde{u}_1$ in (148) will scale like L so that $\pm i/2$ inside the Baxter polynomials can be dropped and we find $Q_2 \simeq \tilde{Q}_1$, that is,

$$\tilde{u}_{1,j} = u_{2,j} + \mathcal{O}(1)$$

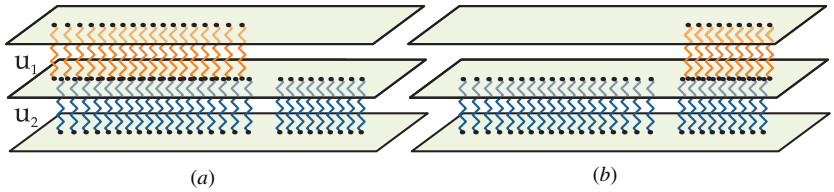

Figure 8. In the scaling limit, to the leading order, the bosonic duality reads as $Q_2 \simeq Q_1\tilde{Q}_1$ with $Q_a = \prod_{k=1}^{K_a}(u-u_a)$. Thus, if we start with the configuration in figure 8(*a*) where the K_1 roots u_1 form a cut of stacks together with K_1 out of the K_2 middle node roots u_2 and apply the bosonic duality to this configuration, the $K_2 - K_1$ new roots $\tilde{u}_1$ must be close to the roots u_2 which were previously *single* while the cut of stacks in the left of figure 8(*a*) will become, after the duality, a cut of simple roots—see figure 8(*b*).

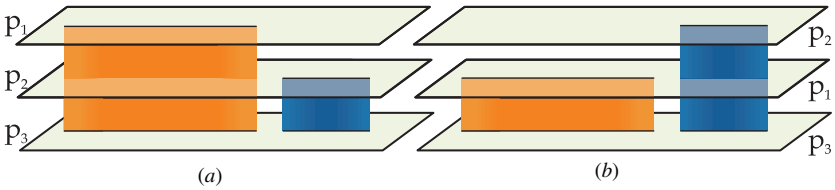

Figure 9. In the scaling limit the configurations in figure 8 condense into some disjoint segments, cuts, and we obtain a Riemann surface whose sheets are quasi-momenta. In this continuous limit, the duality corresponds to the exchange of the Riemann sheets.

and therefore we will indeed obtain a configuration like that depicted in figure 7(*c*). Moreover, the local charges (142) of this dual cut are exactly the same as those of the original cut 7(*a*) since they are carried by the *middle node* roots u_2 which are untouched during the duality transformation.

Finally, if we apply the duality transformation to some configuration like that in figure 8(*a*) in the scaling limit we find, by the same reasons as above, that $Q_2(u) \simeq Q_1(u)\tilde{Q}_1(u)$. This means that the dual roots $\tilde{u}_1$ will be close to roots u_2 which are not yet part of a stack—the ones making the cut in the right in figure 8(*a*). Thus, after the duality, we will obtain a configuration like that in figure 8(*b*).

We conclude that, in the scaling limit with a large number of roots, the distributions of Bethe roots condense into cuts in such a way that the quasi-momenta p_i introduced above become the three sheets of a Riemann surface (see figure 9(*a*)) obeying

$$2\pi n_{ij}^A = \not{p}_i - \not{p}_j, \qquad x \in \mathcal{C}_{ij}^A \tag{149}$$

when x belongs to a cut joining sheets i and j with mode number n_{ij}^A. The duality transformation amounts to a reshuffling of sheets 1 and 2 of this Riemann surface[15] so that a surface like that plotted in figure 9(*a*) transforms into that indicated in figure 9(*b*).

2.2.1. Finite size correction to nested Bethe Ansatz equations. In this section, we will study the leading $1/L$ corrections to the scaling equations (149). Moreover since the charges of the solutions are expressed through *middle node roots* u_2 and since these roots are duality

[15] As we shall see in the following section this interpretation can be made exact, and not only valid in the scaling limit.

invariant, it is useful to write the Bethe equations in terms of these roots only to have duality-invariant equations. Let us then consider a given configuration of roots condensed into some simple cuts $\mathcal{C}_{23}$ and some cuts of stacks $\mathcal{C}_{13}$. Then, to leading order, at cuts $\mathcal{C}_{23}$ we have

$$\frac{1}{x}+2\oint_{\mathcal{C}_{23}}\frac{\rho_2(y)\,\mathrm{d}y}{x-y}+\int_{\mathcal{C}_{13}}\frac{\rho_2(y)\,\mathrm{d}y}{x-y}=2\pi n^A_{23}+\phi_2-\phi_3,\qquad x\in\mathcal{C}_{23} \tag{150}$$

because in cut $\mathcal{C}_{13}$ we have $\rho_1\simeq\rho_2+\mathcal{O}(1/L)$. To study finite size corrections to this equation, two contributions must be considered. On the one hand, as we saw in the previous section, when expanding the *self-interaction* we get [58, 61, 55, 56, 57, 80]

$$\sum_{j\neq k}\mathrm{i}\log\frac{u_{2,k}-u_{2,j}-\mathrm{i}}{u_{2,k}-u_{2,j}+\mathrm{i}}=2\oint_{\mathcal{C}_{23}}\frac{\rho_2(y)\,\mathrm{d}y}{x-y}+2\int_{\mathcal{C}_{13}}\frac{\rho_2(y)\,\mathrm{d}y}{x-y}+\frac{1}{L}\pi\rho_2'\cot\pi\rho_2,$$

where the $1/L$ correction comes from the contribution to the sum from the roots separated by $\mathcal{O}(1)$. On the other hand, the auxiliary roots appear as[16]

$$\sum_j\mathrm{i}\log\frac{u_{2,k}-u_{1,j}+\mathrm{i}/2}{u_{2,k}-u_{1,j}-\mathrm{i}/2}=-\int_{\mathcal{C}_{13}}\frac{\rho_1(y)}{x-y}\,\mathrm{d}y=-\int_{\mathcal{C}_{13}}\frac{\rho_2(y)}{x-y}\,\mathrm{d}y-\int_{\mathcal{C}_{13}}\frac{\rho_1(y)-\rho_2(y)}{x-y}\,\mathrm{d}y$$

where the last term accounts for the mismatch in densities in cuts $\mathcal{C}_{13}$ and is clearly also a $\mathcal{O}(1/L)$ effect. Below, we will compute this mismatch and find

$$\rho_1(x)-\rho_2(x)=\frac{\Delta\cot_{12}}{2\pi\mathrm{i}L}=\frac{\cot^+_{21}-\cot^+_{23}}{2\pi\mathrm{i}L},\qquad x\in\mathcal{C}_{13} \tag{151}$$

where $\Delta f\equiv f(x+\mathrm{i}0)-f(x-\mathrm{i}0)$ and

$$\cot_{ij}\equiv\frac{p_i'-p_j'}{2}\cot\frac{p_i-p_j}{2}. \tag{152}$$

Thus we find, for $x\in\mathcal{C}_{23}$,

$$\frac{1}{x}+2\oint_{\mathcal{C}_{23}}\frac{\rho_2(y)\,\mathrm{d}y}{x-y}+\int_{\mathcal{C}_{13}}\frac{\rho_2(y)\,\mathrm{d}y}{x-y}=2\pi n^A_{23}+\phi_2-\phi_3-\frac{1}{L}\left[\cot_{23}-\int_{\mathcal{C}_{13}}\frac{\Delta\cot_{12}}{x-y}\frac{\mathrm{d}y}{2\pi\mathrm{i}}\right]. \tag{153}$$

As explained before, if we apply the duality transformation, cuts $\mathcal{C}_{23}$ become cuts $\mathcal{C}_{13}$ and vice versa and, to leading order, $p_1\leftrightarrow p_2$. Thus for cuts $\mathcal{C}_{13}$ we find precisely the same equation (153) with $1\leftrightarrow 2$, so that for $x\in\mathcal{C}_{13}$

$$\frac{1}{x}+2\oint_{\mathcal{C}_{13}}\frac{\rho_2(y)\,\mathrm{d}y}{x-y}+\int_{\mathcal{C}_{23}}\frac{\rho_2(y)\,\mathrm{d}y}{x-y}=2\pi n^A_{13}+\phi_1-\phi_3-\frac{1}{L}\left[\cot_{13}-\int_{\mathcal{C}_{23}}\frac{\Delta\cot_{12}}{x-y}\frac{\mathrm{d}y}{2\pi\mathrm{i}}\right]. \tag{154}$$

These two equations describing the finite size corrections for the two types of cuts of the $\mathfrak{su}(1,2)$ spin chain are the main results of this section.

In what follows, we will derive this result from two different approaches. Namely, we will find these finite size corrections using a Baxter formalism, similar to that considered in the previous section, based on transfer matrices for this spin chain in several representations and by exploiting the duality we mentioned in the previous section. It will become clear that the generalization to other NBA equations based on higher rank symmetry groups is straightforward.

[16] Recall that the Bethe roots $u_{2,k}$ belong to a $\mathcal{C}_{23}$ cut and therefore is always well separated from $u_{1,j}$ roots which always belong to $\mathcal{C}_{13}$ cuts.

2.2.2. Derivation using the transfer matrices. The central object in the study of integrable systems is the *transfer matrix* $\hat{T}(u)$. The algebraic Bethe ansatz formalism has the diagonalization of such objects as the main goal and the Bethe equations appear in the process of diagonalization (see [63] and references therein for an introduction to the algebraic Bethe ansatz). As functions of a spectral parameter u and of the Bethe roots $u_{a,j}$, these transfer matrices seem to have some poles at the positions of the Bethe roots. On the other hand, they are defined as a product of R operators which do not have these singularities. This means that the residues of these apparent poles must vanish. These analyticity conditions (on Bethe roots) turn out to be precisely the Bethe equations and, thus, if we manage to obtain the eigenvalues of the transfer matrices, we can use this condition of pole cancelation to obtain the Bethe equations without going through the algebraic Bethe ansatz procedure; see, for example, [72, 78, 81, 82]. For the $\mathfrak{su}(1,2)$ spin chain, we have the following transfer matrices in the anti-symmetric representations:

$$T_{\square}(u) = \mathrm{e}^{-\mathrm{i}\phi_2}\frac{Q_1\left(u-\frac{3\mathrm{i}}{4}\right)}{Q_1\left(u+\frac{\mathrm{i}}{4}\right)}\frac{Q_2\left(u+\frac{3\mathrm{i}}{4}\right)}{Q_2\left(u-\frac{\mathrm{i}}{4}\right)}\left(\frac{u-\frac{5\mathrm{i}}{4}}{u-\frac{3\mathrm{i}}{4}}\right)^L + \mathrm{e}^{-\mathrm{i}\phi_1}\frac{Q_1\left(u+\frac{5\mathrm{i}}{4}\right)}{Q_1\left(u+\frac{\mathrm{i}}{4}\right)}\left(\frac{u-\frac{5\mathrm{i}}{4}}{u-\frac{3\mathrm{i}}{4}}\right)^L + \mathrm{e}^{-\mathrm{i}\phi_3}\frac{Q_2\left(u-\frac{5\mathrm{i}}{4}\right)}{Q_2\left(u-\frac{\mathrm{i}}{4}\right)}\left(\frac{u-\frac{5\mathrm{i}}{4}}{u+\frac{\mathrm{i}}{4}}\right)^L, \tag{155}$$

$$T_{\begin{smallmatrix}\square\\\square\end{smallmatrix}}(u) = \bar{T}_{\square}(\bar{u})\left(\frac{u-\frac{5\mathrm{i}}{4}}{u+\frac{5\mathrm{i}}{4}}\right)^L, \qquad T_{\begin{smallmatrix}\square\\\square\\\square\end{smallmatrix}}(u) = \left(\frac{u-\frac{5\mathrm{i}}{4}}{u+\frac{5\mathrm{i}}{4}}\right)^L.$$

One can easily see that Bethe equations do follow from requiring analyticity of these transfer matrices.

In the previous section, it was shown and emphasized that the TQ Baxter relations are the most powerful method to extract finite size corrections to the scaling limit of Bethe equations.

In this section, we will use the transfer matrices presented above along with the fact that, due to Bethe equations, they are good analytical functions of u to find what are the finite size corrections to this nested Bethe ansatz. Since for generic (super) nested Bethe ansatz the transfer matrices in the several representations are known, this procedure can be easily generalized for other NBAs.

The key idea to find the finite size corrections to the NBA is to use the transfer matrices in the various representations to define a new set of quasi-momenta q_i as the solutions of an algebraic equation whose coefficients are these transfer matrices. For example, to leading order,

$$\begin{aligned} T_{\square}(u) &\simeq \mathrm{e}^{\mathrm{i}p_1} + \mathrm{e}^{\mathrm{i}p_2} + \mathrm{e}^{\mathrm{i}p_3},\\ T_{\begin{smallmatrix}\square\\\square\end{smallmatrix}}(u) &\simeq \mathrm{e}^{\mathrm{i}(p_1+p_2)} + \mathrm{e}^{\mathrm{i}(p_2+p_3)} + \mathrm{e}^{\mathrm{i}(p_3+p_1)},\\ T_{\begin{smallmatrix}\square\\\square\\\square\end{smallmatrix}}(u) &\simeq \mathrm{e}^{\mathrm{i}(p_1+p_2+p_3)}, \end{aligned}$$

so that if we define a set of *exact* quasi-momenta q_i by

$$T_{\begin{smallmatrix}\square\\\square\\\square\end{smallmatrix}}(u) - \mathrm{e}^{\mathrm{i}q}T_{\begin{smallmatrix}\square\\\square\end{smallmatrix}}(u)\left(1-\frac{L}{4u^2}\right) + \mathrm{e}^{2\mathrm{i}q}T_{\square}(u)\left(1-\frac{L}{4u^2}\right) - \mathrm{e}^{3\mathrm{i}q} = 0, \tag{156}$$

then, to leading order, $q_i \simeq p_i$. The factors we add in the definition of q_i look non-natural, but then are chosen to simplify the result. Note however that the coefficients in this equation have no singularities except some fixed poles close to $u = 0$. Thus, defined in this way, the quasi-momenta q_i constitute a four-sheet algebraic surface (modulo 2π ambiguities) such that

$$q_i - q_j = 2\pi n_{ij}^A, \qquad x \in \mathcal{C}_{ij}, \tag{157}$$

and, needless to say, this is an *exact* result in L; it is not a classical (scaling limit) leading result like (149). On the other hand, the expansion at large L of the above algebraic equation yields

$$\begin{aligned} q_1 &= p_1 + \frac{1}{2L}(+\cot_{12} + \cot_{13}) \\ q_2 &= p_2 + \frac{1}{2L}(-\cot_{21} + \cot_{23}) \\ q_3 &= p_3 + \frac{1}{2L}(-\cot_{31} - \cot_{32}), \end{aligned}$$

which follows from the expansion

$$\begin{aligned} T_{\square}(u)\left(1 - \frac{L}{4u^2}\right) &= \mathrm{e}^{\mathrm{i}p_1} + \mathrm{e}^{\mathrm{i}p_2} + \mathrm{e}^{\mathrm{i}p_3} - \frac{1}{4L}[\mathrm{e}^{\mathrm{i}p_1}(2p_1' - p_2' - p_3') \\ &\quad + \mathrm{e}^{\mathrm{i}p_2}(p_1' - p_3') + \mathrm{e}^{\mathrm{i}p_3}(p_1' + p_2' - 2p_3')] + \mathcal{O}\left(\frac{1}{L^2}\right) \\ T_{\begin{smallmatrix}\square\\\square\end{smallmatrix}}(u)\left(1 - \frac{L}{4u^2}\right) &= \mathrm{e}^{\mathrm{i}(p_1+p_2)} + \mathrm{e}^{\mathrm{i}(p_2+p_3)} + \mathrm{e}^{\mathrm{i}(p_3+p_1)} - \frac{1}{4L}[\mathrm{e}^{\mathrm{i}(p_1+p_2)}(p_1' + p_2' - 2p_3') \\ &\quad + \mathrm{e}^{\mathrm{i}(p_1+p_3)}(p_1' - p_3') + \mathrm{e}^{\mathrm{i}(p_2+p_3)}(2p_1' - p_2' - p_3')] + \mathcal{O}\left(\frac{1}{L^2}\right), \\ T_{\begin{smallmatrix}\square\\\square\\\square\end{smallmatrix}}(u) &= \mathrm{e}^{\mathrm{i}(p_1+p_2+p_3)} + \mathcal{O}\left(\frac{1}{L^2}\right) \end{aligned}$$

of the several transfer matrices. Then, to the first order in $1/L$ the exact equation (157) gives, for the quasi-momenta p_i introduced in (258),

$$p_2' - p_3' = 2\pi n_{23}^A - \frac{1}{L}\cot_{23}, \qquad x \in \mathcal{C}_{23}, \tag{158}$$

$$p_1' - p_3' = 2\pi n_{13}^A - \frac{1}{2L}(\cot_{12} + 2\cot_{13} + \cot_{32}), \qquad x \in \mathcal{C}_{13}, \tag{159}$$

where in (158) we use the fact that function $\cot_{31} - \cot_{21}$ vanishes under the slash on the cut $\mathcal{C}_{23}$ since

$$\cot_{ij}^{+} = \cot_{kj}^{-}, \qquad x \in \mathcal{C}_{ik}. \tag{160}$$

Equations (158) and (159) are the finite size corrections we aimed at.

Finally, q_2 must have no discontinuity at cut $\mathcal{C}_{13}$, and therefore

$$\Delta p_2 = 2\pi\mathrm{i}(\rho_1 - \rho_2) = \frac{1}{L}\left(\cot_{21}^{+} - \cot_{23}^{+}\right), \qquad x \in \mathcal{C}_{13}. \tag{161}$$

Thus, replacing the quasi-momenta p_i by its expressions in terms of resolvents (258) and relating the density of *auxiliary roots* ρ_1 to that of the *middle node* roots ρ_2 through (161), we recover precisely (153) and (154) as announced.

We would like to stress the efficiency of the TQ relations. We were able to find the *usual* cot contributions (coming from the expansion of the log's of Bethe equations when the Bethe roots are close to each other) plus the mismatch in densities of the different types of roots making the cuts of stacks using only the fact that due to Bethe equations, the transfer matrices in several representations were analytical functions of u. The computation done in this way is by far more economical than a brute force expansion of the Bethe equations.

Finally, let us make an important remark. To derive (154) from (159), one should use

$$\cot_{12} = -\frac{1}{2\pi\mathrm{i}}\int_{\mathcal{C}_{13}\cup\mathcal{C}_{23}} \frac{\Delta\cot_{12}}{x - y}\,\mathrm{d}y, \tag{162}$$

which is clearly a valid relation if $\cot_{12}$ has only branch cuts as singularities. For generic twists and for small enough cuts $\mathcal{C}_{13}$ and $\mathcal{C}_{23}$, this is the case. Indeed, in the absence of Bethe roots we have no cuts at all and thus $p_1 - p_2 = \phi_2 - \phi_1$. Suppose $\phi_2 - \phi_1 \neq 2\pi n$. Then, by continuity, when we slowly open some cuts $\mathcal{C}_{23}$ and $\mathcal{C}_{13}$, $p_1 - p_2$ will start taking positive values around $\phi_2 - \phi_1$ without ever being zero. Thus, if the cuts are small enough we will never get poles in $\cot_{12}$. In section 2.2.4, we will see that the stacks as described in [14] only exist when this assumption of absence of poles is right and are destroyed when $p_1 - p_2$ reaches $2\pi n$.

2.2.3. Rederivation using the bosonic duality in the scaling limit. In this section, let us rederive the mismatch formula (151) using the bosonic duality (163). Besides the obvious advantage for what concerns our comprehension of having a second derivation, there are systems for which Bethe equations are known but the algebraic formalism behind these equations is still not well developed (this is the case, for example, for the AdS/CFT Bethe equations proposed by Beisert and Staudacher which we will study in section 4.2).

Denoting

$$u_{1,i} = u_{2,i} - \epsilon_i, \qquad \tilde{u}_{1,i} = u_{2,i} - \tilde{\epsilon}_i, \qquad \epsilon \sim 1,$$

and expanding the bosonic duality (163) in the scaling limit ($L \to \infty$), we get

$$\sin(\tau/2) = \sin\left(\frac{1}{2}(\tilde{G}_1 - G_1 + \tau)\right) \exp\left(\sum_{i=1}^{K_1} \frac{\epsilon_i}{u - u_i^1} + \sum_{i=1}^{\tilde{K}_1} \frac{\tilde{\epsilon}_i}{u - u_i^1}\right),$$

where $\tau = \phi_1 - \phi_2$. Taking the logarithm of this equation and differentiating with respect to u, we get

$$\sum \frac{\epsilon_i}{\left(u - u_i^1\right)^2} + \sum \frac{\tilde{\epsilon}_i}{\left(u - u_i^1\right)^2} = \frac{\tilde{G}_1' - G_1'}{2L} \cot \frac{\tilde{G}_1 - G_1 + \tau}{2}$$

where we note that the left-hand side is precisely the difference of resolvents $G_2 - G_1 - \tilde{G}_1$. Thus, we find

$$G_2 - G_1 - \tilde{G}_1 = \frac{\tilde{G}_1' - G_1'}{2L} \cot \frac{\tilde{G}_1 - G_1 + \tau}{2} \simeq \frac{G_2' - 2G_1'}{2L} \cot \frac{G_2 - 2G_1 + \tau}{2} = \frac{1}{L} \cot_{12}.$$

Finally, by computing the discontinuity of this expression at cuts $\mathcal{C}_{13}$ we will get the *mismatch* the densities of the roots in a cut of stacks[17]

$$\rho_1 - \rho_2 = \frac{\Delta \cot_{12}}{2\pi i L} = \frac{\cot_{21}^+ - \cot_{23}^+}{2\pi i L},$$

which was the gap in the chain of arguments presented in the beginning of section 2.2.1 and leading to (153).

Finally, let us show that the bosonic duality amounts to a simple exchange of Riemann sheets in the scaling limit. Consider, for example,

$$\tilde{p}_1 = -\frac{1}{2x} + \tilde{G}_1 - \tilde{\phi}_1 = -\frac{1}{2x} + G_2 - G_1 - \tilde{\phi}_1 = p_2$$

since, as we will see more carefully in the following section, $\tilde{\phi}_{1,2} = \phi_{2,1}$.

[17] $\Delta f = f^+ - f^-$, so that $\rho = -\frac{\Delta G}{2\pi i}$.

2.2.4. More about bosonic duality. In this section, we will explain some details behind the bosonic duality (148) mentioned in section 2.2. There are two main steps to be considered. On one hand, we have to prove that for a set of K_2 generic complex numbers u_2 and K_1 roots u_1 obeying the auxiliary Bethe equations (140) it is possible to write ($\tau = \phi_1 - \phi_2$):

$$2\mathrm{i}\sin(\tau/2)\, Q_2(u) = \mathrm{e}^{\mathrm{i}\tau/2} Q_1(u-\mathrm{i}/2)\tilde{Q}_1(u+\mathrm{i}/2) - \mathrm{e}^{-\mathrm{i}\tau/2} Q_1(u+\mathrm{i}/2)\tilde{Q}_1(u-\mathrm{i}/2), \quad (163)$$

and that, in doing so, we define the position of a new set of numbers $\tilde{u}_1$. *A priori* this is not at all a trivial statement because we have a polynomial of degree K_2 on the left whereas on the right-hand side we have only $K_2 - K_1$ parameters to fix. However, as we will see, if K_1 equations (140) are satisfied it is possible to write $Q_2(u)$ in this form. This will be the subject of section 2.2.4.

Assuming (163) to be proved, we can use this relation to show that in the original Bethe equations we can replace roots u_1 by new roots $\tilde{u}_1$ with the simultaneous exchange $\phi_1 \leftrightarrow \phi_2$. Indeed if we evaluate the duality at $u = u_{2,j}$, we find

$$\frac{Q_1(u_{2,j}-\mathrm{i}/2)}{Q_1(u_{2,j}+\mathrm{i}/2)} = \mathrm{e}^{\mathrm{i}(\phi_2-\phi_1)}\frac{\tilde{Q}_1(u_{2,j}-\mathrm{i}/2)}{\tilde{Q}_1(u_{2,j}+\mathrm{i}/2)},$$

meaning that in equation (141) for the u_2 roots we can replace roots u_1 by the dual roots $\tilde{u}_1$ provided we replace $\phi_1 \leftrightarrow \phi_2$. Moreover if we take $u = \tilde{u}_{1,j} \pm \mathrm{i}/2$, we will get

$$\mathrm{e}^{\mathrm{i}\phi_2 - \mathrm{i}\phi_1} = -\frac{\tilde{Q}_1(\tilde{u}_1+\mathrm{i})}{\tilde{Q}_1(\tilde{u}_1-\mathrm{i})}\frac{Q_2(\tilde{u}_1-\mathrm{i}/2)}{Q_2(\tilde{u}_1+\mathrm{i}/2)},$$

which we recognize as equation (140) with $K_2 - K_1$ roots $\tilde{u}_1$ in place of the K_1 original roots u_1 and with $\phi_1 \leftrightarrow \phi_2$. Finally evaluating (163) at $u = u_{1,j} \pm \mathrm{i}/2$, we will get the original equation (140) so that we see that it must be satisfied in order for equation (163) to be valid.

In section 2.2.4, we will also see that the transfer matrices are invariant under the bosonic duality accompanied by an appropriate reshuffling of phases ϕ_a. In section 2.2.5, some curious examples of dual states will be given.

Decomposition proof. In this section, we shall prove that one can always decompose $Q_2(u)$ as in (163) and that this decomposition uniquely fixes the position of the new set of roots $\tilde{u}_1$. In other words, let us show that we can set the polynomial

$$P(u) \equiv \mathrm{e}^{+\mathrm{i}\frac{\tau}{2}} Q_1(u-\mathrm{i}/2)\tilde{Q}_1(u+\mathrm{i}/2) - \mathrm{e}^{-\mathrm{i}\frac{\tau}{2}} Q_1(u+\mathrm{i}/2)\tilde{Q}_1(u-\mathrm{i}/2) - 2\mathrm{i}\sin\frac{\tau}{2} Q_2(u)$$

to zero through a unique choice of the dual roots $\tilde{u}_1$.

- First, consider the case $K_1 = 0$. Then it is trivial to see that we can always find a unique polynomial $\tilde{Q}_1 = u^{K_2} + \sum_{n=1}^{K_2} a_n u^{n-1}$ such that

  $$\mathrm{e}^{+\mathrm{i}\frac{\tau}{2}}\tilde{Q}_1(u+\mathrm{i}/2) - \mathrm{e}^{-\mathrm{i}\frac{\tau}{2}}\tilde{Q}_1(u-\mathrm{i}/2) = 2\mathrm{i}\sin\frac{\tau}{2} Q_2(u)$$

  because this amounts to solving K_2 linear equations for K_2 coefficients a_n with a non-degenerate triangular matrix.
- Next, let us consider $K_1 \leqslant K_2/2$. First, we choose $\tilde{Q}_1$ to satisfy K_1 equations

  $$\tilde{Q}_1\big(u_p^1\big) = 2\mathrm{i}\mathrm{e}^{-\mathrm{i}\frac{\tau}{2}}\sin\frac{\tau}{2}\frac{Q_2\big(u_p^1-\mathrm{i}/2\big)}{Q_1\big(u_p^1-\mathrm{i}\big)} \equiv c_p, \qquad p = 1,\dots,K_1;$$

  these conditions will define $\tilde{Q}_1(u)$ up to a homogeneous solution proportional to $Q_1(u)$:

  $$\tilde{Q}_1(u) = Q_1(u)\tilde{q}_1(u) + \sum_{p=1}^{K_1}\frac{Q_1(u)}{Q_1'\big(u_p^1\big)\big(u-u_p^1\big)}c_p,$$

where $\tilde{q}_1(u)$ is some polynomial of degree $K_2 - 2K_1$. Now from (140) we note that with this choice of $\tilde{Q}_1$, we have

$$\frac{P\big(u_p^1 + \mathrm{i}/2\big)}{Q_2\big(u_p^1 + \mathrm{i}/2\big)} = \frac{P\big(u_p^1 - \mathrm{i}/2\big)}{Q_2\big(u_p^1 - \mathrm{i}/2\big)} = 0, \qquad p = 1, \ldots, K_3,$$

and thus

$$P(u) = Q_1(u + \mathrm{i}/2)\, Q_1(u - \mathrm{i}/2)\, p(u),$$

where

$$p(u) = \mathrm{e}^{\mathrm{i}\frac{\tau}{2}} \tilde{q}_1(u + \mathrm{i}/2) - \mathrm{e}^{-\mathrm{i}\frac{\tau}{2}} \tilde{q}_1(u - \mathrm{i}/2) - 2\mathrm{i} \sin \frac{\tau}{2} q_2(u)$$

and q_2 is a polynomial. Thus, we are left to the same problem as above where $K_1 = 0$. For completeness, let us note that we can write $q_2(u)$ explicitly in terms of the original roots u_1 and u_2:

$$q_2(u) = \frac{Q_2(u)}{Q_1(u + \mathrm{i}/2) Q_1(u - \mathrm{i}/2)} - \text{poles},$$

where the last term is a simple collection of poles at $u = u_p^1 \pm \mathrm{i}/2$ whose residues are such that $q_2(u)$ is indeed a polynomial.

- We can see that the number of the solutions of (140) with $K_1 = K$ and $K_1 = K_2 - K$ is the same (see [63] for examples of states counting). Thus for each solution with $K_1 \geqslant K_2/2$, we can always find one dual solution with $K_1 \leqslant K_2/2$ and in this way we prove our statement for $K_1 \geqslant K_2/2$.
- Finally, let us stress the uniqueness of $\tilde{Q}_1$. If $K_1 > \tilde{K}_1$, we have nothing to show since we saw explicitly above how the bosonic duality constrains uniquely the dual polynomial $\tilde{Q}_1$. Let us then consider $K_1 < \tilde{K}_1$ and assume that we have two different solutions $\tilde{Q}_1^1$ and $\tilde{Q}_1^2$. Then from the duality relation (163) for either solution, we find

$$\begin{aligned}\mathrm{e}^{\mathrm{i}\frac{\tau}{2}} Q_1(u - \mathrm{i}/2) \big(\tilde{Q}_1^1(u + \mathrm{i}/2) - \tilde{Q}_1^2(u + \mathrm{i}/2)\big) \\ = \mathrm{e}^{-\mathrm{i}\frac{\tau}{2}} Q_1(u + \mathrm{i}/2) \big(\tilde{Q}_1^1(u - \mathrm{i}/2) - \tilde{Q}_1^2(u - \mathrm{i}/2)\big).\end{aligned}$$

Evaluating this expression at $u = u_{1,j} + \mathrm{i}/2$, we find that $\tilde{Q}_1^1(u_{1,j}) - \tilde{Q}_1^2(u_{1,j}) = 0$ so that $\tilde{Q}_1^1(u_1) - \tilde{Q}_1^2(u_1) = Q_1(u)h(u)$ and therefore

$$\mathrm{e}^{\mathrm{i}\frac{\tau}{2}} h(u + \mathrm{i}/2) = \mathrm{e}^{-\mathrm{i}\frac{\tau}{2}} h(u - \mathrm{i}/2),$$

which is clearly impossible for polynomial $h(u)$—for large u, we can neglect $i/2$'s to obtain $\mathrm{e}^{\mathrm{i}\tau} = 1$ thus leading to a contradiction.

Transfer matrix invariance under the bosonic duality. In this section, we will examine the transformation properties of the transfer matrices under the bosonic duality. In appendix A, we consider this problem for the general $\mathfrak{su}(N|M)$ group. For now, let us just take $T_{\square}$ for $\mathfrak{su}(1, 2)$ from (155). Using (163), we can express ratios of Q_1's through $\tilde{Q}_1$ and Q_2 so that

$$\begin{aligned}T_{\square}(u) = \mathrm{e}^{-\mathrm{i}\phi_2} \left(+ \frac{2\mathrm{i} \sin\frac{\tau}{2}\, \mathrm{e}^{-\mathrm{i}\frac{\tau}{2}}\, Q_2\big(u - \frac{\mathrm{i}}{4}\big)}{Q_1\big(u + \frac{\mathrm{i}}{4}\big) \tilde{Q}_1\big(u + \frac{\mathrm{i}}{4}\big)} + \mathrm{e}^{-\mathrm{i}\tau} \frac{\tilde{Q}_1\big(u - \frac{3\mathrm{i}}{4}\big)}{\tilde{Q}_1\big(u + \frac{\mathrm{i}}{4}\big)} \right) \frac{Q_2\big(u + \frac{3\mathrm{i}}{4}\big)}{Q_2\big(u - \frac{\mathrm{i}}{4}\big)} \left(\frac{u - \frac{5\mathrm{i}}{4}}{u - \frac{3\mathrm{i}}{4}} \right)^L \\ + \mathrm{e}^{-\mathrm{i}\phi_1} \left(- \frac{2\mathrm{i} \sin\frac{\tau}{2}\, \mathrm{e}^{+\mathrm{i}\frac{\tau}{2}}\, Q_2\big(u + \frac{3\mathrm{i}}{4}\big)}{Q_1\big(u + \frac{\mathrm{i}}{4}\big) \tilde{Q}_1\big(u + \frac{\mathrm{i}}{4}\big)} + \mathrm{e}^{+\mathrm{i}\tau} \frac{\tilde{Q}_1\big(u + \frac{5\mathrm{i}}{4}\big)}{\tilde{Q}_1\big(u + \frac{\mathrm{i}}{4}\big)} \right) \left(\frac{u - \frac{5\mathrm{i}}{4}}{u - \frac{3\mathrm{i}}{4}} \right)^L \\ + \mathrm{e}^{-\mathrm{i}\phi_3} \frac{Q_2\big(u - \frac{5\mathrm{i}}{4}\big)}{Q_2\big(u - \frac{\mathrm{i}}{4}\big)} \left(\frac{u - \frac{5\mathrm{i}}{4}}{u + \frac{\mathrm{i}}{4}} \right)^L.\end{aligned}$$

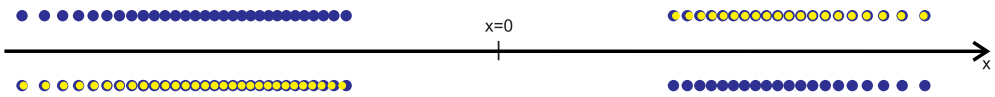

Figure 10. The upper and the lower configurations of Bethe roots are dual to one another. The big blue dots are middle node roots u_2 and the yellow dots are auxiliary roots u_1. The formation of the cuts of stacks is manifest for this situation where the twists are large (like $\pi/2$) and the filling fractions are small.

We see that for $\tau = \phi_1 - \phi_2$, the terms with $\sin\frac{\tau}{2}$ cancel and we get the old expression for $T_\square$ with u_1 replaced by $\tilde{u}_1$ and $\phi_1 \leftrightarrow \phi_2$.

This simple transformation property of the transfer matrices automatically implies that the Riemann surface defined by the algebraic equation (156) is untouched under the duality transformation (to all orders in L), so that the duality can cause at most some reshuffling of the sheets. However, as we will see in the following section, the sheets are not necessarily exchanged as a whole—this operation will be in general done in a piecewise manner.

2.2.5. Examples of the dual configurations. In this section, we will study some curious Bethe root distributions for the twisted $\mathfrak{su}(1,2)$ spin chain described by the nested Bethe equations (140) and (141) and for the usual $\mathfrak{su}(2)$ Heisenberg chain,

$$\left(\frac{u_{1,j}+\frac{\mathrm{i}}{2}}{u_{1,j}-\frac{\mathrm{i}}{2}}\right)^L = -\frac{Q_1(u_{1,j}+\mathrm{i})}{Q_1(u_{1,j}-\mathrm{i})}. \tag{164}$$

Using the first example, we shall understand the importance of twists to stabilize big cuts of stacks like those depicted in figures 7(*a*) and (*b*) and explain how the stacks get destroyed as we decrease the twists.

We can dualize $\mathfrak{su}(2)$ solutions of the twisted[18] Heisenberg ring using the same duality (148) as before with $Q_2(u) \to u^L$. We will consider the dual solutions to the vacuum and to a one-cut solution for the Heisenberg spin chain (164).

Big enough twists, small enough fillings and zippers. In the previous sections, we saw that the introduction of twists in the NBA equations are needed to have a configuration with auxiliary roots u_1 close to some momentum-carrying roots u_2. In figure 10, we have two numerical solutions of Bethe equations which are related by the bosonic duality. In either of them, we see a configuration of Bethe roots with a simple cut with middle roots only (in blue) and a cut of stacks (containing blue and yellow roots). In this situation, it is clearly reasonable to think of stacks as bound states of different types of roots and we see that they indeed condense into *multicolor* cuts.

We will examine what happens when we decrease the twists (or increase filling fractions, which is the same qualitatively). For simplicity we consider the configuration, dual to the simple one-cut solution ($K_2 = K$ and $K_1 = 0$) with no twist for the middle node roots, $\phi_2 - \phi_3 = 0$, and some generic twist $\phi_1 - \phi_2 = \tau$ for the auxiliary roots. Bosonic duality will leave untouched middle node roots u_2 and create K new axillary roots u_1.

In the upper left corner of figure 11, we applied the duality for some big twist $\tau = 4.6$ while in the bottom right corner of the same figure we have a configuration of Bethe roots with some small twist $\tau = 0.2$. In the latter case, the auxiliary (yellow) roots clearly do *not*

[18] For zero twist, the duality becomes degenerate and we will see below that it needs to be slightly modified.

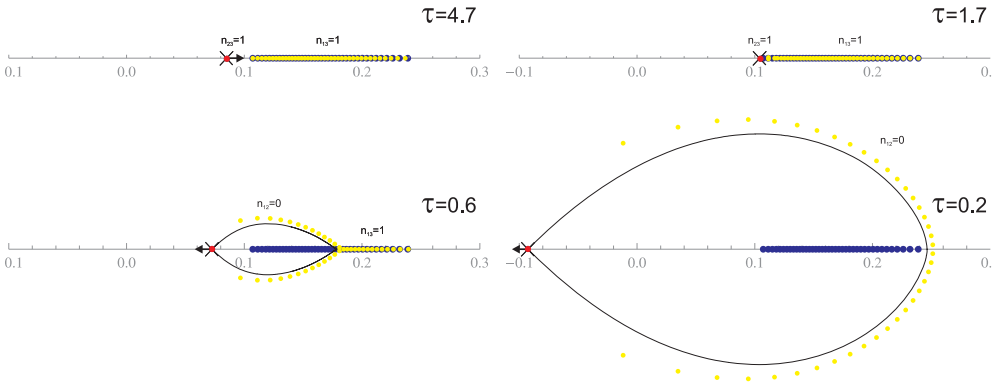

Figure 11. Disintegration of the stack configuration. When the twist is large (the top left corner), the auxiliary roots form bound states together with the middle node ones and constitute a cut of stacks. As we decrease the twist fluctuation $n_{23} = 1$ (the red crossed dot) enters the cut of stacks (the top right corner) and subsequently partly *disintegrates* the cut of stacks forming some zipper-like configuration (the bottom left corner). At some very small value of the twist, the configuration of Bethe roots bears no resemblance to a cut of stacks.

form stacks together with the middle node (blue) roots! rather they form a bubble, containing the original cut of roots u_2.

To understand what happens in the scaling limit consider the position of $n_{23} = 1$ fluctuation, given by (206), which would be a small infinitesimal cut between p_2 and p_3. In figure 11, the position of this virtual fluctuation is marked by a red crossed dot. When the twist is big enough (and the filling fraction is small enough), the fluctuation is to the left from the cut. When we start decreasing the twist the fluctuation approaches the cut (upper right picture on fig 11), and at this point we have at the same time

$$p_2(x_n) - p_3(x_n) = 2\pi$$

and

$$p_1(x_n) - p_3(x_n) = 2\pi,$$

which implies $p_1 - p_2 = 0$ so that equation (162) becomes wrong at this point. When we continue decreasing the twist, the fluctuation passes through the cut and becomes a $n_{12} = 0$ fluctuation. If we think of the fluctuation as being a small cut along the real axis, we see that density becomes negative after crossing the cut:

$$0 < \rho_{23}^{\text{fluc}} = -\frac{\Delta(p_2 - p_3)}{4\pi \mathrm{i}} = -\frac{\Delta(-p_1 - p_2)}{4\pi \mathrm{i}} = -\rho_{12}^{\text{fluc}}.$$

This means that two branch points of the infinitesimal cut should not be connected directly, but rather by some macroscopical curve with real positive density! This curve $z(t)$ can be calculated from the equation $\rho(z)\,\mathrm{d}z \in \mathbb{R}^+$ or

$$\frac{p_1(z) - p_2(z)}{2\pi \mathrm{i}} \partial_t z = \pm 1,$$

and the resulting curve is plotted in black on the two pictures given in the bottom in figure 11. This is very similar to what happens when a fluctuation passes through the one-cut $\mathfrak{su}(2)$ configuration [83]. In the scaling limit, the black curve corresponds to the cut connecting p_1 and p_2 like in figure 12.

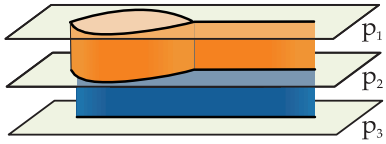

Figure 12. In the scaling limit, the algebraic curves for e^{ip_j} are the same before the duality (blue cut only) and after the duality (when the auxiliary roots are created). The duality causes an interchange of the sheets outside the bubble, while keeping the order untouched inside. This follows from the need of a positive density for the 'virtual' cut. In other words, the duality indeed only interchanges the sheets of the Riemann surface although it interchanges them in a piecewise way.

At first sight, these figures seem to be defying our previous results. Indeed, we checked in the previous section that the transfer matrices themselves are invariant under the bosonic duality. Thus, the algebraic curves obtained from (156) should be the same after and before duality and thus what one naturally expects is a simple interchange of Riemann sheets $p_1 \leftrightarrow p_2$ under the duality transformation. What really happens is a bit more tricky. The quasi-momenta are indeed only exchanged but this exchange operation is done in a piecewise manner. That is, if we denote the new quasi-momenta by p_i^{new} and the old ones by p_i^{old} and if we denote the bubble in figure 12 by $\mathcal{R}$, then we have

$$p_1^{\text{new}} = \begin{cases} p_2^{\text{old}} & \text{outside } \mathcal{R} \\ p_1^{\text{old}} & \text{inside } \mathcal{R}, \end{cases} \qquad p_2^{\text{new}} = \begin{cases} p_1^{\text{old}} & \text{outside } \mathcal{R} \\ p_2^{\text{old}} & \text{inside } \mathcal{R}, \end{cases} \qquad p_3^{\text{new}} = p_3^{\text{old}},$$

where the border of region $\mathcal{R}$ can be precisely determined in the scaling limit as explained above.

Dualizing momentum-carrying roots. In this section, we will consider an example of the application of the bosonic duality to the Heisenberg magnet[19]. The duality (148) can be applied to the roots u_1 obeying (164) provided we replace $Q_2(u) \to u^L$. In fact if we want to strictly consider the zero twist, we need a new duality because that one is clearly degenerate in this limiting case. The proper modified expression is in this case

$$\mathrm{i}(\tilde{K}_1 - K_1)u^L = Q_1(u - \mathrm{i}/2)\tilde{Q}_1(u + \mathrm{i}/2) - Q_1(u + \mathrm{i}/2)\tilde{Q}_1(u - \mathrm{i}/2),$$

and now the number of dual roots is $L - K_1 + 1$. In contrast to what happened with non-zero twists, here, the dual solution is not unique. Indeed if $\tilde{K}_1 > K_1$, we can as well use

$$\tilde{Q}_1^{\alpha} \equiv \alpha Q_1 + \tilde{Q}_1. \tag{165}$$

All these solutions, parameterized by the constant α, have the same charges because the transfer matrix is invariant under this transformation—see appendix A. Note that if initially we have a physical state with $K_1 < L/2$ roots, then all dual states (165) are unphysical with $\tilde{K}_1 > L/2$ violating the half-filling condition. Still, it is interesting, at the level of Bethe equations, to understand how these solutions look like. First, let us single out a particular $\tilde{Q}_1$ out of the various solutions to (165) so that

$$\tilde{Q}_1^{\alpha} = u^{\tilde{K}_1} + \sum_{l=0}^{\tilde{K}_1 - 1} c_l^{\alpha} u^l \tag{166}$$

[19] This section is benefitted a lot from the insightful discussions with T Bargheer and N Beisert whom we should thank.

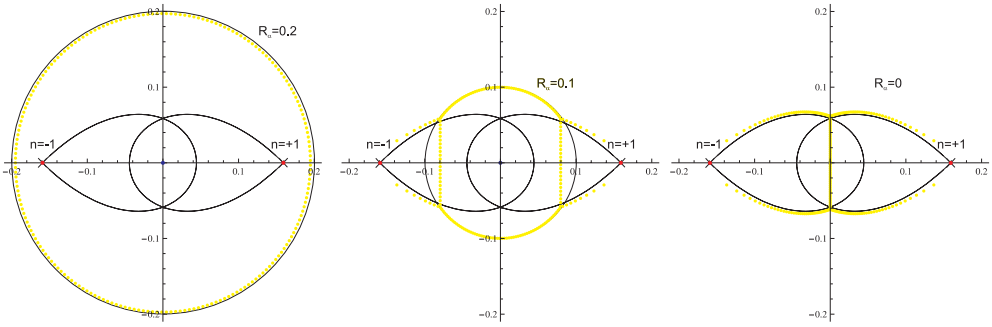

Figure 13. Three configurations of Bethe roots dual to the ferromagnetic vacuum of the untwisted Heisenberg spin chain. For each physical solution (below half filling) of the Bethe equations, there is a one-parameter (α) family of dual unphysical solutions. To the left, α is large and the roots distribute themselves along a circle with radius R_α given by $(R_\alpha L)^L = \alpha$. Decreasing α, the circle will touch the fluctuations $n = \pm 1$. Similar to the previous section, the virtual infinitesimal cuts become macroscopical bubble cuts with cusps at the position of the fluctuations. The intersection points of the new cuts with the circle are connected by condensates, which are logarithmic cuts on the algebraic curve [83].

becomes well defined through (165). We chose $\tilde{Q}_1 = \tilde{Q}_1^0$ to be the dual solution with $c_0^0 = 0$.

Consider for example the vacuum state for which $Q_1 = 1$. Let us first take α to be very large so that we can write

$$\alpha + \tilde{Q}_1^0 \simeq \alpha + (xL)^L. \tag{167}$$

We see that for large α, the dual roots will be on a circle of radius $\frac{|\alpha|^{1/L}}{L}$. The corresponding configuration is present on the first picture in figure 13. In this figure, we also plotted a circle with this radius and one can see that the Bethe roots belong perfectly to the circle.

Let us now understand this configuration from the algebraic curve point of view. The quasi-momenta $p_1 = -p_2 \equiv p = \frac{1}{2x} - G$, in the absence of Bethe roots, are simply given by $p = \frac{1}{2x}$. Let us find the curves with positive densities and mode number $n = 0$. The density is given by $\rho(x) = \frac{1}{2\pi \mathrm{i}} \frac{1}{x}$ and we have to find the curves where $\rho(x)\,\mathrm{d}x$ is real. It is easy to see that the only possibility is the circle centered at the origin with an arbitrary radius. From the above arguments, one can expect that for any α the roots will belong to some circle. However, we analyzed only the curves with the zero mode number and as we see in figure 13 for smaller α's the circle develops four tails and two vertical lines. Along these vertical lines, the roots are separated by i (for $L \to \infty$) forming the so-called *condensates* or *Bethe strings*. The tails meet at the points where the virtual fluctuation is, and the corresponding curves are given by

$$\frac{p(z) \pm \pi}{\pi \mathrm{i}} \partial_t z = \pm 1 \tag{168}$$

analogous to the previous section. In the last configuration, in figure 13, the circle is completely absent. There are only two $n = \pm 1$ curves which, at the interceptions, become a 4π jump log condensate with the Bethe roots separated by $i/2$.

We also built dual configurations to the one-cut solution (see figure 14). The situation is similar to the vacuum, the only difference being that two tails (out of four) do not tend to touch each other, but rather end at the branch points of the initial cut.

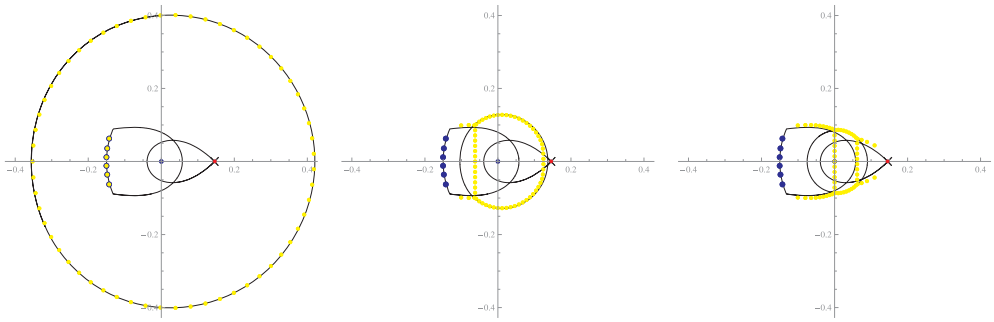

Figure 14. Dual configuration to a one-cut solution. Similar to the previous example for large α, the dual roots are distributed along the big circle and cut (first picture). When α decreases and the circle crosses the cut, we have to choose another curve with a positive density (second and third pictures).

3. Quasi-classical quantization and fluctuations

3.1. Preface

In this section, we will study the semi-classical quantization of the $AdS_5 \times S^5$ Metsaev–Tseytlin superstring [9]. We will see that the semi-classical quantization of this very nontrivial field theory is not conceptually much difficult than the one-dimensional non-relativistic particle in a smooth potential. Let us consider this very instructive example.

In terms of the quasi-momenta

$$p(x) \equiv \frac{\hbar}{\mathrm{i}} \frac{\psi'(x)}{\psi(x)}, \tag{169}$$

the Schrödinger equation for the wavefunction ψ takes the Riccati form

$$p^2 - \mathrm{i}\hbar p' = 2m\,(E - V)\,. \tag{170}$$

What do we know about $p(x)$? It is an analytical function which has, by definition (169), a pole with residue

$$\alpha = \frac{\hbar}{\mathrm{i}} \tag{171}$$

at each of the zeros of the wavefunction. For the Nth excited state, we will have N poles. On the other hand, for very excited states, the right-hand side in (170) is much larger than $\hbar$ and

$$p \simeq p_{\mathrm{cl}} \equiv \sqrt{2m\,(E - V)}$$

now describes a two-sheet Riemann surface. What happened was that, as $N \to \infty$, the poles in $p(x)$ started to be denser and denser, condensing in a square root cut. Thus, in the semi-classical limit, we retrieve the Bohr–Sommerfeld quantization

$$\frac{1}{2\pi\hbar} \oint_{\mathcal{C}} p_{\mathrm{cl}}(z)\,\mathrm{d}z \simeq \frac{1}{2\pi\hbar} \oint_{\mathcal{C}} p(z)\,\mathrm{d}z = N, \tag{172}$$

where $\mathcal{C}$ encircles the cut. The first integral is precisely the action variable of the classical motion.

When we consider more degrees of freedom, in particular when we move to higher dimensions, let us say two, the situation is not just a little worse. Indeed, we have no proper *generic* recipe, except from lattice calculations, to extract the quantum spectrum, or a part

of it, of an interacting quantum field theory. However, if we are lucky, it might happen that the theory is integrable. If it is the case, we can identify the action variables, apply the Bohr–Sommerfeld condition and find the quasi-classical spectrum of the theory.

For a wide class of two-dimensional sigma models, this happens to be the case and the procedure is known explicitly. The central object is a collection of quasi-momenta, $p_i(x)$, whose derivative defines a many-sheet Riemann surface. These sheets can be connected by several cuts, with each of which we can associate a *filling fraction* by integrating the quasi-momenta around the cut as in (172). These are the action variables of the theory. Grosso modo, these filling fractions measure the size of the cut. Finally, when going through these cuts the quasi-momenta can jump by $2\pi n$ with n being an integer labeling the cut.

The superstring on the $AdS_5 \times S^5$ background falls into this class of theories—the model is known to be classically integrable [8, 84], as we showed in section 1. The algebraic curve was built [14], and thus one can try to quasi-classically quantize the string. In the string language, when we choose which Riemann sheets we connect by a cut, we choose which string polarization, i.e. which degree of freedom, to excite. The number n and the filling fraction associated with the cut are in strict analogy with the mode number and the amplitude of a Fourier mode in a free theory such as the string in a flat space [14].

Going back to our simple example, we can see that the existence of such discrete equations is indeed highly natural. For this purpose let us consider a simple harmonic oscillator, $V = \frac{m\omega^2 x^2}{2}$. From (170), it follows that $p(x) = \mathrm{i}m\omega x + \mathcal{O}(1/x)$. Since the quasi-momentum is a meromorphic function with N poles on the real axis, it must be given by

$$p(x) = \mathrm{i}m\omega x + \frac{\hbar}{\mathrm{i}} \sum_{i=1}^{N} \frac{1}{x - x_i}.$$

Then, from the large x behavior in (170) we immediately read

$$E = \hbar\omega \left(N + \tfrac{1}{2}\right)$$

while from the cancelation of each of the x_i poles in the same equation we get[20]

$$x_i = \frac{\hbar}{2\omega m} \sum_{j \neq i}^{N} \frac{1}{x_i - x_j}, \tag{173}$$

which strongly resembles the equations one finds in the Bethe ansatz context.

When we expand the superstring action around some classical solution, characterized by some conserved charges, we obtain, for the oscillations, a quadratic Lagrangian whose quantization yields, for the semi-classical spectrum,

$$E = E_{\mathrm{cl}} + \sum_{A,n} N_{A,n} \mathcal{E}_{A,n}, \tag{174}$$

where we have dropped the zero energy excitation and denoted the number of quanta with energy $\mathcal{E}_{A,n}$ by $N_{A,n}$. The subscript A labels the several possible string polarizations we can excite while the mode number n is the Fourier mode of the quantum fluctuation. In this paper, we shall address the question of finding this quasi-classical spectrum for the $AdS_5 \times S^5$ superstring using the algebraic curve mentioned above.

Let us explain the idea behind the computation. There are basically two main steps involved. First, we construct the curve associated with the classical solution around which we want to consider the quantum fluctuations following the procedure explained in section 1. The second step consists of considering the small excitations around this classical solution in

[20] Its solution is given by the zeros of the Hermite polynomials, $H_N\left(\sqrt{\frac{2m\omega}{\hbar}} x_i\right) = 0$.

the spirit of [57]. In terms of the algebraic curve, this means adding some microscopic cuts to this Riemann surface. By microscopic cuts we mean some finite number of poles, just like in the simple example (171). Then, by construction, the energy of the perturbed configuration is quantized as in (174).

As an application of this method we compute the fluctuation frequencies around the circular $\mathfrak{su}(2)$ and $\mathfrak{sl}(2)$ string. These solutions belong to a family of circular solutions whose quasi-momenta we will compute explicitly in appendix B. The frequencies we compute in this way were obtained in [85, 86] and [87, 88] by direct analysis of the expanded Lagrangian around these solutions in the Metsaev–Tseytlin GS superstring action.

3.2. Circular string solutions

In this section, we will write down an important class of rigid circular strings studied in [87]. As we will explain below, they are particularly simple from the algebraic curve point of view and will therefore provide us an excellent playground to check our method for some simple choice of parameters. In terms of the AdS_5 and S^5 embedding coordinates, we can represent this general class of string solutions with global charges $E = \sqrt{\lambda}\mathcal{E}$, $J_1 = \sqrt{\lambda}\mathcal{J}_1, \ldots$, as [87]

$$\begin{aligned}
u_2 + \mathrm{i}u_1 &= \sqrt{\frac{\mathcal{J}_3}{w_3}}\,\mathrm{e}^{\mathrm{i}(w_3\tau + m_3\sigma)}, & v_2 + \mathrm{i}v_1 &= \sqrt{\frac{\mathcal{S}_2}{\mathrm{w}_2}}\,\mathrm{e}^{\mathrm{i}(\mathrm{w}_2\tau + k_2\sigma)},\\
u_4 + \mathrm{i}u_3 &= \sqrt{\frac{\mathcal{J}_2}{w_2}}\,\mathrm{e}^{\mathrm{i}(w_2\tau + m_2\sigma)}, & v_4 + \mathrm{i}v_3 &= \sqrt{\frac{\mathcal{S}_1}{\mathrm{w}_1}}\,\mathrm{e}^{\mathrm{i}(\mathrm{w}_1\tau + k_1\sigma)},\\
u_6 + \mathrm{i}u_5 &= \sqrt{\frac{\mathcal{J}_1}{w_1}}\,\mathrm{e}^{\mathrm{i}(w_1\tau + m_1\sigma)}, & v_6 + \mathrm{i}v_5 &= \sqrt{\frac{\mathcal{E}}{\kappa}}\,\mathrm{e}^{\mathrm{i}\kappa\tau},
\end{aligned} \tag{175}$$

where the equations of motion and Virasoro constraints impose

$$\begin{aligned}
&1 = \sum_{i=1}^{3}\frac{\mathcal{J}_i}{w_i}, \qquad 1 = \frac{\mathcal{E}}{\kappa} - \sum_{j=1}^{2}\frac{\mathcal{S}_j}{\mathrm{w}_j}, \qquad 0 = \sum_{j=1}^{2} k_j\mathcal{S}_j + \sum_{i=1}^{3} m_i\mathcal{J}_i,\\
&\mathrm{w}_j^2 = \kappa^2 + k_j^2, \qquad \kappa^2 = \sum_{j=1}^{2}\mathcal{S}_j\frac{2k_j^2}{\mathrm{w}_j} + \sum_{i=1}^{3}\mathcal{J}_i\frac{w_i^2 + m_i^2}{w_i},\\
&w_i^2 = \nu^2 + m_i^2, \qquad \nu^2 \equiv \sum_{i=1}^{3}\mathcal{J}_i\frac{w_i^2 - m_i^2}{w_i}.
\end{aligned} \tag{176}$$

As explained in appendix B, for this family of solutions the representative g can be written as

$$g = \mathrm{e}^{\varphi_\sigma\sigma + \varphi_\tau\tau}\cdot g_0,$$

where $\varphi_{\sigma,\tau}$ are linear combinations of Cartan generators and g_0 is a constant matrix. Then we see that the current

$$J = -g^{-1}\,\mathrm{d}g$$

and therefore also the flat connection $A(x)$ in (9) are constant matrices! Then the computation of the path order exponential (10) is trivial and the quasi-momenta $p(x)$ are simply obtained from the eigenvalues of $\frac{2\pi}{\mathrm{i}}A(x)$. For a detailed account, see appendix B.

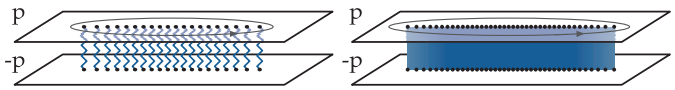

Figure 15. Analytical structure of the quasi-momenta $p(x)$ of a one-dimensional system. Left: for low-lying states, $p(x)$ is a collection of poles. Right: for high energy states, the poles condense into a square root branch cut.

3.3. Frequencies from the algebraic curve

In this section, we will consider the quasi-classical quantization of the $AdS_5 \times S^5$ superstring in the language of the algebraic curve. As an example, we will find the low-lying energy spectrum for the excitations around some simple classical string solutions.

As we have already mentioned in sections 1 and 1.1.1, the *exact* quasi-momenta are made out of a large collection of poles. From (14), we infer the residue of each pole,

$$p \simeq \sum_{a=k}^{S_n} \frac{\alpha(x_k)}{x - x_k} + \cdots,$$

with

$$\alpha(x) = \frac{4\pi}{\sqrt{\lambda}} \frac{x^2}{x^2 - 1}. \tag{177}$$

These poles may then condense into square root cuts forming a classical Riemann surface like in figure 15. The filling fraction and mode number of the cuts are in strict analogy with the amplitude and mode number of a Fourier mode in the usual flat space string. Then, to consider the quantum fluctuations around this classical solution amounts to adding small cuts, i.e. poles, to this curve. The key ingredient allowing us to do so is the knowledge of the residue (177) just like in the example (171) in section 1. The several possible choices of sheets to be connected by these poles correspond to the several possible polarizations of the superstring, i.e. to the different quantum numbers. The 16 physical excitations are the $4+4$ modes in AdS_5 and S^5 (figure 17) plus the 8 fermionic fluctuations (figure 18).

Let us give a bit more of flavor to the above discussion. As we mentioned in section 1, the equations describing the eight-sheet quasi-momenta can be discretized [20] yielding a set of Bethe ansatz equations for the roots x_i making up the cuts. The resulting equations resemble (173) with an extra $2\pi n_i$ on the left-hand side:

$$\sum_{j \neq i} \frac{1}{x_i - x_j} = 2\pi n_i + V(x_i).$$

This means that we can think of x_i as being the position of a particle interacting with many other particles via a two-dimensional Coulomb interaction, placed in an external potential[21] and feeling an external force $2\pi n_i$. What we are doing is, then, first considering a large number of particles which will condense in some disjoint supports, the cuts, with each cut being made out of particles with the same mode number n_i. Then we add an extra particle with some other mode number n. At the leading order, two things happen. The particle will seek its equilibrium point in this background and will backreact, shifting this background slightly by its presence [57]. The (AdS global time) energy E of the new configuration is then shifted. When adding N particles, we get precisely the quantum steps in the spectrum, i.e. (174).

[21] In (173), the potential is a quadratic one; for the actual Bethe equations, it is something else.

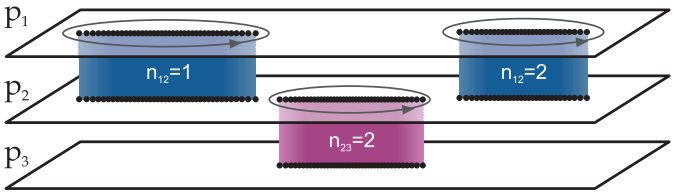

Figure 16. A possible analytical stricture of the quasi-momenta of an integrable sigma model. Many types of cuts are now possible. Cuts can join different sheets and each cut is marked by its 'mode number' n_{ij}. In the flat space limit, they become numbers of Fourier modes. The number of microscopical poles constituting the given cut is called a 'filling fraction' and can be calculated as a contour integral (172).

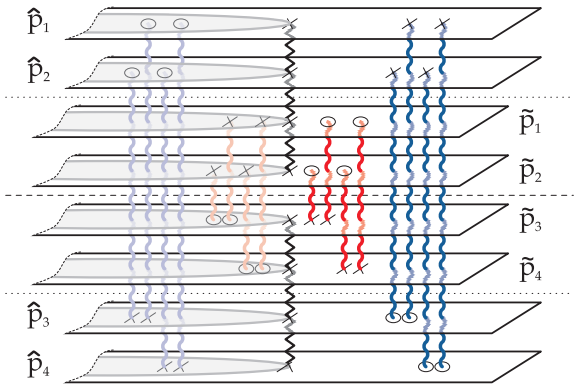

Figure 17. Some configuration of poles on the algebraic curve corresponding to the S^5 excitations (red) and AdS_5 excitations (blue). The black line denotes poles at ± 1, connecting four sheets with equal residues. The crosses correspond to residue $+\alpha(x)$, while circles to residue $-\alpha(x)$. The physical domain of the surface lies outside the unit circle.

Technically, the computations can be divided into two main steps. In what follows, we will use notation (13) intensively. We must solve (11) for all cuts of the Riemann surface where we now have $p(x) \to p(x) + \delta p(x)$, where $p(x)$ is the quasi-momentum associated with the classical solution.

- When applied to the microscopic cut, i.e. pole, equation (11) gives us, to leading order, the position x_n^{ij} of the pole:
$$p_i\left(x_n^{ij}\right) - p_j\left(x_n^{ij}\right) = 2\pi n, \qquad \left|x_n^{ij}\right| > 1, \tag{178}$$
where $i < j$ take values $\hat{1}, \hat{2}, \hat{3}, \hat{4}, \tilde{1}, \tilde{2}, \tilde{3}, \tilde{4}$ and indicate which two sheets share the pole. We refer to domain $|x| > 1$ as a *physical domain*. The interior of the unit circle is just the mirror image of the physical domain, as we saw in the previous section (15).
- Then, to find δp, and in particular the energy shift δE, we must solve the same equations but now in the macroscopic cuts:
$$\delta p_i^+ - \delta p_j^- = 0, \qquad x \in \mathcal{C}_n^{ij}. \tag{179}$$
This linear problem is to be supplemented with the known analytical properties of $\delta p(x)$, namely the asymptotic behavior presented below and the simple pole singularities with residues (177). In this way, we compute the backreaction described above.

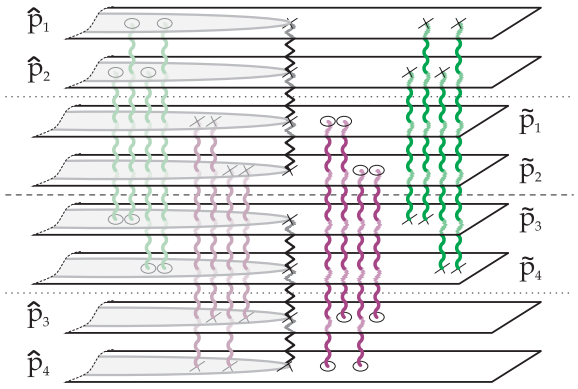

Figure 18. Some configuration of poles on the algebraic curve corresponding to eight fermionic excitations. The black line denotes poles at ± 1, connecting four sheets with equal residues. The crosses correspond to residue $\alpha(x)$, while circles to residue $-\alpha(x)$. The physical domain of the surface lies outside the unit circle.

Before proceeding, it is useful to introduce some simple notation. We shall consider N_n^{ij} excitations with mode number n between sheets p_i and p_j such that

$$N_{ij} \equiv \sum_n N_n^{ij}$$

is the total number of poles connecting these two sheets. Moreover, each excitation has its own quantum numbers according to the global symmetry. The S^5, AdS_5 and fermionic excitations can then be identified as the several possible choices of sheets to be connected (see figures 17 and 18),

$$\begin{aligned} &S^5, && (i,j) = (\tilde{1},\tilde{3}), (\tilde{1},\tilde{4}), (\tilde{2},\tilde{3}), (\tilde{2},\tilde{4}) \\ &AdS_5, && (i,j) = (\hat{1},\hat{3}), (\hat{1},\hat{4}), (\hat{2},\hat{3}), (\hat{2},\hat{4}) \\ &\text{Fermions}, && (i,j) = (\tilde{1},\hat{3}), (\tilde{1},\hat{4}), (\tilde{2},\hat{3}), (\tilde{2},\hat{4}), \\ & && \quad (\hat{1},\tilde{3}), (\hat{1},\tilde{4}), (\hat{2},\tilde{3}), (\hat{2},\tilde{4}) \end{aligned} \tag{180}$$

The 16 physical degrees of freedom of the superstring are precisely these 16 elementary excitations, also called *momentum-carrying excitations* [14, 19].

When adding extra poles to the classical solutions, their energy will be shifted by

$$\delta E = \delta\Delta + \sum_{AdS^5} N_{ij} + \frac{1}{2}\sum_{Ferm} N_{ij}, \tag{181}$$

where we isolated the anomalous part $\delta\Delta$ of the energy shift from the trivial bare part. Then, it is convenient to recast (17), for the excitations, as

$$\delta \begin{pmatrix} \hat{p}_1 \\ \hat{p}_2 \\ \hat{p}_3 \\ \hat{p}_4 \\ \hline \tilde{p}_1 \\ \tilde{p}_2 \\ \tilde{p}_3 \\ \tilde{p}_4 \end{pmatrix} \simeq \frac{4\pi}{x\sqrt{\lambda}} \left(\begin{array}{ccc} +\delta\Delta/2 & +N_{\hat{1}\hat{4}} + N_{\hat{1}\hat{3}} & +N_{\hat{1}\tilde{3}} + N_{\hat{1}\tilde{4}} \\ +\delta\Delta/2 & +N_{\hat{2}\hat{3}} + N_{\hat{2}\hat{4}} & +N_{\hat{2}\tilde{4}} + N_{\hat{2}\tilde{3}} \\ -\delta\Delta/2 & -N_{\hat{2}\hat{3}} - N_{\hat{1}\hat{3}} & -N_{\tilde{1}\hat{3}} - N_{\tilde{2}\hat{3}} \\ -\delta\Delta/2 & -N_{\hat{1}\hat{4}} - N_{\hat{2}\hat{4}} & -N_{\tilde{2}\hat{4}} - N_{\tilde{1}\hat{4}} \\ \hline -N_{\tilde{1}\tilde{4}} - N_{\tilde{1}\tilde{3}} & -N_{\tilde{1}\tilde{3}} - N_{\tilde{1}\tilde{4}} \\ -N_{\tilde{2}\tilde{3}} - N_{\tilde{2}\tilde{4}} & -N_{\tilde{2}\tilde{4}} - N_{\tilde{2}\tilde{3}} \\ +N_{\tilde{2}\tilde{3}} + N_{\tilde{1}\tilde{3}} & +N_{\tilde{1}\tilde{3}} + N_{\tilde{2}\tilde{3}} \\ +N_{\tilde{1}\tilde{4}} + N_{\tilde{2}\tilde{4}} & +N_{\tilde{2}\tilde{4}} + N_{\tilde{1}\tilde{4}} \end{array}\right). \tag{182}$$

These filling fractions N_{ij}^n are not independent. Any algebraic curve must obey the Riemann bilinear identity (see equation (3.38) and (3.44) in [14]). Since this was already the case for the classical solution around which we expand, the new filling fractions are constrained by

$$\sum_n n \sum_{\text{All} ij} N_n^{ij} = 0, \tag{183}$$

which is nothing but the string level matching condition in the algebraic curve language.

It is also important to note that sign of the residues can be summarized by the following formula:

$$\operatorname*{res}_{x=x_n^{ij}} \hat{p}_k = (\delta_{i\hat{k}} - \delta_{j\hat{k}})\alpha\big(x_n^{ij}\big)N_n^{ij}, \qquad \operatorname*{res}_{x=x_n^{ij}} \tilde{p}_k = (\delta_{j\tilde{k}} - \delta_{i\tilde{k}})\alpha\big(x_n^{ij}\big)N_n^{ij}, \tag{184}$$

with $k = 1, 2, 3, 4$ and $i < j$ taking values $\hat{1}, \hat{2}, \hat{3}, \hat{4}, \tilde{1}, \tilde{2}, \tilde{3}, \tilde{4}$, as summarized in figures 17 and 18.

In the following sections, we shall analyze the quantum fluctuations around some simple classical solutions belonging to the family of rigid circular strings (175). We will do it in three main steps. First, we compute the quasi-momenta[22] associated with each classical solution as explained in section 3.2 and in greater detail in appendix B. Then we shall consider the fluctuations around the classical solution which appear as new poles in the quasi-momenta. As explained above, we start by finding the position of these new roots using (178) and then we shall compute the perturbation δp of the quasi-momenta by using, again, the analytical properties described in section 1.1.1 plus the knowledge of the poles' positions found in the second step.

We can already note that, using this procedure, one relies uniquely on considerations of analyticity and *need not* introduce any particular parameterization of the group element $g(\sigma, \tau)$ for the fluctuations around the classical solution, in contrast to what is usually done in this type of analysis [85–88]. It is also nice to see that the fermionic and bosonic frequencies appear, in our approach, on a completely equal footing, both corresponding to simple poles which differ only by the sheets they unite—see figures 17 and 18. Finally, in principle, we can apply our method to any classical solution whereas the same generalization seems to be highly non-trivial to do directly in the action since we no longer have a simple field redefinition to make it time and space independent as was the case in [86, 88]. This method will allow us to prove some general statements about the quasi-classical spectrum and its relation to the finite-size corrections in the BS equations.

3.3.1. The BMN string. We shall consider the simplest possible solution amongst the family of circular strings presented in section 3.2, the rotating point-like BMN string [89] moving around a big circle of S^5. For this solution, all spins except for

$$\mathcal{J}_1 = \mathcal{J}$$

are set to zero. Then we have $m_1 = 0$, $w_1 = \mathcal{J}$, $\mathcal{E} = \kappa = \mathcal{J}$. For this solution the connection $A(x)$ presented in appendix B is not only constant but also diagonal, so we immediately find

$$\tilde{p}_{1,2} = -\tilde{p}_{3,4} = \hat{p}_{1,2} = -\hat{p}_{3,4} = \frac{2\pi\mathcal{J}x}{x^2 - 1}. \tag{185}$$

[22] Due to the simplicity of these solutions we could have computed the quasi-momenta by an alternative method, namely using just the analytical properties presented in section 1.1.1. This was done for the $\mathfrak{su}(2)$ and $\mathfrak{sl}(2)$ circular solutions in [18] and [24] respectively.

We see that this is indeed the simplest eight-sheet algebraic curve we could have built—it has neither poles nor cuts connecting its sheets other than the trivial ones at $x = \pm 1$ (16).

We shall now study the quantum fluctuations around this solution. For the sake of clarity, we shall not write explicitly many of the quantities computed in the intermediate steps—they can be found in appendix C.

To consider the 16 types of physical excitations, we add all types of poles in figures 17 and 18. From (178) we find that the poles in the physical domain with $|x| > 1$, for this simple case, are all located at the same position

$$x_n^{ij} = x_n = \frac{1}{n}\big(\mathcal{J} + \sqrt{\mathcal{J}^2 + n^2}\big). \tag{186}$$

Now we must find the quasi-momenta $p(x) + \delta p(x)$

- with poles located at (186) with residues (184) connecting the several sheets,
- obeying the $x \to 1/x$ symmetry property (15),
- with residues ± 1 grouped as in (16),
- with large x behavior given by (182).

From the requirements listed above, one can easily write the expression for the quasi-momenta. For example,

$$\delta \hat{p}_2 = \hat{a} + \frac{\delta\alpha_+}{x-1} + \frac{\delta\alpha_-}{x+1} + \sum_{i=\hat{3},\hat{4},\bar{3},\bar{4}} \sum_n \frac{\alpha\big(x_n^{\hat{2}i}\big) N_n^{\hat{2}i}}{x - x_n^{\hat{2}i}} - \sum_{i=\hat{3},\hat{4},\bar{3},\bar{4}} \sum_n \frac{\alpha\big(x_n^{\hat{1}i}\big) N_n^{\hat{1}i}}{1/x - x_n^{\hat{1}i}} \tag{187}$$

$$\delta \hat{p}_3 = \hat{b} + \frac{\delta\beta_+}{x-1} + \frac{\delta\beta_-}{x+1} - \sum_{i=\hat{1},\hat{2},\bar{1},\bar{2}} \sum_n \frac{\alpha\big(x_n^{\hat{3}i}\big) N_n^{\hat{3}i}}{x - x_n^{\hat{3}i}} + \sum_{i=\hat{1},\hat{2},\bar{1},\bar{2}} \sum_n \frac{\alpha\big(x_n^{\hat{4}i}\big) N_n^{\hat{4}i}}{1/x - x_n^{\hat{4}i}}, \tag{188}$$

where $\hat{a}$, $\hat{b}$ and $\delta\alpha_\pm$, $\delta\beta_\pm$ are constants to be fixed and the last terms ensure the right poles in physical domain for $\delta\hat{p}_{1,4}(x) = -\delta\hat{p}_{2,3}(1/x)$. Similar expressions can be immediately written down for $\delta\hat{p}_{2,3}$ with the introduction of two new constants $\tilde{a}$ and $\tilde{b}$.

At this point, we are left with the problem of fixing the eight constants

$$\hat{a}, \hat{b}, \tilde{a}, \tilde{b}, \delta\alpha_+, \delta\alpha_-, \delta\beta_+, \delta\beta_-.$$

This is precisely the number of conditions one obtains by imposing the $1/x$ behavior at large x for the quasi-momenta (182). The asymptotic of $\hat{p}_2$, $\hat{p}_3$, $\tilde{p}_2$, $\tilde{p}_3$ fixes the first four constants while the remaining four equations, solvable only if the level matching condition (183) is satisfied, fix the remaining coefficients and yield

$$\delta E = \sum_{\text{All}} \sum_n \frac{\sqrt{n^2 + \mathcal{J}^2} - \mathcal{J}}{\mathcal{J}} N_n^{ij} + \sum_{\text{AdS}^5} N^{ij} + \frac{1}{2} \sum_{\text{Ferm}} N^{ij}, \tag{189}$$

where we indeed recognize the famous BMN frequencies [89] in the anomalous part of the energy shift.

3.3.2. The circular string in S^3, the one-cut $\mathfrak{su}(2)$ solution. The next less trivial example is the simple $\mathfrak{su}(2)$ rigid circular string [85]. Still it is simple enough so that all results

are explicit. This solution is obtained from the family of circular strings in section 3.2 by setting

$$m_1 = -m_2 = m, \qquad \mathcal{J}_1 = \mathcal{J}_2 = \mathcal{J}$$

with all other spins set to zero. For this solution,

$$\mathcal{E} = \kappa = \sqrt{\mathcal{J}^2 + m^2}.$$

The quasi-momenta can be computed as explained in appendix B. The AdS_5 quasi-momenta are obtained as for the BMN string

$$\hat{p}_{1,2} = -\hat{p}_{3,4} = \frac{2\pi\kappa x}{x^2 - 1}, \tag{190}$$

while for the S^5 components $\tilde{p}_i$ we find that this solution corresponds to a one-cut between $\tilde{p}_2$ and $\tilde{p}_3$ with mode number $k = -2m$, given by [18]

$$\begin{pmatrix} \tilde{p}_1 \\ \tilde{p}_2 \\ \tilde{p}_3 \\ \tilde{p}_4 \end{pmatrix} = 2\pi \begin{pmatrix} +\frac{x}{x^2-1} K(1/x) \\ +\frac{x}{x^2-1} K(x) - m \\ -\frac{x}{x^2-1} K(x) + m \\ -\frac{x}{x^2-1} K(1/x) \end{pmatrix}, \qquad K(x) \equiv \sqrt{m^2 x^2 + \mathcal{J}^2}, \tag{191}$$

where we assume that $m > 0$ and branch cut goes to the left of $x = -1$ so that

$$K(x) = mx + \mathcal{O}(1/x),\ K(x) = \mathcal{J} + \mathcal{O}(x)$$
$$K(1) = K(-1) = \kappa > 0.$$

In the rest of this section, we will compute the quantum spectrum of the low-lying excitations around this solution. For simplicity, we will consider the AdS_5, S^5 and fermionic fluctuations independently assuming the level matching condition (183) to be satisfied *for each of the sectors separately*. The result we give, however, is valid under the softer constraint (183) for all sectors, as one can easily check.

Method of computation. Suppose we want to compute the variation of the quasi-momenta $\delta p(x)$ when a small pole is added to some general finite gap solution with some square root cuts. Since the branch points will be slightly displaced, we conclude that $\delta p(x)$ behaves like $\partial_{x_0}\sqrt{x - x_0} \sim 1/\sqrt{x - x_0}$ near each such point.

We deal with a one-cut finite gap solution. Then, for $\delta\tilde{p}_2$, we can assume the most general analytical function with one branch cut, namely $f(x) + g(x)/K(x)$ where f and g are some rational functions and $K(x)$ was defined in (191). To obtain $\delta\tilde{p}_3$, it suffices to note that (179) simply tells us that $\delta\tilde{p}_3$ is the analytical continuation of $\delta\tilde{p}_2$ through the cut. The remaining quasi-momentum $\delta\tilde{p}_{1,4}$ can then be obtained from this by the inversion symmetry (15). We conclude that

$$\begin{pmatrix} \delta\tilde{p}_1 \\ \delta\tilde{p}_2 \\ \delta\tilde{p}_3 \\ \delta\tilde{p}_4 \end{pmatrix} = \begin{pmatrix} -f(1/x) - \frac{g(1/x)}{K(1/x)} \\ f(x) + \frac{g(x)}{K(x)} \\ f(x) - \frac{g(x)}{K(x)} \\ -f(1/x) + \frac{g(1/x)}{K(1/x)} \end{pmatrix}. \tag{192}$$

The only singularity of $\delta\tilde{p}_2$ apart from the branch cut is eventual simple poles at ± 1 and x_n and so the same must be true for $f(x)$ and $g(x)$. Then, just like in the previous example,

these functions are uniquely fixed by the large x asymptotics (182) and by the residues at x_n (184) of the quasi-momenta.

Finally, since the AdS_5 part of the quasi-momenta of the non-perturbed finite gap solution has no branch cuts their variations $\delta\hat{p}_i$ have the same form (187) and (188) as for the simplest BMN string.

The AdS_5 excitations. This part is the simplest. The excitations live in the empty AdS_5 sheets where the only impact of the S^5 classical solution comes through the Virasoro constraints, by the residues at ±1 (16). Thus, $\tilde{p}$ are nonperturbed and $\delta\hat{p}_i$ are the same as in the BMN case (187), (188) with only AdS_5 filling fractions N's being nonzero. Indeed, comparing (185) and (190) we see that we can completely recycle the previous computation provided we replace $\mathcal{J}$ by κ in expression (186) for the pole's position. This immediately leads to

$$\delta E = \sum_{\mathrm{AdS}^5} \sum_n \frac{\sqrt{\mathcal{J}^2+m^2+n^2}}{\sqrt{\mathcal{J}^2+m^2}} N_n^{ij}. \tag{193}$$

The S^5 excitations. We must now analyze the shift in quasi-momenta due to the excitation of the algebraic curve by the four types of poles $(\tilde{1}\tilde{3}, \tilde{2}\tilde{4}, \tilde{2}\tilde{3}, \tilde{1}\tilde{4})$. Since the AdS quasi-momenta are trivial, with no cuts, we obtain for $\delta\hat{p}$ the same kind of expression we had for the BMN string (185), that is,

$$\delta\hat{p}_{1,2} = -\delta\hat{p}_{3,4} = \frac{2\pi\,\delta E}{\sqrt{\lambda}} \frac{x}{x^2-1}, \tag{194}$$

where the constant factor was fixed by the asymptotics (182)

$$\delta\hat{p}_{1,2} \simeq -\delta\hat{p}_{3,4} \simeq \frac{2\pi\,\delta E}{\sqrt{\lambda}} \frac{1}{x}.$$

Due to the Virasoro constraints, the poles at ±1 in the AdS_5 and S^5 sectors are synchronized (16) so that we merely need to compute $f(x)$ and $g(x)$ from the large x asymptotics (182) and the residue condition (184) and extract, from these two functions, the residues at ±1. This is done in appendix D.1. Let us just provide a glimpse of reasoning involved. Since the difference

$$\delta\tilde{p}_3 = f(x) - g(x)/K(x)$$

must have a single pole at $x_n^{\tilde{1}\tilde{3}}$ with residue $\alpha\big(x_n^{\tilde{1}\tilde{3}}\big)$ whereas the sum

$$\delta\tilde{p}_2 = f(x) + g(x)/K(x)$$

must be analytical, we can, in this way, read the residues of both f and g at this point. Similar reasoning should be carried over for all the other excitations and for the points $x = \pm1$ and leads to the ansatz (D.1), (D.2) where the only three constants left to be found can be fixed by the large x asymptotics of the quasi-momenta.

One can then read off the energy shift from the large x asymptotics of the quasi-momenta:

$$\delta E = \sum_n \big(N_n^{\tilde{1}\tilde{3}} + N_n^{\tilde{2}\tilde{4}}\big) \frac{x_n^{\tilde{1}\tilde{3}}(m+n) - \mathcal{J} - K\big(x_n^{\tilde{1}\tilde{3}}\big)}{\kappa} + N_n^{\tilde{1}\tilde{4}} \frac{n x_n^{\tilde{1}\tilde{4}} - 2\mathcal{J}}{\kappa} + N_n^{\tilde{2}\tilde{3}} \frac{2m+n}{x_n^{\tilde{2}\tilde{3}}\kappa} \tag{195}$$

in terms of the positions of the roots obtained from the original algebraic curve through (178).

Fermionic excitations. We have eight fermionic excitations but since $\hat{p}_1 = \hat{p}_2 = -\hat{p}_3 = -\hat{p}_4$ and $\tilde{p}_{1,2} = -\tilde{p}_{4,3}$, we will get the same result for the $(\hat{1}\tilde{3}, \hat{2}\tilde{3}, \hat{3}\tilde{2}, \hat{4}\tilde{2})$ poles and possibly another result for the $(\hat{1}\tilde{4}, \hat{2}\tilde{4}, \hat{3}\tilde{1}, \hat{4}\tilde{1})$ excitations. We can repeat the same kind of calculations we did for the S^5 excitations to fix completely the quasi-momenta—see appendix D.2. Then, from the asymptotics (182) we get

$$\delta\Delta = \sum_n \left(N_n^{\hat{1}\tilde{3}} + N_n^{\hat{2}\tilde{3}} + N_n^{\hat{3}\tilde{2}} + N_n^{\hat{4}\tilde{2}}\right)\frac{m+n}{x_n^{\hat{1}\tilde{3}}\kappa} + \left(N_n^{\hat{1}\tilde{4}} + N_n^{\hat{2}\tilde{4}} + N_n^{\hat{3}\tilde{1}} + N_n^{\hat{4}\tilde{1}}\right)\frac{nx_n^{\hat{1}\tilde{4}} - \mathcal{J} - \kappa}{\kappa}. \tag{196}$$

3.3.3. The circular string in AdS_3, the one-cut $\mathfrak{sl}(2)$ solution. In section 3.3.2, we analyzed in detail a simple $\mathfrak{su}(2)$ solution with a particular mode number $k = -2m$. In appendix E, we repeat the analysis for the general $\mathfrak{sl}(2)$ circular string [87, 88] which also corresponds to a one-cut algebraic curve but this time with an arbitrary mode number k for the cut [24]. This solution is again contained in the family of circular strings written in section 3.2. It corresponds to two non-zero spins:

$$\mathcal{S}_1 = \mathcal{S}, \qquad \mathcal{J}_1 = \mathcal{J}$$

with mode numbers $m_1 = m$ and $k_1 = k$ constrained by the level matching condition

$$\mathcal{S}k + \mathcal{J}m = 0$$

and frequencies $w_1 = \mathcal{J}$ and $\mathrm{w}_1 = w$ fixed by

$$w^3 - (k^2 + m^2 + \mathcal{J}^2)w + 2km\mathcal{J} = 0. \tag{197}$$

For this solution $\kappa = \sqrt{w^2 - k^2}$ and the energy can be found from

$$\mathcal{E} = \kappa\left(1 + \frac{\mathcal{S}}{w}\right).$$

In appendix E, we present the quasi-momenta associated with this classical solution and compute the fluctuation frequencies as we did for the $\mathfrak{su}(2)$ string. These results, together with those for the $\mathfrak{su}(2)$ circular string, are summarized and discussed in the following sections.

3.4. Results, interpretation and one-loop shift

In this section, we list all our results and introduce the notations usually used in the literature. In the following section, we shall analyze them, compare them and draw some conclusions.

3.4.1. Simple $\mathfrak{su}(2)$ circular string. In section 3.3.2, we found the level spacings around the simple $\mathfrak{su}(2)$ circular solution, that is, the fluctuation frequencies of the effective quadratic Lagrangian obtained by expanding the Metsaev–Tseytlin action (3) around this classical solution. In [86], this computation was performed keeping in mind the stability analysis and computation of the one-loop shift. The various frequencies and corresponding degeneracies and origin can be summarized in table 1.[23] Using the notation introduced in this table, we can replace the explicit expressions for the position of the roots found from (178) and recast our

[23] By expanding the GS action without imposing the Virasoro conditions from the beginning, one obtains, apart from the frequencies listed in the above table, some massless modes with $\omega = n$ [85]. In section 5, we will see these Virasoro modes from the Bethe ansatz point of view if an extra level of particles with rapidities θ is introduced [90].

Table 1. Simple $\mathfrak{su}(2)$ frequencies.

	Eigenmodes	Notation
S^5	$\sqrt{2\mathcal{J}^2+n^2\pm 2\sqrt{\mathcal{J}^4+n^2\mathcal{J}^2+m^2n^2}}$	$\omega_n^{S_\pm}$
	$\sqrt{\mathcal{J}^2+n^2-m^2}$	ω_n^S
Fermions	$\sqrt{\mathcal{J}^2+n^2}$	ω_n^F
AdS_5	$\sqrt{\mathcal{J}^2+n^2+m^2}$	ω_n^A

Table 2. General $\mathfrak{sl}(2)$ frequencies.

	Eigenmodes	Notation
AdS_5	$(\omega^2-n^2)^2+\frac{4\mathcal{S}}{\mathrm{w}}\kappa^2\omega^2-\frac{4\mathcal{E}}{\kappa}(\omega\mathrm{w}-kn)^2=0$	$\omega_n^{A_+}>\omega_n^{A_-}$
	$\sqrt{n^2+\kappa^2}$	ω_n^A
Fermions	$\sqrt{\left(n+\frac{\sqrt{w^2-\mathcal{J}^2}}{2}\right)^2+\frac{1}{2}(\kappa^2+\mathcal{J}^2-m^2)}$	ω_n^F
S^5	$\sqrt{\mathcal{J}^2+n^2-m^2}$	ω_n^S

results (193), (195), (196) as

$$\begin{aligned}\kappa\delta E=&\sum_n\left(N_n^{\hat1\hat3}+N_n^{\hat2\hat4}\right)\left(\omega_{n+m}^S-\mathcal{J}\right)+N_n^{\hat2\hat3}\omega_{n+2m}^{S_-}+N_n^{\hat1\hat4}\left(\omega_n^{S_+}-2\mathcal{J}\right)\\&+\sum_n\left(N_n^{\hat1\hat4}+N_n^{\hat2\hat4}+N_n^{\hat3\hat1}+N_n^{\hat4\hat1}\right)\left(\omega_n^F-\mathcal{J}+\frac{\kappa}{2}\right)\\&+\sum_n\left(N_n^{\hat1\hat3}+N_n^{\hat2\hat3}+N_n^{\hat3\hat2}+N_n^{\hat4\hat2}\right)\left(\omega_{n+m}^F-\frac{\kappa}{2}\right)\\&+\sum_n\left(N_n^{\hat1\hat3}+N_n^{\hat1\hat4}+N_n^{\hat2\hat3}+N_n^{\hat2\hat4}\right)\omega_n^A.\end{aligned}\tag{198}$$

We note the appearance of constant shifts and relabeling of the frequencies when compared to those in table 1. We shall discuss this point below.

3.4.2. General $\mathfrak{sl}(2)$ circular string. The same analysis can be carried over for the $\mathfrak{sl}(2)$ circular string. In [87, 88], these frequencies were computed and the result is summarized in table 2.[24]

In the notation of the above table, the results (E.12), (E.9), (E.5) and (E.4) derived in appendix E can be put together as

$$\begin{aligned}\kappa\delta E=&\sum_n\left(N_n^{\hat1\hat3}+N_n^{\hat2\hat4}\right)\omega_n^A+N_n^{\hat2\hat3}\left(\omega_{n-k}^{A_-}+w\right)+N_n^{\hat1\hat4}\left(\omega_{n+k}^{A_+}-w\right)\\&+\sum_n\left(N_n^{\hat2\hat3}+N_n^{\hat2\hat4}+N_n^{\hat3\hat1}+N_n^{\hat3\hat2}\right)\left(\omega_{n+m/2-k/2}^F-\omega_{m/2-k/2}^F+\frac{1}{2}\kappa\right)\\&+\sum_n\left(N_n^{\hat1\hat3}+N_n^{\hat1\hat4}+N_n^{\hat4\hat1}+N_n^{\hat4\hat2}\right)\left(\omega_{-n-m/2-k/2}^F-\omega_{-m/2-k/2}^F+\frac{1}{2}\kappa\right)\\&+\sum_n\left(N_n^{\tilde1\tilde3}+N_n^{\tilde1\tilde4}+N_n^{\tilde2\tilde3}+N_n^{\tilde2\tilde4}\right)\left(\omega_{n+m}^S-\mathcal{J}\right).\end{aligned}\tag{199}$$

[24] The results in this table are slightly simplified compared to those usually presented in the literature, especially the fermionic frequencies.

3.4.3. Explanation of shifts. Let us first look at the $\mathfrak{su}(2)$ result (198) and pick one of the frequencies, say the first one

$$\omega^S_{n+m} - \mathcal{J}. \tag{200}$$

We find two kinds of shifts relatively to the frequencies listed in the table 1, namely the constant shift $\mathcal{J}$ and the shift in the Fourier mode $n \to n+m$, the same shifts we observe for the $\mathfrak{sl}(2)$ frequencies.

Let us understand the origin of these shifts. For this purpose, consider a system of two harmonic oscillators,

$$L_x = \frac{\dot{x}_1^2 + \dot{x}_2^2}{2} - \frac{\omega^2}{2}\left(x_1^2 + x_2^2\right),$$

and suppose that, instead of quantizing this system, we chose to quantize the system obtained by rotating x_1, x_2 with angular velocity $\mathcal{J}$, i.e. we move to the y frame

$$x_1 + \mathrm{i}x_2 = (y_1 + \mathrm{i}y_2)\,\mathrm{e}^{\mathrm{i}\mathcal{J}t}.$$

Then, we obtain[25]

$$H_y = H_x + \mathcal{J}L_z,$$

where L_z is the usual angular momentum, so that

$$E^y_{n_1,n_2} = \omega + (\omega - \mathcal{J})\,n_1 + (\omega + \mathcal{J})\,n_2.$$

Thus for the radially symmetric wavefunction, for which $n_1 = n_2$ (and in particular for the ground-state energy), the constant shifts cancel and we obtain the same energies as for the first system. That, in general, the two results are different is obvious since the energy depends on the observer.

The constant shifts mentioned above have exactly this origin. In fact, when expanding the Metsaev–Tseytlin string action around the classical $\mathfrak{su}(2)$ circular string, one obtains an effective *time- and space-dependent* Lagrangian whose σ, τ dependence can be killed by a change of frame:

$$\delta X = R(\sigma, \tau)\delta Y,$$

where δX are the (bosonic) components of the fluctuations and R is a time- and space-dependent rotation matrix—see, for instance, expression (2.14) in [86][26]. The same kind of field redefinitions is also present for the fermion fields. The time dependence of the rotation matrix gives the constant shifts as in the simple example we just considered while the space dependence in this change of frame is responsible for the relabeling of the mode numbers.

To make contact with the algebraic curve, let us return to the frequency (200) we picked as illustration. It corresponds to a pole from sheet $\tilde{p}_1$ to $\tilde{p}_3$ (or from $\tilde{p}_2$ to $\tilde{p}_4$) whose position is fixed by (178). The result in the rotated frame, ω^S_n, would correspond to a pole with mode number $n+m$ whose position is given by

$$\tilde{p}_1\left(x_n^{\tilde{1}\tilde{3}}\right) - \tilde{p}_3\left(x_n^{\tilde{1}\tilde{3}}\right) = 2\pi n + 2\pi m.$$

When plugging the actual expressions (191) for $\tilde{p}_1$ and $\tilde{p}_3$ in this equation, we see that $2\pi m$ disappears and the equation looks simpler than (178). However, for several cut solutions there is no such obvious choice of mode numbers (or field redefinition which kills the time dependence in the Lagrangian).

[25] In the y frame, the Lagrangian takes the form $2L_y = \dot{y}_1^2 + \dot{y}_2^2 - (\omega^2 - \mathcal{J}^2)\left(x_1^2 + x_2^2\right) + 2\mathcal{J}y_1\dot{y}_2 - 2\mathcal{J}\dot{y}_1 y_2$.

[26] The same is true for the $\mathfrak{sl}(2)$ circular string. The authors have moved to a different frame through a time- and space-dependent rotation—see, for instance, equation (4.11) in [88]—and should, therefore, measure shifted energies.

3.4.4. One-loop shift and prescription for labeling fluctuation frequencies. To compute the one-loop shift to the classical energy of a given solution, according to [53], one has to sum over all energies of the modes in the expansion around the classical configuration

$$\delta E_{1-\text{loop}} = \frac{1}{2\kappa} \lim_{N\to\infty} \sum_{n=-N}^{N} \left(\sum_{i=1}^{8} \Omega^B_{i,n} - \sum_{i=1}^{8} \Omega^F_{i,n} \right).$$

However, the right-hand side is hard to define rigorously. For $n \to \pm\infty$, each frequency behaves like

$$\Omega^B_{i,n} \simeq |n| \pm c^B_i + d^B_i, \qquad \Omega^F_{i,n} \simeq |n| \pm c^F_i + d^F_i,$$

and thus the sum is sensible to the labeling of the frequencies. The seemingly innocent redefinition

$$\Omega^B_{i,n} \to \Omega^B_{i,n+k_i}, \qquad \Omega^F_{i,n} \to \Omega^F_{i,n+l_i}, \tag{201}$$

with integer shifts constrained by $\sum_i k_i - l_i = 0$ to ensure the convergence of the sum, *does* change the result

$$\delta E_{1-\text{loop}} \to \delta E_{1-\text{loop}} + \sum \left(k_i^2 - l_i^2 + 2c^B_i k_i - 2c^F_i l_i \right). \tag{202}$$

In appendix F, we discuss in greater detail the effect of these shifts.

One way to compute the frequencies is to expand the Metsaev–Tseytlin action around some classical solution. Generically, the resulting quadratic Lagrangian is time and space dependent. To eliminate this dependence, when possible, a field redefinition is performed. However, there are several ways to do the field redefinition to get a time- and space-independent action. Different choices will give different sets of frequencies related by transformations such as (201) and will therefore lead to different results. In appendix F, we analyze this kind of dangers by focusing on two explicit examples. Thus, we need a solid prescription for the labeling of the frequencies.

Suppose we were semi-classically quantizing around some classical string solution in a flat space. Then we would expect to find some fluctuation frequencies, the zero modes, corresponding to an overall translation of the string solution and which should, therefore, carry no energy at all. Then the usual prescription is to take $\Omega_{i,0} = 0$.

The zero modes should also exist for a string in the $\text{AdS}_5 \times S^5$ space with a large number of isometries. Indeed, let us take our results and denote the contribution at $n = 0$ in (198) and (199) by $\delta E_0^{\mathfrak{su}(2)}$ and $\delta E_0^{\mathfrak{sl}(2)}$ respectively. Then, we find that they are equal and given by

$$\delta E_0 = \sum_{\text{AdS}^5} N_{ij} + \frac{1}{2} \sum_{\text{Ferm}} N_{ij}. \tag{203}$$

In other words, the contribution to the anomalous part $\delta\Delta$ of zero modes for our labeling is zero! Thus, the prescription we used seems to be the precise analogue of the flat space Fourier modes prescription.

Moreover, by construction, we have a good BMN limit. That is, when in the limit of very small cuts with $m \to 0$ we recover the result (189) without any unusual shifts[27].

[27] This is not the case for the frequencies listed in table 2 for instance. For example, from this expression, we find, for the fermionic frequencies, $\omega^F_n \simeq \sqrt{(n + k/2)^2 + \mathcal{J}^2}$. See also the discussion in appendix F.

Table 3. General $\mathfrak{su}(2)$ frequencies.

	Eigenmodes	Notation
S^5	$(\omega^2-n^2)^2-\frac{4\mathcal{J}_2}{w_2}(\omega w_1-m_1 n)^2-\frac{4\mathcal{J}_1}{w_1}(\omega w_2-m_2 n)^2=0$	$\omega_n^{S_+}>\omega_n^{S_-}$
	$\sqrt{n^2+\nu^2}$	ω_n^S
Fermions	$\sqrt{\left(n-\frac{\sqrt{w_1^2+m_2^2-\kappa^2}}{2}\right)^2+\mathcal{J}_1 w_1+\mathcal{J}_2 w_2}$	ω_n^F
AdS_5	$\sqrt{n^2+\kappa^2}$	ω_n^A

Then, from (198) and (199), we can write the one-loop shifts for the one-cut circular solutions[28]:

$$E^{\mathfrak{su}(2)}_{\text{one-loop}}=\frac{1}{2\kappa}\lim_{N\to\infty}\sum_{n=-N}^{N}4\omega_n^A+\omega_{n+m}^S+\omega_{n+2m}^{S_-}+\omega_n^{S_+}-4\omega_n^F-4\omega_{n+m}^F,$$

$$E^{\mathfrak{sl}(2)}_{\text{one-loop}}=\frac{1}{2\kappa}\lim_{N\to\infty}\sum_{n=-N}^{N}2\omega_n^A+\omega_{n+k}^{A_+}+\omega_{n-k}^{A_-}+4\omega_{n+m}^S-4\omega^F_{n+\frac{m-k}{2}}-4\omega^F_{-n-\frac{m+k}{2}}.$$

3.4.5. General $\mathfrak{su}(2)$ *results.* Another interesting solution contained in the family of circular solutions described in section 3.2 is the generalization of the simple $\mathfrak{su}(2)$ solution to the case of two non-equal spins $\mathcal{J}_{1,2}$ with two different mode numbers $m_{1,2}$. The fluctuation frequencies associated with this solution can be listed in table 3 [87].[29]

Now, armed with our prescription, we can write the one-loop shift unambiguously. Imposing

- good BMN limit (189) for vanishing filling fractions,
- proper zero-mode behavior with $n=0$ frequencies having trivial anomalous, part (203).
- for $m_1=-m_2=m$ we should retrieve the simple $\mathfrak{su}(2)$ result (198),

we get (for $m_1+m_2\leqslant 0$)

$$\begin{aligned}\kappa\delta E=&\sum_n\left(N_n^{\check1\check3}+N_n^{\check2\check4}\right)\left(\omega^S_{n+m_1}-w_1\right)+N_n^{\check2\check3}\left(\omega^{S_-}_{n+m1-m2}+w_2-w_1\right)\\&+\sum_n N_n^{\check1\check4}\left(\omega^{S_+}_{n+m_1+m_2}-w_2-w_1\right)+\sum_n\left(N_n^{\hat1\hat3}+N_n^{\hat1\hat4}+N_n^{\hat2\hat3}+N_n^{\hat2\hat4}\right)\omega_n^A\\&+\sum_n\left(N_n^{\hat1\check4}+N_n^{\hat2\check4}+N_n^{\hat3\check1}+N_n^{\hat4\check1}\right)\left(\omega^F_{n+\frac{m_1+m_2}{2}}-\omega^F_{\frac{m_1+m_2}{2}}+\frac{\kappa}{2}\right)\\&+\sum_n\left(N_n^{\hat1\check3}+N_n^{\hat2\check3}+N_n^{\hat3\check2}+N_n^{\hat4\check2}\right)\left(\omega^F_{-n-\frac{m_1-m_2}{2}}-\omega^F_{-\frac{m_1-m_2}{2}}+\frac{\kappa}{2}\right).\end{aligned}$$

3.5. Summary

In this section, we explain how to compute the quantum fluctuations around *any* classical superstring motion in $AdS_5\times S^5$. These excitations include the fermionic, AdS_5 and S^5

[28] As for the simple example of the harmonic oscillators in the previous section, the sum of all constant shifts appearing in (198) and (199) cancel so that only the shifts in the mode number lead to a change of the final result. The difference with respect to the sum with no shifts can be obtained from (202) and is equal to m^2/κ in both cases.

[29] The fermionic frequencies for the general circular string of section 3.2 can be computed (we shall publish our findings elsewhere). In particular, for the $\mathfrak{su}(2)$ general circular string we find the results listed in table 3.

modes. We showed that each mode corresponds to adding a pole to a specific pair of sheets i, j of the algebraic curve. The position of the pole is determined from the equation

$$p_i\big(x_n^{ij}\big) - p_j\big(x_n^{ij}\big) = 2\pi n,$$

and thus provides one with an *unambiguous* labeling for the frequencies. In particular we observe the nice feature that for $n = 0$ this equation prescribes the pole at infinity, that is, we find the expected zero modes associated with global transformations under the isometries of the target super-space.

Technically, we computed the change in quasi-momenta due to the addition of these new poles and read, from the large x asymptotics, the global charge corresponding to the AdS energy, that is, the frequencies. However, since we computed explicitly the perturbed quasi-momenta we have obtained not only the energy shift but actually all conserved charges!

In the following sections, we will use this method to prove some general statements about the quasi-classical spectrum around *any* classical string solution.

4. Matching finite size corrections and fluctuations

In section 2, we developed a method to compute the finite size corrections in the thermodynamical limit. The conjectured BS equations depend on the 't Hooft coupling λ and should describe the spectrum of the AdS/CFT system (in the planar limit) for the asymptotic states, i.e. for large angular momentum $\mathcal{J} = L/\sqrt{\lambda} \gg 1$. The analogue of the thermodynamical limit for the BS equations is $K_a \sim L \sim \sqrt{\lambda} \to \infty$ as we already mentioned in section 1. The BS equations are constructed to reproduce the classical algebraical curve of the 'finite-gap' method in the leading thermodynamical limit. The finite size $1/L$ corrections are also $1/\sqrt{\lambda}$ corrections to the classical spectrum and thus should be related to the quasi-classical quantization considered in section 3.

In this section, we will apply the method developed in section 2 to the BS equations to extract their finite size corrections. Then, we will show that they are, in fact, related to the fluctuations, considered in the previous section, in such a way, that the one-loop $1/\sqrt{\lambda}$ correction to the classical energy of a state is given by a sum of zero point oscillations. This proves the complete one-loop consistency of the BS equations.

4.1. Heisenberg spin chain

In this section, we will demonstrate the interplay between fluctuations and finite size corrections in NBAs in the scaling limit. For simplicity, we first consider the $\mathfrak{su}(1,2)$ spin chain and then generalize to the general $\mathfrak{su}(N)$ case.

In section 2, we explained how to obtain the spectrum of the fluctuation energies around any classical string solution using the algebraic curve by adding a pole to this curve. In particular, we reproduced in this way some previous results [85–88] where the semi-classical quantization around some simple circular string motions was computed by directly expanding the Metsaev–Tseytlin action [9] around some classical solutions and quantizing the resulting quadratic action. Using the fact that one extra pole in the algebraic curve means one quantum fluctuation, we can compute the leading quantum corrections to the classical energy of a state from the field theory considerations using the algebraic curve alone, as we mentioned in section 1. This implies a nontrivial relation between the fluctuations on the algebraic curve and finite size corrections in the Bethe ansatz.

- Suppose we compute the energy shift $\delta\mathcal{E}_n^{ij}$ due to the addition of a stack with mode number n uniting sheets p_i and p_j to a given configuration with some finite cuts $\mathcal{C}$.

- Suppose, on the other hand, that we compute $1/L$ energy expansion $\mathcal{E} = \mathcal{E}^{(0)} + \frac{1}{L}\mathcal{E}^{(1)} + \cdots$ of the configuration with the finite cuts $\mathcal{C}$.

From the field theory point of view, the first quantity corresponds to *one of the fluctuation energies* around a classical solution parameterized by the configuration with cuts $\mathcal{C}$ whereas the second quantity, $\mathcal{E}^{(1)}$, is the *one-loop shift* [53] around this classical solution with energy $\mathcal{E}^{(0)}$. This one-loop shift, or ground-state energy, is given by the sum of halves of the fluctuation energies [53]:

$$\mathcal{E}^{(1)} = \frac{1}{2}\sum_{n=-N}^{N}\sum_{ij}\delta\mathcal{E}_n^{ij}. \tag{204}$$

In fact for usual (non super-symmetric) field theories, this sum is divergent and needs to be regularized. We will see that (204) can be generalized and holds for arbitrary local charges

$$\mathcal{Q}_r^{(1)} = \frac{1}{2}\sum_{n=-N}^{N}\sum_{ij}\delta\mathcal{Q}_{r,n}^{ij}, \tag{205}$$

where N is some large cutoff.

Let us once more stress that from the Bethe ansatz point of view, these quantities are computed independently and there is *a priori* no obvious reason why such a relation between fluctuations and finite size corrections should hold. In this section, we will show that nested Bethe ansä tze describing (super) spin chains with an arbitrary rank do indeed obey such a property with some particular regularization procedure (for the Heisenberg $su(2)$ spin chain, a similar treatment was carried in [57]). Moreover, we will see that the regularization mentioned above also appears naturally from the Bethe ansatz point of view as some integrals around the origin.

4.1.1. One-loop shift and fluctuations. We will follow the logic of the previous section to compute the charges of the fluctuations, around a given configuration of the roots. Let us pick the leading order integral equation for the densities of the Bethe roots in the scaling limit (150) and perturb it by a single stack, connecting p^i with p^j. According to (144) this simply implies $\rho_2 \to \rho_2 + \frac{1}{L}\delta(x - x^{ij})$, where x^{ij} is position of the new stack. Finally, the positions where one can put an extra stack, as it follows from the BAE (140), (141), can be parameterized by one integer mode number n

$$p_i\big(x_n^{ij}\big) - p_j\big(x_n^{ij}\big) = 2\pi n. \tag{206}$$

Therefore, for $i = 2$, $j = 3$ the perturbed equation (150) reads as

$$\frac{1}{x} + 2\fint_{\mathcal{C}_{23}}\frac{\rho(y)}{x-y} + \int_{\mathcal{C}_{13}}\frac{\rho(y)}{x-y} + \frac{1}{L}\frac{2}{x - x_n^{23}} = 2\pi k_{23} + \phi_2 - \phi_3, \qquad x \in \mathcal{C}_{23}, \tag{207}$$

and this perturbation will lead to some perturbation of the density $\delta\rho(y)$, which will lead to the perturbation in the local charges (142) as

$$\delta\mathcal{Q}_{r,n}^{23} = \int\frac{\delta\rho(y)}{y^r}\,\mathrm{d}y + \frac{1}{L\big(x_n^{23}\big)^r}, \tag{208}$$

the local charges of the fluctuation with polarization 23 and mode number n.

Thus, by linearity, if we want to obtain the one-loop shift (205) (or rather a large N regularized version of this quantity where the sum over n goes from $-N$ to N) we have to solve the following integral equation for densities:

$$\frac{1}{x} + 2\fint_{\mathcal{C}_{23}}\frac{\rho(y)}{x-y} + \int_{\mathcal{C}_{13}}\frac{\rho(y)}{x-y} + \sum_{n=-N}^{N}\frac{1}{2L}\left[\frac{2}{x - x_n^{23}} + \frac{1}{x - x_n^{13}}\right] = 2\pi k_{23}, \quad x \in \mathcal{C}_{23}, \tag{209}$$

and then the one-loop shifted charges are given

$$\mathcal{Q}_r = \int_{\mathcal{C}_{13}\cup\mathcal{C}_{23}} \frac{\rho(y)}{y^r}\,\mathrm{d}y + \sum_{n=-N}^{N} \frac{1}{2L}\left[\frac{1}{\left(x_n^{23}\right)^r} + \frac{1}{\left(x_n^{13}\right)^r}\right] \tag{210}$$

$$= \int_{\mathcal{C}_{13}\cup\mathcal{C}_{23}} \frac{\rho(y)}{y^r}\,\mathrm{d}y + \sum_{n=-N}^{N} \frac{1}{2L}\left[\oint_{x_n^{23}} \frac{\cot_{23}}{y^r}\frac{\mathrm{d}y}{2\pi\mathrm{i}} + \oint_{x_n^{13}} \frac{\cot_{13}}{y^r}\frac{\mathrm{d}y}{2\pi\mathrm{i}}\right]. \tag{211}$$

To pass from the first line to the second in the above expression, we use that $\cot_{ij}$ has poles at x_n^{ij} with unit residue. We will now understand how to redefine the density in such a way that the second term is absorbed into the first one. We start by opening the contours in (211) around the excitation points x_n^{ij}. These contours will then end up around the cuts $\mathcal{C}_{\mathrm{kl}}$ of the classical solution and around the origin. We will not consider the contour around $x = 0$—this contribution would lead to a regularization of the divergent sum on rhs of (205). We will analyze it carefully in the superstring case, where it leads to the Hernandez–Lopez phase factor. Then we get

$$\mathcal{Q}_r = \int_{\mathcal{C}_{13}\cup\mathcal{C}_{23}} \frac{\rho(y)}{y^r}\,\mathrm{d}y + \frac{1}{2L}\left[\oint_{\mathcal{C}_{13}} \frac{\cot_{23}}{y^r}\frac{\mathrm{d}y}{2\pi\mathrm{i}} + \oint_{\mathcal{C}_{23}} \frac{\cot_{13}}{y^r}\frac{\mathrm{d}y}{2\pi\mathrm{i}}\right]. \tag{212}$$

Noting that

$$\cot_{ij}^{+} = \cot_{kj}^{-}, \qquad x \in \mathcal{C}_{ik}, \tag{213}$$

where the superscript + (−) indicates that x is slightly above (below) the cut, we can write

$$\mathcal{Q}_r = \int_{\mathcal{C}_{13}\cup\mathcal{C}_{23}} \frac{\rho(y)}{y^r}\,\mathrm{d}y - \frac{1}{2L}\int_{\mathcal{C}_{13}\cup\mathcal{C}_{23}} \frac{\Delta\cot_{12}}{y^r}\frac{\mathrm{d}y}{2\pi\mathrm{i}} \tag{214}$$

so that we see that it is natural to introduce a new density, 'dressed' by the virtual particles

$$\varrho = \rho - \frac{1}{2L}\frac{\Delta\cot_{12}}{2\pi\mathrm{i}} \tag{215}$$

so that the expression for the local charges takes the standard form

$$\mathcal{Q}_r = \int_{\mathcal{C}_{13}\cup\mathcal{C}_{23}} \frac{\varrho(y)}{y^r}\,\mathrm{d}y.$$

Let us now rewrite our original integral equation (209) in terms of this dressed density. We will see that the integral equation we construct for this density by requiring a proper semi-classical quantization will be precisely equation (153) (up to some contribution coming from the region around $x = 0$; subtraction of this contribution could be considered as a regularization of the divergent sum (205) which is the finite-size-corrected integral equation arising from the NBA for the spin chain! This will thus prove the announced property relating finite size corrections and one-loop shift.

Consider for example the first summand in (209) (recall that $x \in \mathcal{C}_{23}$):

$$\sum_n \frac{1}{x - x_n^{23}} = \sum_n \oint_{x_n^{23}} \frac{\cot_{23}}{x-y}\frac{\mathrm{d}y}{2\pi\mathrm{i}} = \cot_{23} + \oint_{\mathcal{C}_{13}} \frac{\cot_{23}}{x-y}\frac{\mathrm{d}y}{2\pi\mathrm{i}} = \cot_{23} - \int_{\mathcal{C}_{13}} \frac{\Delta\cot_{12}}{x-y}\frac{\mathrm{d}y}{2\pi\mathrm{i}}. \tag{216}$$

Note that $\cot_{23}$ has branch cut singularities at $\mathcal{C}_{13}$ which we have to encircle when we blow up the contour, which leads to the second term. The first term comes from the pole at $x = y$.

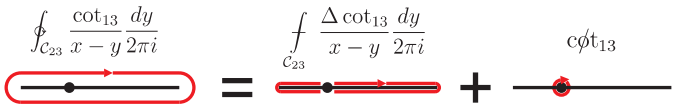

Figure 19. Illustration of an identity used in the main text.

Finally, to write the second term as it is we used (160). Analogously (see figure 19 for a pictorial explanation of the second equality),

$$\sum_n \frac{1}{x-x_n^{13}} = \oint_{\mathcal{C}_{23}} \frac{\cot_{13}}{x-y}\frac{\mathrm{d}y}{2\pi \mathrm{i}} = \mathrm{c}\not{\mathrm{o}}\mathrm{t}_{13} + \int_{\mathcal{C}_{23}} \frac{\Delta\cot_{13}}{x-y}\frac{\mathrm{d}y}{2\pi \mathrm{i}} = \mathrm{c}\not{\mathrm{o}}\mathrm{t}_{13} - \int_{\mathcal{C}_{23}} \frac{\Delta\cot_{12}}{x-y}\frac{\mathrm{d}y}{2\pi \mathrm{i}}. \tag{217}$$

Then we note that (see (162))

$$\mathrm{c}\not{\mathrm{o}}\mathrm{t}_{13} = \mathrm{c}\not{\mathrm{o}}\mathrm{t}_{12} = -\int_{\mathcal{C}_{13}\cup\mathcal{C}_{23}} \frac{\Delta\cot_{12}}{x-y}\frac{\mathrm{d}y}{2\pi \mathrm{i}}$$

so that (209) reads as

$$\frac{1}{x} + 2\int_{\mathcal{C}_{23}} \frac{\rho(y)}{x-y} + \int_{\mathcal{C}_{13}} \frac{\rho(y)}{x-y} + \frac{1}{2L}\left[2\cot_{23} - 2\int_{\mathcal{C}_{23}} \frac{\Delta\cot_{12}}{x-y}\frac{\mathrm{d}y}{2\pi \mathrm{i}} - 3\int_{\mathcal{C}_{13}} \frac{\Delta\cot_{12}}{x-y}\frac{\mathrm{d}y}{2\pi \mathrm{i}}\right] = 2\pi k_{23} + \phi_2 - \phi_3,$$

which in terms of the redefined density ϱ becomes

$$\frac{1}{x} + 2\int_{\mathcal{C}_{23}} \frac{\varrho(y)}{x-y} + \int_{\mathcal{C}_{13}} \frac{\varrho(y)}{x-y} + \frac{1}{L}\left[\cot_{23} - \int_{\mathcal{C}_{13}} \frac{\Delta\cot_{12}}{x-y}\frac{\mathrm{d}y}{2\pi \mathrm{i}}\right] = 2\pi k_{23} + \phi_2 - \phi_3,$$

which coincides precisely with (153) as announced above! Thus the finite size corrections to the charge of any given configuration will indeed be equal to the field theoretical prediction, that is, to the one-loop shift around the classical solution.

4.1.2. Generalization. Here, we consider a $\mathfrak{su}(n)$ NBA with the Dynkin labels V_a being +1 for a particular a only. In this section, we generalize the results from section 4.1.1. For the spin chain $\mathfrak{su}(n)$ NBA, in the classical limit, we will have n quasi-momenta, each above or below each of the $n-1$ Dynkin nodes[30]. We label these quasi-momenta by p_i (p_j) with i, i' (j, j') taking positive (negative) values for quasi-momenta above (below) the node for which $V_a \neq 0$. Then let us mention how the equations in the previous section are generalized. We consider a *middle node* cut $\mathcal{C}_{1,-1}$. Now the analogue of equation (209) is

$$-\frac{1}{x} + \sum_j \int_{\mathcal{C}_{1,j}} \frac{\delta\rho(y)}{x-y} + \sum_i \int_{\mathcal{C}_{i,-1}} \frac{\delta\rho(y)}{x-y} + \sum_{n=-N}^{N} \frac{1}{2L}\left[\sum_i \frac{1}{x-x_n^{i,-1}} + \sum_j \frac{1}{x-x_n^{1,j}}\right] = 0, \tag{218}$$

and the charges (210)–(212) and (214) become[31]

[30] See figure 20 for an example of such a pattern for a supergroup which clearly resembles $\mathfrak{su}(8)$.

[31] As in the previous section, we ignore the regularization of the charges coming from the contribution of the contour around the origin which would appear in the second line by opening the contours around the excitation points x_n^{ij}.

$$\mathcal{Q}_r - \int_{\mathcal{C}} \frac{\rho(y)}{y^r}\,\mathrm{d}y = +\sum_n \sum_{ij} \frac{1}{2L}\frac{1}{\left(x_n^{ij}\right)^r} = +\frac{1}{2L}\sum_{ij}\frac{1}{2J}\oint_{x_n^{ij}} \frac{\cot_{ij}}{y^r}\frac{\mathrm{d}y}{2\pi\mathrm{i}} \tag{219}$$

$$= +\frac{1}{2L}\sum_{ii'j}\oint_{\mathcal{C}_{i'j}} \frac{\cot_{ij}}{y^r}\frac{\mathrm{d}y}{2\pi\mathrm{i}} + \frac{1}{2L}\sum_{ijj'}\oint_{\mathcal{C}_{ij'}} \frac{\cot_{ij}}{y^r}\frac{\mathrm{d}y}{2\pi\mathrm{i}} \tag{220}$$

$$= -\frac{1}{2L}\sum_{ii'j}\oint_{\mathcal{C}_{i'j}} \frac{\cot_{ii'}}{y^r}\frac{\mathrm{d}y}{2\pi\mathrm{i}} - \frac{1}{2L}\sum_{ijj'}\oint_{\mathcal{C}_{ij'}} \frac{\cot_{jj'}}{y^r}\frac{\mathrm{d}y}{2\pi\mathrm{i}} \tag{221}$$

$$= -\frac{1}{2L}\int_{\mathcal{C}} \frac{\sum_{i<i'}\Delta\cot_{ii'} + \sum_{j<j'}\Delta\cot_{jj'}}{y^r}\frac{\mathrm{d}y}{2\pi\mathrm{i}}, \tag{222}$$

so that the natural definition of the dressed density now becomes

$$\varrho = \rho + \frac{1}{4L\pi\mathrm{i}}\Delta\left(\sum_{i<i'}\cot_{ii'} + \sum_{j<j'}\cot_{jj'}\right). \tag{223}$$

The next step is to rewrite the integral equation (218) in terms of this new density. We proceed exactly as in (216), (217) now using

$$\cot_{1,i} = -\sum_j \left(\mathcal{I}^{1i}_{1,j} + \mathcal{I}^{1i}_{i,j}\right), \qquad \mathcal{I}^{kl}_{ij} \equiv \int_{\mathcal{C}_{ij}} \frac{\cot_{kl}(y)}{x-y}\frac{\mathrm{d}y}{2\pi\mathrm{i}},$$

which is the analogue of (162) for this $\mathfrak{su}(n)$ setup, so that at the end we obtain the following equation:

$$\sum_j \int_{\mathcal{C}_{1,j}} \frac{\delta\varrho(y)}{x-y} + \sum_i \int_{\mathcal{C}_{i,-1}} \frac{\delta\varrho(y)}{x-y} + \frac{1}{L}\left(\cot_{1,-1} - \sum_{ij}\int_{\mathcal{C}_{ij}} \frac{\Delta\cot_{1,i} + \Delta\cot_{j,-1}}{x-y}\frac{\mathrm{d}y}{2\pi\mathrm{i}}\right) = 0 \tag{224}$$

for $\delta\varrho = \varrho - \varrho_0$ where ϱ_0 obeys the leading order equation

$$-\frac{1}{x} + \sum_j \int_{\mathcal{C}_{1,j}} \frac{\varrho_0(y)}{x-y} + \sum_i \int_{\mathcal{C}_{i,-1}} \frac{\varrho_0(y)}{x-y} = 2\pi k_{1,-1}. \tag{225}$$

This corrected equation is precisely the one we would obtain from finite size corrections to the $\mathfrak{su}(n)$ NBA equations. To find this equation from the Bethe ansatz point of view, one can simply repeat either of the derivations in section 2.2.1, that is, the known transfer matrices in various representations or the bosonic duality described in the previous sections. In section 4.2, we consider the AdS/CFT Bethe ansatz equations which are based on a large rank symmetry group, namely $PSU(2,2|4)$. There one can see an example of how this could be done explicitly.

4.2. Matching of finite size corrections and fluctuations in AdS/CFT

4.2.1. Middle node anomaly. In this section, we will expand the BS equations in the scaling limit for the roots belonging to a cut containing middle node roots x_4 only. We do not assume that all the other cuts are of the same type, rather they can be cuts of stacks of several sizes. In section 2.2.5, we will generalize the results obtained in this section to an arbitrary cut, assuming, as in the previous section, that the cuts are small enough and twists are not zero so that stacks are stable. We will discus in section 18 what happens when one takes all twists to zero.

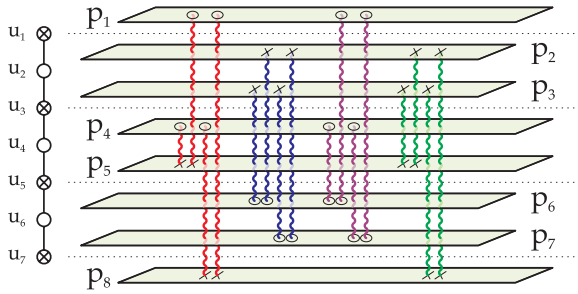

Figure 20. The several physical fluctuations in the string Bethe ansatz. The 16 elementary physical excitations are the stacks (bound states) containing the middle node root. From the left to the right, we have four S^5 fluctuations, four AdS_5 modes and eight fermionic excitations. The bosonic (fermionic) stacks contain an even (odd) number of fermionic roots represented by a cross in the $psu(2,2|4)$ Dynkin diagram in the left.

To leading order, the middle node equation (31) can simply be written as $\not{p}_4 - \not{p}_5 = 2\pi n$ while at one loop the first product on the rhs of (31) corrects this equation due to (62):

$$\frac{1}{\mathrm{i}} \log \prod_{j\neq k}^{K_4} \left(\frac{u_{4,k} - u_{4,j} + \mathrm{i}}{u_{4,k} - u_{4,j} - \mathrm{i}} \right) \simeq 2\not{F}_4(x) + \alpha(x)\pi\rho'(x)\cot(\pi\rho(x)), \tag{226}$$

where $F_4(x) = \sum_j^{K_4} \frac{1}{u(x)-u_{4,j}}$, $\rho(x) = \frac{\mathrm{d}k}{\mathrm{d}u_k}$. Expansion of the remaining terms in (31) will not lead to the appearance of such *anomaly*-like terms since the roots of other types are separated by ~ 1 from $x_{4,k}$. Thus, we simply have

$$2\pi n = \not{p}_4 - \not{p}_5 - \eta\alpha(x)\pi\rho'(x)\cot(\pi\rho(x)), \qquad x \in \mathcal{C}_{45}.$$

In the following sections, we will use dualities of the BS equations to get some extra information about the cuts of stacks and generalize the above equation to any possible type of cut. To achieve this, we shall recast this equation in terms of the middle node roots x_4 only. Finally, in this section we will use

$$\cot_{ij} \equiv \alpha(x)\frac{p_i' - p_j'}{2}\cot\frac{p_i - p_j}{2},$$

which is similar to (but should not be confused with) (152).

4.2.2. Dualities in the string Bethe ansatz. Obviously, the behavior of the Bethe roots will be as described in section 2.2 for a simpler example of a $\mathfrak{su}(1,2)$ spin chain, that is, we will have simple cuts made out of x_4 roots only and also cuts of stacks with x_2, x_3 and x_4 roots for example. Consider such a cut of stacks. Clearly, to be able to write the middle node equation (31) or (227) we need to compute the density mismatches $\rho_2 - \rho_3$ and $\rho_3 - \rho_4$ which are one-loop contributions we must take into account if we want to write an integral equation for the middle node equation in terms of the density ρ_4 of momentum-carrying roots only. In this section, we shall analyze the dualities present in the BS Bethe equations. By analyzing them in the scaling limit, we will then be able to derive the desired density mismatches.

Fermionic duality in the scaling limit. In [21], it was shown that the BS equations obey a very important fermionic duality. Since we chose to work with a subset of the possible Bethe equations, that is, those with $\eta_1 = \eta_2 = \eta$ present in [21], we should apply the duality present below not only to the fermionic roots x_1 and x_3 (as described below) but also to the Bethe

roots x_5 and x_7. Obviously, the duality for x_5 and x_7 is exactly the same as for x_1 and x_3 and so we will focus simply on the latter while keeping implicit that we always dualize all the fermionic roots at the same time.

We construct the polynomial ($\tau = \eta\,(\phi_4 - \phi_3)$)

$$P(x) = \mathrm{e}^{+\mathrm{i}\frac{\tau}{2}} \prod_{j=1}^{K_4} \big(x - x^+_{4,j}\big) \prod_{j=1}^{K_2} \big(x - x^-_{2,j}\big)\big(x - 1/x^-_{2,j}\big) - \mathrm{e}^{-\mathrm{i}\frac{\tau}{2}} \prod_{j=1}^{K_4} \big(x - x^-_{4,j}\big) \prod_{j=1}^{K_2} \big(x - x^+_{2,j}\big)\big(x - 1/x^+_{2,j}\big) \tag{227}$$

of degree $K_4 + 2K_2$ which clearly admits $x = x_{3,j}$ and $x = 1/x_{1,j}$ as $K_3 + K_1$ zeros[32]. The remaining $K_4 + 2K_2 - K_3 - K_1$ roots are denoted by $\tilde{x}_{3,j}$ or $1/\tilde{x}_{1,j}$ depending on whether they are outside or inside the unit circle respectively,

$$P(x) = 2\mathrm{i}\sin(\tau/2) \prod_{j=1}^{K_1} (x - 1/x_{1,j}) \prod_{j=1}^{\tilde{K}_1} (x - 1/\tilde{x}_{1,j}) \prod_{j=1}^{K_3} (x - x_{3,j}) \prod_{j=1}^{\tilde{K}_3} (x - \tilde{x}_{3,j}). \tag{228}$$

Then we can replace the roots $x_{1,j}, x_{3,j}$ by the roots $\tilde{x}_{1,j}, \tilde{x}_{3,j}$ in the BS equations provided we change the grading $\eta \to -\eta$ and interchange the twists $\phi_1 \leftrightarrow \phi_2$ and $\phi_3 \leftrightarrow \phi_4$. In fact, since we should also dualize the remaining fermionic roots, we should also change $\phi_5 \leftrightarrow \phi_6$ and $\phi_7 \leftrightarrow \phi_8$ and replace the remaining fermionic roots x_5 and x_7.

Since to the leading order $x^\pm \simeq x$, each root will belong to a stack which must always contain a momentum-carrying root x_4. Therefore, we have $\tilde{K}_1 = K_2 - K_1$ and $\tilde{K}_3 = K_2 + K_4 - K_3$. Thus, we label the Bethe roots as

$$\begin{aligned}
x_{1,j} &= x_{4,j} - \epsilon_{1,j}, && j = 1, \dots, K_1\\
\tilde{x}_{1,j} &= x_{4,j+K_1} - \tilde{\epsilon}_{1,j}, && j = 1, \dots, \tilde{K}_1\\
x_{2,j} &= x_{4,j} - \epsilon_{2,j}, && j = 1, \dots, K_2\\
x_{3,j} &= x_{4,j} - \epsilon_{3,j}, && j = 1, \dots, K_3\\
\tilde{x}_{3,j} &= x_{4,j+K_3} - \tilde{\epsilon}_{3,j}, && j = 1, \dots, \tilde{K}_3,
\end{aligned}$$

with $\epsilon \sim 1/\sqrt{\lambda}$. Dividing (227) and (228) by $\prod_{j=1}^{K_4}(x - x_{4,j}) \prod_{j=1}^{K_2}(x - x_{4,j})(x - 1/x_{4,j})$, we have

$$\mathrm{e}^{+\mathrm{i}\frac{\tau}{2}} \prod_{j=1}^{K_4} \frac{x - x^+_{4,j}}{x - x_{4,j}} \prod_{j=1}^{K_2} \frac{x - x^-_{2,j}}{x - x_{4,j}} \frac{x - 1/x^-_{2,j}}{x - 1/x_{4,j}} - \mathrm{e}^{-\mathrm{i}\frac{\tau}{2}} \prod_{j=1}^{K_4} \frac{x - x^+_{4,j}}{x - x_{4,j}} \prod_{j=1}^{K_2} \frac{x - x^+_{2,j}}{x - x_{4,j}} \frac{x - 1/x^+_{2,j}}{x - 1/x_{4,j}} = 2\mathrm{i}\sin(\tau/2) \prod_{j=1}^{K_1} \frac{x - 1/x_{1,j}}{x - 1/x_{4,j}} \prod_{j=1}^{\tilde{K}_1} \frac{x - 1/\tilde{x}_{1,j}}{x - 1/x_{4,K_1+j}} \prod_{j=1}^{K_3} \frac{x - x_{3,j}}{x - x_{4,j}} \prod_{j=1}^{\tilde{K}_3} \frac{x - \tilde{x}_{3,j}}{x - x_{4,K_3+j}}. \tag{229}$$

In this form, it is easy to expand the duality relation in powers of $1/\sqrt{\lambda}$. By expanding all factors in (229) such as

$$\prod_{j=1}^{K_2} \frac{x - x^\pm_{2,j}}{x - x_{4,j}} = \exp\left(\sum_{j=1}^{K_2} \log \frac{x - x^\pm_{2,j}}{x - x_{4,j}}\right) \simeq \exp\left(\mp\frac{\mathrm{i}}{2} G_2(x) + \sum_{j}^{K_2} \frac{\epsilon_{2,j}}{x - x_{2,j}}\right),$$

[32] We also have $1/x_1$ zeros because, due to (32), the equation for $x_{1,j}$ is the same as the equation for $x_{3,j}$ if we replace $x_{3,j}$ by $1/x_{1,j}$. This is why the restriction (32) of the twists is so important.

we find

$$\sin\left(\frac{\eta(p_4-p_3)}{2}\right)=\sin\left(\frac{\tau}{2}\right)\exp\left(+\sum\frac{\epsilon_3}{x-x_3}+\sum\frac{\tilde{\epsilon}_3}{x-x_3}-\sum\frac{\epsilon_2}{x-x_2}\right)$$
$$\times\exp\left(-\sum\frac{\epsilon_1/x_1^2}{x-1/x_1}-\sum\frac{\tilde{\epsilon}_1/\tilde{x}_1^2}{x-1/\tilde{x}_1}+\sum\frac{\epsilon_2/x_2^2}{x-1/x_2}\right).$$

Then, similar to what we had in section 2.2.3 for the bosonic duality, we note that

$$\alpha(x)\partial_x\left(\sum\frac{\epsilon_3}{x-x_3}+\sum\frac{\tilde{\epsilon}_3}{x-\tilde{x}_3}-\sum\frac{\epsilon_2}{x-\tilde{x}_2}\right)=H_3+H_{\bar{3}}-H_4-H_2,$$

with a similar expression for the argument of the second exponential. Thus, finally, we get

$$(H_4+H_2-H_3-H_{\bar{3}})+(\bar{H}_2-\bar{H}_1-\bar{H}_{\bar{1}})=-\mathrm{cot}_{34}$$

or, alternatively, using the $x\to 1/x$ symmetry transformation properties of the quasi-momenta,

$$(\bar{H}_4+\bar{H}_2-\bar{H}_3-\bar{H}_{\bar{3}})+(H_2-H_1-H_{\bar{1}})=-\mathrm{cot}_{12}\,.$$

From these expressions, we can deduce several properties of the density mismatches we wanted to obtain. For example, if we compute the discontinuity of (4.2.2) at a cut containing roots x_1, that is, in a large cut of stacks $\mathcal{C}_{1,i>4}$, we immediately get

$$\rho_1-\rho_2=-\frac{\Delta\,\mathrm{cot}_{12}}{2\pi\mathrm{i}},\qquad x\in\mathcal{C}_{1,i>4}. \tag{230}$$

Proceeding in a similar way, we find

$$\rho_3-\rho_4=-\frac{\Delta\,\mathrm{cot}_{34}}{2\pi\mathrm{i}},\qquad x\in\mathcal{C}_{3,i>4}, \tag{231}$$

$$\rho_3-\rho_4=\rho_2-\rho_{\bar{3}},\qquad x\in\mathcal{C}_{1,i>4}\cup\mathcal{C}_{2,i>4}. \tag{232}$$

Let us now show that in the scaling limit, the fermionic duality corresponds just to the exchange of the sheets $\{p_i\}$ of the Riemann surface. For illustration, let us pick p_1 and see how it transforms under the duality. By definition the fermionic duality corresponds to the replacement $\eta\to-\eta$, $H_1\to H_{\bar{1}}$, $H_3\to H_{\bar{3}}$ and $\phi_1\leftrightarrow\phi_2$, $\phi_3\leftrightarrow\phi_4$, so that

$$p_1\to\frac{2\pi\mathcal{J}x-\delta_{\eta,-1}Q_1+\delta_{\eta,+1}Q_2x}{x^2-1}-\eta(-H_{\bar{1}}-\bar{H}_{\bar{3}}+\bar{H}_4)+\phi_2=p_2+\eta\,\mathrm{cot}_{12}$$

In the same way we get

$$p_2\to p_1+\eta\,\mathrm{cot}_{12},\qquad p_3\to p_4-\eta\,\mathrm{cot}_{34},\qquad p_4\to p_3-\eta\,\mathrm{cot}_{34},$$

and since $\mathrm{cot}_{ij}\sim 1/\sqrt{\lambda}$ we see that to the leading order the duality indeed just exchanges the sheets.

Bosonic duality in the scaling limit. The bosonic nodes of the BS equations are precisely as in the usual Bethe ansatz discussed in the first sections, so we can just briefly mention the results. The duality ($\tau=\eta(\phi_2-\phi_3)$)

$$\mathrm{e}^{+\mathrm{i}\frac{\tau}{2}}\tilde{Q}_2(u-\mathrm{i}/2)Q_2(u+\mathrm{i}/2)-\mathrm{e}^{-\mathrm{i}\frac{\tau}{2}}\tilde{Q}_2(u+\mathrm{i}/2)Q_2(u-\mathrm{i}/2)=2\mathrm{i}\sin\frac{\tau}{2}Q_1(u)Q_3(u)$$

leads to

$$(H_1+H_3-H_2-H_{\bar{2}})+(\bar{H}_1+\bar{H}_3-\bar{H}_2-\bar{H}_{\bar{2}})=\mathrm{cot}_{23}, \tag{233}$$

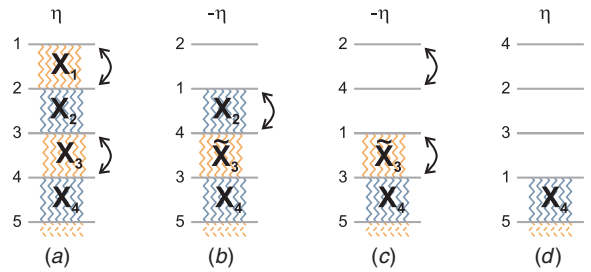

Figure 21. Action of the duality on a long stack. By successively applying the fermionic and the bosonic dualities, we can reduce the size of any large cut. One should not forget to change the sign of the grading η after applying the fermionic duality.

which implies

$$\rho_2 - \rho_3 = +\frac{\Delta\,\mathrm{cot}_{23}}{2\pi\,\mathrm{i}}, \qquad x \in \mathcal{C}_{2,i>4}.$$

As we already discussed in section 2.2, the bosonic duality also amounts to an exchange of Riemann sheets. Indeed, under the replacement $H_2 \to H_{\tilde{2}}$ and $\phi_2 \leftrightarrow \phi_3$, we find

$$p_2 \to p_3 - \eta\,\mathrm{cot}_{23}, \qquad p_3 \to p_2 + \eta\,\mathrm{cot}_{23},$$

which again, to the leading order in $\sqrt{\lambda}$, is just the exchange of the sheets of the curve.

Dualities and the missing mismatches. Using bosonic and fermionic dualities separately, we already got some information about the several possible mismatches of the densities inside the stack. To compute the missing mismatches, we have to use both dualities together. For example, suppose we want to compute $\rho_3 - \rho_4$ in a cut $\mathcal{C}_{1,i>4}$. We start by one such large cut of stacks (see figure 21(*a*)) and we apply the fermionic duality to this configuration so that we obtain a smaller cut as depicted in figure 21(*b*). For this configuration, we can use (4.2.2) to get

$$\rho_2 - \rho_{\tilde{3}} = +\frac{\Delta\,\mathrm{cot}_{14}}{2\pi\,\mathrm{i}}.$$

However, from (232), this is also equal to the mismatch we wanted to compute, that is,

$$\rho_3 - \rho_4 = +\frac{\Delta\,\mathrm{cot}_{14}}{2\pi\,\mathrm{i}}, \qquad x \in \mathcal{C}_{1,i>4}.$$

To compute the last mismatch, we apply the bosonic duality to get a yet smaller cut as in figure 21(*c*) for which we use (231) to get

$$\rho_{\tilde{3}} - \rho_4 = -\frac{\Delta\,\mathrm{cot}_{13}}{2\pi\,\mathrm{i}}.$$

Again, from (232), we can revert this result into a mismatch for the configuration before duality, that is,

$$\rho_2 - \rho_3 = -\frac{\Delta\,\mathrm{cot}_{13}}{2\pi\,\mathrm{i}}, \qquad x \in \mathcal{C}_{1,i>4}.$$

Let us then summarize all density mismatches in table 4.

Table 4. Density mismatches.

	$\mathcal{C}_{1,i}$	$\mathcal{C}_{2,i}$	$\mathcal{C}_{3,i}$
$2\pi\mathrm{i}(\rho_1-\rho_2)$	$-\Delta\cot_{12}$		
$2\pi\mathrm{i}(\rho_2-\rho_3)$	$-\Delta\cot_{13}$	$+\Delta\cot_{23}$	
$2\pi\mathrm{i}(\rho_3-\rho_4)$	$+\Delta\cot_{14}$	$-\Delta\cot_{24}$	$-\Delta\cot_{34}$

4.2.3. Integral equation. In this section, we shall recast equation (227) or

$$\eta\frac{4\pi\mathcal{J}x-2\delta_{\eta,+1}\mathcal{Q}_1-2\delta_{\eta,-1}\mathcal{Q}_2x}{x^2-1}+2H\!\!\!/_4-H_3-H_5-\bar{H}_1-\bar{H}_7 \\ =2\pi n+\eta\phi_4-\eta\phi_5-\cot_{45} \tag{234}$$

in terms of the density $\rho_4(x)$ of the middle roots x_4. To do so, we only need to replace the several densities by the middle node density $\rho_4(x)$ using the several density mismatches presented in table 4. Defining

$$H_{ij}(x)\equiv\int_{\mathcal{C}_{ij}}\frac{\alpha(x)}{\alpha(y)}\frac{\rho_4(y)}{x-y}\,\mathrm{d}y,$$

we can then rewrite equation (234) in terms of the middle node roots only:

$$\eta\frac{4\pi\mathcal{J}x-2\delta_{\eta,+1}\mathcal{Q}_1-2\delta_{\eta,-1}\mathcal{Q}_2x}{x^2-1}+2H\!\!\!/_{45}+H_{15}+H_{48}-2\bar{H}_{18}-\bar{H}_{15}-\bar{H}_{48} \\ =2\pi n+\eta\phi_4-\eta\phi_5-\cot_{45}+\sum_{\substack{1\leqslant i\leqslant 4\\ 5\leqslant j\leqslant 8}}\left(\mathcal{I}_{ij}^{i4}+\mathcal{I}_{ij}^{5j}\right)+\sum_{\substack{1\leqslant i\leqslant 4\\ 5\leqslant j\leqslant 8}}\left(\bar{\mathcal{I}}_{1j}^{i1}+\bar{\mathcal{I}}_{i8}^{8j}\right), \tag{235}$$

where $x\in\mathcal{C}_{45}$ and

$$\mathcal{I}_{ij}^{kl}(x)=(-1)^{F_{kl}}\int_{\mathcal{C}_{ij}}\frac{\alpha(x)}{\alpha(y)}\frac{\Delta\cot_{kl}}{x-y}\frac{\mathrm{d}y}{2\pi\mathrm{i}},\qquad \mathcal{I}_{ij}^{kk}(x)\equiv 0,\qquad \bar{\mathcal{I}}_{ij}^{kl}(x)=\mathcal{I}_{ij}^{kl}(1/x).$$

The several dualities amount to an exchange of Riemann sheets so that the cuts $\mathcal{C}_{ij}\to\mathcal{C}_{i'j'}$ with the subscripts in H_{ij} changing accordingly. The middle roots x_4 are never touched in the process. Moreover, to leading order, $p_i\leftrightarrow p_{i'}$ and thus the rhs of (235) is also trivially changed under the dualities. Therefore, as in section 2.2.1 (see (153) and (154)), we can now trivially write the corrected equation when x belongs to any possible type of cut of stacks by applying the several dualities to equation (235).

4.2.4. Fluctuations. In this section, we shall find the integral equation (235) from the field theoretical point of view like we did in section 4.1.1. That is, we will find what the corrections to the classical (leading order) equations [14]

$$\eta\frac{4\pi\mathcal{J}x-2\delta_{\eta,+1}\mathcal{Q}_1-2\delta_{\eta,-1}\mathcal{Q}_2x}{x^2-1}+2H\!\!\!/_4-H_3-H_5-\bar{H}_1-\bar{H}_7=2\pi n+\eta\phi_4-\eta\phi_5, \tag{236}$$

should be in order to describe properly the semi-classical quantization of the string (and not only the classical limit). We will find that this construction leads precisely to the integral equation (235), thus showing that the BS nested Bethe ansatz equations do reproduce the one-loop shift around any (stable) classical solution with exponential precision (in some large charge of the classical solution). This section is very similar to section 4.1.1 and thus we will often omit lengthy but straightforward intermediate steps. We assume $i=1,\ldots,4$ and $j=5,\ldots,8$ in all sums.

As in (209) and (218), we add $\frac{1}{2}(-1)^F$ of a virtual excitation for each possible mode number n and polarization ij to each quasi-momenta. Note that for this super-symmetric model, the fluctuations can also be fermionic and indeed the grading $(-1)^F$ equals +1 (-1) for bosonic (fermionic) fluctuations (see figure 20) as usual for bosonic (fermi-onic) harmonic oscillators.

We denote $\rho = \rho_0 + \delta\rho$ where ρ_0 is the leading density, the solution of the leading (classical) equation (236), while ρ obeys the corrected (semi-classical) equation. For example, if we consider $x \in \mathcal{C}_{4,5}$, the starting point should be (see [93] for a similar analysis)

$$\begin{aligned}0 = {}& \frac{-2x\delta_{\eta,-1}\delta\mathcal{Q}_1}{x^2-1} + 2\int_{\mathcal{C}_{45}} \frac{\alpha(x)}{\alpha(y)}\frac{\delta\rho(y)}{x-y} + \int_{\mathcal{C}_{15}} \frac{\alpha(x)}{\alpha(y)}\frac{\delta\rho(y)}{x-y} + \int_{\mathcal{C}_{48}} \frac{\alpha(x)}{\alpha(y)}\frac{\delta\rho(y)}{x-y} \\ & - 2\int_{\mathcal{C}_{18}} \frac{\alpha(1/x)}{\alpha(y)}\frac{\delta\rho(y)}{1/x-y} - \int_{\mathcal{C}_{15}} \frac{\alpha(1/x)}{\alpha(y)}\frac{\delta\rho(y)}{1/x-y} - \int_{\mathcal{C}_{48}} \frac{\alpha(1/x)}{\alpha(y)}\frac{\delta\rho(y)}{1/x-y} + \sum_{n=-N}^{N}\frac{1}{2} \\ & \times \left[\sum_{i\leqslant 4}\frac{(-1)^{F_{i5}}\alpha(x)}{x-x_n^{i5}} + \sum_{j\geqslant 5}\frac{(-1)^{F_{4j}}\alpha(x)}{x-x_n^{4j}} - \sum_{i\leqslant 4}\frac{(-1)^{F_{i8}}\alpha(1/x)}{1/x-x_n^{i8}} - \sum_{j\geqslant 5}\frac{(-1)^{F_{1j}}\alpha(1/x)}{1/x-x_n^{1j}}\right].\end{aligned} \tag{237}$$

Then, by construction, the charges

$$\mathcal{Q}_r = \int_{\mathcal{C}}\frac{\rho(y)}{y^r}\,\mathrm{d}y + \sum_n\sum_{ij}(-1)^{F_{ij}}\frac{\alpha\left(x_n^{ij}\right)}{2\left(x_n^{ij}\right)^r} = \int_{\mathcal{C}}\frac{\rho(y)}{y^r}\,\mathrm{d}y + \sum_{ij}\frac{(-1)^{F_{ij}}}{2}\oint_{x_n^{ij}}\frac{\cot_{ij}}{y^r}\frac{\mathrm{d}y}{2\pi\mathrm{i}} \tag{238}$$

will take the $1/\sqrt{\lambda}$-corrected values. It is clear that, as before, we do not include the new *virtual* excitations in the density $\rho(x)$. Similar to (215) and (223), if we want the charges to have the standard form

$$\mathcal{Q}_r = \int\frac{\varrho(y)}{y^r}\,\mathrm{d}y,$$

we must redefine the density as

$$\varrho = \rho + \frac{1}{4\pi\mathrm{i}}\left(\sum_{i<i'\leqslant 4}(-1)^{F_{ii'}}\Delta\cot_{ii'} + \sum_{j>j'\geqslant 5}(-1)^{F_{jj'}}\Delta\cot_{jj'}\right).$$

Now we want to go back to the integral equation (237) and rewrite it using the density $\delta\varrho = \varrho - \rho_0$. For example, for $x \in \mathcal{C}_{45}$,

$$\begin{aligned}& 2\int_{\mathcal{C}_{45}}\frac{\alpha(x)}{\alpha(y)}\frac{\delta\rho(y)}{x-y} + \int_{\mathcal{C}_{15}}\frac{\alpha(x)}{\alpha(y)}\frac{\delta\rho(y)}{x-y} + \int_{\mathcal{C}_{48}}\frac{\alpha(x)}{\alpha(y)}\frac{\delta\rho(y)}{x-y} \\ & \qquad + \sum_{n=-N}^{N}\frac{1}{2}\left[\sum_i\frac{(-1)^{F_{i5}}\alpha(x)}{x-x_n^{i5}} + \sum_j\frac{(-1)^{F_{4j}}\alpha(x)}{x-x_n^{4j}}\right] \\ & = 2\int_{\mathcal{C}_{45}}\frac{\alpha(x)}{\alpha(y)}\frac{\delta\varrho(y)}{x-y} + \int_{\mathcal{C}_{15}}\frac{\alpha(x)}{\alpha(y)}\frac{\delta\varrho(y)}{x-y} + \int_{\mathcal{C}_{48}}\frac{\alpha(x)}{\alpha(y)}\frac{\delta\varrho(y)}{x-y} \\ & \qquad + \cot_{45} - \sum_{ij}\left(\mathcal{I}_{ij}^{4i} + \mathcal{I}_{ij}^{j5}\right) - \frac{1}{2}\sum_{ij}\left(\bar{\mathcal{I}}_{8j}^{8i} + \bar{\mathcal{I}}_{1i}^{1j} + \bar{\mathcal{I}}_{ij}^{8i} + \bar{\mathcal{I}}_{ij}^{1j}\right),\end{aligned}$$

where the identity

$$(-1)^{F_{4i}}\cot_{4,i} = -\sum_j\left(\mathcal{I}_{4j}^{4i} + \mathcal{I}_{ij}^{4i}\right) - \sum_j\left(\bar{\mathcal{I}}_{1j}^{1\bar{i}} + \bar{\mathcal{I}}_{\bar{i}j}^{1\bar{i}}\right),$$

where $\bar{\bar{i}} = i$, $\bar{1} = 4$, $\bar{2} = 3$ are being used. Now, when $x \in \mathcal{C}_{18}$, we will get

$$2\int_{\mathcal{C}_{18}} \frac{\alpha(x)}{\alpha(y)}\frac{\delta\rho(y)}{x-y} + \int_{\mathcal{C}_{15}} \frac{\alpha(x)}{\alpha(y)}\frac{\delta\rho(y)}{x-y} + \int_{\mathcal{C}_{48}} \frac{\alpha(x)}{\alpha(y)}\frac{\delta\rho(y)}{x-y}$$
$$+ \sum_{n=-N}^{N} \frac{1}{2}\left[\sum_i \frac{(-1)^{F_{i8}}\alpha(x)}{x - x_n^{i8}} + \sum_j \frac{(-1)^{F_{1j}}\alpha(x)}{x - x_n^{1j}}\right]$$
$$= 2\int_{\mathcal{C}_{18}} \frac{\alpha(x)}{\alpha(y)}\frac{\delta\varrho(y)}{x-y} + \int_{\mathcal{C}_{15}} \frac{\alpha(x)}{\alpha(y)}\frac{\delta\varrho(y)}{x-y} + \int_{\mathcal{C}_{48}} \frac{\alpha(x)}{\alpha(y)}\frac{\delta\varrho(y)}{x-y}$$
$$- \frac{1}{2}\sum_{ij}\left(\mathcal{I}_{ij}^{1i} + \mathcal{I}_{ij}^{j8} - \mathcal{I}_{8j}^{8i} - \mathcal{I}_{1i}^{1j}\right).$$

Finally we can use the x to $1/x$ symmetry to translate the last equality into one for $x \in \mathcal{C}_{45}$. Subtracting it from the previous equation, we see that the $1/\sqrt{\lambda}$-corrected equation will correspond to adding

$$-\mathrm{cot}_{45} + \sum_{ij}\left(\mathcal{I}_{ij}^{4i} + \mathcal{I}_{ij}^{5i} + \bar{\mathcal{I}}_{1j}^{1i} + \bar{\mathcal{I}}_{8i}^{8j}\right)$$

to the rhs of (236) thus obtaining, after the identification $\varrho = \rho_4$, precisely the finite-size-corrected equation (235) obtained from the NBA point of view!

In this section, we showed that the one-loop shift as a sum of all fluctuation energies (or other local charges) perfectly matches the finite size corrections in the NBA equations. However we systematically dropped the contours around the unit circle. In the following section, we will accurately take it into account.

4.3. The unit circle and the Hernandez–Lopez phase

Consider again the sum in equation (237). We can rewrite it as an integral around each x_n^{ij} and then blow the contour to encircle all the singularities of cot_{ij} and the circle going through the points x_N^{ij} and x_{-N}^{ij}, which are close to 1 and -1 correspondingly. In the previous section, we have already considered the contributions coming from the contours encircling the cuts of cot_{ij} and showed that they reproduce the finite size corrections in the BS equations. Let us show that the unit circle contributions account for the HL phase factor. We will drop systematically the contributions considered in the previous section:

$$\sum_{n=-N}^{N}\frac{1}{2}\left[\sum_{i\leqslant 4}\frac{(-1)^{F_{i5}}\alpha(x)}{x - x_n^{i5}} + \sum_{j\geqslant 5}\frac{(-1)^{F_{4j}}\alpha(x)}{x - x_n^{4j}} - \sum_{i\leqslant 4}\frac{(-1)^{F_{i8}}\alpha(1/x)}{1/x - x_n^{i8}} - \sum_{j\geqslant 5}\frac{(-1)^{F_{1j}}\alpha(1/x)}{1/x - x_n^{1j}}\right]$$
$$= \frac{1}{2}\left[\sum_{i\leqslant 4}\oint \frac{\alpha(x)}{\alpha(y)}\frac{(-1)^{F_{i5}}\,\mathrm{cot}_{i5}}{x-y}\frac{\mathrm{d}y}{2\pi\,\mathrm{i}} + \cdots\right]. \tag{239}$$

Now let us assume that we can replace $\cot\left(\frac{p_i(x)-p_j(x)}{2}\right)$ by $\mathrm{i}\,\mathrm{sign}(\mathrm{Im}\,x)$ everywhere with exponential precision in $\frac{L}{\sqrt{\lambda}} \gg 1$. This is reasonable for generic points in the unit circle, where the imaginary part of $p_i(x) - p_j(x)$ is large, but one has to carefully analyze the neighborhood of the real axis, where this imaginary part vanishes. We will analyze this step carefully in the following section. Assuming that this could be done, we will get

$$\frac{1}{2}\left[\sum_{i\leqslant 4}\oint \alpha(x)\frac{(-1)^{F_{i5}}(p_i' - p_5')}{x-y}\,\mathrm{sign}(\mathrm{Im}\,y)\frac{\mathrm{d}y}{2\pi} + \cdots\right]$$

$$= \oint \left[\frac{\alpha(x)}{x-y} - \frac{\alpha(1/x)}{1/x-y} \right] (p_4' - p_3' - p_2' + p_1') \operatorname{sign}(\operatorname{Im} y) \frac{\mathrm{d}y}{2\pi} = -2\eta \mathcal{V}(x). \tag{240}$$

Finally, as we can see from (46), the combination of quasi-momenta appearing in (240) is precisely the one from which one reads the local charges Q_n,

$$p_4' - p_3' - p_2' + p_1' = -\eta \partial_y \left[G_4(y) - G_4(1/y) \right], \tag{241}$$

where

$$G_4(y) = -\sum_{n=0}^{\infty} \mathcal{Q}_{n+1} y^n, \tag{242}$$

so that we can expand the denominators in (240) for large x and obtain

$$\mathcal{V}(x) = \alpha(x) \sum_{\substack{r,\, s\, =\, 2 \\ r+s \,\in\, \text{Odd}}}^{\infty} \frac{1}{\pi} \frac{(r-1)(s-1)}{(s-r)(r+s-2)} \left(\frac{\mathcal{Q}_r}{x^s} - \frac{\mathcal{Q}_s}{x^r} \right), \tag{243}$$

where we recognize precisely the Hernandez–Lopez coefficients! To obtain the values of the potential for $|x| < 1$, we can simply use the exact symmetry $\mathcal{V}(x) = -\mathcal{V}(1/x)$ which is not manifest in form (243).

Unit circle contribution. In this section, we show that for the 'unit circle' contribution we can replace $\cot_{ij}$ by $\mathrm{i} \operatorname{sign} \operatorname{Im}(x)$ if the ratio $L/\sqrt{\lambda}$ is large.

Let us focus on the vicinity of $x = 1$ where we have the following expansion of the quasi-momenta:

$$\frac{p_i(x) - p_j(x)}{2} = \frac{\beta_{ij}}{x-1} + \cdots,$$

where β_{ij} is usually of order $L/\sqrt{\lambda}$. We will consider the circle with radius $x^{ij}_{N+1/2} \simeq 1 + \frac{1}{\pi N \beta_{ij}}$, where N is some large cutoff in the sum of fluctuations (237). We want to estimate

$$\int \alpha(x) f(x) \left[\cot\left(\frac{p_i - p_j}{2} \right) + \mathrm{i} \operatorname{sign}(\operatorname{Im} x) \right] (p_i' - p_j') \, \mathrm{d}x.$$

This integral is dominated for $x \simeq \pm 1$ and can be performed by the saddle point. The contribution for $x \simeq 1$ is

$$\int \alpha(x) f(x) \left[\cot\left(\frac{p_i - p_j}{2} \right) + \mathrm{i} \operatorname{sign}(\operatorname{Im} x) \right] (p_i' - p_j') \, \mathrm{d}x = \frac{\mathrm{i}\pi^3 f(1)}{6\beta_{ij}\sqrt{\lambda}} + \mathcal{O}\left(\frac{1}{N} \right),$$

which is zero under the sum over all polarizations. For example,

$$\frac{(-1)^{F_{45}}}{\beta_{45}} = -\frac{(-1)^{F_{35}}}{\beta_{35}}.$$

Thus, we can indeed can replace cot's when integrating over the unit circle by a simple sign function. In the appendix G, we will carefully analyze the $N \to \infty$ limit and the numbering of the frequencies problem.

Summary. Although we always assumed the twists to be sufficiently large and the fillings to be sufficiently small, we can always analytically continue the results toward zero twists or large filling fractions. Let us briefly explain why. In the scaling limit, for large twists, the bosonic duality we introduced amounts to a simple exchange of sheets in some Riemann surface, $p_a(x) \leftrightarrow p_b(x)$. As we saw in section 2.2.5, what happens when the twists start to become very small is that the quasi-momenta are still simply exchanged but in a piecewise

manner, that is, we can always split the complex planes in some finite number of regions where the bosonic duality simply means $p_a(x) \leftrightarrow p_b(x)$. Thus, from the e^{ip} algebraic curve point of view nothing special occurs for what analyticity is concerned and therefore we can safely analytically continue our findings to any value of the twists. Exactly the same analysis holds for the filling fractions. Moreover, for the usual Bethe system, we defined a set of quasi-momenta, which constitute an algebraic curve to any order in $1/L$, and therefore we do not expect analyticity to break down at any order in $1/L$.

We also preformed a high precision numerical check concluding that there is no singularity when the configuration of the Bethe roots is affected by this partial reshuffling of the sheets and that finite size corrections are still related to the same sum of fluctuations, which are analytical functions w.r.t. the twists.

5. Relativistic bootstrap approach in AdS/CFT

The classical integrable two-dimensional nonlinear sigma models are relatively easy to solve. At least, when the corresponding Lax pair is known, one can construct a large class of the so-called classical finite gap solutions [94]. These solutions are known to constitute a dense (in the sense of parameters of initial conditions) subset in the space of solutions of the model.

However, the quantization of such classically integrable sigma models usually creates substantial problems and is known to be virtually impossible to do in the direct way, in terms of the original degrees of freedom of the classical action. The existing quantum solutions are usually based on plausible assumptions which are difficult to prove in a systematic way.

There were a few successful, though not completely justified, attempts to find the quantum solutions of the $SU(N)$ principal chiral field model (PCF), starting from the original action. Zamolodchikov and Zamolodchikov [95] found the factorizable bootstrap S-matrices for the $O(N)$ sigma models, later generalized to many other sigma models. The $O(4)$ case on which we focused in this section is equivalent to the $SU(2)$ PCF. Polyakov and Wiegmann [96] and Wiegmann [97] found the equivalent non-relativistic integrable Thirring model reducible in a special limit to the PCF. Faddeev and Reshetikhin [98] proposed the 'equivalent' double spin chain for the $SU(2)$ PCF. In both cases, the equivalence is based on subtle assumptions, difficult to verify.

The verification of such solutions is usually based on the perturbation theory, large N limit or Monte Carlo simulations [95, 99–101].

Here, we address this question in a more systematic way. Namely, we will reproduce all classical finite gap solutions of a sigma model from the Bethe ansatz solution for a system of physical particles on the space circle, in a special large density and large energy limit. We shall call it the continuous limit though, as we show, it is the actual classical limit of the theory. We will see that in this limit, the BAEs diagonalizing the periodicity condition will be reduced to a Riemann–Hilbert problem. This section is inspired by Mann and Polchinski [102] and contains many original results.

In [90], we also repeated this construction for the $O(6)$ sigma model and explained how the generalization to the $O(2n)$ model can be done in a trivial way. In fact, as will be clear below, the method seems to be general enough to work for all sigma models described by a factorizable bootstrap S-matrix. Hence it gives a new way to relate, in a general and systematic way, the classical and quantum integrability.

The classical action of the $SU(2)$ PCF is

$$S = \frac{\sqrt{\lambda}}{8\pi} \int d\sigma\, d\tau\ \mathrm{tr}\ \partial_a g^\dagger \partial_a g, \qquad g \in SU(2). \tag{244}$$

It is equivalent to the $O(4)$ sigma model where the fundamental field is the four-dimensional unit vector $\vec{X}(\sigma, \tau)$. Therefore, at least classically, it can be used to study a string on the $S^3 \times R_1$ background. Indeed, our main motivation for this study was the search for new approaches in the quantization of the Green–Schwarts–Metsaev–Tseytlin superstring on $AdS_5 \times S^5$ which is classically (and most likely quantum-mechanically as well) an integrable field theory as we discussed in section 1. The simplest nontrivial sub-sector of it is described by the sigma model on the subspace $S^3 \times R_t$, where R_t is the coordinate corresponding to the AdS time. The time direction will be almost completely decoupled from the dynamics of the rest of the string coordinates, appearing only through the Virasoro conditions. These conditions are a selection rule for the states of the theory or, better to say, for the classical solutions appearing when we pick the classical limit in Bethe equations. The degrees of freedom eliminated in this way are the longitudinal modes associated with the reparameterization invariance of the string.

Of course, in the absence of the fermions and of the AdS part of the full 10D superstring theory, this model will be asymptotically free and will not be suitable to describe the quantum string theory. Nevertheless, in the classical limit we shall encounter the full finite gap solution of the string in the $SO(4)$ sector found in [18]. The method can be generalized to the $SO(6)$ sector in [15] and hopefully to the full Green–Schwarts–Metsaev–Tseytlin superstring on the $AdS_5 \times S^5$ space, including fermions, where the finite gap solution was constructed in [15] (although it appears to be more difficult for the last, and the most interesting, system).

At the end of this paper, we go slightly further and derive from these BAEs the conjectured asymptotic string Bethe ansatz (the so-called AFS equation [20]) with its nontrivial dressing factor to the leading order in large λ. According to the quasi-classical analysis in the previous sections, it captures the information about the quantum spectrum up to the $1/\sqrt{\lambda}$ order for large $L/\sqrt{\lambda}$.

5.1. Classical $SU(2)$ principal chiral field

In this section, we will review the classical finite gap solution of the $SU(2)$ principal chiral field. This construction can be obtained by the reduction of the full $PSU(2, 2|4)$ algebraic curve constructed in the introduction to the $SU(2)$ sub-sector. This can be achieved by dropping all quasi-momenta except $\tilde{p}_2$ and $\tilde{p}_3$. But for self-consistency of this section and to fix some notations, we will go through the construction of [18][33] for the easy comparison with the quantum Bethe ansatz solution of the model.

Classically, this model can be used to describe the string on $S^3 \times R_t \subset AdS_5 \times S^5$. At the quantum level, even dropping all the rest of the degrees of freedom, one might still expect to capture some features of the full superstring theory. As we will see in the later sections, this is indeed the case.

The action (244) possesses the obvious global symmetry under the right and left multiplication by the $SU(2)$ group element. The currents associated with this symmetry are, respectively,

$$j^R \equiv j = g^{-1}dg, \qquad j^L = dgg^{-1}, \tag{245}$$

and the corresponding Noether charges read as

$$Q_R = \frac{i\sqrt{\lambda}}{4\pi}\int_0^{2\pi} d\sigma \ \mathrm{tr}\left(j_\tau^R \tau^3\right), \qquad Q_L = \frac{i\sqrt{\lambda}}{4\pi}\int_0^{2\pi} d\sigma \ \mathrm{tr}\left(j_\tau^L \tau^3\right). \tag{246}$$

In the quantum theory, these charges are positive integers[34].

[33] With a little generalization to the excitations of both left and right sectors.

[34] For future comparisons, tt will be important to note that the normalization of the generators is such that the smallest possible charge is 1 as follows from the Poisson brackets for the current.

Virasoro conditions read as $\mathrm{tr}\,(j_\tau \pm j_\sigma)^2 = -2\kappa_\pm^2$, where we used the residual reparameterization symmetry to fix the AdS global time Y to

$$Y = \frac{\kappa_+}{2}(\tau+\sigma) + \frac{\kappa_-}{2}(\tau-\sigma). \tag{247}$$

Finally, from the action, we read off the energy and momentum as

$$E^{\rm cl} \pm P^{\rm cl} = -\frac{\sqrt{\lambda}}{8\pi}\int_0^{2\pi} \mathrm{tr}\,(j_\tau \pm j_\sigma)^2\,\mathrm{d}\sigma = \frac{\sqrt{\lambda}}{2}\kappa_\pm^2. \tag{248}$$

5.1.1. Classical integrability and finite gap solution. The equations of motion can be encoded into a single flatness condition for a Lax connection over the worldsheet [94]:

$$\left[\partial_\sigma - \frac{x j_\tau + j_\sigma}{x^2-1}, \partial_\tau - \frac{x j_\sigma + j_\tau}{x^2-1}\right] = 0. \tag{249}$$

In particular, we can then use this flat connection to define the monodromy matrix

$$\Omega(x) = \overleftarrow{P}\exp\int_0^{2\pi} \mathrm{d}\sigma \frac{x j_\tau + j_\sigma}{x^2-1}. \tag{250}$$

By construction, $\Omega(x)$ is a unimodular matrix (and also unitary for real x) whose eigenvalues can therefore be written as

$$(\mathrm{e}^{\mathrm{i}\tilde{p}(x)}, \mathrm{e}^{-\mathrm{i}\tilde{p}(x)}), \tag{251}$$

where $\tilde{p}(x)$ is called the quasi-momentum. These *functions of x* do not depend on time τ due to (249) and therefore provide an infinite set of classical integrals of motion of the model.

From the explicit expression (250), we can determine the behavior of the quasi-momentum close to $x = \pm 1, 0, \infty$. Using (248) and (246), we obtain

$$\tilde{p}(x) \simeq -\frac{\pi\kappa_\pm}{x \mp 1}, \tag{252}$$

$$\tilde{p}(x) \simeq 2\pi m + \frac{2\pi Q_L}{\sqrt{\lambda}}x, \tag{253}$$

$$\tilde{p}(x) \simeq -\frac{2\pi Q_R}{\sqrt{\lambda}}\frac{1}{x}. \tag{254}$$

Since, by construction, $\Omega(x)$ is analytical in the whole plane except at $x = \pm 1$ where it develops essential singularities, it follows from (255) that for $x \neq \pm 1$ the only singularities of

$$\tilde{p}'(x) = -\frac{1}{\sqrt{4-(\mathrm{tr}\;\Omega(x))^2}}\frac{\mathrm{d}}{\mathrm{d}x}\,\mathrm{tr}\;\Omega(x) \tag{255}$$

are of the form

$$\tilde{p}'(x \to x_k) \simeq \frac{1}{\sqrt{x-x_k}}. \tag{256}$$

If we look for a finite gap solution, the number K of these cuts is finite and we conclude that $\tilde{p}'(x)$ and $-\tilde{p}'(x)$ are two branches of an analytical function defined by a hyperelliptic curve (see figure 1):

$$(p')^2 = \frac{P^2(x)}{Q(x)}, \tag{257}$$

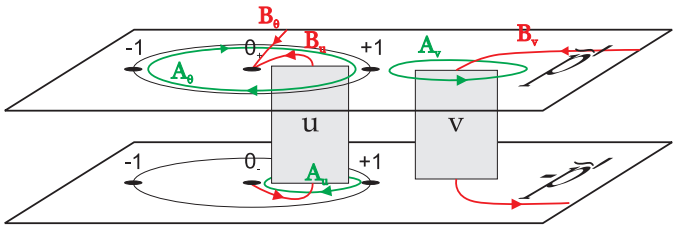

Figure 22. Algebraic curve from the finite gap method. u and v cuts correspond to cuts inside and outside the unit circle respectively.

where $Q(x)$ has $2K$ zeros and the order of $P(x)$ is fixed by the large x asymptotics (254). We denote the branch cuts of $p'(x)$ by u (v) cuts if they are inside (outside) the unit circle. These cuts are the loci where the eigenvalues of the monodromy matrix become degenerate. Thus, when crossing such a cut the quasi-momentum may at most jump by a multiple of 2π which characterizes each cut:

$$\tilde{p}'(x) = \pi n_k, \qquad x \in \mathcal{C}_k, \tag{258}$$

where $\tilde{p}'(x)$ is the average of the quasi-momentum above and below the cut:

$$\tilde{p}'(x) \equiv \tfrac{1}{2}(\tilde{p}(x + \mathrm{i}0) + \tilde{p}(x - \mathrm{i}0)). \tag{259}$$

Each cut is also parameterized by the filling fraction numbers which we define as integrals along A cycles of the curve (see figure 1)[35]:

$$S_i^v = -\frac{\sqrt{\lambda}}{8\pi^2\mathrm{i}} \oint_{A_i^v} \tilde{p}(x)\left(1 - \frac{1}{x^2}\right) \mathrm{d}x, \qquad S_i^u = \frac{\sqrt{\lambda}}{8\pi^2\mathrm{i}} \oint_{A_i^u} \tilde{p}(x)\left(1 - \frac{1}{x^2}\right) \mathrm{d}x. \tag{260}$$

Finally, imposing (252)–(254), (258), (260), one fixes completely the undetermined constants in (257).

5.2. *Quantum Bethe ansatz and classical limit: $O(4)$ sigma model*

We will describe a quantum state of the $O(4)$ sigma model by a system of L relativistic particles of mass $\mu/2\pi$ put on a circle of length 2π. The momentum and the energy of each particle can be suitably parameterized by its rapidity as $p = \frac{\mu}{2\pi}\sinh\theta$ and $e = \frac{\mu}{2\pi}\cosh\theta$, respectively, so that the total energy and momentum will be given by

$$P = \frac{\mu}{2\pi}\sum_{\alpha=1}^{L} \sinh(\pi\theta_\alpha), \tag{261}$$

$$E = \frac{\mu}{2\pi}\sum_{\alpha=1}^{L} \cosh(\pi\theta_\alpha). \tag{262}$$

These particles transform in the vector representation under the $O(4)$ symmetry group or in the bi-fundamental representations of $SU(2)_R \times SU(2)_L$. The scattering of the particles in

[35] It was pointed out in [15, 19] and shown in [16] that $S_i^{u,v}$ are the action variables so that quasi-classically, they indeed become integers. We will also find a striking evidence of this quantization on the string side when finding the classics from the quantum Bethe ansatz where these quantities are naturally quantized. Indeed, from the AdS/CFT correspondence these filling fractions are expected to be integers since this is obvious on the SYM side [18, 19]. We used their integrability to quasi-classically quantize the AdS/CFT string in section 3.

this theory is known to be elastic and factorizable; the relativistic S-matrix $\hat{S}(\theta_1 - \theta_2)$ depends only on the difference of rapidities of scattering particles θ_1 and θ_2 and obeys the Yang–Baxter equations. As was shown in [95] (and in [97, 99, 103, 104] for the general principle chiral field) these properties, together with the unitarity and crossing invariance, define essentially unambiguously the S-matrix $\hat{S}$. Let us briefly recall how the bootstrap program goes. From the symmetry of the problem, we know that

$$\hat{S} = \hat{S}_L \times \hat{S}_R, \tag{263}$$

where $S_{L,R}$ are built by using the two $SU(2)$-invariant tensors and can therefore be written as

$$\hat{S}_{R,L}(\theta)^{a'b'}_{ab} = \frac{S_0(\theta)}{\theta - \mathrm{i}}\big(\theta\delta^{a'}_a\delta^{b'}_b - \mathrm{i}f(\theta)\delta^{b'}_a\delta^{a'}_b\big).$$

Imposing the Yang–Baxter equation on $\hat{S}$ yields $f(\theta) = 1$, while the unitarity constrains the remaining unknown function to obey

$$S_0(\theta)S_0(-\theta) = 1 \tag{264}$$

and the crossing symmetry requires

$$S_0(\theta) = \left(1 - \frac{\mathrm{i}}{\theta}\right) S_0(\mathrm{i} - \theta). \tag{265}$$

From (264) and (265) and the absence of poles on the physical strip $0 < \theta < 2$, one can compute the scalar factor: $S_0(\theta) = \frac{\Gamma(-\frac{\theta}{2\mathrm{i}})\Gamma(\frac{1}{2}+\frac{\theta}{2\mathrm{i}})}{\Gamma(\frac{\theta}{2\mathrm{i}})\Gamma(\frac{1}{2}-\frac{\theta}{2\mathrm{i}})}$. For our purpose, we just need the much easier to extract large θ asymptotics. From (265) and (264), it immediately follows that

$$\mathrm{i}\log S_0^2(\theta) = 1/\theta + O(1/\theta^3). \tag{266}$$

5.2.1. Bethe equations for particles on a circle. When this system of particles is put into a finite one-dimensional periodic box of length $\mathcal{L}$, the set of rapidities of the particles $\{\theta_\alpha\}$ is constrained by the condition of periodicity of the wavefunction $|\psi\rangle$ of the system,

$$|\psi\rangle = \mathrm{e}^{\mathrm{i}\mu\sinh\pi\theta_\alpha}\prod_{1}^{\overleftarrow{\alpha-1}}\hat{S}(\theta_\alpha - \theta_\beta)\prod_{N}^{\overrightarrow{\alpha+1}}\hat{S}(\theta_\alpha - \theta_\beta)|\psi\rangle, \tag{267}$$

where the first term is due to the free phase of the particle and the second is the product of the scattering phases with the other particles. The arrows stand for the ordering of the terms in the product and $\mu = m_0\mathcal{L}$ is a dimensionless parameter. Diagonalization of both the L and R factors in the process of fixing the periodicity (267) leads to the following set of Bethe equations [105] which may be found from (267) by the algebraic Bethe ansatz method [69, 106]. We took the logarithms of the Bethe ansatz equations in their standard, product form. This leads to the integers m_α, n^u_j, n^v_j defining the choice of the branch of logarithms:

$$\begin{aligned} 2\pi m_\alpha = {} & \mu\sinh\pi\theta_\alpha - \sum_{\beta\neq\alpha}^{L}\mathrm{i}\log S_0^2(\theta_\alpha - \theta_\beta) \\ & - \sum_{j}^{J_u}\mathrm{i}\log\frac{\theta_\alpha - u_j + \mathrm{i}/2}{\theta_\alpha - u_j - \mathrm{i}/2} - \sum_{k}^{J_v}\mathrm{i}\log\frac{\theta_\alpha - v_k + \mathrm{i}/2}{\theta_\alpha - v_k - \mathrm{i}/2}, \end{aligned} \tag{268}$$

$$2\pi n^u_j = \sum_{\beta}^{L}\mathrm{i}\log\frac{u_j - \theta_\beta - \mathrm{i}/2}{u_j - \theta_\beta + \mathrm{i}/2} + \sum_{i\neq j}^{J_u}\mathrm{i}\log\frac{u_j - u_i + \mathrm{i}}{u_j - u_i - \mathrm{i}}, \tag{269}$$

$$2\pi n_j^v = \sum_{\beta}^{L} \mathrm{i} \log \frac{v_k - \theta_\beta - \mathrm{i}/2}{v_k - \theta_\beta + \mathrm{i}/2} + \sum_{l \neq k}^{J_v} \mathrm{i} \log \frac{v_k - v_l + \mathrm{i}}{v_k - v_l - \mathrm{i}}, \tag{270}$$

where u's and v's are the Bethe roots appearing from the diagonalization of (267) and characterizing each quantum state. A quantum state with no such roots corresponds to the highest weight ferromagnetic state where all spins of both kinds are up. Adding u (v) roots corresponds to flipping one of the right (left) $SU(2)$ spins, thus creating a magnon. The left and right charges of the wavefunction, associated with the two $SU(2)$ spins, are given by

$$Q_L = L - 2J_u, \qquad Q_R = L - 2J_v. \tag{271}$$

This model with massive relativistic particles and the asymptotically free UV behavior cannot look like a consistent quantum string theory. Only in the classical limit can we view it as a string toy model obeying the classical conformal symmetry. In the classical case, it is also easy to impose the Virasoro conditions. In the quasi-classical limit, we can still try to impose the Virasoro conditions as some natural constraints on the quantum states. We will discuss this point later.

5.3. Quasi-classical limit

In the classical limit, the physical mass of the particle[36]

$$\frac{\mu}{2\pi} \sim \mathrm{e}^{-\sqrt{\lambda}/2}, \tag{272}$$

where λ is the physical coupling at the scale of the size of the box 2π, vanishes since $\lambda \to \infty$. Moreover we should focus on quantum states with large quantum numbers, i.e. we shall consider a large number $L \to \infty$ of particles on the ring.

Let us now think of (268)–(270) as the equations for the equilibrium condition for a system of three kinds of particles: (θ_α, u_j and v_k), interacting between themselves and experiencing the external constant forces ($2\pi m_\alpha$, $2\pi n_j^u$ and $2\pi n_k^v$). The particles of the θ kind are also placed into the external confining potential

$$V(z) = \mu \cosh(\pi M z), \qquad z = \theta/M, \tag{273}$$

where

$$M \equiv -\frac{\log \mu}{2\pi} \simeq \frac{\sqrt{\lambda}}{4\pi}. \tag{274}$$

In the classical limit, the potential becomes a square box potential with the infinite walls at $z = \pm 2$ (see figure 23). Moreover, since this is a large box for the original variables we can use the asymptotics (266) for the force between particles of the θ (or z) type. The box potential provides the appropriate boundary conditions for the density of particles interacting by the Coulomb force. Since they repeal each other, the density should be peaked around $z = \pm 2$. To find the correct asymptotics close to these two points, we can consider (268) as the equilibrium condition for the gas of Coulomb particles in the box.

[36] For the $O(N)$ sigma model, the beta function for the coupling is given by $\beta \equiv \frac{\partial}{\partial \log \Lambda} \sqrt{\lambda(\Lambda)} = N - 2$ where Λ is the cutoff of the theory. The dynamically generated mass must be of the form $\mu = \Lambda f(\sqrt{\lambda})$. The functional form of f is fixed by the β function upon imposing independence on the cutoff of this physical quantity. Thus, for general N, $-\log \mu = \frac{\sqrt{\lambda}}{N-2} + \mathcal{O}(1)$.

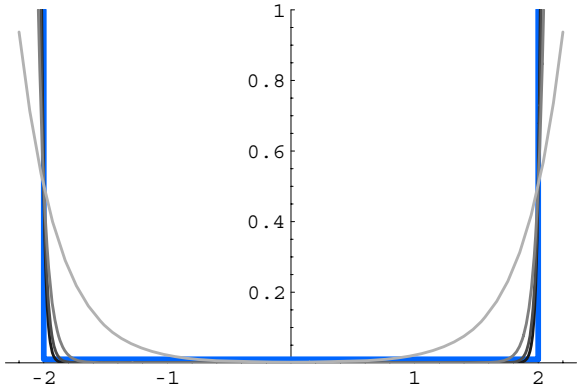

Figure 23. We plot $V(z)$ for $M = 1, 5, 9, 13$ (lighter to darker gray). It is clear that the potential approaches the blue box potential as $M \to \infty$.

If the right and left modes (magnons) are not excited, we have only the states with $U(1)$ modes. In the classical limit, using the Coulomb approximation (266), we have for this sector the following Bethe equation:

$$\mu \sinh \pi M z_\alpha - 2\pi m = -\frac{1}{M} \sum_{\beta \neq \alpha}^{L} \frac{1}{z_\alpha - z_\beta}.$$

In the continuous limit, the equation for the asymptotic density, $L \sim M \to \infty$, is given, through the resolvent $G_\theta(z) = \frac{1}{M} \sum_{\beta=1}^{L} \frac{1}{z-z_\beta}$, by

$$G_\theta(z) = -2\pi m, \qquad z \in \mathcal{C}_\theta, \tag{275}$$

with inverse square root boundary conditions near ± 2. The analytical function $G_\theta(x)$ having a real part on the cut defined by (275), with support $[-2, 2]$, with inverse square root boundary conditions (the only compatible with the asymptotics at $z \to \infty$: $G_\theta(z) \to \frac{L}{M} \frac{1}{z}$, is completely fixed:

$$G_\theta(z) = \left(\frac{2\pi m z + \frac{L}{M}}{\sqrt{z^2 - 4}} - 2\pi m \right), \qquad L > 4\pi |m| M, \tag{276}$$

which gives for the density

$$\rho_\theta(z) = \frac{1}{\pi} \left(\frac{2\pi m z + \frac{L}{M}}{\sqrt{4 - z^2}} \right). \tag{277}$$

For a general solution with u and v magnons, we will also find the same asymptotics

$$\rho(z) \equiv \frac{1}{M} \sum_{\alpha=1}^{L} \delta(z - z_\alpha) \simeq \frac{2\kappa_\pm}{\sqrt{2 \mp z}}, \qquad z \to \pm 2, \tag{278}$$

with $\kappa_\pm$ yet to be determined through the energy and momentum of the solution, as we shall explain in the following section.

We will consider the scenario where we have the same mode number $m_\alpha = m$ for all z particles. As proposed in [90, 102], this is the adequate set of states which will obey the Virasoro constraints in the classical limit.

First, we will relate the z behavior close to the walls, characterized by the constants $\kappa_\pm$ with the energy and momentum E, P of the quantum state, as given by (279) and (262) respectively. Then we shall eliminate θ's from the system of Bethe equations by explicitly solving the first one in the limit considered. Finally, we will justify why we take the same mode number m for all θ's by identifying the longitudinal modes to the excited mode numbers m_i in the Bethe ansatz setup. This constraint on the states will correspond to the Virasoro conditions, at least in the classical limit.

5.3.1. Energy and momentum. The total momentum can be calculated exactly, before any classical limit[37]:

$$P = \frac{\mu}{2\pi}\sum_\alpha \sinh(\pi\theta_\alpha) = m_p L_p - \sum_p n_p S^u_p - \sum_p n_p S^v_p, \tag{279}$$

where L_p, S^u_p and S^v_p are the numbers of Bethe roots with given mode numbers m_p, $n_{u,p}$ and $n_{v,p}$ respectively. To prove this, it suffices to sum (268) for all roots θ_α. The contribution of $S_0(\theta)$ terms cancels due to anti-symmetry while the second and third sums on the rhs of (268) are replaced using (269) and (270), respectively.

Let us show how to calculate the energy (262) which is a fair less trivial task [90]. As a byproduct, we will also reproduce the total momentum from the behavior at the singularities at $z = \pm 2$ described by residua $\kappa_\pm$. We want to compute the sum

$$E \equiv \frac{\mu}{2\pi}\sum_\alpha \cosh(\pi\theta_\alpha),$$

but we *cannot* simply replace this sum by an integral and use the asymptotic density $\rho_\theta(z)$ to compute the energy. This is because the main contribution to the energy comes from large θ's, near the walls, where the expression for the asymptotic density is no longer accurate. It is natural for the classical limit since the particles become effectively massless and the contributions of right and left modes are clearly distinguishable and located far from $\theta = 0$. We note that the energy is dominated by large θ's where, with exponential precision, we can replace $\cosh\pi\theta_\alpha$ by $\pm\sinh\pi\theta_\alpha$ for positive (negative) θ_α. Furthermore, the contribution from θ's in the middle of the box is also exponentially suppressed since μ is very small. Thus, we can pick a point a somewhere in the box not too close to the walls. One can think of a as being somewhere in the middle. Then,

$$E = \sum_{z_\alpha > a}\frac{\mu}{2\pi}\sinh(\pi z_\alpha M) - \sum_{z_\alpha < a}\frac{\mu}{2\pi}\sinh(\pi z_\alpha M),$$

where, let us stress, the result is *correct independent of point a within the interval* $-2 < a < 2$ *with the exponential precision*. Each sum of $\sinh\pi\theta_\alpha$ can be substituted by the corresponding rhs of the Bethe equation (268), thus giving

$$\begin{aligned} E \simeq \frac{\mathrm{i}}{\pi}\sum_{z_\beta < a < z_\alpha}\log S_0^2(M[z_\alpha - z_\beta]) + \sum_\alpha m\,\mathrm{sign}(z_\alpha - a) \\ - \frac{1}{2\pi}\sum_{j,\alpha}\mathrm{sign}(z_\alpha - a)\mathrm{i}\log\frac{Mz_\alpha - u_j + \mathrm{i}/2}{Mz_\alpha - u_j - \mathrm{i}/2} \\ - \frac{1}{2\pi}\sum_{k,\alpha}\mathrm{sign}(z_\alpha - a)\mathrm{i}\log\frac{Mz_\alpha - v_k + \mathrm{i}/2}{Mz_\alpha - v_k - \mathrm{i}/2} \end{aligned} \tag{280}$$

[37] For the closed string theory, we should take $P = 0$ which gives the level matching condition. Moreover, as we shall explain later, we should also pick the same mode number for all particles, $m_\alpha = m$.

As mentioned above we assume all m_α to be the same[38]. Now we can safely go to the continuous limit since in the first term the distances between z's are now mostly of order 1.[39] This allows one to rewrite the energy, with $1/M$ precision, as follows:

$$E \simeq -\frac{M}{\pi}\int_{-2}^{a} \mathrm{d}z \int_{a}^{2} \mathrm{d}w \frac{\rho_\theta(z)\rho_\theta(w)}{z-w} - \frac{M}{2\pi}\int \frac{\rho_\theta(z)\rho_u(w)}{z-w}\mathrm{sign}(z-a)\,\mathrm{d}z\,\mathrm{d}w$$
$$-\frac{M}{2\pi}\int \frac{\rho_\theta(z)\rho_v(w)}{z-w}\mathrm{sign}(z-a)\,\mathrm{d}z\,\mathrm{d}w + mM\int \rho_\theta(z)\,\mathrm{sign}(z-a)\,\mathrm{d}z, \quad (281)$$

where we are now free to use the asymptotic density $\rho_\theta(z)$. By the use of Bethe equations, we managed to transform the original sum over cosh's, highly peaked at the walls, into a much smoother sum where the main contribution is now softly distributed along the bulk and where the continuous limit does not look suspicious. From the previous discussion, we know that this expression does not depend on a provided a is not too close to the walls. In fact, we can easily see that it does not depend on a at all after taking the continuous limit leading to the perfect box-like potential. To prove it, one notes that due to Bethe equations (268) the a derivative of (281) is zero for all $a \in\ ]-2, 2[$. Hence, we can even send a close to a wall: $a = -2+\epsilon$, where ϵ is very small. But then the last three terms in (281) are precisely the momentum (279), as explained in the beginning of this section. To compute the first term, we can now use asymptotics (266) and (278). The contribution of this term is then given by

$$-\frac{M}{\pi}\int_{-2}^{-2+\epsilon} \mathrm{d}z \int_{-2+\epsilon}^{2} \mathrm{d}w \frac{\rho_\theta(z)\rho_\theta(w)}{z-w}$$
$$\simeq -\int_{-2}^{-2+\epsilon} \mathrm{d}z \int_{-2+\epsilon}^{2} \mathrm{d}w \frac{4M\kappa_-^2}{\pi(z-w)\sqrt{2+z}\sqrt{2+w}} \simeq 2\pi M\kappa_-^2 \quad (282)$$

so that

$$E \simeq 2M\kappa_-^2\pi + P. \quad (283)$$

If we compute the a-independent integral (281) near the other wall, i.e. for $a = 2-\epsilon$, we find

$$E \simeq 2M\kappa_+^2\pi - P.$$

Therefore, equating the results one obtains the desired expressions for the energy and momentum:

$$E \pm P = 2\pi M\kappa_\pm^2 \quad (284)$$

through the singularities of the density of rapidities at $z = \pm 2$, described by $\kappa_\pm$. Together with (274), this is precisely the classical formula (248)!

5.4. Elimination of θ's and AFS equations

In this section, we will show how the AFS equations (29), which are restriction of the BS equations on the $\mathfrak{su}(2)$ sub-sector, can be derived from the bootstrap approach. It is useful for what follows, to introduce some new notations. Using the Zhukovsky map

$$z = x(z) + \frac{1}{x(z)}, \qquad |x(z)| > 1, \quad (285)$$

[38] as we will show it is this choice of states which reproduces the finite gap solution of [18] we mentioned in the first section. We will come back to this point at a latter stage

[39] Moreover, it is very important that the contribution from z's near the walls ± 2 is now suppressed since (266)

$$|\log S_0^2(M(2-z_\beta))| > |\log S_0^2(M(2-a))| \sim 1/M.$$

we define

$$y_j^{\pm} \equiv x\left(\frac{u_j \pm \mathrm{i}/2}{M}\right), \qquad y_j \equiv x\left(\frac{u_j}{M}\right) \tag{286}$$

with the similar expressions for v_l given by $\tilde{y}_l^{\pm}$ and $\tilde{y}_l$ respectively.

In this section, for the purposes of comparison with the asymptotic AFS Bethe ansatz for the $N = 4$ SYM theory, let us drop the v magnons, $J_v = 0$. Their contributions will be easily restored later. As explained at the beginning of this section, we can write the first Bethe equation, (268), as

$$\not{G}_\theta(z) + 2\pi m = \sum_{j=1}^{K} \mathrm{i}\log\frac{Mz - u_j - \mathrm{i}/2}{Mz - u_j + \mathrm{i}/2}, \tag{287}$$

where

$$G_\theta(z) = \frac{1}{M}\sum_{\alpha}\frac{1}{z - \theta_\alpha/M} = \int_{-2}^{2}\frac{\mathrm{d}z'\rho_\theta(z')}{z - z'} \tag{288}$$

and $\not{G}_\theta(z)$ is a real part of $G_\theta(z)$. We can find $G_\theta(z)$ as a function of u_j.

Performing the inverse Zhukovsky map (285) and (286), we obtain the equation

$$\not{G}_\theta(z) + 2\pi m = \mathrm{i}\sum_{j=1}^{K}\left(\log\frac{x - y_j^+}{x - y_j^-} + \log\frac{x - 1/y_j^+}{x - 1/y_j^-}\right). \tag{289}$$

Introducing

$$H(x) = G_\theta\left(z(x)\right), \tag{290}$$

we obtain from (289)

$$\frac{1}{2}\left[H(x) + H(1/x)\right] = -2\pi m + \mathrm{i}\sum_{j=1}^{K}\left(\log\frac{x - y_j^+}{x - y_j^-} + \log\frac{x - 1/y_j^+}{x - 1/y_j^-}\right). \tag{291}$$

The solution of this equation, with the right asymptotics at infinity $H(1/\epsilon) = G_\theta\,(1/\epsilon) \simeq L/M\epsilon$, is as follows:

$$H(x) = \mathrm{i}\sum_{j=1}^{K}\left[\frac{2x}{x^2-1}\left(\frac{1}{y_j^+} - \frac{1}{y_j^-}\right) - \frac{2x^2\log\frac{y_j^+}{y_j^-}}{x^2-1} + 2\log\frac{y_j^+ x - 1}{y_j^- x - 1}\right] + \frac{\frac{L}{2M} + 2\pi m}{x-1} + \frac{\frac{L}{2M} - 2\pi m}{x+1}. \tag{292}$$

We can also compute the density of θ's as the imaginary part of the resolvent $G_\theta(z)$:

$$\rho_\theta(Z(x)) = \frac{\mathrm{Im}\,G_\theta(Z(x))}{\pi} = \frac{\mathrm{i}}{2\pi}\left[H(x) - H(1/x)\right]. \tag{293}$$

Then from (284) and (278) we see that in classical limit (279), (262) can be expressed through poles of $H(x)$ in $x = \pm 1$. Extracting the residues of $H(x)$ at the poles $x = \pm 1$, we can see that

$$\Delta = L + 2\mathrm{i}M\sum_{j=1}^{K}\left(\frac{1}{y_j^+} - \frac{1}{y_j^-}\right) \tag{294}$$

$$P = \left(m - \frac{\mathrm{i}}{2\pi}\sum_{j=1}^{K}\log\frac{y_j^+}{y_j^-}\right)\Delta = 0. \tag{295}$$

(294) is precisely the expression for the anomalous dimension (33) and (295) gives precisely the zero momentum condition for the AFS equation (32) (for zero twists)!

5.4.1. Derivation of the AFS formula. In this section we will exclude θ variables from (269) and (270), using the θ-density calculated above, and obtain the AFS equation (29). We here try to go the same way as the authors of [107], where similar variables were excluded in favor of the magnon variables in Lieb–Wu equations for the Hubbard model.

Let us now exclude θ's from (269), using the result (292). Taking the log of (269), we obtain

$$\sum_{j\neq k}\log\frac{u_k-u_j+\mathrm{i}}{u_k-u_j-\mathrm{i}}+2\pi\mathrm{i}n_k=\sum_{\beta}\log\frac{u_k-\theta_\beta+\mathrm{i}/2}{u_k-\theta_\beta-\mathrm{i}/2}\equiv\mathrm{i}p_k. \tag{296}$$

Rewriting p_k through density, we have

$$\mathrm{i}p_k=M\int_{-2}^{2}\log\frac{z-w_k^+}{z-w_k^-}\rho_\theta(z)\,\mathrm{d}z, \tag{297}$$

where $w_k^\pm=\frac{u_k\pm i/2}{M}$. The function $\rho_\theta(z)$ is given by equations (292) and (293). In appendix H, we perform the integration and obtain the following result:

$$\begin{aligned}\mathrm{i}p_k=\sum_j\left[2\log\frac{y_k^-y_j^+\left(y_j^-y_k^+-1\right)}{y_k^+y_j^-\left(y_j^+y_k^--1\right)}-2\mathrm{i}(u_j-u_k)\log\frac{\left(y_j^-y_k^--1\right)\left(y_j^+y_k^+-1\right)}{\left(y_j^-y_k^+-1\right)\left(y_j^+y_k^--1\right)}\right]\\ -2M\left(\frac{1}{y_k^+}-\frac{1}{y_k^-}\right)\left[2\pi m-\mathrm{i}\sum_j\log\frac{y_j^+}{y_j^-}\right]+L\log\frac{y_k^+}{y_k^-}.\end{aligned} \tag{298}$$

It leads to the following equations:

$$\left(\frac{y_k^+}{y_k^-}\right)^L=\prod_{j\neq k}^{K}\frac{y_k^+-y_j^-}{y_k^--y_j^+}\left(\frac{1-1/\left(y_j^-y_k^+\right)}{1-1/\left(y_j^+y_k^-\right)}\right)^{-1}\left(\frac{\left(y_j^-y_k^--1\right)}{\left(y_j^-y_k^+-1\right)}\frac{\left(y_j^+y_k^+-1\right)}{\left(y_j^+y_k^--1\right)}\right)^{2\mathrm{i}(u_j-u_k)}, \tag{299}$$

which precisely coincide with the AFS [20] (29), including the expressions for energy and momentum (294), (295).

5.4.2. Classical limit and KMMZ algebraic curve. To consider the classical limit, we trivially restore the v roots from the previous calculation to find

$$\left(\frac{y_k^+}{y_k^-}\right)^L=\prod_{j\neq k}^{J_u}\frac{u_k-u_j+\mathrm{i}}{u_k-u_j-\mathrm{i}}\sigma^2(u_j,u_k)\prod_{l=1}^{J_v}\sigma^2(v_l,u_k), \tag{300}$$

and similarly for $\tilde{y}_k$, and consider the limit where $J_u, J_v, L\sim M$, so that the u and v roots also scale as M. Then the expansion of this equation, after taking the log's, gives to the leading order in $1/M$

$$\pi n_k=\frac{\frac{L}{2M}y_k+2\pi m}{1-y_k^2}+\frac{1}{y_k^2-1}\frac{1}{M}\sum_{l=1}^{J_v}\frac{1}{1/y_k-\tilde{y}_l}+\frac{y_k^2}{y_k^2-1}\frac{1}{M}\sum_{j\neq k}^{J_u}\frac{1}{y_k-y_j}. \tag{301}$$

Finally, we can define the quasi-momentum [108]

$$p(x)=\frac{\frac{L}{2M}x+2\pi m}{1-x^2}+\frac{1}{x^2-1}\frac{1}{M}\sum_{j=1}^{J_v}\frac{1}{1/x-\tilde{y}_j}+\frac{x^2}{x^2-1}\frac{1}{M}\sum_{j=1}^{J_u}\frac{1}{x-y_j}. \tag{302}$$

Let us explain how it becomes precisely the quasi-momentum we had in the context of the algebraic curve in section 5.1.1 in the classical theory. It is clear that we indeed have

asymptotics (253) and (254) close to $x = 0, \infty$. Then, to relate the residues of (302) to those found from the algebraic curve in (252), we expand (294) in our limit as follows

$$\Delta = L + \sum_j \frac{2}{y_j^2 - 1} + \sum_l \frac{2}{\tilde{y}_l^2 - 1} \tag{303}$$

and check that this is indeed what one finds from the quasi-momenta we just defined. Finally, when we consider a large number of magnons J_u, J_v the roots in (302) condense into a number of one-dimensional supports, the sums becoming the integrals along these lines giving the same square root cuts as we had in the finite gap construction.

5.4.3. Geometric proof. The roots solving (268)–(270) with the same mode number will condense into a single square root cut. When we consider more than one type of mode numbers we see that the particles condense into a few distinct supports, one for each distinct mode number:

$$\mathcal{C} = \mathcal{C}_1 \cup \cdots \cup \mathcal{C}_K.$$

We can now rescale the Bethe roots

$$(u, v, \theta) = M(x, y, z) \tag{304}$$

and define

$$\begin{aligned} p_1 = -p_2 &= \frac{1}{M} \sum_{i=1}^{J_u} \frac{1}{z - x_i} - \frac{1}{2M} \sum_{\beta=1}^{L} \frac{1}{z - z_\beta} \\ p_3 = -p_4 &= \frac{1}{M} \sum_{l=1}^{J_v} \frac{1}{z - y_l} - \frac{1}{2M} \sum_{\beta=1}^{L} \frac{1}{z - z_\beta}. \end{aligned} \tag{305}$$

Then we can recast the Bethe equations in this scaling limit as follows:

$$\begin{aligned} x \in \mathcal{C}_u, &\qquad {p_1}^+ - {p_2}^- = 2\pi n_u \\ x \in \mathcal{C}_\theta, &\qquad {p_2}^+ - {p_3}^- = 2\pi m \\ x \in \mathcal{C}_v, &\qquad {p_3}^+ - {p_4}^- = 2\pi n_v \\ x \in \mathcal{C}_\theta, &\qquad {p_4}^+ - {p_1}^- = 2\pi m, \end{aligned} \tag{306}$$

where we

- considered, as in the preceding section, one single mode number m for all rapidities;
- dropped the momentum $\mu \sinh\theta$; as we explained in section 5.3, we can do this provided we replace it by the boundary conditions (278).

These equations tell us that $p_1'(z)$, $p_2'(z)$, $p_3'(z)$, $p_4'(z)$ form four sheets of the Riemann surface of an analytical function $p'(z)$ (see figure 24).

They can also be written as holomorphic integrals around the infinite B cycles:

$$\begin{aligned} \oint_{B_j^u} \mathrm{d}p &= 2\pi n_{u,j} \qquad n_j = 1, \ldots, K_u \\ \oint_{B_j^v} \mathrm{d}p &= 2\pi n_{v,j} \qquad n_j = 1, \ldots, K_v \\ \oint_{B^\theta} \mathrm{d}p &= 2\pi m, \end{aligned} \tag{307}$$

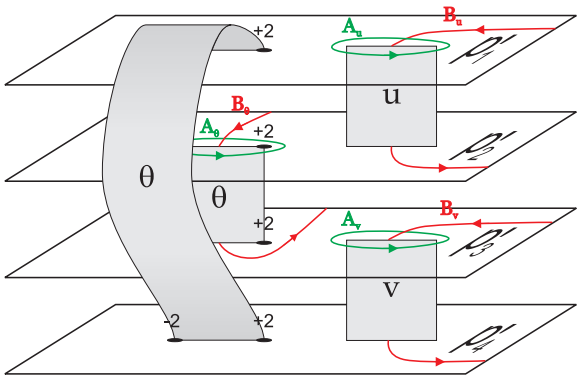

Figure 24. Structure of the curve coming from the Bethe ansatz side. This figure is related to figure 1 by means of the Zhukovsky map.

where the first two conditions correspond to the equations in the first and third lines of (143), respectively, while the last one corresponds to any of the equations of the second and fourth lines of (143). The B cycles are defined as in figure 24.

We found two Riemann surfaces which we plotted in figures 1 and 24, respectively. The equivalence between these two curves is achieved through the Zhukovsky map [90]:

$$z = x + \frac{1}{x}$$

and amounts to the equivalence between the finite gap solutions for the classical theory and the Bethe ansatz solutions in the scaling limit.

5.5. Virasoro modes

We established the equivalence between

- all classical solutions following from the PCF action (244) and subject to the Virasoro conditions $\mathrm{tr}\,(j_\tau \pm j_\sigma)^2 = -2\kappa_\pm^2$ as described by the construction of the algebraic curve of section 5.1.1,
- the Bethe ansatz quantum solution (268) and (269) in the scaling limit (304) with all rapidities θ_α having the same mode number m.

In the context of string theory, one is interested in quantizing the Polyakov string action

$$S = \frac{\sqrt{\lambda}}{8\pi} \int \mathrm{d}\sigma\, \mathrm{d}\tau \sqrt{h} h^{ab} (\mathrm{tr}\ \partial_a g^\dagger \partial_b g - \partial_a Y \partial_b Y). \tag{308}$$

Due to its local reparameterization and Weyl symmetries, one can then fix the target spacetime Y as in (247) and reduce the action to (244). However, due to the residual reparameterization symmetry

$$\tau \pm \sigma \to f_\pm(\tau \pm \sigma), \tag{309}$$

one must keep in mind that the original presence of the worldsheet metric field imposes the fcat that the stress energy tensor vanishes. This is precisely the Virasoro conditions.

On the other hand, from the field theory point of view the Bethe ansatz equations (268)–(270) should describe all possible states of the theory, and not only those for which

$$\langle \psi | T^{ab} | \phi \rangle = 0. \tag{310}$$

Thus, in view of the equivalence we proved, we are led to the conclusion that if we start with some classical solution with one θ cut and some u and v cuts, the excitation of additional microscopic θ cuts should correspond to the inclusion of the longitudinal modes which we drop in the context of string theory. Indeed, these massless (from the worldsheet point of view) excitations coming from our conformal gauge choice appear if one expands the action around the classical solution without fixing the Virasoro conditions from the beginning (see, for instance, expression (2.7) and the discussion following it in [86]). In this section we verify this claim therefore justifying this single θ cut restriction, first proposed in [102] and given the interpretation as the Virasoro condition in [90].

In (280), we computed the energy of a quantum state where all mode numbers $m_\alpha = m$ were the same. If we change the mode numbers of a few θ's we will have a macroscopic support with particles having the mode number m surrounded by some microscopic domains, linear supports, with mode numbers $m_\beta < m$ (to the left of it) and $m_\beta > m$ (to its right).

Let us assume that we excite them one at a time and focus on the first particle whose mode number we change. Before we do it, it is in equilibrium due to the exponential force exerted by the wall of the box (273) and by (an equal) force produced by all the other particles and by the constant force $2\pi m$—see (268). When we change the particle mode number, the constant force increases pushing the particle against the wall. However since the forces are exponential the shift will be very small, much smaller than $1/M$—the characteristic distance between the neighboring rapidities. Then let us consider the particles in the middle of the box, those whose position is well described by the asymptotic density $\rho(z)$. They only feel the change in the mode number through the new position of the corresponding θ particle. Since this shift is very small the asymptotic density, to the order we are interested, is not changed. Thus, in this procedure of changing a few mode numbers we conclude that, when going to the continuous limit in (280), only the second term will lead to a different result so that

$$\delta E = \sum_n |n| N_{m+n}, \tag{311}$$

where N_n is the number of particles with mode number n. We found in this way the massless (worldsheet) modes associated with the local reparameterization symmetry of the worldsheet. These modes appear when considering the fluctuations around a classical solution [86] and are the only ones not taken into account by the finite gap algebraic curve (see section 3).

6. Summary

In this work, we review some aspects of integrability in AdS/CFT. Particular attention is paid to quasi-classical effects in integrable classical sigma models, describing strings in curved AdS backgrounds, and finite size effects in the integrable spin chains arising in the CFT side of the duality.

- In section 1, we review the most important constructions such as the classical algebraic curve for the superstring action and the quantum Bethe equations—including the all-loop Beisert–Staudacher (BS) equations—and their scaling limit.
- In section 2, we show how the finite size corrections to the scaling limit could be computed in a systematic way to arbitrary order in $1/L$, where L is the spin chain length. The procedure is similar to the standard WKB expansion. Close to the edges of the distribution of Bethe roots, we find a universal Airy-type behavior governing the solutions to Bethe equations. For a single cut solution in the $\mathfrak{sl}(2)$ sub-sector, we explicitly computed the energy up to the $1/L^2$ order. The explicit result is quite involved and is given in (123).

This method was recently applied to the strong coupling limit of the BS equations [123] where a prediction for the two-loop correction to the energy of the folded string was made (extending earlier one-loop results of [124]). The results have been partly recovered using different methods [66, 67].

Then we consider the nested Bethe ansatz. As a technical tool we make use of a curious duality among the systems of Bethe ansatz equations, which we call bosonic duality. In the scaling limit, it amounts to the interchange of the Riemann surface sheets. An integral equation describing the leading finite size corrections in a closed form is presented.

- In section 3, we develop a method of computation of the quasi-classical corrections to the classical spectrum of string theory in the $AdS_5 \times S^5$ background, based solely on the classical integrable structure of the theory. The idea of this method is inspired by the analytical structure of the quasi-momenta of one-dimensional quantum mechanical systems. Quantum excitations are identified with poles on the algebraic surface (see figure 1) whose residue is fixed by the integer value of the classical action variables. In this way, we reproduced results of the previous direct calculations based on the string worldsheet action. The method we developed can be applied to a wide range of integrable field theories with a known classical algebraic curve description. In particular, strings in the $AdS_4/\mathbb{CP}^3$ background can be studied using the technology developed here [125, 126].

  Furthermore, from a more mathematical point of view, the algebraic curve method has been rederived for the $SU(2)$ subsector of the AdS_5/CFT_4 duality [17].

  Moreover, this formalism allows one to compute the quantum corrections to the classical energies of complicated string configurations, going beyond the simplest circular string solutions. In particular, the method was applied to the giant magnon solution [127–130] with perfect agreement with the finite size Lücsher correction [131–134]. A direct computation of the one-loop shift around the finite volume giant magnon from the string worldsheet action seems to be an almost impossible task. Another example where the method could be efficiently applied is the folded string solution dual to the twist two operators in the YM theory. These operators are relevant in the study of gluon scattering amplitudes and are therefore particularly interesting.
- In section 4, we show that the finite size corrections to the Bethe equations in the scaling limit can be seen as describing a sea of virtual quasi-classical fluctuations in the sense that they can be interpreted as an infinite sum over all the zero point energy oscillations. The condition that the finite size corrections match the quasi-classical excitations is a very nontrivial self-consistency restriction on the underlying system of Bethe ansatz equations. At strong coupling, such reasoning allows one to derive the leading quantum correction to the dressing factor, the Hernandez–Lopez phase (37). The same sort of arguments proved to be extremely useful [125, 126] in the context of the novel AdS^4/CFT_3 duality [110].
- Finally, in section 5 we consider standard relativistic sigma models, such as the S^3 sigma model which can be thought of as toy models for the full superstring theory. Such models are described by relativistic particles with some isotopic degrees of freedom. Surprisingly, and interestingly, we found out that once the momenta of the physical particles is integrated out we are left with a complicated system of effective Bethe equations for the isotopic degrees of freedom which precisely coincide with the BS equations in the $\mathfrak{su}(2)$ sector! This constitutes very strong evidence in favor of a more elegant (and yet to be found) description of the full spectrum of AdS/CFT, containing such an extra (hidden) level of degrees of freedom.

Acknowledgments

First, I would like to thank my thesis supervisor V Kazakov for introducing me to the beautiful subject, my collaborators during my PhD in Paris K Sakai and especially P Vieira, members of the jury I Kostov, A Zabrodin, K Zarembo, J-B Zuber and especially M Staudacher and A Tseytlin. I would like also to thank my master supervisors D Diakonov and V Petrov who established my scientistic style and T Bargheer, N Beisert, C Kristjansen, L Lipatov, J Penedones, A Rej, P Ribeiro, D Serban, F Smirnov, J Troost, D Volin and Al Zamolodchikov for numerous discussions. The work was partially supported by RSGSS-1124.2003.2, RFBR grant 08-02-00287 and ANR grant INT-AdS/CFT (contract ANR36ADSCSTZ).

Appendix A. Transfer matrix invariance and the bosonic duality for $SU(K|M)$ supergroups

In this section, we review the formalism of [78] which allows one to derive the transfer matrices of usual (super) spin chains in any representation. We will use this general formalism to prove the invariance under the bosonic dualities of all possible transfer matrices one can build. The transfer matrices presented in section 2.2.2 can be obtained trivially using this formalism[40].

As mentioned in section 2.2, for the standard $SU(K|M)$ super spin chains (based on the standard R-matrix $R(u) = u + \mathrm{i}\mathcal{P}$ with $\mathcal{P}$ being the superpermutation), we can find the (twisted) transfer matrix eigenvalues for the single column young tableau with a boxes through the *non-commutative generating functions* [78, 79]

$$\sum_{a=0}^{\infty}(-1)^a\,\mathrm{e}^{\mathrm{i}a\partial_u}\frac{T_a(u)}{Q_{K,M}(u+(a-K+M+1)i/2)}\,\mathrm{e}^{\mathrm{i}a\partial_u}=\overrightarrow{\prod}_{(x,n)\in\gamma}\hat{V}^{-1}_{x,n}(u), \tag{A.1}$$

where γ is a path starting from (M, K) and finishing at $(0, 0)$ (always approaching this point with each step) in a rectangular lattice of size $M \times K$ as in figure 6,[41] $x = (m, k)$ is point in this path and $n = (0, -1)$ or $(-1, 0)$ is the unit vector looking along the next step of the path. Each path describes in this way a possible Dynkin diagram of the $SU(K|M)$ supergroup with corners denoting fermionic nodes and straight lines denoting bosonic ones; see figure 6. Finally,

$$\hat{V}^{-1}_{(m,k),(0,-1)}(u)=\mathrm{e}^{\mathrm{i}\phi_k}\frac{Q_{k,m}(u+\mathrm{i}(m-k-1)/2)}{Q_{k,m}(u+\mathrm{i}(m-k+1)/2)}\frac{Q_{k-1,m}(u+\mathrm{i}(m-k+2)/2)}{Q_{k-1,m}(u+\mathrm{i}(m-k+0)/2)}-\mathrm{e}^{\mathrm{i}\partial_u}$$

$$\hat{V}^{-1}_{(m,k),(-1,0)}(u)=\left(\mathrm{e}^{\mathrm{i}\varphi_m}\frac{Q_{k,m-1}(u+\mathrm{i}(m-k-2)/2)}{Q_{k,m-1}(u+\mathrm{i}(m-k+0)/2)}\frac{Q_{k,m}(u+\mathrm{i}(m-k+1)/2)}{Q_{k,m}(u+\mathrm{i}(m-k-1)/2)}-\mathrm{e}^{\mathrm{i}\partial_u}\right)^{-1},$$

where $Q_{k,m}$ is the Baxter polynomial for the roots of the corresponding node[42] and $\{\phi_k, \varphi_m\}$ are twists introduced in the transfer matrix [79]. Let us then consider a bosonic node like that in the middle of figure 6 (the *vertical* bosonic node is treated in the same fashion). If the position of this node on the $M \times K$ lattice is given by (m, k), then it is obvious that the

[40] We should mention that the transfer matrices in section 2.2.2 are not exactly the same we have in this appendix but can be obtained from these via a trivial rescaling in u which obviously does not spoil the invariance of these objects.
[41] Notice that the path goes in opposite direction compared to the labeling a of the Baxter polynomial Q_a used before. In the notation of this section $Q_{k,m}$ corresponds to the node is at position (m,k) in this lattice.
[42] $\hat{Q}_{0,0}$ is normalized to 1. If we are considering a spin in the representation where the first Dynkin node has a nonzero Dynkin label then $Q_{M,K}$ will play the role of the potential term. In general the situation is more complicated, see [78]. In any case we are mainly interested in the dualization of roots which are not momentum carrying thus we need not care about such matters.

only combination containing $Q_{m,k}$ on the right-hand side of (A.1) comes from the product of $\hat{V}^{-1}_{(m,k),(-1,0)}(u)\hat{V}^{-1}_{(m+1,k),(-1,0)}(u)$ which reads as

$$\left[\mathrm{e}^{\mathrm{i}\varphi_m+\varphi_{m+1}}\frac{Q_{k,m+1}(u+\mathrm{i}(m-k+2)/2)}{Q_{k,m+1}(u+\mathrm{i}(m-k+0)/2)}\frac{Q_{k,m-1}(u+\mathrm{i}(m-k-2)/2)}{Q_{k,m-1}(u+\mathrm{i}(m-k+0)/2)}+\mathrm{e}^{2\mathrm{i}\partial_u}\right.$$
$$-\left(\mathrm{e}^{\mathrm{i}\varphi_{m+1}}\frac{Q_{k,m}(u+\mathrm{i}(m-k-1)/2)}{Q_{k,m}(u+\mathrm{i}(m-k+1)/2)}\frac{Q_{k,m+1}(u+\mathrm{i}(m-k+2)/2)}{Q_{k,m+1}(u+\mathrm{i}(m-k+0)/2)}\right.$$
$$\left.\left.+\mathrm{e}^{\mathrm{i}\varphi_m}\frac{Q_{k,m-1}(u+\mathrm{i}(m-k+0)/2)}{Q_{k,m-1}(u+\mathrm{i}(m-k+2)/2)}\frac{Q_{k,m}(u+\mathrm{i}(m-k+3)/2)}{Q_{k,m}(u+\mathrm{i}(m-k+1)/2)}\right)\mathrm{e}^{\mathrm{i}\partial_u}\right]^{-1}. \tag{A.2}$$

So, if we want to study the bosonic duality on the node (k, m) and its relation with the invariance of several transfer matrices, we need to study the last two lines of this expression. For simplicity let us shift u, omit the subscript k in the Baxter polynomials $Q_{k,m-1}$, $Q_{k,m}$, $Q_{k,m+1}$ and define the reduced transfer matrix as

$$t(u,\varphi_m,\varphi_{m+1})\equiv\mathrm{e}^{\mathrm{i}\varphi_{m+1}}\frac{Q_m(u-\mathrm{i})}{Q_m(u)}\frac{Q_{m+1}(u+\mathrm{i}/2)}{Q_{m+1}(u-\mathrm{i}/2)}+\mathrm{e}^{\mathrm{i}\varphi_m}\frac{Q_{m-1}(u-\mathrm{i}/2)}{Q_{m-1}(u+\mathrm{i}/2)}\frac{Q_m(u+\mathrm{i})}{Q_m(u)}. \tag{A.3}$$

Note that the absence of poles at the zeros of Q_m yields precisely the Bethe equations for this auxiliary node.

A.1. Bosonic duality ⇒ transfer matrix invariance

Thus, to check the invariance of the transfer matrices in all representations it suffices to verify that the reduced transfer matrix $t(u, \varphi_m, \varphi_{m+1})$ is invariant under $\varphi_m \leftrightarrow \varphi_{m+1}$ and $Q_m \to \tilde{Q}_m$ where

$$2\mathrm{i}\sin\left(\frac{\varphi_{m+1}-\varphi_m}{2}\right)Q_{m-1}(u)Q_{m+1}(u)$$
$$=\mathrm{e}^{\mathrm{i}\frac{\varphi_{m+1}-\varphi_m}{2}}Q_m(u-\mathrm{i}/2)\tilde{Q}_m(u+\mathrm{i}/2)-\mathrm{e}^{-\mathrm{i}\frac{\varphi_{m+1}-\varphi_m}{2}}Q_m(u+\mathrm{i}/2)\tilde{Q}_m(u-\mathrm{i}/2), \tag{A.4}$$

which can be easily verified. If suffices to replace, in $t(u, \varphi_m, \varphi_{m+1})$ in (A.3),

$$\frac{Q_m(u-\mathrm{i})}{Q_m(u)}\to\mathrm{e}^{-\mathrm{i}(\varphi_{m+1}-\varphi_m)}\frac{\tilde{Q}_m(u-\mathrm{i})}{\tilde{Q}_m(u)}$$
$$+2\mathrm{i}\,\mathrm{e}^{-\mathrm{i}\frac{\varphi_{m+1}-\varphi_m}{2}}\sin\left(\frac{\varphi_{m+1}-\varphi_m}{2}\right)\frac{Q_{m-1}(u+\mathrm{i}/2)Q_{m+1}(u+\mathrm{i}/2)}{Q_m(u)\tilde{Q}_m(u)},$$
$$\frac{Q_m(u+\mathrm{i})}{Q_m(u)}\to\mathrm{e}^{+\mathrm{i}(\varphi_{m+1}-\varphi_m)}\frac{\tilde{Q}_m(u+\mathrm{i})}{\tilde{Q}_m(u)}$$
$$-2\mathrm{i}\,\mathrm{e}^{-\mathrm{i}\frac{\varphi_{m+1}-\varphi_m}{2}}\sin\left(\frac{\varphi_{m+1}-\varphi_m}{2}\right)\frac{Q_{m-1}(u-\mathrm{i}/2)Q_{m+1}(u-\mathrm{i}/2)}{Q_m(u)\tilde{Q}_m(u)},$$

which are obvious consequences of the bosonic duality.

A.2. Transfer matrix invariance ⇒ bosonic duality

On the other hand suppose that we have two solutions of Bethe equations, one of them characterized by the Baxter polynomials $\{\ldots, Q_{m-1}, Q_m, Q_{m+1}, \ldots\}$ with twists $\{\ldots, \varphi_m, \varphi_{m+1}, \ldots$ and the other with $\{\ldots, Q_{m-1}, \tilde{Q}_m, Q_{m+1}, \ldots\}$ with twists $\{\ldots, \varphi_{m+1}, \varphi_m, \ldots\}$ for which the transfer matrices are the same, that is,

$$t(u,\varphi_m,\varphi_{m+1})=\tilde{t}(u,\varphi_{m+1},\varphi_m). \tag{A.5}$$

Then we can show that these two solutions are related by the bosonic duality (A.4). Indeed if we build the Wronskian[43] like object

$$W(u) \equiv \mathrm{e}^{\mathrm{i}\frac{\varphi_{m+1}-\varphi_m}{2}} \frac{Q_m(u-\mathrm{i}/2)\tilde{Q}_m(u+\mathrm{i}/2)}{Q_{m-1}(u)Q_{m+1}(u)} - \mathrm{e}^{-\mathrm{i}\frac{\varphi_{m+1}-\varphi_m}{2}} \frac{Q_m(u+\mathrm{i}/2)\tilde{Q}_m(u-\mathrm{i}/2)}{Q_{m-1}(u)Q_{m+1}(u)},$$

we can easily check that

$$W(u+\mathrm{i}/2) - W(u-\mathrm{i}/2)$$
$$= -\mathrm{e}^{-\mathrm{i}\frac{\varphi_{m+1}+\varphi_m}{2}} \frac{Q_m(u)\tilde{Q}_m(u)}{Q_{m-1}(u-\mathrm{i}/2)Q_{m+1}(u+\mathrm{i}/2)}(t(u,\varphi_m,\varphi_{m+1}) - \tilde{t}(u,\varphi_{m+1},\varphi_m)) = 0.$$

Since by definition $W(u)$ is a rational function, this means that it must be a constant. Thus if $\varphi_m \neq \varphi_{m+1}$, we must have $K_m + \tilde{K}_m = K_m + K_{m+1}$ and the value of W can be read from the large u behavior. In this way, we obtain precisely the bosonic duality (A.4). If $\varphi_m = \varphi_{m+1}$, then we see that $K_m + \tilde{K}_m = K_m + K_{m+1} + 1$ and we will obtain a different value for constant W which will correspond to the untwisted bosonic duality described in section 2.2.5.

Appendix B. Quasi-momenta for a generic rigid circular string

To establish the link between the embedding coordinate solution (175) with the coset's notations, we introduce the matrices

$$\mathcal{R} = \prod_{i=1}^{3} \mathrm{e}^{\frac{\mathrm{i}}{2}(w_i\tau + m_i\sigma)\Phi_i} \cdot \mathcal{R}_0 \in SU(4)$$

and

$$\mathcal{Q} = \mathrm{e}^{\frac{\mathrm{i}}{2}\kappa\tau\Phi_1} \cdot \prod_{i=1}^{2} \mathrm{e}^{-\frac{\mathrm{i}}{2}(\mathrm{w}_i\tau + k_i\sigma)\Phi_{i+1}} \cdot \mathcal{Q}_0 \in SU(2,2),$$

where Φ_i are the Cartan generators:

$$\Phi_1 = \mathrm{diag}(+,+,-,-), \qquad \Phi_2 = \mathrm{diag}(+,-,+,-), \qquad \Phi_3 = \mathrm{diag}(-,+,+,-),$$

and $\mathcal{R}_0 = \mathrm{e}^{\Phi_{42}\theta}\,\mathrm{e}^{\Phi_{64}\gamma}$ and $\mathcal{Q}_0 = \mathrm{e}^{\Phi'_{42}\psi}\,\mathrm{e}^{\Phi'_{64}\rho}$ are constant matrices with

$$(\cos\gamma, \sin\gamma\cos\theta, \sin\gamma\sin\theta) = \left(\sqrt{\frac{\mathcal{J}_1}{w_1}}, \sqrt{\frac{\mathcal{J}_2}{w_2}}, \sqrt{\frac{\mathcal{J}_3}{w_3}}\right),$$

$$(\cosh\rho, \sinh\rho\cos\psi, \sinh\rho\sin\psi) = \left(\sqrt{\frac{\mathcal{E}}{\kappa}}, \sqrt{\frac{\mathcal{S}_1}{\mathrm{w}_1}}, \sqrt{\frac{\mathcal{S}_2}{\mathrm{w}_2}}\right)$$

and Φ_{42}, Φ_{64}, Φ'_{42}, Φ'_{64} given respectively by

$$\frac{1}{2}\begin{pmatrix} 0 & -1 & 0 & 0 \\ 1 & 0 & 0 & 0 \\ 0 & 0 & 0 & -1 \\ 0 & 0 & 1 & 0 \end{pmatrix}, \qquad \begin{pmatrix} 0 & 0 & 0 & 0 \\ 0 & 0 & -1 & 0 \\ 0 & 1 & 0 & 0 \\ 0 & 0 & 0 & 0 \end{pmatrix},$$

$$\frac{1}{2}\begin{pmatrix} 0 & -1 & 0 & 0 \\ 1 & 0 & 0 & 0 \\ 0 & 0 & 0 & 1 \\ 0 & 0 & -1 & 0 \end{pmatrix}, \qquad \frac{1}{2}\begin{pmatrix} 0 & 0 & 0 & 1 \\ 0 & 0 & -1 & 0 \\ 0 & -1 & 0 & 0 \\ 1 & 0 & 0 & 0 \end{pmatrix}.$$

[43] We would like to thank A Zabrodin and V Kazakov for suggesting this nice interpretation for the bosonic duality.

Let us ignore for a moment the fact that, for a generic choice of mode numbers m_i, k_j, these matrices are not always periodic. Then, to describe the circular solutions we can use, as representative $g \in PSU(2,2|4)$, the block diagonal matrix

$$g = \left(\begin{array}{c|c} \mathcal{Q} & 0 \\ \hline 0 & \mathcal{R} \end{array}\right), \tag{B.1}$$

which indeed leads to (175) under the map (5).

What is particular about this solution is that, as follows trivially from the form of the matrices $\mathcal{R}$ and $\mathcal{Q}$, the current

$$J = -g^{-1}\,\mathrm{d}g,$$

and therefore also the flat connection $A(x)$ in (9) are constant matrices! Then the computation of (10) is trivial and the quasi-momenta $p(x)$ are simply obtained from the eigenvalues of $\frac{2\pi}{\mathrm{i}}A(x)$.

Before going on, let us comment on the subtle point ignored above—the periodicity of the rotation matrices $\mathcal{R}$ (and $\mathcal{Q}$). For some integers m_i, we see that this matrix could become anti-periodic. This means that in principle we should use another representative, $\mathcal{R}^{\text{periodic}}$, for which we should still have (5) but which should be periodic. However, if both $\mathcal{R}$ and $\mathcal{R}^{\text{periodic}}$ obey these equations this means that they are related by an anti-periodic $SP(4)$ gauge transformation. This means that for the purpose of computing the quasi-momenta $p(x)$, we can indeed always use the element (139) provided we keep in mind that if $\mathcal{R}$ is anti-periodic we can recover the real quasi-momenta through

$$\begin{aligned}\{\mathrm{e}^{\mathrm{i}\hat{p}_1}, \mathrm{e}^{\mathrm{i}\hat{p}_2}, \mathrm{e}^{\mathrm{i}\hat{p}_3}, \mathrm{e}^{\mathrm{i}\hat{p}_4}|\mathrm{e}^{\mathrm{i}\tilde{p}_1}, \mathrm{e}^{\mathrm{i}\tilde{p}_2}, \mathrm{e}^{\mathrm{i}\tilde{p}_3}, \mathrm{e}^{\mathrm{i}\tilde{p}_4}\}_{\text{For the true representative } \mathcal{R}^{\text{periodic}}} \\ = \{\mathrm{e}^{\mathrm{i}\hat{p}_1}, \mathrm{e}^{\mathrm{i}\hat{p}_2}, \mathrm{e}^{\mathrm{i}\hat{p}_3}, \mathrm{e}^{\mathrm{i}\hat{p}_4}| -\mathrm{e}^{\mathrm{i}\tilde{p}_1}, -\mathrm{e}^{\mathrm{i}\tilde{p}_2}, -\mathrm{e}^{\mathrm{i}\tilde{p}_3}, -\mathrm{e}^{\mathrm{i}\tilde{p}_4}\}_{\text{Using the anti-periodic } \mathcal{R}^{\text{instead}}}.\end{aligned}$$

The same kind of statement hold for the AdS element $\mathcal{Q}$.

The computation of the quasi-momenta is then straightforward. The S^5 components $\tilde{p}_i$ are given in terms of the eigenvalues[44] of the symmetric matrix:

$$\tilde{A}(x) = \pi \begin{pmatrix} -\tilde{a}_+(1/x) & \tilde{b}_+ & -\tilde{c}(1/x) & \tilde{d}(x) \\ \tilde{b}_+ & \tilde{a}_+(x) & \tilde{d}(1/x) & \tilde{c}(x) \\ -\tilde{c}(1/x) & \tilde{d}(1/x) & \tilde{a}_-(x) & \tilde{b}_- \\ \tilde{d}(x) & \tilde{c}(x) & \tilde{b}_- & -\tilde{a}_-(1/x) \end{pmatrix} \tag{B.2}$$

with

$$\begin{aligned}\tilde{a}_\pm(x) &= \pm\tilde{a}(x) - m_3\cos\theta \\ \tilde{a}(x) &= -\frac{m_1 - w_1 x + (m_2 - w_2 x)\cos\theta + x\cos 2\gamma\,(-w_1 + m_1 x + (w_2 - m_2 x)\cos\theta)}{x^2 - 1} \\ \tilde{b}_\pm &= (m_2 \mp m_3)\cos\gamma\,\sin\theta \\ \tilde{c}(x) &= \frac{(m_2 + m_3)x^2 - (m_2 - m_3) - 2w_3 x}{x^2 - 1}\sin\gamma\,\sin\theta \\ \tilde{d}(x) &= \frac{-m_1 + w_1 x + (m_2 - w_2 x)\cos\theta}{x^2 - 1}\sin 2\gamma\end{aligned}$$

[44] To each eigenvalue, we might need to add a multiple of π in such a way that its asymptotics become those prescribed in section 1.1.1. If $\mathcal{R}$ is periodic this multiple should contain an even number of π's whereas if it is anti-periodic, we should add πn with n odd to each quasi-momentum—see discussion in the text.

while the AdS quasi-momenta $\hat{p}_i$ are the eigenvalues of

$$\hat{A}(x) = \pi \begin{pmatrix} -\hat{a}_+(1/x) & \hat{b}_+ & -\hat{c}(x) & \hat{d}(x) \\ \hat{b}_+ & \hat{a}_+(x) & \hat{d}(x) & \hat{c}(x) \\ \hat{c}(x) & -\hat{d}(x) & \hat{a}_-(x) & \hat{b}_- \\ -\hat{d}(x) & -\hat{c}(x) & \hat{b}_- & -\hat{a}_-(1/x) \end{pmatrix} \tag{B.3}$$

with

$$\begin{aligned} \hat{a}_\pm(x) &= \pm\frac{2\pi\kappa - k_1(x^2-1)\cos\theta}{x^2-1}\cosh\rho + k_2\cos\psi \\ \hat{b}_\pm &= (k_2\cosh\rho \mp k_1)\sin\psi \\ \hat{c}(x) &= \frac{k_2(x^2+1) - 2w_2 x}{x^2-1}\sin\psi\sinh\rho \\ \hat{d}(x) &= \frac{k_1(x^2+1) - 2w_1 x}{x^2-1}\cos\psi\sinh\rho. \end{aligned}$$

For the simple $\mathfrak{su}(2)$ or $\mathfrak{sl}(2)$ solutions we have, amongst other conditions, $\theta = \psi = 0$ which simplifies the computation drastically.

Appendix C. BMN string, details

This appendix serves as a complement to section 3.3.1. The quasi-momenta with the correct poles located at (186) and residues given by (184) are given by

$$\begin{aligned} \delta\hat{p}_2 &= \hat{a} + \frac{\delta\alpha_+}{x-1} + \frac{\delta\alpha_-}{x+1} + \sum_{i=\hat{3},\hat{4},\tilde{3},\tilde{4}}\sum_n \frac{\alpha\big(x_n^{\hat{2}i}\big)N_n^{\hat{2}i}}{x - x_n^{\hat{2}i}} - \sum_{i=\hat{3},\hat{4},\tilde{3},\tilde{4}}\sum_n \frac{\alpha\big(x_n^{\hat{1}i}\big)N_n^{\hat{1}i}}{1/x - x_n^{\hat{1}i}} \\ \delta\hat{p}_3 &= \hat{b} + \frac{\delta\beta_+}{x-1} + \frac{\delta\beta_-}{x+1} - \sum_{i=\hat{1},\hat{2},\tilde{1},\tilde{2}}\sum_n \frac{\alpha\big(x_n^{\hat{3}i}\big)N_n^{\hat{3}i}}{x - x_n^{\hat{3}i}} + \sum_{i=\hat{1},\hat{2},\tilde{1},\tilde{2}}\sum_n \frac{\alpha\big(x_n^{\hat{4}i}\big)N_n^{\hat{4}i}}{1/x - x_n^{\hat{4}i}}, \end{aligned}$$

where the last term guarantees that $\delta\hat{p}_{1,4}(x) = -\delta\hat{p}_{2,3}(1/x)$ have right poles with appropriate residues in the physical domain. Analogously,

$$\delta\tilde{p}_2 = \tilde{a} + \frac{\delta\alpha_+}{x-1} + \frac{\delta\alpha_-}{x+1} - \sum_{i=\hat{3},\hat{4},\tilde{3},\tilde{4}}\sum_n \frac{\alpha\big(x_n^{\tilde{2}i}\big)N_n^{\tilde{2}i}}{x - x_n^{\tilde{2}i}} + \sum_{i=\hat{3},\hat{4},\tilde{3},\tilde{4}}\sum_n \frac{\alpha\big(x_n^{\tilde{1}i}\big)N_n^{\tilde{1}i}}{1/x - x_n^{\tilde{1}i}} \tag{C.1}$$

$$\delta\tilde{p}_3 = \tilde{b} + \frac{\delta\beta_+}{x-1} + \frac{\delta\beta_-}{x+1} + \sum_{i=\hat{1},\hat{2},\tilde{1},\tilde{2}}\sum_n \frac{\alpha\big(x_n^{\tilde{3}i}\big)N_n^{\tilde{3}i}}{x - x_n^{\tilde{3}i}} - \sum_{i=\hat{1},\hat{2},\tilde{1},\tilde{2}}\sum_n \frac{\alpha\big(x_n^{\tilde{4}i}\big)N_n^{\tilde{4}i}}{1/x - x_n^{\tilde{4}i}} \tag{C.2}$$

and $\delta\tilde{p}_{1,4}(x) = -\delta\tilde{p}_{2,3}(1/x)$. From the large x behavior of these quasi-momenta, one obtains

$$\begin{aligned} \hat{a} &= -\sum_n \frac{2\pi n}{\sqrt{\lambda}\mathcal{J}}\sum_{i=\hat{3},\hat{4},\tilde{3},\tilde{4}} N_n^{\hat{1}i}, \qquad \hat{b} = +\sum_n \frac{2\pi n}{\sqrt{\lambda}\mathcal{J}}\sum_{i=\hat{1},\hat{2},\tilde{1},\tilde{2}} N_n^{\hat{4}i}, \\ \tilde{a} &= +\sum_n \frac{2\pi n}{\sqrt{\lambda}\mathcal{J}}\sum_{i=\hat{3},\hat{4},\tilde{3},\tilde{4}} N_n^{\tilde{1}i}, \qquad \tilde{b} = -\sum_n \frac{2\pi n}{\sqrt{\lambda}\mathcal{J}}\sum_{i=\hat{1},\hat{2},\tilde{1},\tilde{2}} N_n^{\tilde{4}i}, \end{aligned}$$

the level matching condition (183) and

$$\delta\alpha^+ - \delta\alpha^- = -\sum_n \frac{2\pi n}{\sqrt{\lambda}\mathcal{J}}\sum_{i=\hat{3},\hat{4},\tilde{3},\tilde{4}}\sum_{j=\hat{1},\hat{2}} N_n^{ij},$$

$$\delta\beta^+ - \delta\beta^- = -\sum_n \frac{2\pi n}{\sqrt{\lambda}\mathcal{J}} \sum_{i=\hat{3},\hat{4},\tilde{3},\tilde{4}} \sum_{j=\tilde{3},\tilde{4}} N_n^{ij}.$$

Appendix D. $\mathfrak{su}(2)$ circular string, details

In this appendix, we present the details of the calculations from section 3.3.2 of the fluctuation frequencies around the one-cut $\mathfrak{su}(2)$ solution.

D.1. S^5 modes

We start from the ansatz (192). We have four types of poles ($\tilde{1}\tilde{3}$, $\tilde{2}\tilde{4}$, $\tilde{2}\tilde{3}$, $\tilde{1}\tilde{4}$). Thus,

$$f(x) = \tfrac{1}{2}(\delta\tilde{p}_2(x) + \delta\tilde{p}_3(x))$$

must have simple poles at $x_n^{\tilde{2}\tilde{4}}$ and $x_n^{\tilde{1}\tilde{3}}$ with residues $\frac{1}{2}\alpha\big(x_n^{\tilde{1}\tilde{3}}\big)$ and $-\frac{1}{2}\alpha\big(x_n^{\tilde{2}\tilde{4}}\big)$ respectively (see figure 17 or (184). The same holds for

$$f(1/x) = -\tfrac{1}{2}(\delta\tilde{p}_4(x) + \delta\tilde{p}_1(x)).$$

Moreover, since the residues of $\delta\tilde{p}_i$ are connected to the AdS quasi-momenta (16) and these are given by (194) we conclude that $f(x)$ should be regular at $x = \pm 1$. Thus, we obtain

$$f(x) = -\sum_n \left(\frac{N_n^{\tilde{2}\tilde{4}}}{2} \left[\frac{\alpha\big(x_n^{\tilde{2}\tilde{4}}\big)}{x - x_n^{\tilde{2}\tilde{4}}} + \frac{\alpha\big(x_n^{\tilde{2}\tilde{4}}\big)}{x_n^{\tilde{2}\tilde{4}}(1 - x x_n^{\tilde{2}\tilde{4}})} \right] - (\tilde{2}\tilde{4} \to \tilde{1}\tilde{3}) \right). \tag{D.1}$$

Then

$$g(x) = \frac{K(x)}{2}\,(\delta\tilde{p}_2(x) - \delta\tilde{p}_3(x))$$

must have simple poles at $x_n^{\tilde{2}\tilde{4}}$, $x_n^{\tilde{1}\tilde{3}}$ and $x_n^{\tilde{2}\tilde{3}}$ with residues $-\frac{1}{2}\alpha\big(x_n^{\tilde{1}\tilde{3}}\big)$, $-\frac{1}{2}\alpha\big(x_n^{\tilde{2}\tilde{4}}\big)$ and $-\alpha\big(x_n^{\tilde{2}\tilde{3}}\big)$ respectively while

$$g(1/x) = \frac{K(x)}{2}\,(\delta\tilde{p}_4(x) - \delta\tilde{p}_1(x))$$

must have simple poles at $x_n^{\tilde{2}\tilde{4}}$, $x_n^{\tilde{1}\tilde{3}}$ and $x_n^{\tilde{1}\tilde{4}}$ with residues $\frac{1}{2}\alpha\big(x_n^{\tilde{1}\tilde{3}}\big)$, $\frac{1}{2}\alpha\big(x_n^{\tilde{2}\tilde{4}}\big)$ and $\alpha\big(x_n^{\tilde{1}\tilde{4}}\big)$ respectively. In contrast to $f(x)$, this function may have poles at ± 1 so we arrive at

$$\begin{aligned} g(x) = a + \frac{\alpha_-}{x^2-1} + \frac{x\alpha_+}{x^2-1} &+ \sum_n \left(N_n^{\tilde{1}\tilde{4}} \frac{\alpha\big(x_n^{\tilde{1}\tilde{4}}\big) K\big(1/x_n^{\tilde{1}\tilde{4}}\big)}{x_n^{\tilde{1}\tilde{4}}\big(1 - x x_n^{\tilde{1}\tilde{4}}\big)} - N_n^{\tilde{2}\tilde{3}} \frac{\alpha\big(x_n^{\tilde{2}\tilde{3}}\big) K\big(x_n^{\tilde{2}\tilde{3}}\big)}{x - x_n^{\tilde{2}\tilde{3}}} \right) \\ &+ \sum_n \left(\frac{N_n^{\tilde{2}\tilde{4}}}{2} \left[\frac{\alpha\big(x_n^{\tilde{2}\tilde{4}}\big) K\big(1/x_n^{\tilde{2}\tilde{4}}\big)}{x_n^{\tilde{2}\tilde{4}}\big(1 - x x_n^{\tilde{2}\tilde{4}}\big)} - \frac{\alpha\big(x_n^{\tilde{2}\tilde{4}}\big) K\big(x_n^{\tilde{2}\tilde{4}}\big)}{x - x_n^{\tilde{2}\tilde{4}}} \right] + (\tilde{2}\tilde{4} \to \tilde{1}\tilde{3}) \right). \end{aligned} \tag{D.2}$$

Finally, the remaining constants are fixed by the large x asymptotic (182) to be

$$a = -\frac{2\pi}{\sqrt{\lambda}} \sum_n \big[m\big(N_n^{\tilde{1}\tilde{3}} + N_n^{\tilde{2}\tilde{4}}\big) + 2m N_n^{\tilde{2}\tilde{3}} \big]$$

$$\alpha_+ = \frac{2\pi}{\sqrt{\lambda}} \sum_n \left[\big(N_n^{\tilde{1}\tilde{3}} + N_n^{\tilde{2}\tilde{4}}\big)\big(x_n^{\tilde{1}\tilde{3}}(m+n) - \mathcal{J} - K\big(x_n^{\tilde{1}\tilde{3}}\big)\big) + N_n^{\tilde{1}\tilde{4}}\big(x_n^{\tilde{1}\tilde{4}} n - 2\mathcal{J}\big) + N_n^{\tilde{2}\tilde{3}} \frac{2m+n}{x_n^{\tilde{2}\tilde{3}}} \right]$$

$$\alpha_- = \frac{2\pi}{\sqrt{\lambda}} \sum_n \big[N_n^{\tilde{1}\tilde{3}} + N_n^{\tilde{1}\tilde{4}} + N_n^{\tilde{2}\tilde{3}} + N_n^{\tilde{2}\tilde{4}} \big] n.$$

Then, from the residue at $x = 1$ we read $\delta E = \frac{\alpha_+}{\sqrt{m^2 + \mathcal{J}^2}}$.

D.2. Fermionic modes

Arguments similar to those in the previous section lead to

$$f(x)=\frac{2\pi}{\sqrt{\lambda}}\frac{x}{x^2-1}\sum_n\left[\frac{N_n^{\hat1\bar4}+N_n^{\hat2\bar4}-N_n^{\hat3\bar1}-N_n^{\hat4\bar1}}{xx_n^{\hat1\bar4}-1}+x\frac{N_n^{\hat3\bar2}+N_n^{\hat4\bar2}-N_n^{\hat1\bar3}-N_n^{\hat2\bar3}}{x-x_n^{\hat3\bar2}}\right]$$

and

$$\begin{aligned}g(x)=b&+\frac{\beta_-}{x^2-1}+\frac{x\beta_+}{x^2-1}\\&+\frac{2\pi}{\sqrt{\lambda}}\sum_n\left[\frac{\left(\sqrt{m^2+\mathcal{J}^2}x_n+n\left(1-x_n^2\right)\right)\left(N_n^{\hat1\bar4}+N_n^{\hat2\bar4}+N_n^{\hat3\bar1}+N_n^{\hat4\bar1}\right)}{(1-xx_n)\left(x_n^2-1\right)}\right.\\&\left.-x_n\frac{\left(\sqrt{m^2+\mathcal{J}^2}x_n+(n+m)\left(1-x_n^2\right)\right)\left(N_n^{\hat3\bar2}+N_n^{\hat4\bar2}+N_n^{\hat1\bar3}+N_n^{\hat2\bar3}\right)}{(x-x_n)\left(x_n^2-1\right)}\right],\end{aligned}$$

where

$$b=\frac{2\pi m}{\sqrt{\lambda}}\sum_n\left(N_n^{\hat1\bar3}+N_n^{\hat2\bar3}+N_n^{\hat1\bar3}+N_n^{\hat1\bar3}\right)$$

$$\beta_-=\frac{2\pi}{\sqrt{\lambda}}\sum_n\left(\frac{x_n\sqrt{m^2+\mathcal{J}^2}}{x_n^2-1}-n\right)\left(N_n^{\hat1\bar3}+N_n^{\hat1\bar4}+N_n^{\hat2\bar3}+N_n^{\hat2\bar4}+N_n^{\hat3\bar1}+N_n^{\hat3\bar2}+N_n^{\hat4\bar1}+N_n^{\hat4\bar2}\right)$$

$$\begin{aligned}\beta_+=\frac{2\pi}{\sqrt{\lambda}}\sum_n\left[\left(\mathcal{J}-nx_n+\frac{x_n^2\sqrt{m^2+\mathcal{J}^2}}{x_n^2-1}\right)\left(N_n^{\hat1\bar4}+N_n^{\hat2\bar4}+N_n^{\hat3\bar1}+N_n^{\hat4\bar1}\right)\right.\\\left.+\left(\frac{\sqrt{m^2+\mathcal{J}^2}}{x_n^2-1}-\frac{m+n}{x_n}\right)\left(N_n^{\hat1\bar3}+N_n^{\hat2\bar3}+N_n^{\hat3\bar2}+N_n^{\hat4\bar2}\right)\right].\end{aligned}$$

The AdS_5 part of the quasi-momenta is given by

$$\delta\hat p_2(x)=\frac{2\pi}{\sqrt{\lambda}}\frac{x}{x^2-1}\left(+\delta\Delta-2\frac{N_n^{\hat1\bar3}+N_n^{\hat1\bar4}}{xx_n-1}-2x\frac{N_n^{\hat2\bar3}+N_n^{\hat2\bar4}}{x_n-x}\right)$$

$$\delta\hat p_3(x)=\frac{2\pi}{\sqrt{\lambda}}\frac{x}{x^2-1}\left(-\delta\Delta+2\frac{N_n^{\hat4\bar1}+N_n^{\hat4\bar2}}{xx_n-1}+2x\frac{N_n^{\hat3\bar1}+N_n^{\hat3\bar2}}{x_n-x}\right),$$

and $\delta\hat p_{1,4}(x)=-\delta\hat p_{2,3}(1/x)$. The constant Δ can be found by fixing the residues at ±1 for $\delta\hat p_i$ and $\delta\tilde p_i$ to be equal (16) and is given in the main text (196).

Appendix E. $\mathfrak{sl}(2)$ circular string

The eigenvalues of (B.2) and (B.3) for the $\mathfrak{sl}(2)$ circular string described in the beginning of section 3.3.3 yield the most general one-cut quasi-momentum connecting $\hat p_2$ and $\hat p_3$. (Due to the $x\to1/x$ symmetry, $\hat p_1$ and $\hat p_4$ will also be connected by a cut, but this will be in an unphysical domain, that is, inside the unit circle.) Explicitly, we find

$$\tilde p_{1,2}=-\tilde p_{3,4}=2\pi\frac{\mathcal{J}x+m}{x^2-1},\tag{E.1}$$

and

$$\begin{pmatrix}\hat{p}_1\\ \hat{p}_2\\ \hat{p}_3\\ \hat{p}_4\end{pmatrix}=\begin{pmatrix}-\hat{p}_2(1/x)\\ +\hat{p}_2(x)\\ -\hat{p}_2(x)\\ +\hat{p}_2(1/x)\end{pmatrix},$$

where [24]

$$\hat{p}_2=k\pi\left(1-\frac{(Cx+1)\sqrt{x^2-2BCx+C^2}}{C(x^2-1)}\right) \tag{E.2}$$

and

$$w\equiv\frac{k}{2}\left(C+\frac{1}{C}\right),\qquad B=1+\frac{2\mathcal{S}}{w}. \tag{E.3}$$

From all solutions of (197) and (E.3) for solutions for C and B, we should pick that for which we have a real cut outside the unit circle.

In the rest of this appendix, we will excite this solution by adding poles to quasi-momenta as we did for the $\mathfrak{su}(2)$ solution. In this way, we shall find the energy shifts around this classical solution. Moreover, as for the $\mathfrak{su}(2)$ string, we shall consider the AdS_5, S^5 and fermions separately, assuming for simplicity the Riemann identity (183) to be satisfied *for each of the sectors separately*—the result, as before, holds if we relax this stronger assumption.

E.1. The AdS$_5$ excitations

For these excitations, the S^5 quasi-momentum remains untouched because its asymptotics do not change and it is still only allowed to have simple poles at ±1. Due to the Virasoro coupling of these quasi-momenta to the AdS_5 ones through the poles at ±1 (16), we see that $\delta\hat{p}_i$ must have no poles at these points. The only poles of these quasi-momenta should be located at $x_n^{\hat{i}\hat{j}}$ with residues given by (184)—see figure 17. Finally, as explained in section 3.3.2, the perturbed quasi-momenta should have inverse square behavior close to the branch points of the classical solution.

Thus, from the same kind of reasoning we saw in the previous section for the $\mathfrak{su}(2)$ circular string, we find (E.6) for the AdS_3 excitations connecting sheets $(\hat{p}_2,\hat{p}_3)$ and $(\hat{p}_1,\hat{p}_4)$ and (E.7) for the remaining AdS_5 excitations uniting $(\hat{p}_1,\hat{p}_3)$ and $(\hat{p}_2,\hat{p}_4)$. From the large x behavior (182) of these quasi-momenta, we read the energy shifts[45]

$$\delta E=\sum_n\left(N_n^{\hat{2}\hat{3}}\left[\frac{k-n}{k}\frac{x_n^{\hat{2}\hat{3}}-C^{-1}}{x_n^{\hat{2}\hat{3}}+C^{-1}}+\frac{nw}{k\kappa}\right]+N_n^{\hat{1}\hat{4}}\left[\frac{k+n}{k}\frac{x_n^{\hat{1}\hat{4}}-C}{x_n^{\hat{1}\hat{4}}+C}+\frac{nw}{k\kappa}\right]\right) \tag{E.4}$$

and

$$\delta E=\sum_n N_n^{\hat{1}\hat{3}}\left[\frac{K\left(x_n^{\hat{1}\hat{3}}\right)k+n\left(x_n^{\hat{1}\hat{3}}-C\right)}{k\left(x_n^{\hat{1}\hat{3}}+C\right)}+\frac{nw}{k\kappa}\right]+N_n^{\hat{2}\hat{4}}\left[\frac{K\left(x_n^{\hat{2}\hat{4}}\right)k+n\left(x_n^{\hat{2}\hat{4}}-C\right)}{k\left(x_n^{\hat{2}\hat{4}}+C\right)}+\frac{nw}{k\kappa}\right], \tag{E.5}$$

where, as for the $\mathfrak{su}(2)$ string, we denote the square root in the classical solution (E.2) by $K(x)$.

[45] These AdS_3 excitations were also found in a similar way by K Zarembo in relation with the finite size corrections computation [61] (according to the private communication).

E.1.1. AdS_3 excitations—details. In strict analogy to what we have already seen for the $\mathfrak{su}(2)$ solution, the two (left and right) physical excitations inside the $\mathfrak{sl}(2)$ sector described by the $AdS_3\sigma$ model are given by the poles, connecting the pairs of sheets $(\hat{p}_2, \hat{p}_3)$ and $(\hat{p}_1, \hat{p}_4)$. We denote the number of such poles by $N_{\hat{2}\hat{3}}$ and $N_{\hat{1}\hat{4}}$ respectively.

As explained above, the AdS_5 excitation shifts of $\hat{p}$'s have no poles at ± 1 and must present an inverse square root behavior close to the branch points of the classical solution. Thus, we can write

$$\delta\hat{p}_2(x) = \frac{2\pi}{\sqrt{\lambda}K(x)} \sum_n \left(N_n^{\hat{2}\hat{3}} \frac{x a_n}{x - x_n^{\hat{2}\hat{3}}} + N_n^{\hat{1}\hat{4}} \frac{x \bar{a}_n}{x - 1/x_n^{\hat{1}\hat{4}}} \right), \tag{E.6}$$

where

$$K(x) \equiv \sqrt{x^2 - 2BCx + C^2}$$

and the position of the roots is given by (178). Fixing the residues at $x_n^{\hat{2}\hat{3}}$ and $x_n^{\hat{1}\hat{4}}$ according to (184), we have

$$a_n = \frac{2Cx_n^{\hat{2}\hat{3}}(k-n)}{k\left(Cx_n^{\hat{2}\hat{3}} + 1\right)}, \qquad \bar{a}_n = -\frac{2C(k+n)}{k\left(C + x_n^{\hat{1}\hat{4}}\right)}.$$

The large x asymptotic (182) is consistent if the Riemann bilinear identity (183) is satisfied

$$\sum_n \left(N_n^{\hat{2}\hat{3}} + N_n^{\hat{1}\hat{4}}\right) n = 0,$$

and the energy shift is then given by (E.4)).

E.1.2. The remaining AdS_5 excitations—details. These correspond to simple poles connecting $(\hat{p}_1, \hat{p}_3)$ and $(\hat{p}_2, \hat{p}_4)$ for which

$$\delta\hat{p}_2(x) = \frac{2\pi}{\sqrt{\lambda}} \sum_n \left[\frac{N_n^{\hat{1}\hat{3}} x \left(a_n + \frac{b_n + c_n x}{K(x)}\right)}{\left(x - x_n^{\hat{1}\hat{3}}\right)\left(x - 1/x_n^{\hat{1}\hat{3}}\right)} + \frac{N_n^{\hat{2}\hat{4}} x \left(\bar{a}_n + \frac{\bar{b}_n + \bar{c}_n x}{K(x)}\right)}{\left(x - x_n^{\hat{2}\hat{4}}\right)\left(x - 1/x_n^{\hat{2}\hat{4}}\right)} \right]. \tag{E.7}$$

Then $\delta\hat{p}_3$, just as we saw for the $\mathfrak{su}(2)$ solution, is the analytical continuation of $\delta\hat{p}_2$ through the cut. In simpler terms, it corresponds to a simple change of sign of $K(x)$ in the above expression. Finally, $\delta\hat{p}_{1,4}(x) = -\delta\hat{p}_{2,3}(1/x)$.

The undetermined coefficients are fixed by the residues

$$\operatorname*{res}_{x=x_n^{\hat{1}\hat{3}}} \hat{p}_{1,3} = \pm\alpha\left(x_n^{\hat{1}\hat{3}}\right) N_n^{\hat{1}\hat{3}}, \qquad \operatorname*{res}_{x=x_n^{\hat{1}\hat{3}}} \hat{p}_{2,4} = 0,$$

$$\operatorname*{res}_{x=x_n^{\hat{2}\hat{4}}} \hat{p}_{2,4} = \pm\alpha\left(x_n^{\hat{2}\hat{4}}\right) N_n^{\hat{2}\hat{4}}, \qquad \operatorname*{res}_{x=x_n^{\hat{2}\hat{4}}} \hat{p}_{1,3} = 0$$

to be

$$a_n = -1, \qquad b_n = C\frac{2nx_n^{\hat{1}\hat{3}} + kK\left(x_n^{\hat{1}\hat{3}}\right)}{k\left(x_n^{\hat{1}\hat{3}} + C\right)}, \qquad c_n = \frac{kK\left(x_n^{\hat{1}\hat{3}}\right) - 2Cn}{k\left(C + x_n^{\hat{1}\hat{3}}\right)}$$

$$\bar{a}_n = 1, \qquad \bar{b}_n = C\frac{2nx_n^{\hat{2}\hat{4}} + kK\left(x_n^{\hat{2}\hat{4}}\right)}{k\left(x_n^{\hat{2}\hat{4}} + C\right)}, \qquad \bar{c}_n = \frac{kK\left(x_n^{\hat{2}\hat{4}}\right) - 2Cn}{k\left(C + x_n^{\hat{2}\hat{4}}\right)}.$$

Hence, with the level matching condition

$$\sum_n \left(N_n^{\hat{1}\hat{3}} + N_n^{\hat{2}\hat{4}}\right) n = 0,$$

we find, from the large x behavior, the energy shift (E.5).

E.2. The S^5 excitations

The S^5 quasi-momentum (E.1) has no branch cuts and thus $\delta\tilde{p}_i$ will be of the same form as we found for the BMN string except that the position of the roots, found from (178), is now given by

$$\tilde{x}_n \equiv x_n^{\tilde{1}\tilde{3}} = x_n^{\tilde{1}\tilde{4}} = x_n^{\tilde{2}\tilde{3}} = x_n^{\tilde{1}\tilde{4}} = \frac{\mathcal{J} + \sqrt{\mathcal{J}^2 + (n+m)^2 - m^2}}{n} \tag{E.8}$$

instead of (186). The explicit expressions for $\delta\tilde{p}_i$ are given in (E.10). This perturbation shifts the residues at ± 1 from

$$\pi\,(\mathcal{J} \mp m)$$

to some other values, which we parameterize by

$$\pi(\mathcal{J} + \delta\mathcal{J}^{\text{eff}} \mp (m + \delta m^{\text{eff}})).$$

The precise expressions for these shifts can be found in (E.10) and (E.11). But then, since the AdS_5 quasi-momenta only know about the S^5 sector through the residues at these points, the perturbed quasi-momenta $\hat{p}_i + \delta\hat{p}_i$ will be given by the same expression (E.2) with the trivial replacement

$$\mathcal{J}, m \to \mathcal{J} + \delta\mathcal{J}^{\text{eff}}, m + \delta m^{\text{eff}}.$$

The same is true for the energy given in (E.3) so that—see appendix D.2 for details—we can immediately find

$$\delta E = \frac{1}{\kappa}\sum_n \left(N_n^{\tilde{1}\tilde{3}} + N_n^{\tilde{1}\tilde{4}} + N_n^{\tilde{2}\tilde{3}} + N_n^{\tilde{2}\tilde{4}}\right)\left(\sqrt{(n+m)^2 - m^2 + \mathcal{J}^2} - \mathcal{J}\right). \tag{E.9}$$

E.2.1. The S^5 excitations—details. As explained above, the perturbed S^5 quasi-momenta are of the BMN form (C.1) and (C.2):

$$\delta\tilde{p}_2(x) = +\frac{4\pi}{\sqrt{\lambda}}\frac{x^2}{x^2-1}\sum_n\left(\frac{N_n^{\tilde{2}\tilde{3}} + N_n^{\tilde{2}\tilde{4}}}{\tilde{x}_n - x} + \frac{N_n^{\tilde{1}\tilde{3}} + N_n^{\tilde{1}\tilde{4}}}{x^2\tilde{x}_n - x}\right)$$

$$\delta\tilde{p}_3(x) = -\frac{4\pi}{\sqrt{\lambda}}\frac{x^2}{x^2-1}\sum_n\left(\frac{N_n^{\tilde{1}\tilde{3}} + N_n^{\tilde{2}\tilde{3}}}{\tilde{x}_n - x} + \frac{N_n^{\tilde{2}\tilde{4}} + N_n^{\tilde{1}\tilde{4}}}{x^2\tilde{x}_n - x}\right),$$

where $\tilde{x}_n$ is given by (E.8). Then, in the notation introduced above, the shift in the $x = \pm 1$ residues is given by

$$\delta\mathcal{J}^{\text{eff}} = \frac{\sum_n \left(N_n^{\tilde{1}\tilde{3}} + N_n^{\tilde{1}\tilde{4}} + N_n^{\tilde{2}\tilde{3}} + N_n^{\tilde{2}\tilde{4}}\right)\left(mn + \mathcal{J}^2 - \mathcal{J}\sqrt{\mathcal{J}^2 + n^2 + 2mn}\right)}{\sqrt{\lambda}(m^2 - \mathcal{J}^2)} \tag{E.10}$$

while δm^{eff} is given by

$$\mathcal{J}\delta m^{\text{eff}} + \delta\mathcal{J}^{\text{eff}} m = \frac{1}{\sqrt{\lambda}}\sum_n \left(N_n^{\tilde{1}\tilde{3}} + N_n^{\tilde{1}\tilde{4}} + N_n^{\tilde{2}\tilde{3}} + N_n^{\tilde{2}\tilde{4}}\right)n = 0 \tag{E.11}$$

due to the Riemann condition. Then, from (E.3) and (197), we have

$$\delta\mathcal{E} = \frac{w^3 - km\mathcal{J}}{w^2\kappa}\delta w = \frac{w(k^2 + m^2 + \mathcal{J}^2) - 3km\mathcal{J}}{w^2\kappa}\delta w$$

where, using (197) and (E.11), we have

$$\delta w = -\frac{\delta\mathcal{J}^{\text{eff}}}{\mathcal{J}}\frac{w^2(m^2 - \mathcal{J}^2)}{w(k^2 + m^2 + \mathcal{J}^2) - 3km\mathcal{J}}$$

so that δE will be given by (E.9).

E.3. Fermionic excitations

The fermionic excitations can be treated as for the $\mathfrak{su}(2)$ string. As before, we expect at most two different answers for the energy shifts—one coming from the poles uniting the $(\hat{1}\tilde{3}, \hat{1}\tilde{4}, \hat{4}\tilde{1}, \hat{4}\tilde{2})$ sheets and the other coming from the poles uniting the $(\hat{2}\tilde{3}, \hat{2}\tilde{4}, \hat{3}\tilde{1}, \hat{3}\tilde{2})$ sheets. From the expressions in appendix C.3, we find

$$\delta\Delta = \sum_n \big(N_n^{\hat{1}\tilde{3}} + N_n^{\hat{1}\tilde{4}} + N_n^{\hat{4}\tilde{1}} + N_n^{\hat{4}\tilde{2}}\big)\delta\Delta_n^{(1)} + \sum_n \big(N_n^{\hat{2}\tilde{3}} + N_n^{\hat{2}\tilde{4}} + N_n^{\hat{3}\tilde{1}} + N_n^{\hat{3}\tilde{2}}\big)\delta\Delta_n^{(2)}, \tag{E.12}$$

where

$$\delta\Delta_n^{(1)} = \frac{(2m+k) - 2\mathcal{J}C - kC^2}{k(C^2-1)\big(C^{-1}x_n^{\hat{1}\tilde{3}}+1\big)} + \frac{n\big(C^{-1}x_n^{\hat{1}\tilde{3}}-1\big)}{k\big(C^{-1}x_n^{\hat{1}\tilde{3}}+1\big)} + \frac{nw}{k\kappa}$$

$$\delta\Delta_n^{(2)} = \frac{(2m-k)C^2 - 2\mathcal{J}C + k}{k(C^2-1)\big(Cx_n^{\hat{2}\tilde{3}}+1\big)} - \frac{n\big(Cx_n^{\hat{2}\tilde{3}}-1\big)}{k\big(Cx_n^{\hat{2}\tilde{3}}+1\big)} + \frac{nw}{k\kappa}$$

with the position of the fermionic poles being given by (178), in terms of the algebraic curve for the classical solution.

E.3.1. Fermionic excitations—details. The S^5 part of the quasi-momenta is given by

$$\tilde{p}_2(x) = +\frac{4\pi x}{\sqrt{\lambda}(x^2-1)}\sum_n\left(\frac{N_n^{\hat{3}\tilde{1}}+N_n^{\hat{4}\tilde{1}}}{xx_n^{\hat{3}\tilde{1}}-1} - x\frac{N_n^{\hat{3}\tilde{2}}+N_n^{\hat{4}\tilde{2}}}{x-x_n^{\hat{3}\tilde{1}}}\right)$$

$$\tilde{p}_3(x) = -\frac{4\pi x}{\sqrt{\lambda}(x^2-1)}\sum_n\left(\frac{N_n^{\hat{1}\tilde{4}}+N_n^{\hat{2}\tilde{4}}}{xx_n^{\hat{3}\tilde{1}}-1} - x\frac{N_n^{\hat{1}\tilde{3}}+N_n^{\hat{2}\tilde{3}}}{x-x_n^{\hat{3}\tilde{1}}}\right)$$

whereas the AdS_5 part is more complicated. Parameterizing $\delta\hat{p}$ as we did for the $\mathfrak{su}(2)$ string in (192), we have

$$f(x) = \frac{x}{x^2-1}\sum_n\left(x\frac{N_n^{\hat{2}\tilde{3}}+N_n^{\hat{2}\tilde{4}}-N_n^{\hat{3}\tilde{1}}-N_n^{\hat{3}\tilde{2}}}{x-x_n^{\hat{2}\tilde{3}}} + \frac{N_n^{\hat{2}\tilde{3}}+N_n^{\hat{2}\tilde{4}}-N_n^{\hat{3}\tilde{1}}-N_n^{\hat{3}\tilde{2}}}{xx_n^{\hat{2}\tilde{3}}-1}\right)$$

$$g(x) = \frac{x}{x^2-1}\sum_n\left(\left[\frac{xK\big(x_n^{\hat{2}\tilde{3}}\big)}{x-x_n^{\hat{2}\tilde{3}}} + a_nx + b_n\right]\big(N_n^{\hat{2}\tilde{3}}+N_n^{\hat{2}\tilde{4}}+N_n^{\hat{3}\tilde{1}}+N_n^{\hat{3}\tilde{2}}\big)\right.$$
$$\left. - \left[\frac{xx_n^{\hat{1}\tilde{3}}K(1/x_n^{\hat{1}\tilde{3}})}{xx_n^{\hat{1}\tilde{3}}-1} + \bar{a}_nx + \bar{b}_n\right]\big(N_n^{\hat{1}\tilde{3}}+N_n^{\hat{1}\tilde{4}}+N_n^{\hat{4}\tilde{1}}+N_n^{\hat{4}\tilde{2}}\big)\right),$$

where the remaining constants are given by

$$a_n = C\frac{(C^2-1)(k-2n)x_n^{\hat{2}\tilde{3}} + 2Cm - 2\mathcal{J}}{(C^2-1)\big(Cx_n^{\hat{2}\tilde{3}}+1\big)k}$$

$$\bar{a}_n = C\frac{(C^2-1)k - 2(m+n) + 2C(Cn+\mathcal{J})}{(C^2-1)\big(C+x_n^{\hat{1}\tilde{3}}\big)k}$$

$$b_n = C\frac{(C^2-1)k - 2C^2(m+n) + 2(n+C\mathcal{J})}{(C^2-1)\big(C+x_n^{\hat{2}\tilde{3}}\big)k}$$

$$\bar{b}_n = -C\frac{(C^2-1)(k+2n)x_n^{\hat{1}\tilde{3}} + 2Cm - 2C^2\mathcal{J}}{(C^2-1)\big(C+x_n^{\hat{1}\tilde{3}}\big)k}.$$

Then the energy shifts can be read from the large x asymptotics and are given in (E.12).

Appendix F. Ambiguities due to shifts

To compute the one-loop shift, one must sum all frequencies. This sum, however, is sensitive to the way the frequencies are labeled. Let us demonstrate this on a simple example. Consider the sum

$$\frac{1}{2}\sum_{n=-\infty}^{\infty}(2\omega_n-\omega_{n+m}-\omega_{n-m})$$

with $\omega_n=\omega_{-n}$ and assume that for a large mode number, $\omega_n\simeq|n|+\cdots$. Naively this sum is zero if m is an integer, since all terms cancel among each other if we allow the renumbering of the terms. However, a more careful analysis shows that this is not the case:

$$\frac{1}{2}\sum_{n=-N}^{N}(2\omega_n-\omega_{n+m}-\omega_{n-m})=\sum_{n=N-m+1}^{N}(\omega_n-\omega_{n-m})=m^2+\mathcal{O}(1/N)\,.$$

Thus, one should be very careful while calculating the one-loop shift with frequencies in hand because ambiguities can easily arise. Consider, for example, the equation for the bosonic frequencies for the general $3\mathcal{J}$ solution [87]:

$$P_8^{J_1J_2J_3}(\omega)=(\omega^2-n^2)^4-4(\omega^2-n^2)^2\sum_{i\neq j}^{3}\frac{\mathcal{J}_i}{w_i}(w_j\omega-m_jn)^2$$
$$+8\sum_{i\neq j\neq k\neq i}^{3}\frac{\mathcal{J}_i}{w_i}(w_j\omega-m_jn)^2(w_k\omega-m_kn)^2=0.$$

This solution can be smoothly deformed to a general $\mathfrak{su}(2)$ solution for which $J_3\to 0$ while preserving all constraints (6). In this limit, we find

$$P_8^{J_1J_20}(\omega)=P_4^{\mathfrak{su}(2)}(\omega)\big((\omega^2-n^2)^2-4\big(m_3n-\omega\sqrt{m_3^2+\nu^2}\big)^2\big),$$

where the quartic polynomial $P_4^{\mathfrak{su}(2)}(\omega)$ is that appearing in table 3 and gives us the usual $\mathfrak{su}(2)$ modes whereas the remaining equations yield the frequencies

$$\sqrt{(n+m_3)^2+\nu^2}+w_3,\qquad \sqrt{(n-m_3)^2+\nu^2}-w_3$$

instead of the two $\sqrt{n^2+\nu^2}$ we read from table 3. From the above explanation, this ambiguity converts into an extra contribution of m_3^2/κ to the one-loop shift.

Moreover, we also found contradictory results in the literature. For the simple $\mathfrak{su}(2)$ solution, in [86, 91, 92] the sum over fermionic frequencies ω_n^F is taken over the integers for even m and over $\mathbb{Z}+1/2$ for odd m while in [39, 55] the sum always goes over the integers. We found that the fermions will indeed be summed over integer n's. The same kind of mismatch appears for the $\mathfrak{sl}(2)$ circular string. For example, in [39, 58, 61, 88] the fermionic frequencies ω_n^F are summed with n integer whereas we found $\omega^F_{n+m/2-k/2}$ and $\omega^F_{-n-m/2-k/2}$, that is, the frequencies have half-integer arguments if $m+k$ is odd—see (199). In view of these discrepancies, we also repeated the calculation for the frequencies directly from the expansion of the string action using a coset representative parameterized as in [11]. We also found the same kind of field redefinitions which are trivially related to the $\mathcal{R}$ and $\mathcal{Q}$ matrices written in section 3.2. For the simple $\mathfrak{su}(2)$ solution, the field redefinitions always leave the fermions periodic whereas for the $\mathfrak{sl}(2)$ string they are periodic (anti-periodic) for $m+k$ even (odd) in agreement with the calculation presented in this paper. Shifts changing integers into half-integers are no longer related by the simple expressions of form m^2/κ like in the previous example. However, the sum over fermions can be replaced by an integral with exponential precision and therefore these shifts may end up being not so harmful.

Appendix G. Large N limit

In the x plane, the contour in figure 4(a) is mapped to that in figure 4(b). For large N, the contour starts at $-1-\epsilon_-^{ij}(N)$ and ends at $+1+\epsilon_+^{ij}(N)$. In this appendix, we perform a careful analysis of the large N limit.

G.1. Asymptotics of quasi-momenta and expansion of x_n

Let us take $\eta=1$ and use notations (47). Large n's are mapped to the vicinity of ±1 where

$$\hat{p}_2 \simeq +\frac{\alpha_\pm}{x\mp 1}+\sum_{n=0}\hat{a}_n^\pm(x\mp 1)^n, \qquad \tilde{p}_2 \simeq +\frac{\alpha_\pm}{x\mp 1}+\sum_{n=0}\tilde{a}_n^\pm(x\mp 1)^n,$$
$$\hat{p}_3 \simeq -\frac{\alpha_\pm}{x\mp 1}+\sum_{n=0}\hat{b}_n^\pm(x\mp 1)^n, \qquad \tilde{p}_3 \simeq -\frac{\alpha_\pm}{x\mp 1}+\sum_{n=0}\tilde{b}_n^\pm(x\mp 1)^n.$$

The remaining quasi-momenta are fixed by the $x\to 1/x$ symmetry:

$$\begin{aligned}\tilde{p}_{1,2}(x) &= -2\pi m-\tilde{p}_{2,1}(1/x)\\ \tilde{p}_{3,4}(x) &= +2\pi m-\tilde{p}_{4,3}(1/x)\\ \hat{p}_{1,2,3,4}(x) &= -\hat{p}_{2,1,4,3}(1/x).\end{aligned} \tag{G.1}$$

From this expansion, we can read the large n behavior of x_n^{ij} defined by (5). Let us, however, use a more general definition

$$p_i\big(x_n^{ij}\big)-p_j\big(x_n^{ij}\big)=2\pi(n-m_i+m_j). \tag{G.2}$$

For $n\to\pm\infty$, all x_n^{ij} are close to ±1 and we find

$$x_n^{ij}=\pm1+\frac{\alpha^\pm}{\pi n}+\mathcal{O}(1/n^2), \tag{G.3}$$

where we note that the first $1/n$ coefficient is universal and fixed uniquely by the residues of the quasi-momenta.

G.2. Large N versus ϵ regularization

The main goal of this appendix is to justify the integration path used in the main text where for all ij, the integral in the x plane starts from $-1-\epsilon$ and ends at $1+\epsilon$ as depicted in figure 20(b). However, by definition (205) we have to start from the large N regularization. These two regularizations, in principle, are not equivalent, since x_N^{ij}'s are not exactly equal for all ij and thus we should calculate the difference between both regularizations. In particular in (239), we will have slightly different contours of integrations after replacement of cot's by sign. One would like to make all the contours to be the circle of the radius $1+\epsilon$. However, while changing the contours of integration one will get some unwelcome contributions proportional to

$$\left(\frac{1}{\alpha_+}-\frac{1}{\alpha_-}\right)(m+m_{\hat{1}}+m_{\hat{2}}-m_{\tilde{1}}-m_{\tilde{2}})(m+m_{\tilde{3}}+m_{\tilde{4}}-m_{\hat{3}}-m_{\hat{4}}).$$

Fortunately it is possible to choose m_i in such a way that it is always zero, and this transformation is possible. For example,

$$m_{\tilde{1}}=m, \qquad m_{\tilde{4}}=-m \tag{G.4}$$

and all the other m_i are zero. This amounts to some prescription for the mode numbers. For obvious reasons, let us denote it by the Bethe ansatz friendly prescription. In contrast to what we had in section 3, we have no obvious argument in favor of this new prescription. For the $sl(2)$ and $su(2)$ one-cut solutions, this prescription gives the same result (with exponential precision in large $\mathcal{J}$) as in [58, 61, 85–88].

Appendix H. Derivation of the AFS formula for asymptotic string BAEs

In this appendix, we evaluate integral (297) and obtain the AFS BAE.

We can simplify expression for $H(x)$ (292) assuming that in (295) $P = 0$:

$$H(x) = -4\pi m + \frac{\Delta}{M}\frac{x}{x^2-1} + 2\mathrm{i}\sum_j \log\frac{y_j^+ x - 1}{y_j^- x - 1}. \tag{H.1}$$

We rewrite (297) in the x variable:

$$\mathrm{i}p_k = -\frac{M}{2}\oint \frac{\mathrm{i}}{2\pi}(H(x) - H(1/x))\left(\log\frac{x-y_k^+}{x-y_k^-} + \log\frac{x-1/y_k^+}{x-1/y_k^-}\right)\left(1-\frac{1}{x^2}\right)\mathrm{d}x, \tag{H.2}$$

where the contour goes in the counterclockwise direction around the unit circle, $y_k^\pm = X\left(w_k^\pm\right)$. Note that terms with $H(1/x)$ are equal to those with $H(x)$ after a change of the variable $x \to 1/x$ so that

$$\mathrm{i}p_k = M\oint H(x)\left(\log\frac{x-y_k^+}{x-y_k^-} + \log\frac{x-1/y_k^+}{x-1/y_k^-}\right)\left(\frac{x^2-1}{x^2}\right)\frac{\mathrm{d}x}{2\pi\mathrm{i}}. \tag{H.3}$$

Various terms are

$$I_1 \equiv \oint\left(-4\pi m + \frac{\Delta}{M}\frac{x}{x^2-1}\right)\log\frac{x-y_k^+}{x-y_k^-}\left(\frac{x^2-1}{x^2}\right)\frac{\mathrm{d}x}{2\pi\mathrm{i}} \tag{H.4}$$

$$I_2 \equiv \oint\left(-4\pi m + \frac{\Delta}{M}\frac{x}{x^2-1}\right)\log\frac{x-1/y_k^+}{x-1/y_k^-}\left(\frac{x^2-1}{x^2}\right)\frac{\mathrm{d}x}{2\pi\mathrm{i}} \tag{H.5}$$

$$I_3 \equiv 2\mathrm{i}\oint \log\frac{y_j^+ x - 1}{y_j^- x - 1}\log\frac{x-y_k^+}{x-y_k^-}\left(\frac{x^2-1}{x^2}\right)\frac{\mathrm{d}x}{2\pi\mathrm{i}} \tag{H.6}$$

$$I_4 \equiv 2\mathrm{i}\oint \log\frac{y_j^+ x - 1}{y_j^- x - 1}\log\frac{x-1/y_k^+}{x-1/y_k^-}\left(\frac{x^2-1}{x^2}\right)\frac{\mathrm{d}x}{2\pi\mathrm{i}}. \tag{H.7}$$

Integral I_1 can be calculated by residue in $x = 0$, since $|y_k^\pm| > 1$:

$$I_1 = \frac{\Delta}{M}\log\frac{y_k^+}{y_k^-} - 4\pi m\left(\frac{1}{y_k^+} - \frac{1}{y_k^-}\right). \tag{H.8}$$

Similar I_2 and I_4 are given by residue at infinity:

$$I_2 = 4\pi m\left(\frac{1}{y_k^+} - \frac{1}{y_k^-}\right) \tag{H.9}$$

$$I_4 = -2\mathrm{i}\left(\frac{1}{y_k^+} - \frac{1}{y_k^-}\right)\log\frac{y_j^+}{y_j^-}. \tag{H.10}$$

Calculation of I_3 is slightly more difficult. One can differentiate it with respect to y_j^+ to kill one of the logarithms and then calculate it by poles at $x = 0$:

$$\partial_{y_j^+} I_3 = 2\mathrm{i}\log\frac{y_k^+}{y_k^-} + 2\mathrm{i}\left(\frac{1}{y_j^{+2}} - 1\right)\log\frac{y_k^+ y_j^+ - 1}{y_k^- y_j^+ - 1}, \qquad I_3 = \int_{y_j^-}^{y_j^+}\partial_{y_j^+} I_3 \mathrm{d}y_j^+; \tag{H.11}$$

thus,

$$I_3 = 2\mathrm{i}\frac{u_j - u_k}{M}\log\frac{\left(y_j^+ y_k^- - 1\right)\left(y_j^- y_k^+ - 1\right)}{\left(y_j^+ y_k^+ - 1\right)\left(y_j^- y_k^- - 1\right)} + \frac{2}{M}\log\frac{y_j^- y_k^+ - 1}{y_j^+ y_k^- - 1}$$
$$+ 2\mathrm{i}\left(\left(y_j^+ - y_j^-\right)\log\frac{y_k^+}{y_k^-} - \left(y_k^+ - y_k^-\right)\log\frac{y_j^+}{y_j^-}\right). \tag{H.12}$$

Finally,

$$\mathrm{i}p_k = M\sum_{a=1}^{4} I_a = L\log\frac{y_k^+}{y_k^-}$$
$$+ \sum_j \left(2\log\frac{1 - 1/y_j^- y_k^+}{1 - 1/y_j^+ y_k^-} + 2\mathrm{i}(u_j - u_k)\log\frac{\left(y_j^+ y_k^- - 1\right)\left(y_j^- y_k^+ - 1\right)}{\left(y_j^+ y_k^+ - 1\right)\left(y_j^- y_k^- - 1\right)}\right); \tag{H.13}$$

thus, we prove (298) assuming $P = 0$. This immediately leads to the AFS BAE (299).

References

[1] Polyakov A M 1998 String theory and quark confinement *Nucl. Phys. Proc. Suppl.* **68** 1–8 (arXiv: hep-th/9711002)

[2] Maldacena J M 1998 The large N limit of superconformal field theories and supergravity *Adv. Theor. Math. Phys.* **2** 231–52 (arXiv:hep-th/9711200)

[3] Gubser S S, Klebanov I R and Polyakov A M 1998 Gauge theory correlators from non-critical string theory *Phys. Lett.* B **428** 105–14 (arXiv:hep-th/9802109)

[4] Witten E 1998 Anti-de Sitter space and holography *Adv. Theor. Math. Phys.* **2** 253–91 (arXiv:hep-th/9802150)

[5] Minahan J A and Zarembo K 2003 The Bethe-ansatz for $N = 4$ super Yang–Mills *J. High Energy Phys.* JHEP03(2003)013 (arXiv:hep-th/0212208)

[6] Lipatov L N 1994 Asymptotic behavior of multicolor QCD at high energies in connection with exactly solvable spin models *JETP Lett.* **59** 596–9

[7] Faddeev L D and Korchemsky G P 1995 High-energy QCD as a completely integrable model *Phys. Lett.* B **342** 311–22 (arXiv:hep-th/9404173)

[8] Bena I, Polchinski J and Roiban R 2004 Hidden symmetries of the AdS(5) $\times$ S^5 superstring *Phys. Rev.* D **69** 046002 (arXiv:hep-th/0305116)

[9] Metsaev R R and Tseytlin A A 1998 Type IIB superstring action in AdS(5) $\times$ S(5) background *Nucl. Phys.* B **533** 109–26 (arXiv:hep-th/9805028)

[10] Berkovits N, Bershadsky M, Hauer T, Zhukov S and Zwiebach B 2000 Superstring theory on AdS(2) $\times$ S(2) as a coset supermanifold *Nucl. Phys.* B **567** 61 (arXiv:hep-th/9907200)

[11] Alday L F, Arutyunov G and Frolov S 2006 New integrable system of 2dim fermions from strings on AdS(5) $\times$ S^5 *J. High Energy Phys.* JHEP01(2006)078 (arXiv:hep-th/0508140)

[12] Das A K, Maharana J, Melikyan A and Sato M 2004 The algebra of transition matrices for the AdS(5) $\times$ S^5 superstring *J. High Energy Phys.* JHEP12(2004)055 (arXiv:hep-th/0411200)

[13] Berkovits N 2005 BRST cohomology and nonlocal conserved charges *J. High Energy Phys.* JHEP02(2005)060 (arXiv:hep-th/0409159)

[14] Beisert N, Kazakov V A, Sakai K and Zarembo K 2006 The algebraic curve of classical superstrings on AdS(5) $\times$ S^5 *Commun. Math. Phys.* **263** 659–710 (arXiv:hep-th/0502226)

[15] Beisert N, Kazakov V A and Sakai K 2006 Algebraic curve for the SO(6) sector of AdS/CFT *Commun. Math. Phys.* **263** 611–57 (arXiv:hep-th/0410253)

[16] Dorey N and Vicedo B 2006 On the dynamics of finite-gap solutions in classical string theory *J. High Energy Phys.* JHEP07(2006)014 (arXiv:hep-th/0601194)

[17] Vicedo B 2008 *J. High Energy Phys.* JHEP06(2008)086 (arXiv:0803.1605 [hep-th])

[18] Kazakov V A, Marshakov A, Minahan J A and Zarembo K 2004 Classical/quantum integrability in AdS/CFT *J. High Energy Phys.* JHEP05(2004)024 (arXiv:hep-th/0402207)

[19] Beisert N, Kazakov V A, Sakai K and Zarembo K 2005 Complete spectrum of long operators in $N = 4$ SYM at one loop *J. High Energy Phys.* JHEP07(2005)030 (arXiv:hep-th/0503200)

[20] Arutyunov G, Frolov S and Staudacher M 2004 Bethe ansatz for quantum strings *J. High Energy Phys.* JHEP10(2004)016 (arXiv:hep-th/0406256)

[21] Beisert N and Staudacher M 2005 Long-range PSU(2,2|4) Bethe ansaetze for gauge theory and strings *Nucl. Phys.* B **727** 1–62 (arXiv:hep-th/0504190)

[22] Sutherland B 1995 Low-lying eigenstates of the one-dimensional Heisenberg ferromagnet for any magnetization and momentum *Phys. Rev. Lett.* **74** 816–9

[23] Beisert N, Minahan J A, Staudacher M and Zarembo K 2003 Stringing spins and spinning strings *J. High Energy Phys.* JHEP09(2003)010 (arXiv:hep-th/0306139)

[24] Kazakov V A and Zarembo K 2004 Classical/quantum integrability in non-compact sector of AdS/CFT *J. High Energy Phys.* JHEP10(2004)060 (arXiv:hep-th/0410105)

[25] Arutyunov G and Frolov S 2005 Integrable Hamiltonian for classical strings on AdS(5) $\times$ S^5 *J. High Energy Phys.* JHEP02(2005)059 (arXiv:hep-th/0411089)

[26] Babelon M T O and Bernard D 2003 *Introduction to Classical Integrable Systems* (Cambridge: Cambridge University Press)

[27] Belokolos D and Bobenko A I 1994 *AlgebroGeometric Approach to Nonlinear Integrable Equations* (Berlin: Springer)

[28] Beisert N 2004 The complete one-loop dilatation operator of $N = 4$ super Yang–Mills theory *Nucl. Phys.* B **676** 3–42 (arXiv:hep-th/0307015)

[29] Beisert N and Staudacher M 2003 The $N = 4$ SYM integrable super spin chain *Nucl. Phys.* B **670** 439–63 (arXiv:hep-th/0307042)

[30] Beisert N, Dippel V and Staudacher M 2004 A novel long range spin chain and planar $N = 4$ super Yang–Mills *J. High Energy Phys.* JHEP07(2004)075 (arXiv:hep-th/0405001)

[31] Staudacher M 2005 The factorized S-matrix of CFT/AdS *J. High Energy Phys.* JHEP05(2005)054 (arXiv: hep-th/0412188)

[32] Beisert N 2008 The su(2|2) dynamic S-matrix *Adv. Theor. Math. Phys.* **12** 945 (arXiv:hep-th/0511082)

[33] Beisert N, Hernandez R and Lopez E 2006 A crossing-symmetric phase for AdS(5) $\times$ S^5 strings *J. High Energy Phys.* JHEP11(2006)070 (arXiv:hep-th/0609044)

[34] Beisert N 2007 On the scattering phase for AdS(5) $\times$ S^5 strings *Mod. Phys. Lett.* A **22** 415–24 (arXiv: hep-th/0606214)

[35] Janik R A 2006 The AdS(5) $\times$ S^5 superstring worldsheet S-matrix and crossing symmetry *Phys. Rev.* D **73** 086006 (arXiv:hep-th/0603038)

[36] Beisert N, Eden B and Staudacher M 2007 Transcendentality and crossing *J. Stat. Mech.* **0701** P021 (arXiv: hep-th/0610251)

[37] Eden B and Staudacher M 2006 Integrability and transcendentality *J. Stat. Mech.* **0611** P014 (arXiv: hep-th/0603157)

[38] Kotikov A V and Lipatov L N 2003 DGLAP and BFKL evolution equations in the $N = 4$ supersymmetric gauge theory *Nucl. Phys.* B **661** 19–61 (arXiv:hep-ph/0208220)

[39] Hernandez R and Lopez E 2006 Quantum corrections to the string Bethe ansatz *J. High Energy Phys.* JHEP07(2006)004 (arXiv:hep-th/0603204)

[40] Bern Z, Czakon M, Dixon L J, Kosower D A and Smirnov V A 2007 The four-loop planar amplitude and cusp anomalous dimension in maximally supersymmetric Yang–Mills theory *Phys. Rev.* D **75** 085010 (arXiv:hep-th/0610248)

[41] Beisert N, McLoughlin T and Roiban R 2007 The four-loop dressing phase of $N = 4$ SYM *Phys. Rev.* D **76** 046002 (arXiv:0705.0321)

[42] Kotikov A V, Lipatov L N, Rej A, Staudacher M and Velizhanin V N 2007 Dressing and wrapping *J. Stat. Mech.* **0710** P10003 (arXiv:0704.3586)

[43] Dorey N, Hofman D M and Maldacena J M 2007 On the singularities of the magnon S-matrix *Phys. Rev.* D **76** 025011 (arXiv:hep-th/0703104)

[44] Ambjorn J, Janik R A and Kristjansen C 2006 Wrapping interactions and a new source of corrections to the spin-chain/string duality *Nucl. Phys.* B **736** 288–301 (arXiv:hep-th/0510171)

[45] Kruczenski M, Roiban R, Tirziu A and Tseytlin A A 2008 Strong-coupling expansion of cusp anomaly and gluon amplitudes from quantum open strings in AdS5 $\times$ S5 *Nucl. Phys.* B **791** 93–124 (arXiv:0707.4254)

[46] Roiban R and Tseytlin A A 2007 Strong-coupling expansion of cusp anomaly from quantum superstring *J. High Energy Phys.* JHEP11(2007)016 (arXiv:0709.0681)

[47] Klose T and Zarembo K 2007 Reduced sigma-model on AdS5 $\times$ S5: one-loop scattering amplitudes *J. High Energy Phys.* JHEP02(2007)071 (arXiv:hep-th/0701240)

[48] Klose T, McLoughlin T, Minahan J A and Zarembo K 2007 World-sheet scattering in AdS(5) $\times$ S^5 at two loops *J. High Energy Phys.* JHEP08(2007)051 (arXiv:0704.3891)

[49] Maldacena J M and Swanson I 2007 Connecting giant magnons to the pp-wave: an interpolating limit of $AdS_5 \times S^5$ *Phys. Rev.* D **76** 026002 (arXiv:hep-th/0612079)
[50] Bern Z, Dixon L J and Smirnov V A 2005 Iteration of planar amplitudes in maximally supersymmetric Yang–Mills theory at three loops and beyond *Phys. Rev.* D **72** 085001 (arXiv:hep-th/0505205)
[51] Cachazo F, Spradlin M and Volovich A 2007 Four-loop cusp anomalous dimension from obstructions *Phys. Rev.* D **75** 105011 (arXiv:hep-th/0612309)
[52] Gubser S S, Klebanov I R and Polyakov A M 2002 A semi-classical limit of the gauge/string correspondence *Nucl. Phys.* B **636** 99–114 (arXiv:hep-th/0204051)
[53] Frolov S and Tseytlin A A 2002 Semiclassical quantization of rotating superstring in AdS(5) $\times$ S(5) *J. High Energy Phys.* JHEP06(2002)007 (arXiv:hep-th/0204226)
[54] Roiban R, Tirziu A and Tseytlin A A 2007 Two-loop world-sheet corrections in AdS5 $\times$ S5 superstring *J. High Energy Phys.* JHEP07(2007)056 (arXiv:0704.3638)
[55] Beisert N, Tseytlin A A and Zarembo K 2005 Matching quantum strings to quantum spins: one-loop versus finite-size corrections *Nucl. Phys.* B **715** 190–210 (arXiv:hep-th/0502173)
[56] Hernandez R, Lopez E, Perianez A and Sierra G 2005 Finite size effects in ferromagnetic spin chains and quantum corrections to classical strings *J. High Energy Phys.* JHEP06(2005)011 (arXiv:hep-th/0502188)
[57] Beisert N and Freyhult L 2005 Fluctuations and energy shifts in the Bethe ansatz *Phys. Lett.* B **622** 343–8 (arXiv:hep-th/0506243)
[58] Beisert N and Tseytlin A A 2005 On quantum corrections to spinning strings and Bethe equations *Phys. Lett.* B **629** 102–10 (arXiv:hep-th/0509084)
[59] Minahan J A, Tirziu A and Tseytlin A A 2006 1/J corrections to semiclassical AdS/CFT states from quantum Landau–Lifshitz model *Nucl. Phys.* B **735** 127–71 (arXiv:hep-th/0509071)
[60] Minahan J A, Tirziu A and Tseytlin A A 2005 $1/J^2$ corrections to BMN energies from the quantum long range Landau–Lifshitz model *J. High Energy Phys.* JHEP11(2005)031 (arXiv:hep-th/0510080)
[61] Schafer-Nameki S, Zamaklar M and Zarembo K 2005 Quantum corrections to spinning strings in AdS(5) $\times$ S^5 and Bethe ansatz: a comparative study *J. High Energy Phys.* JHEP09(2005)051 (arXiv:hep-th/0507189)
[62] Schafer-Nameki S and Zamaklar M 2005 Stringy sums and corrections to the quantum string Bethe ansatz *J. High Energy Phys.* JHEP10(2005)044 (arXiv:hep-th/0509096)
[63] Faddeev L D 1996 How algebraic Bethe ansatz works for integrable model arXiv:hep-th/9605187
[64] Reshetikhin N Yu and Smirnov V A 1983 Quantum Floquet functions *Zapiski nauchnikh seminarov LOMI* vol 131 pp 128–41
Reshetikhin N Yu and Smirnov V A 1983 *J. Math. Sci.* **30** (4) 326–2336
[65] Korchemsky G P 1998 WKB quantization of reggeon compound states in high-energy QCD arXiv: hep-ph/9801377
[66] Bajnok Z, Balog J, Basso B, Korchemsky G P and Palla L 2008 arXiv:0809.4952 [hep-th]
[67] Volin D 2008 arXiv:0812.4407 [hep-th]
[68] Beisert N 2005 The dilatation operator of $N = 4$ super Yang–Mills theory and integrability *Phys. Rep.* **405** 1–202 (arXiv:hep-th/0407277)
[69] Kulish P P, Reshetikhin N Y and Sklyanin E K 1981 Yang–Baxter equation and representation theory: I *Lett. Math. Phys.* **5** 393–403
[70] Matytsin A 1994 On the large N limit of the Itzykson–Zuber integral *Nucl. Phys.* B **411** 805–20 (arXiv: hep-th/9306077)
[71] Daul J-M and Kazakov V A 1994 Wilson loop for large N Yang–Mills theory on a two-dimensional sphere *Phys. Lett.* B **335** 371–6 (arXiv:hep-th/9310165)
[72] Krichever I, Lipan O, Wiegmann P and Zabrodin A 1997 Quantum integrable models and discrete classical Hirota equations *Commun. Math. Phys.* **188** 267–304 (arXiv:hep-th/9604080)
[73] Bleher P 1991 Quasi-Classical Expansions and the Problem of Quantum Chaos (*Lecture Notes in Mathematics* vol 1469) (Berlin: Springer)
[74] Brezin E and Kazakov V A 1990 Exactly solvable field theories of closed strings *Phys. Lett.* B **236** 144–50
[75] Mehta M L 1967 *Random Matrices* (New York: Academic)
[76] Beisert N, Kristjansen C and Staudacher M 2003 The dilatation operator of $N = 4$ super Yang–Mills theory *Nucl. Phys.* B **664** 131–84 (arXiv:hep-th/0303060)
[77] Serban D and Staudacher M 2004 Planar $N = 4$ gauge theory and the Inozemtsev long range spin chain *J. High Energy Phys.* JHEP06(2004)001 (arXiv:hep-th/0401057)
[78] Kazakov V, Sorin A and Zabrodin A 2008 Supersymmetric Bethe ansatz and Baxter equations from discrete Hirota dynamics *Nucl. Phys.* B **790** 345–413 (arXiv:hep-th/0703147)
[79] Zabrodin A 2007 Backlund transformations for difference Hirota equation and supersymmetric Bethe ansatz arXiv:0705.4006

[80] Gromov N and Kazakov V 2006 Double scaling and finite size corrections in sl(2) spin chain *Nucl. Phys.* B **736** 199–224 (arXiv:hep-th/0510194)
[81] Reshetikhin N y 1983 A method of functional equations in the theory of exactly solvable quantum systems *Lett. Math. Phys.* **7** 205–13
[82] Reshetikhin N Y 1985 Integrable models of quantum one-dimensional magnets with O(N) and SP(2K) symmetry *Theor. Math. Phys.* **63** 555–69
[83] Bargheer T, Beisert N and Gromov N 2008 Quantum stability for the Heisenberg ferromagnet *New J. Phys.* **10** 103023 (arXiv:0804.0324)
[84] Mandal G, Suryanarayana N V and Wadia S R 2002 Aspects of semiclassical strings in AdS(5) *Phys. Lett.* B **543** 81–8 (arXiv:hep-th/0206103)
[85] Frolov S and Tseytlin A A 2003 Multi-spin string solutions in AdS(5) $\times$ S^5 *Nucl. Phys.* B **668** 77–110 (arXiv:hep-th/0304255)
[86] Frolov S and Tseytlin A A 2003 Quantizing three-spin string solution in AdS(5) $\times$ S^5 *J. High Energy Phys.* JHEP07(2003)016 (arXiv:hep-th/0306130)
[87] Arutyunov G, Russo J and Tseytlin A A 2004 Spinning strings in AdS(5) $\times$ S^5: new integrable system relations *Phys. Rev.* D **69** 086009 (arXiv:hep-th/0311004)
[88] Park I Y, Tirziu A and Tseytlin A A 2005 Spinning strings in AdS(5) $\times$ S^5: one-loop correction to energy in SL(2) sector *J. High Energy Phys.* JHEP03(2005)013 (arXiv:hep-th/0501203)
[89] Berenstein D E, Maldacena J M and Nastase H S 2003 Strings in flat space and pp waves from $N = 4$ super Yang–Mills *AIP Conf. Proc.* **646** 3–14
[90] Gromov N, Kazakov V, Sakai K and Vieira P 2007 Strings as multi-particle states of quantum sigma- models *Nucl. Phys.* B **764** 15–61 (arXiv:hep-th/0603043)
[91] Frolov S A, Park I Y and Tseytlin A A 2005 On one-loop correction to energy of spinning strings in S(5) *Phys. Rev.* D **71** 026006 (arXiv:hep-th/0408187)
[92] Schafer-Nameki S 2006 Exact expressions for quantum corrections to spinning strings *Phys. Lett.* B **639** 571–8 (arXiv:hep-th/0602214)
[93] Gromov N and Vieira P 2008 Constructing the AdS/CFT dressing factor *Nucl. Phys.* B **790** 72–88 (arXiv:hep-th/0703266)
[94] Novikov S, Manakov S V, Pitaevsky L P and Zakharov V E 1984 *Theory of Solitons. The Inverse Scattering Method (Contemporary Soviet Mathematics)* (New York: Consultants Bureau) p 276
[95] Zamolodchikov A B and Zamolodchikov A B 1978 Relativistic factorized S matrix in two-dimensions having O(N) isotopic symmetry *Nucl. Phys.* B **133** 525
[96] Polyakov A M and Wiegmann P B 1983 Theory of nonabelian Goldstone bosons in two dimensions *Phys. Lett.* B **131** 121–6
[97] Wiegmann P B 1984 Exact solution for the SU(N) main chiral field in two-dimensions *JETP Lett.* **39** 214–8
[98] Faddeev L D and Reshetikhin N Y 1986 Integrability of the principal chiral field model in (1+1)-dimension *Ann. Phys.* **167** 227
[99] Wiegmann P 1984 Exact factorized s matrix of the chiral field in two-dimensions *Phys. Lett.* B **142** 173–6
[100] Fateev V A, Kazakov V A and Wiegmann P B 1994 Principal chiral field at large N *Nucl. Phys.* B **424** 505–20 (arXiv:hep-th/9403099)
[101] Balog J, Naik S, Niedermayer F and Weisz P 1992 The exact mass gap of the chiral SU(n) $\times$ SU(n) model *Phys. Rev. Lett.* **69** 873–6
[102] Mann N and Polchinski J 2005 Bethe ansatz for a quantum supercoset sigma model *Phys. Rev.* D **72** 086002 (arXiv:hep-th/0508232)
[103] Wiegmann P B 1984 On the theory of nonabelian Goldstone bosons in two-dimensions: exact solution of the O(3) nonlinear sigma model *Phys. Lett.* B **141** 217
[104] Ogievetsky E, Reshetikhin N and Wiegmann P 1987 The principal chiral field in two-dimension and classical lie algebra (NORDITA-84/38) *Nucl. Phys.* B **280** 45
[105] Zamolodchikov A B and Zamolodchikov A B 1992 Massless factorized scattering and sigma models with topological terms *Nucl. Phys.* B **379** 602–23
[106] Faddeev L D, Sklyanin E K and Takhtajan L A 1980 The quantum inverse problem method: I *Theor. Math. Phys.* **40** 688–706
[107] Rej A, Serban D and Staudacher M 2006 Planar $N = 4$ gauge theory and the Hubbard model *J. High Energy Phys.* JHEP03(2006)018 (arXiv:hep-th/0512077)
[108] Gromov N and Kazakov V 2007 Asymptotic Bethe ansatz from string sigma model on $S^3 \times$ R *Nucl. Phys.* B **780** 143–60 (arXiv:hep-th/0605026)
[109] Gromov N and Vieira P 2008 The all loop AdS4/CFT3 Bethe ansatz arXiv:0807.0777
[110] Aharony O, Bergman O, Jafferis D L and Maldacena J 2008 $N = 6$ superconformal Chern–Simons-matter theories, M2-branes and their gravity duals *J. High Energy Phys.* JHEP10(2008)091 (arXiv:0806.1218)

[111] Bandres M A, Lipstein A E and Schwarz J H 2008 Ghost-free superconformal action for multiple M2-branes *J. High Energy Phys.* JHEP07(2008)117 (arXiv:0806.0054)
[112] Benna M, Klebanov I, Klose T and Smedback M 2008 Superconformal Chern–Simons theories and AdS4/CFT3 correspondence *J. High Energy Phys.* JHEP09(2008)072 (arXiv:0806.1519)
[113] Ezhuthachan B, Mukhi S and Papageorgakis C 2008 D2 to D2 *J. High Energy Phys.* JHEP07(2008)041 (arXiv:0806.1639)
[114] Nishioka T and Takayanagi T 2008 On type IIA Penrose limit and $N = 6$ Chern–Simons theories *J. High Energy Phys.* JHEP08(2008)001 (arXiv:0806.3391)
[115] Minahan J A and Zarembo K 2008 The Bethe ansatz for superconformal Chern–Simons *J. High Energy Phys.* JHEP09(2008)040 (arXiv:0806.3951)
[116] Gaiotto D, Giombi S and Yin X 2008 Spin chains in $N = 6$ superconformal Chern–Simons-matter theory arXiv:0806.4589
[117] Arutyunov G and Frolov S 2008 Superstrings on AdS4 × CP3 as a coset sigma-model *J. High Energy Phys.* JHEP09(2008)129 (arXiv:0806.4940)
[118] Stefanski B Jr 2009 Green–Schwarz action for type IIA strings on $AdS_4 \times CP^3$ *Nucl. Phys.* B **808** 80–7 (arXiv:0806.4948)
[119] Grignani G, Harmark T and Orselli M 2008 The SU(2) × SU(2) sector in the string dual of $N = 6$ superconformal Chern–Simons theory arXiv:0806.4959
[120] Hosomichi K, Lee K-M, Lee S, Lee S and Park J 2008 N = 5, 6 superconformal Chern–Simons theories and M2-branes on orbifolds *J. High Energy Phys.* JHEP09(2008)002 (arXiv:0806.4977)
[121] Bagger J and Lambert N 2008 Three-algebras and $N = 6$ Chern–Simons gauge theories arXiv:0807.0163
[122] Ahn C and Nepomechie R I 2008 $N = 6$ super Chern–Simons theory S-matrix and all-loop Bethe ansatz equations *J. High Energy Phys.* JHEP09(2008)010 (arXiv:0807.1924)
[123] Gromov N 2008 Generalized scaling function at strong coupling arXiv:0805.4615
[124] Casteill P Y and Kristjansen C 2007 The strong coupling limit of the scaling function from the quantum string Bethe ansatz *Nucl. Phys.* B **785** 1 (arXiv:0705.0890 [hep-th])
[125] Gromov N and Vieira P 2008 The AdS4/CFT3 algebraic curve arXiv:0807.0437
[126] Gromov N and Mikhaylov V 2008 Comment on the scaling function in AdS4 × CP3 arXiv:0807.4897
[127] Gromov N, Schafer-Nameki S and Vieira P 2008 Quantum wrapped giant magnon *Phys. Rev.* D **78** 026006 (arXiv:0801.3671)
[128] Gromov N, Schafer-Nameki S and Vieira P 2008 Efficient precision quantization in AdS/CFT arXiv:0807.4752
[129] Hatsuda Y and Suzuki R 2008 Finite-size effects for multi-magnon states *J. High Energy Phys.* JHEP09(2008)025 (arXiv: 0807.0643)
[130] Bombardelli D and Fioravanti D 2008 Finite-size corrections of the $\mathbb{CP}^3$ giant magnons: the Lúscher terms arXiv:0810.0704
[131] Bajnok Z and Janik R A 2009 Four-loop perturbative Konishi from strings and finite size effects for multiparticle states *Nucl. Phys.* **B807** 625–50 (arXiv:0807.0399)
[132] Janik R A and Lukowski T 2007 Wrapping interactions at strong coupling—the giant magnon *Phys. Rev.* D **76** 126008 (arXiv:0708.2208)
[133] Heller M P, Janik R A and Lukowski T 2008 A new derivation of Luscher F-term and fluctuations around the giant magnon *J. High Energy Phys.* JHEP06(2008)036 (arXiv:0801.4463)
[134] Bajnok Z, Janik R A and Lukowski T 2008 Four loop twist two, BFKL, wrapping and strings arXiv:0811.4448